The role of the transcriptional regulators NFATc1 and Blimp-1 in follicular T-cells

Die Rolle der Transkriptionsregulatoren NFATc1 und Blimp-1 in follikulären T-Zellen

Doctoral thesis for a doctoral degree
at the Graduate School of Life Sciences,
Julius-Maximilians-Universität Würzburg,
Section Infection and Immunity

submitted by Anika König
from Hanau

Würzburg 2020

Submitted on: ……..……..

Office stamp

Members of the Thesis Committee

Chairperson:	Prof. Dr. med. Georg Gasteiger
Primary Supervisor:	PD Dr. Friederike Berberich-Siebelt
Supervisor (Second):	PD Dr. Robert Hock
Supervisor (Third):	PD Dr. med. Niklas Beyersdorf

Date of Public Defence: ……..……

Date of Receipt of Certificates: …….

Table of Contents

1 Affidavit

I hereby confirm that my thesis entitled “The role of the transcriptional regulators NFATc1 and Blimp-1 in follicular T-cells” is the result of my own work. I did not receive any help or support from commercial consultants. All sources and / or materials applied are listed and specified in the thesis.

Furthermore, I confirm that this thesis has not yet been submitted as part of another examination process neither in identical nor in similar form.

Place, Date Signature

Eidesstattliche Erklärung

Hiermit erkläre ich an Eides satt, die Dissertation „Die Rolle der Transkriptionsregulatoren NFATc1 und Blimp-1 in follikulären T-Zellen“ eigenständig, d.h. insbesondere selbständig und ohne Hilfe eines kommerziellen Promotionsberaters, angefertigt und keine anderen als die von mir angegebenen Quellen und Hilfsmittel verwendet zu haben.

Ich erkläre außerdem, dass die Dissertation weder in gleicher noch in ähnlicher Form bereits in einem anderen Prüfungsverfahren vorgelegen hat.

Ort, Datum Unterschrift

2 Acknowledgements

At this point I would like to thank all my colleagues, collaborators and people who supported me in the creation of my doctoral thesis.

First, I would like to sincerely thank my first supervisor PD Dr. Friederike Berberich-Siebelt who supported me via all means, scientifically and personally. The door was always open for encouraging discussions, which were full of curiosity for my work. Many thanks for the positive input theoretically and practically whenever open questions were encountered. Last but not least, my particular thanks for the granted freedom and the patience it took to finalize this project.

Furthermore, I would like to thank the members of my thesis committee PD Dr. Robert Hock and PD Dr. Niklas Beyersdorf for the accelerating discussions within the annual meetings. Additionally, I would like to thank PD Dr. Niklas Beyersdorf for the preparation of the second report on my thesis.

My devoted thanks go to Dr. Martin Vaeth for the pioneering work on this project and for answering any kind of question. Special thanks to Dr. Lena Diez for teaching me how to get around in the lab as a starter.

All of my current and former colleagues I would like to joyfully thank for the positive atmosphere in the lab, for fruitful discussions and the help with some experimental work. Without the support of Dr. Raghu Erapaneedi, Dr. Stefan-Klein Hessling, Dr. Khalid Muhammad, Benjamin Lunz, Nadine Winter, Musga Qureishi, Lara Schwab, Katharina Schwarz, Felix Schüssler, Alexander Lenhart, Markus Haßler, Yosif Tumbev, Cristina Chiarolla, Sabrina Giampaolo, Yin Xiao, Snigdha Majumder and Rishav Seal this work would not have been the same.

I gratefully thank all my collaborators for sharing their expertise and manpower to support me: Prof. Dr. Ingolf Berberich, Dr. Nora Müller and Jun.-Prof. Dr. Florian Erhard from the VIM Wuerzburg, Dr. Matthias Klein, Prof. Dr. Magdalena Huber and Dr. Lucia Campos Carrascosa from the University of Marburg, Tabea Steinmüller, Sabine Roth and the immunohistochemistry laboratory from the Institute of Pathology Wuerzburg.

I would like to appreciate the organization of the GSLS and especially the section “immunomodulation” which was enormous helpful in shaping my immunological expertise.

Finally, I would like to thank my huge and colorful family and especially Björn who supported me throughout this journey in every sense.

3 Abstract

The defense against invading pathogens is, amongst other things, mediated via the action of antibodies. Class-switched antibodies and antibodies of high affinity are produced by plasma cells descending from germinal center B (GCB) cells. GCB cells develop in the germinal center (GC), a specialized microstructure found in the B-cell follicle of secondary lymphoid organs. GCB-cell maturation and proliferation are supported by follicular T-helper (Tfh) cells. On the other hand, follicular regulatory T (Tfr) cells control this process in quantity and quality preventing, for instance, the formation of autoantibodies directed against endogenous structures. The development of GCB, Tfh and Tfr cells essentially depends on the migration into the GC, which is mediated via the expression of the chemokine receptor CXCR5.

One transcription factor highly expressed in follicular T cells, comprising Tfh and Tfr cells, is NFATc1. Tfr cells additionally express the transcriptional repressor Blimp-1, which is not expressed in Tfh cells. We found that NFATc1 is transactivating *Cxcr5* via response elements in the promoter and enhancer *in vitro*. Blimp-1 binds to the same elements, transactivating *Cxcr5* expression in cooperation with NFATc1, whilst mediating *Cxcr5*-repression on its own. In Tfr cells Blimp-1 suppresses CXCR5 expression in the absence of NFATc1. Blimp-1 itself is necessary to restrict Tfr-cell frequencies and to mediate Tfr-cell function as in mice with Blimp-1-ablated Tregs high frequencies of Tfr cells do not reduce GCB- or Tfh cell frequencies. NFATc1 and Blimp-1 double deficient Tfr cells show additional loss of function, which becomes visible in clearly expanded antibody titers.

To evaluate the function of NFATc1 in Tfr cells, we not only deleted it, but also overexpressed a constitutive active form of NFATc1/αA (caNFATc1/αA) in regulatory T cells (Tregs). The latter is leading to an upregulation of CXCR5 per cell, without changing Tfh or Tfr-cell frequencies. However, the high density of surface CXCR5 enhances the migration of Tfr cells deep into the GC, which results in a tighter control of the antigen-specific humoral immune response. Additionally, caNFATc1/αA increases the expression of genes coding for Tfr effector molecules like *Il1rn*, *Il10*, *Tigit* and *Ctla4*. Interestingly, this part of the transcriptional change is dependent on the presence of Blimp-1. Furthermore, Blimp-1 regulates the expression of multiple chemokine receptor genes on the background of caNFATc1/αA.

In contrast, when caNFATc1/αA is overexpressed in all T cells, the frequencies of Tfh- and GCB cells are dominantly reduced. This effect seems to stem from the conventional T-cell (Tcon) side, most probably originating from increased secretion of interleukin-2 (IL-2) via the caNFATc1/αA overexpressing Tcons. IL-2 is known to hinder the germinal center reaction (GCR) and it might in its abundance not be neutralizable by Tfr cells.

Taken together, NFATc1 and Blimp-1 cooperate to control the migration of Tfr cells into the GC. Tfr cells in the GC depend on NFATc1 and Blimp-1 to perform their proper function. Overexpression of caNFATc1 in Tregs strengthens Tfr function in a Blimp-1-dependent manner, whilst overexpression of caNFATc1 in all T cells dominantly diminishes the GCR.

4 Zusammenfassung

Die Abwehr von Krankheitserregern durch das Immunsystem wird unter anderem (u.a.) durch die Wirkung von Antikörpern vermittelt. Antikörper, welche einen Klassenwechsel und eine hohe Affinität aufweisen, werden von Plasmazellen gebildet, welche sich von Keimzentrums-B (GCB) -Zellen ableiten. GCB-Zellen evolvieren innerhalb des Keimzentrums (GC), einer Mikrostruktur, welche sich innerhalb des B-Zellfollikels sekundärer lymphoider Organe bildet. Die GCB-Zell-Reifung und -Proliferation wird durch follikuläre T-Helfer (Tfh) -Zellen unterstützt und durch follikuläre regulatorische T (Tfr) -Zellen kontrolliert, wodurch u.a. die Bildung von Autoantikörpern, welche körpereigene Strukturen angreifen, unterbunden wird. Die Entwicklung von GCB-, Tfh- und Tfr-Zellen ist in entscheidender Weise abhängig von der Expression des Chemokinrezeptors CXCR5 und der damit verbundenen Migration in das GC.

NFATc1 ist ein Transkriptionsfaktor, welcher in follikulären T-Zellen, bestehend aus Tfh- und Tfr-Zellen, stark exprimiert wird. Im Gegensatz zu Tfh-Zellen exprimieren Tfr-Zellen zusätzlich den Transkriptionsrepressor Blimp-1. Wir haben herausgefunden, dass NFATc1 die Expression von *Cxcr5* über die Bindung an Elemente innerhalb des *Cxcr5*-Promotors und -Enhancers *in vitro* transakiviert. Blimp-1 bindet an selbige Elemente und transaktiviert in Kooperation mit NFATc1 die *Cxcr5*-Expression, während es die *Cxcr5*-Expression alleine hemmt. In Tfr-Zellen supprimiert Blimp-1 die CXCR5-Expression in Abwesenheit von NFATc1. Blimp-1 beschränkt darüber hinaus das Vorkommen von Tfr-

Zellen und spielt eine Rolle in der Effektorfunktion von Tfr-Zellen. Dies wird deutlich da das verstärkte Tfr-Zell-Vorkommen in Mäusen mit Blimp-1 defizienten Tregs nicht zu einer Reduktion der GCB-oder Tfh-Zellen führt. Der Verlust der Effektorfunktion akkumuliert in NFATc1 und Blimp-1 doppel-defizienten Tfr-Zellen, was sich in einem deutlichen Anstieg der Antikörpertiter im Serum immunisierter Tiere zeigt.

Zur Überprüfung der Funktion von NFATc1 in Tfr-Zellen untersuchten wir sowohl dessen Deletion, als auch die Überexpression einer konstitutiv aktiven Form von NFATc1/αA (caNFATc1/αA) in regulatorischen T-Zellen (Tregs). Letztere steigert die CXCR5-Expression pro Zelle ohne das Vorkommen von Tfh- oder Tfr-Zellen zu verändern. Jedoch führte die erhöhte Oberflächenexpression von CXCR5 zu einer verstärkten Migration der Tfr-Zellen in das GC, was in einer verstärkten Kontrolle der antigenspezifischen Antikörpertiter resultierte. Darüber hinaus erhöht caNFATc1/αA in Abhängigkeit von Blimp-1, die Expression der Gene *Il1rn*, *Il10*, *Tigit* und *Ctla4*, welche mit der Effektorfunktion von Tfr-Zellen assoziiert werden. Blimp-1 wirkt auf dem Hintergrund der Überexpression von NFATc1 vor allem regulierend auf die Expression von Chemokinrezeptorgenen.

Im Gegensatz zur Überexpression von caNFATc1/αA in Tregs allein, führt selbige Veränderung in allen T-Zellen zu einer deutlichen Reduktion des Vorkommens von Tfh- und GCB-Zellen nach Immunisierung. Dieser Effekt scheint durch konventionelle T-Zellen (Tcons) vermittelt zu sein und entsteht vermutlich durch eine erhöhte Sekretion von Interleukin-2 (IL-2) durch die caNFATc1/αA überexprimierenden Tcons. Dieses IL-2 scheint in seiner Menge nicht durch die vorliegenden Tfr-Zellen neutralisierbar zu sein und die Keimzentrumsreaktion (GCR) zu hemmen.

Die vorliegende Arbeit zeigt, dass NFATc1 und Blimp-1 kooperieren, um die Migration von Tfr-Zellen in das GC zu kontrollieren. Tfr-Zellen im GC sind in der Erfüllung ihrer ordnungsgemäßen Funktion abhängig von NFATc1 und Blimp-1. Die Überexpression von caNFATc1 in Tregs stärkt die Funktion von Tfr-Zellen in einer Blimp-1-abhängigen Weise, während die Überexpression von caNFATc1 in allen T-Zellen die GCR extrem minimiert.

5 Introduction

5.1 The immune system

The immune system is constituted of cells and molecules responsible to provide protection from infectious diseases. It responds to the introduction of foreign substances into the body as well as injured cells. Substances recognized as foreign include components of microbes (pathogens), macromolecules, such as proteins, polysaccharides and small chemicals. Under certain circumstances also self-molecules can be mistakenly recognized as foreign and elicit an immune response, which can cause damage to the body. The defense against microbes is mediated via two lines of defense. Early defense responses are provided via the innate immunity, whilst later responses are taken over by the adaptive immunity. The innate immunity is the phylogenetically older part of the immune system. It is built of physical and chemical barriers, cells and blood proteins. The physical and chemical barriers of this system consist of epithelia and antimicrobial chemicals produced at epithelial surfaces [1]. Cells of the innate immunity comprise phagocytic cells (neutrophils and macrophages), dendritic cells (DCs), natural killer cells (NK) and innate lymphoid cells (ILCs). Within the blood are proteins that are preformed and ready to react to invading pathogens such as the complement system and other mediators of inflammation. The innate immunity reacts against structures that are common to groups of related microbes, the so-called pathogen-associated molecular patterns (PAMPs), as well as endogenous molecules that are produced from damaged or dying cells, the so-called damage-associated molecular patterns (DAMPs) [2]. The receptors that recognize these classes of molecules are called pattern recognition receptors (PRR). Mechanisms of innate immunity respond to repeated exposures in essentially the same way [1].

The adaptive immunity is phylogenetically younger than the innate immunity and can be found in vertebrates only. It can recognize a broad spectrum of microbial and non-microbial substances. Different from the innate immunity, which can only recognize classes of molecules, it can even distinguish different substances, a property which is called specificity. It is also capable to react more forcefully to repeatedly exposures with the same pathogen, this characteristic is known as memory. The adaptive immunity consists of cells that are named lymphocytes and their secreted products, for example antibodies and cytokines. Substances that are recognized by lymphocytes or antibodies, therewith

inducing an immune response, are called antigens [1]. There are subpopulations of lymphocytes that differ in their functions and in the way how they recognize antigens. In mammals, B lymphocytes (B cells) undergo the early stages of differentiation within the bone marrow. B cells recognize extracellular soluble and cell surface antigens via the B-cell receptor (BCR). They can differentiate into antibody-secreting plasma cells. Antibodies recognize antigens and bind to them. In case of a microbial antigen this process leads to the neutralization of infectivity and targeting for elimination via various effector mechanisms. T lymphocytes (T cells) also arise in the bone marrow before they migrate into the thymus where they mature [3]. T cells recognize peptides derived from foreign proteins that are bound to a complex of endogenous proteins named major histocompatibility complex (MHC), which is located on the surface of other cells. The recognition of this peptide that is presented via the MHC is mediated via the T-cell receptor (TCR) on the surface of the T cell. This TCR-MHC interaction leads to the stimulation of the T cell, which secretes cytokines in response [4]. These cytokines can stimulate the proliferation and differentiation of the T cells themselves and activate other cells such as B cells, macrophages and other leukocytes. In this way, T cells recognize intracellular microbes and either help phagocytes to destroy these microbes or kill the infected cells themselves. Every T- and B cell expresses a unique antigen recognizing TCR or BCR, respectively. This high diversity allows the immune system to combat a high diversity of pathogens. Prior to recognition of an antigen, T- and B cells are called naïve. Upon encounter with an antigen presented via the MHC on the surface of an antigen presenting cell (APC) T- and B-cells become activated and rapidly divide. This leads to a rapid expansion of cells with the same antigen-recognizing receptor, a process which is called clonal selection. Following neutralization of an antigen, only a small percentage of these cells become long lasting memory cells, which can be activated more rapidly upon reactivation [1].

5.2 Development of T cells in the thymus

T-lymphoid progenitor cells migrate from the bone marrow into the thymus. These progenitors lack the TCR as well as the coreceptors CD4 and CD8 that are necessary for the proper activation of the T cell via the TCR. The developing T cells pass through different stages of development marked via the expression of CD4 and/or CD8. Until the proper rearrangement of the pre-TCR, the developing T cell expresses neither of the coreceptors and are called double negative (DN). The successful expression of the pre-TCR

upregulates CD4 and CD8, as well as the proper TCR. These double positive (DP) thymocytes then interact with cortical epithelial cells, which express high levels of MHC molecules associated with self-peptides on their surface. There are two classes of MHC molecules, which distinguish themselves via the ability to interact with the coreceptors CD4 and CD8. MHCI molecules are interacting with the CD8 coreceptor, whilst MHCII molecules interact with CD4 [5]. The fate of these DP thymocytes depends on the signaling strength of the TCR-MHC interaction. A weak signal leads to the induction of programmed cell death (death by neglect), whilst strong TCR signaling either leads to the induction of apoptosis (negative selection) or induces the generation of a regulatory phenotype mostly within the $CD4^+$ lineage (nTreg). This mechanism generates the central tolerance against antigens deriving from the organism itself. Intermediate TCR-signaling mediates the survival of the cell (positive selection), creating a conventional T cell without regulatory attributes (Tcon) [6]. If a DP thymocyte becomes a $CD4^+$ or $CD8^+$ T cell, depends on the successful interaction either with the MHCI molecule (CD8) or the MHCII molecule (CD4) [5].

5.3 Differentiation of different T-helper cell lineages

Mature T cells leave the thymus and are then called naïve. Upon TCR engagement, naïve $CD4^+$ T cells differentiate into various T helper (Th) cell lineages as shown in Figure 5.1. The fate decision for a Th lineage is made by the cytokines being present during the interaction of a naïve cell with the APC. The naïve $CD4^+$ T cell becomes activated via the interaction of the TCR with the MHCII-peptide complex and the costimulus it gets via the interaction of CD28 with its ligands CD80 (B7-1) or CD86 (B7-2). The cytokine signal induces the expression of the lineage specific transcription factor that in turn mediates a transcriptional program that is characteristic for the Th lineage. The different Th lineages are distinguished primarily via the cytokines they secrete. Th1 cells dominantly produce IFN-γ and lymphotoxin, whilst Th2 cells are characterized via their IL-4, IL-5 and IL-13 production. Further Th lineages are named according to the cytokines they predominantly express, e.g. Th17 and Th9. Naïve $CD4^+$ T cells can furthermore differentiate post thymically into a regulatory subset called induced Treg (iTreg). T cells that provide help to B cells to differentiate into plasma cells that are secreting class switched antibodies with a high affinity are called follicular T helper cells (Tfh). It is discussed if these cells represent an own Th lineage or if they represent a phenotypic state of the other Th lineages [7-10].

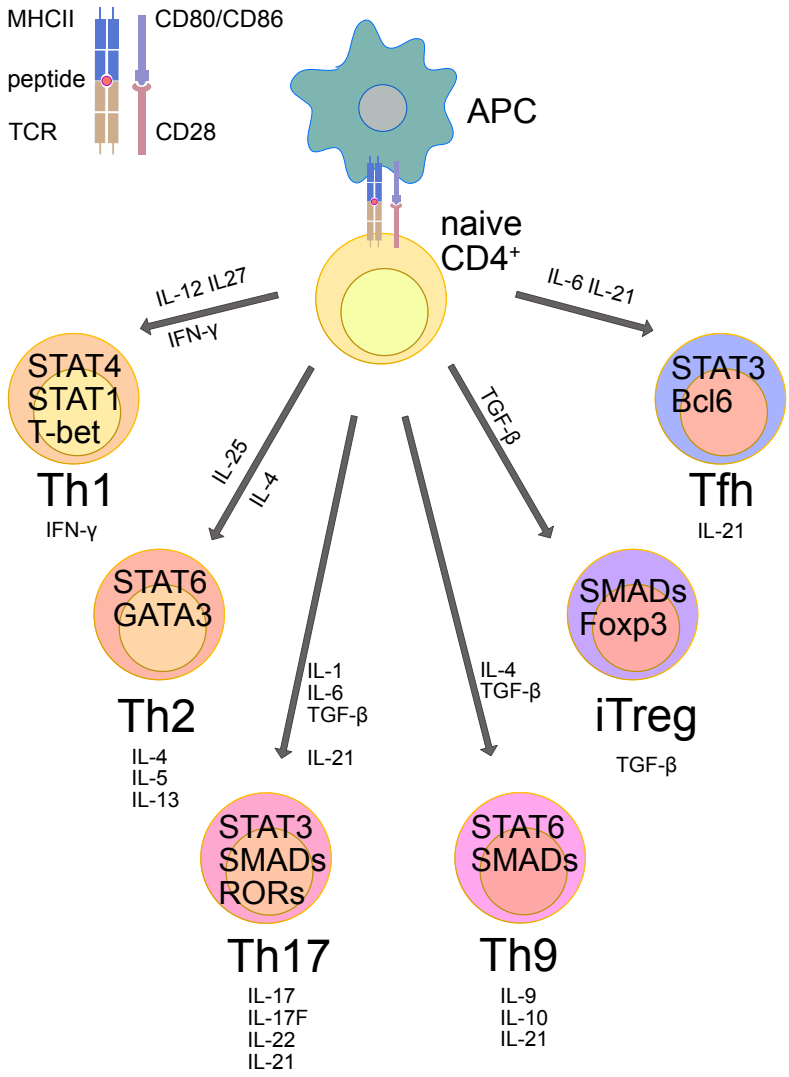

Figure 5.1: Differentiation of Th lineages

The naïve T cell becomes activated via the interaction of the TCR with the MHCII-peptide complex and the co-stimulus it receives via the ligation of CD28 with CD80 or CD86. The cytokines being present during this process direct the differentiation into different Th lineages, which differ in lineage specific transcription factors and in the cytokines they express. Cytokines directing the differentiation are indicated next to the arrows. Th lineage names are indicated below the cells and the lineage specific transcription factors are indicated within the cell. The cytokines which are finally secreted via the different Th lineages are written below the Th-lineage names [7-10].

5.4 Lymphoid organs

The anatomy of the immune system is set up of multiple lymphoid organs. The bone marrow and the thymus are the primary lymphoid organs where lymphocytes first express

their antigen receptors and mature. Naïve lymphocytes leave the bone marrow via the circulation and home to the secondary lymphoid organs, such as lymph nodes (LNs), the spleen and mucosal-associated lymphoid tissues [3]. Mucosal-associated lymphoid tissues comprise the Peyer's patches, tonsils, nasal-associated lymphoid tissue and bronchial-associated lymphoid tissue. Multiple LNs are strategically placed and build a protective network over the body in order to detect antigens stemming from the interstitium. The spleen is important in detecting blood-borne antigens and mucosal-associated lymphoid tissues 'collect' antigens directly from the local environment such as lungs, the gastro-intestinal tract and the reproductive tract. Adult LNs are encapsulated structures that separate into three distinct regions, the cortex, the paracortex and the medulla (Fig. 5.2) [11]. Naïve T and B cells enter the paracortex of the LN via fine blood vessels named high endothelial venules (HEV). HEV express the peripheral node addressin (PNAd), which interacts with L-selectin, expressed on the naïve lymphocyte. The cortex is densely packed with B cells as well as follicular dendritic cells that are arranged into distinct clusters named primary follicles. The paracortex is an accumulation of less densely packed T cells and DCs. The architecture of these distinct zones is arranged via pairs of chemokines and their corresponding receptors. CCL19 and CCL21 are constitutively expressed by stromal cells in the T-cell zone and share the chemokine receptor CCR7. CCR7 is expressed on naïve and central memory T cells and DCs, which home to the T-cell compartment. Follicular stromal cells in the follicular compartment constitutively express CXCL13. B cells and also a small subset of T cells home to the follicular compartment; this requires the expression of CXCR5, the chemokine receptor for CXCL13. DCs and soluble antigen enter the LN via the afferent lymphatic vessels. The activation of naïve T cells via the interaction with an APC is called priming. T cells can be primed via antigen presenting DCs, as DCs present antigen in the form of peptide-MHCI or -MHCII complexes. FDCs present unprocessed antigen in the form of antigen-antibody immune complexes. Antigen challenge leads to massive proliferation of B cells and the formation of germinal centers (GC) in the B-cell follicles. Within these GC, FDCs present antigen to activated B cells, therewith shaping the B-cell response to the antigen [11]. Similar to the LNs, the spleen also separates into distinct regions of T and B cells that are orchestrated via the same chemokine-chemokine receptor pairs. The presentation of blood-borne antigens to T cells mediates the downregulation of CCR7, whilst upregulating CXCR5 allowing them to migrate to the edge of the B-cell follicles. The presentation of antigen to the B cell upregulates CCR7,

mediating the migration of the B cell to the edge of the B-cell follicle, where B cells receive help from T cells resulting in the formation of a GC [12].

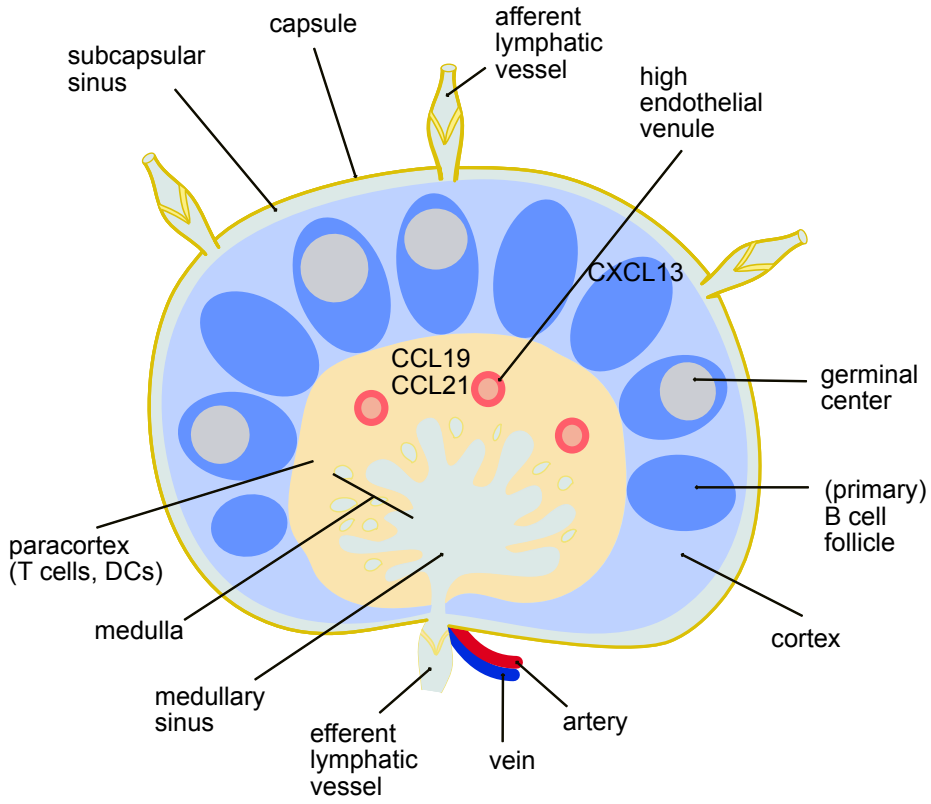

Figure 5.2: Scheme of a LN

The LN is a vascularized encapsulated lymphoid organ. DCs and soluble antigen enter the LN via the afferent lymphatic vessels, which are connected to the subcapsular sinus and the medullary sinus. T and B cells enter the LN via the HEV. Different zones can be distinguished within the LN, according to the cell types which reside there. The paracortex is rich in T cells and DCs (T-cell zone), whilst the cortex contains densely packed clusters of B cells and FDCs (primary B cell follicles). Upon antigen challenge a GC can develop within the follicle. Within the T-cell zone, stromal cells constitutively express CCL19 and CCL21, whilst follicular stromal cells in the B cell follicles of the cortex express CXCL13. These chemokine gradients orchestrate the architecture of the different zones of the LN [3, 11].

5.5 The germinal center

The GC is a specialized microstructure that arises in secondary lymphoid organs upon antigen stimulation via infection or immunization with a T cell-dependent antigen [13]

(Fig. 5.3). Such an antigen needs the help of T cells towards B cells in order to generate a productive antibody response. The help is provided in form of a contact-dependent signal via CD40 and T cell-secreted cytokines [14]. In multiple inflammatory states such as autoimmune diseases, cancer and during infection, ectopic GCs can also arise in nonlymphoid tissues. B cells can directly bind soluble antigen or bind to antigen presented on the surface of FDCs, macrophages or DCs. In response to the specific antigen encounter via the unique BCR, B cells upregulate CCR7 to migrate toward the T-cell zone. At the border between the T cell- and the B-cell follicle (T-B border) B cells present processed antigen via their MHCII to $CD4^+$ pre-Tfh cells, which provide survival and costimulatory signals to the B cell. In response, B cells undergo cell division and will either initiate a GCR or differentiate into short-lived extra-follicular plasma cells or memory B cells. B cells seeding the GC migrate from the T-B border into the center of the follicle where they undergo rapid clonal expansion and become germinal center B cells (GCB). The GC then divides into two distinct compartments, the light- (LZ) and the dark zone (DZ). These zones are created via chemokine gradients. CXCL12 is produced by a network of CXCL12-producing reticular cells (CRCs) in the DZ and recognized via CXCR4 on highly proliferative B cells, that are called centroblasts [13]. Within the DZ, centroblasts undergo two processes that shape their BCR, the somatic hypermutation (SHM) and the class-switch recombination (CSR). Both processes are mediated via the enzyme activation-induced deaminase (AID). AID deaminates cytidine residues within the VDJ and switch regions that code for the BCR. This leads to a high rate of point mutations (SHM) within the variable regions of the BCR that recognizes the antigen, as well as the switching of the constant region of the BCR to another (Iso-) type (CSR) [15]. Centroblasts will then upregulate CXCR5 in order to migrate into the LZ, which they enter as centrocytes. The CXCL13 gradient is produced via FDCs, which are also presenting antigen to the centrocytes within the LZ. The mutation of the BCR coding genes occurs randomly, which can lead to an increase in the binding capacity to the antigen (higher affinity), the loss of antigen recognition, or the binding to an autoantigen. Centrocytes with a beneficial BCR therefore need to be selected. In order to survive, centrocytes need to take up antigen from the surface of FDCs, process it and present it via the MHCII to follicular T helper cells (Tfh), that are localized within the LZ. Centrocytes that receive help from Tfh cells can cycle back to the DZ where they might undergo another round of SHM following selection in the LZ or develop into antibody secreting plasma cells or long-lived memory B cells that leave the GC. The randomness of SHM poses the risk to generate autoreactive GCB cells.

Specialized regulatory T cells, which enter the follicle (Tfr), regulate the germinal center reaction (GCR) [13].

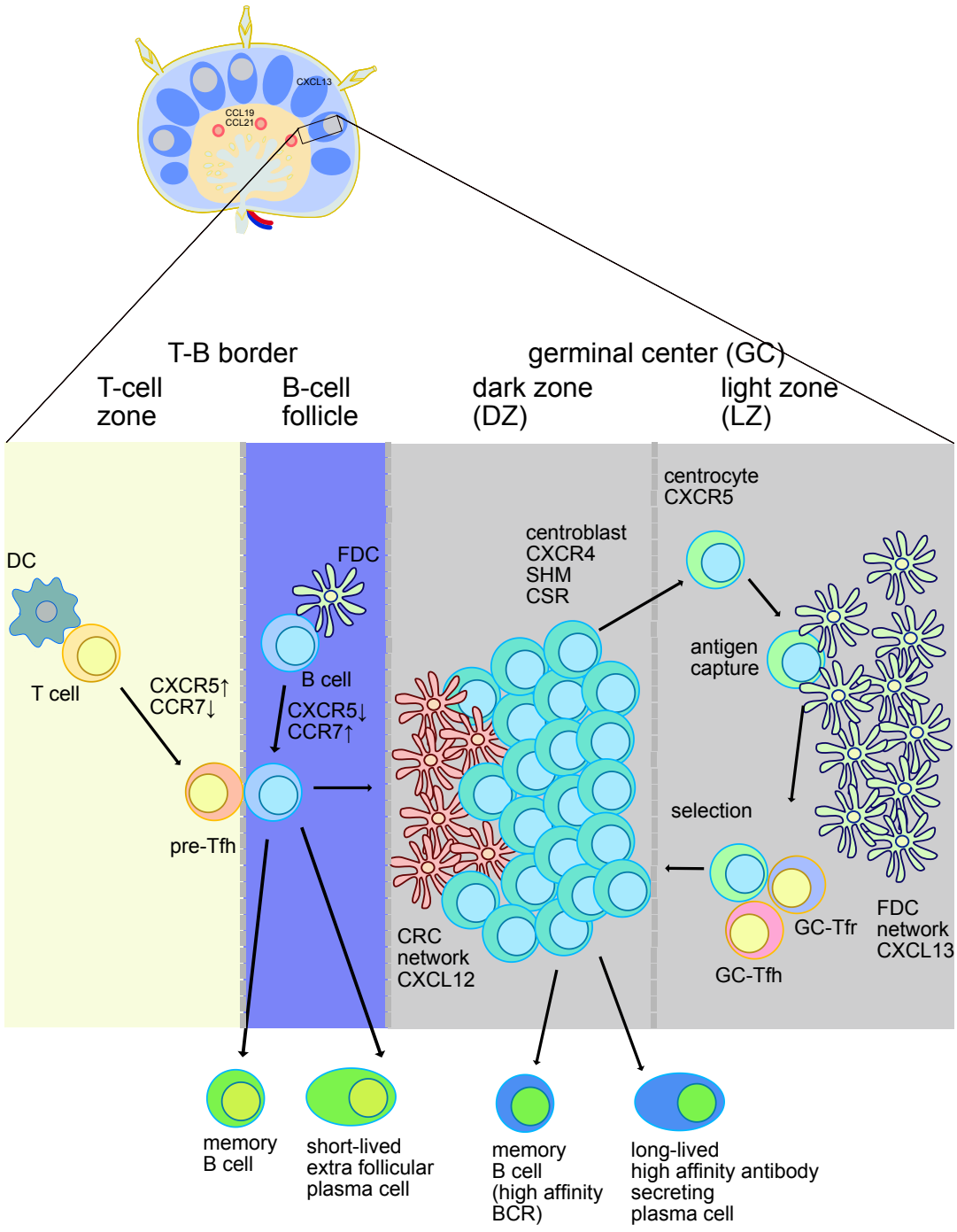

Figure 5.3: Scheme of a GCR in a LN

The GC arises in B cell follicles of secondary lymphoid organs upon infection or immunization. The GCR happens as a sequence of events: T cells and B cells become primed in their designated zones, which are

orchestrated via chemokine-chemokine receptor pairs. Yellow: T-cell zone: The priming of the T cell via the DC in followed by the upregulation of the chemokine receptor CXCR5 and downregulation of CCR7. The T cell migrates towards the T-B border, differentiating into a pre-Tfh cell. Blue: B cell follicle: In response to antigen encounter via the BCR, the B cell upregulates CCR7 and migrates towards the T-cell zone. T-B-border: The B cell presents processed antigen as an MHCII-peptide complex (not visualized) to the pre-Tfh cell. B cell and pre-Tfh cell exchange costimulatory signals. The B cell might develop into a GCB cell seeding a GC or become a memory B cell or short-lived extra follicular plasma cell. Grey: GC DZ: CRCs produce the chemokine CXCL12. The centroblasts expressing CCR4 are rapidly dividing and undergo SHM and CSR. Grey: GC LZ, FDCs produce the chemokine CXCL13 and display antigen on their surface. Centrocytes expressing CXCR5, take up antigen from the FDCs, process it and present it to the GC-Tfh cell. If the TCR of GC-Tfr cell recognizes the antigen presented as MHCII-peptide complex (not visualized) via the centrocyte, it provides help to the centrocyte to cycle back into the GC DZ where it either becomes a centroblast undergoing SHM and CSR or develop into a memory B cell or long-lived plasma cell, which leaves the GC. The selection process in the GC LZ is regulated via GC-Tfr cell [13, 15].

5.6 Development and function of Tfh cells

Tfh cells are a specialized subset of Th cells that provide help to GCB cells during the GCR. The development of Tfh cells starts during the priming of the naïve $CD4^+$ T cell with the DC. The DC presents the antigen that is recognized by the naïve $CD4^+$ T cell and provides costimulatory signals via the engagement of the surface molecules CD28, ICOS, CD40L and OX40 on the T cell. This process is supported via the additional secretion of the cytokines IL-6 and IL-12 via the DC, which bind to the designated cytokine receptors on the T cell (Fig. 5.4) [16]. Both kind of interactions induce signaling cascades within the T cell, which will be discussed in detail. The stimulatory receptor CD28 on the surface of the T cell interacts with its ligand CD80 or CD86 on the surface of the DC. This signal induces the phosphatidylinositol-3-kinase (PI3K)-mediated signaling, which is essential for the expression of Bcl6 in the pre-Tfh cell [17]. The interaction of the ICOS-ligand on the surface of the DC with the costimulatory molecule ICOS on the surface of T cells similarly induces PI3K signaling, subsequently leading to the phosphorylation of the protein kinase B (Akt). Akt becomes activated via this phosphorylation and in turn phosphorylates the transcription factor Foxo1. The phosphorylated Foxo1 is subsequently degraded in the cytoplasm. This removes a transcriptional blockade of the Tfh cell development, as Foxo1

positively regulates the transcription of the transcription factor Klf2. One function of Klf2 is the conservation of the chemokine receptor profile of a naïve T cell, namely the expression of CCR7, S1PR1 and PSGL1. The Tfh cell development requires the upregulation of CXCR5 in order to migrate closer to the T-B-border. Therefore, ICOS-signaling is needed for the Tfh cell development [17-19]. Furthermore, ICOS-signaling might induce the expression of IL-21, which supports Tfh cell function within the GC [20, 21]. The interaction of CD28 on the T cell with its ligands CD80 and CD86 on the DC was mentioned earlier. These two ligands of CD28 increase on the surface of DC due to CD40 signaling. Naïve $CD4^+$ T cells express the ligand of CD40 (CD40L). The interaction of CD40L on the naïve T cell with CD40 on the DC activates the DC and leads to the upregulation of CD80 and CD86 as well as the secretion of cytokines, such as IL-12 [9]. IL-12 and IL-6 both help during the priming with the DC to induce the Tfh differentiation [16]. The CD40-CD40L is a bidirectional signaling, and CD40L signaling might additionally help in the differentiation of the naïve T cell into the pre-Tfh [22, 23]. The transcription factor Bcl6 defines the fate of a Tfh, because it induces the Tfh-related gene expression and suppresses the differentiation of the other Th lineages [22, 24, 25]. The induction of the Bcl6 expression is supported via the secretion of IL-6 and IL-12 via the DC in a STAT1 and STAT3-dependent manner [16, 26]. At this early stage of Tfh differentiation the transcription factors Bcl6 and Ascl2 both mediate the expression of CXCR5, whilst downregulating the expression of the chemokine receptors CCR7 and PSGL1 [16, 27, 28]. The pre-Tfh then migrates to the T-B-border where it interacts with a B cell that has migrated to the T-B border due to the activation with an antigen. This step is necessary for the further development into a Tfh cell. The primed B cell presents the antigen-MHCII complex to the pre-Tfh cell, therewith providing signals for the further development into a Tfh cell. On the other side the primed B cells receive help from the pre-Tfh cell and either develop into a GCB cells or differentiate into plasma cells in these extrafollicular foci [29]. The pre-Tfh cell receives help from the primed B cell in the same manner as from the DC before. The conjugates of T and B cells are stabilized via SLAM family members. This stable interaction mediated via SLAM is essential for the further Tfh cell development [22, 30]. Tfh cells that received help from primed B cells at the T-B-border then migrate into the LZ of the GC where they interact with GCB cells. GCB cells express high levels of Fas and are bound by the antibody GL-7, as well as peanut agglutinin (PNA) [15]. Within the LZ of the GC, GCB cells compete for the help of Tfh cells. GCB cells with a high affinity receptor for the antigen presented by the FDC more likely receive

help from a Tfh cell. The higher affinity for the antigen facilitates the uptake of more antigen from the FDC, which will be processed and presented to the Tfh cell via MHCII [15]. This selection is important, as help of Tfh cells to low and high affinity B cells leads to the generation of antibodies with a lower affinity over time [31]. GCB cells are prone to die due to the induction of apoptosis via Fas signaling. Tfh cells provide survival signals to the GCB cells via CD40L, IL-4, IL-21, PD-1 and BAFF, therewith competing with the induction of cell death via the apoptosis inducing Fas-FasL interaction [22]. The CD40L signaling in a GCB induces AID, which mediates SHM and the class-switch recombination (CSR) in the GCB cells [32]. The antibody class switch is further guided via cytokines that are secreted via Tfh cells. IL-4 and IFN-γ for example support the class switching to IgG1 or IgG2a, whilst IL-4 and/or IL-13 support the switching to IgE [16, 33]. Via the secretion of IL-4 and IL-21, Tfh cells furthermore direct the fate decisions of GCB cells. IL-21 producing Tfh cells promote SHM, whilst IL-4 producing Tfh cells induce CSR and plasma-cell differentiation. IL-4 and IL-21 double producing Tfh cells support larger GC responses [21]. The interaction of PD-1 on the Tfh cell with PD-L1 and PD-L2 on the GCB has a bidirectional function [22]. PD-1 signaling in the Tfh cell counter-regulates the TCR signal, allowing the Tfh cell to provide help to the GCB cell without undergoing massive proliferation itself [34]. The interaction of PD-L1 and PD-L2 on GCB cells with PD-1 on Tfh cells is important for the formation of long-lived plasma cells. The lack of PD-1 signaling results in more Tfh cells, which produce less IL-4 and IL-21 [35]. Finally, GCB cells differentiate either into memory B cells or long-lived plasma cells. Memory B cells recirculate, reside in tissues, such as the lung or stay in the LN in a subcapsular niche, whilst long lived plasma cells migrate to the bone marrow [36]. Tfh cells on the other hand can give rise to memory Tfh cells, which also can be found in the circulation [37-39].

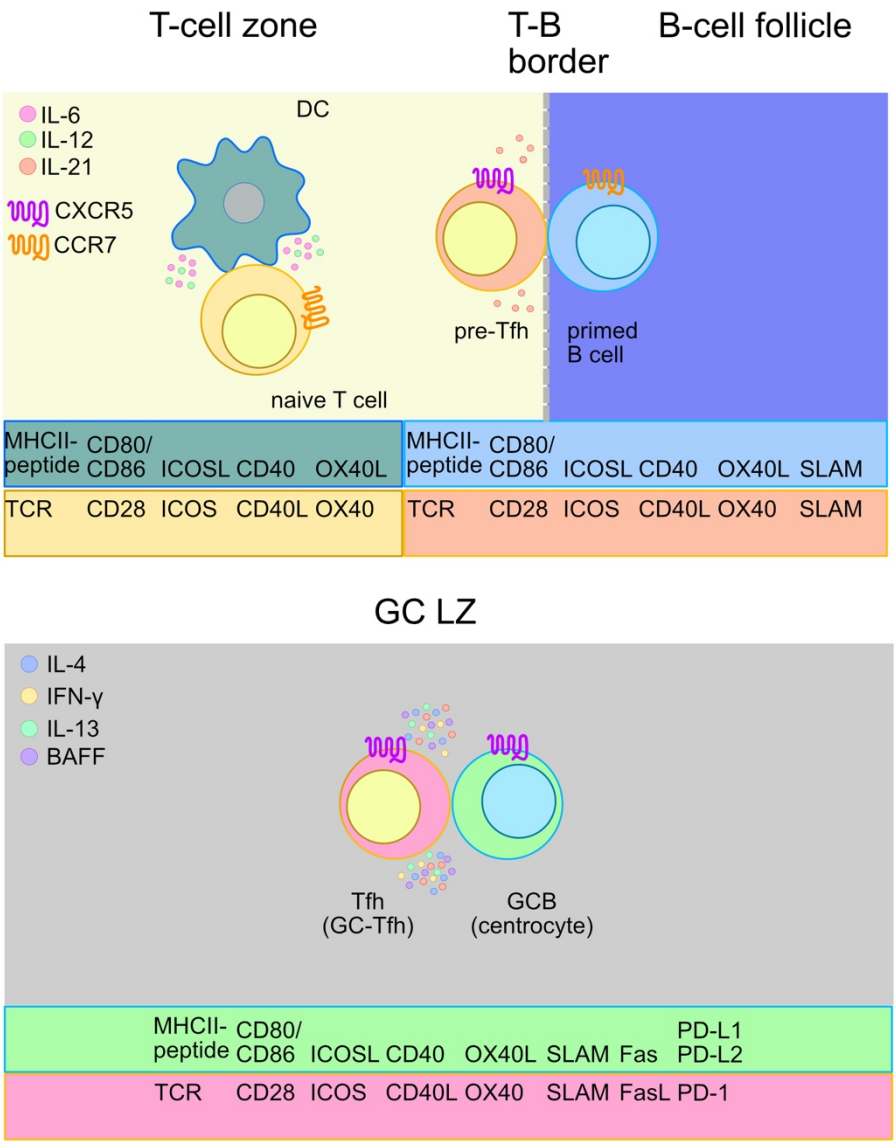

Figure 5.4: Tfh cell development and function within the GC

The development of Tfh cells is a multistep process, which requires the interaction with multiple APCs. In the T cell zone (yellow) naïve T cells become primed via the interaction with a DC. The DC engages the TCR via the ligation to the MHCII-peptide complex. On its surface, the DC displays a set of ligands (CD80/CD86, ICOSL, CD40, OX40), which bind to costimulatory molecules on the surface of the naïve T cell (CD28, ICOS, CD40L, OX40). The secretion of the cytokines IL-6 and IL-12 via the DC further supports the development of the naïve T cell into the pre-Tfh cell. The pre-Tfh cell upregulates CXCR5, downregulates CCR7 and migrates to the T-B-border (grey dashed line), where it secretes IL-21 and interacts with a primed B cell via the same surface molecules as before with the DC. This interaction is stabilized via interactions of the SLAM-family members, which are expressed on T and B cells [16]. The interaction with the primed B cell drives the further development of the pre-Tfh cell into the Tfh cell (GC-Tfh), which migrates into the GC LZ (grey), where it provides help to

GCB cells via the secretion of multiple cytokines, such as BAFF, IL-21 and IL-4. Similar to the interaction at the T-B-border, Tfh cells and GCB cells exchange stimulatory signals via surface molecules. The interaction of Fas on the surface of the GCB cell with FasL on the surface of the Tfh cell renders the GCB cell prone to apoptosis. The Tfh cell compensates the induction of apoptosis in the GCB via the secretion of BAFF, IL-4, IL-21 as well as CD40-CD40L and PD-1-PD-L1/L2 signaling [16, 22]. Tfh cells also might secrete other cytokines, such as IL-4, IL-13 and IFN-γ [16, 33]. The surface molecules are indicated in boxes sharing the same coloring with the cell type on which they are expressed.

5.7 Development of Tfr cells

Similar to the development of Tfh cells, Tfr cells presumably develop via a multistep process [40, 41]. Tfr cells mostly derive from nTregs originating from the thymus [42, 43]. Under circumstances that support the conversion of naïve $CD4^+$ Tcons to peripherally induced pTregs Tfr cells can derive from naïve $CD4^+$ Tcons [44]. If Tfr cells originate from naïve Tcons or nTregs therefore is still a matter of debate [45]. Two different groups propose similar models, in which nTregs undergo a multistep process to develop into Tfr cells [40, 41] (Fig. 5.5). In these models $Foxp3^+CD25^+$ naïve Tregs become primed via a DC within the T-cell zone. The development of Tfr cells needs CD28 as well as ICOS signaling, which is provided via the DC during priming [41, 45-48]. This early Tfr cell can either leave the LN to become a circulating Tfr cell (cTfr) with less suppressive capacity [38, 41, 49] or undergo further differentiation into a tissue resident Tfr. Further Tfr differentiation needs the interaction with the primed B cell at the T-B-border [40, 41]. In order to localize to the T-B-border, the early Tfr cell needs to upregulate CXCR5. PD-1 signaling has a negative influence on the CXCR5 expression already at this stage [41, 48]. The upregulation of CXCR5 in Tfr cells is mediated via the transcription factor NFATc1 [50]. NFATc1 is activated upon TCR signaling in a calcium-dependent manner. In line with this STIM1 and STIM2, which mediate the opening of Ca^{2+} channels in the plasma membrane upon TCR stimulation are important in Tfr cell differentiation [51, 52]. The early Tfr cell needs to interact with the primed B cell at the T-B-border in order to further develop into a mature Tfr. This interaction is most probably antigen-independent due to a bystander effect [41, 42, 53]. The bystander effect occurs, because a B cell with a specificity for a certain antigen will take up whole proteins from the FDC, process them and present multiple peptides deriving from one protein in form of MHCII-peptide complexes to many T cells each are having a different specificity. The interaction with the primed B cell leads

to upregulation of Bcl6, ICOS and PD-1 and forms an intermediate Tfr cell (iTfr) [41]. The productive interaction between the early Tfr and the B cell needs SAP [41, 46]. The induction of Bcl6 in Tfr cells is to a certain extend mediated via the mTOR complex 1 (mTORC1). mTORC1 contains a serin/threonin protein kinase that phosphorylates STAT3. STAT3-P induces the transcription of TCF-1, which itself induces Bcl6 expression. The induction of mTORC1 is discussed to be mediated via ICOS and IL-2 signaling [54]. Whilst the Tfr differentiates further, it downregulates CD25 successively [40, 41, 55, 56]. Therefore, ICOS might be then becoming more important to keep the Bcl6 expression. In line with this ICOS signaling saves Bcl6 from proteosomal degradation. Upon ICOS stimulation, a component of the PI3K complex named p85α interacts with osteopontin (OPN). OPN interferes with the proteosomal degradation of Bcl6, therewith stabilizing it [57]. From the T-B-border, the iTfr needs to migrate into the GC to become a mature Tfr (mTfr). This final differentiation stage is marked by further downregulation of CD25 [41]. This downregulation might be the result of pronounced Bcl6 expression caused by high levels of IL-21 within the GC [58]. One mechanism that also plays a role in Tfr differentiation is the gradual shift in the balance of the transcriptional regulators Id2 and Id3 versus (vs.) E2A. Upon TCR signaling, *Id2* and *Id3* levels decline, allowing the binding of E2A to its designated sites to induce the Tfr signature. It is proposed that the increase of Id2 and Id3 levels is required during the development of Tfr cells to allow the maturation of Tfr cells via the modulation of Bcl6 and Blimp-1 abundance [41, 59]. If this mechanism works repetitively at the different developmental stages is not known yet. One could imagine that the lowering of Id2 and Id3 levels is happening mostly at the T-B-border where the prolonged interaction of early Tfr and primed B cell via SAP also might allow the strongest TCR signal. In order to mature fully, the Tfr needs then to upregulate Id2 and Id3 again, which could then happen in the GC.

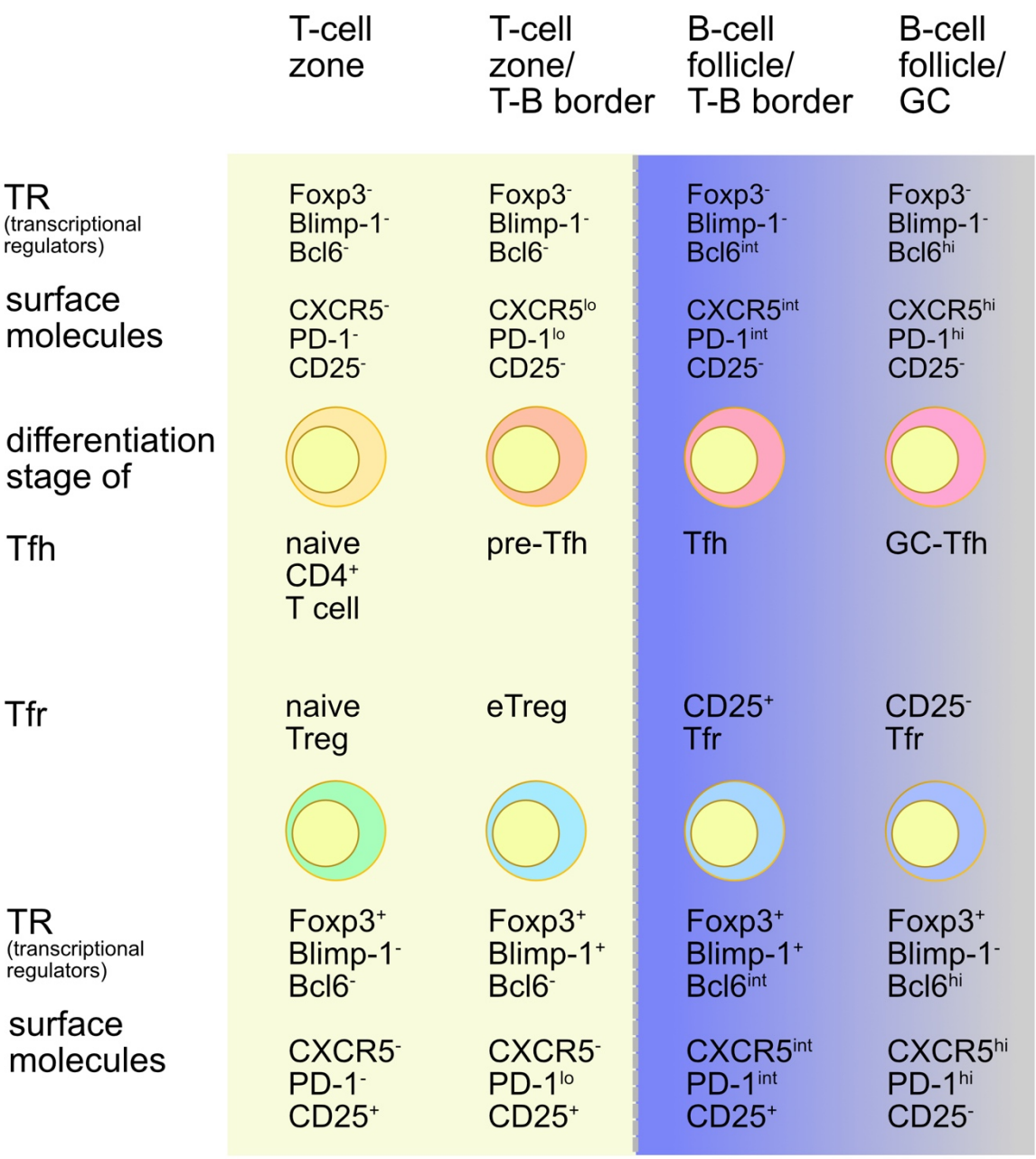

Figure 5.5: Model of developmental stages of Tfr and Tfh cells

Tfr cells develop similar to Tfh cells in sequence during their migration from the T cell zone into the GC. The consecutive stages of Tfh and Tfh cell development are marked via differences in the expression levels of the transcriptional regulators (TR) Foxp3, Blimp-1 and Bcl6, as well as the surface molecules CXCR5, PD-1 and CD25. Adapted from [40]

5.8 Regulation of the humoral immune response via Tfr cells

The regulation of the humoral immune response is mediated via Tfr cells in their different developmental stages in the T-cell zone, at the T-B-border and in the GC itself. Tfr cells might suppress Tfh cells as well as GCB cells via multiple mechanisms, which are shared with Tregs [40]. Tfr cells express high levels of the inhibitory molecule CTLA-4 [40, 60]. CTLA-4 binds with high affinity to the costimulatory molecules CD80/CD86 on the surface of APCs. It competes with the CD28-CD80/86 interaction and even removes CD80/CD86 from the surface of the APC. The complex of CD80/CD86 and CTLA-4 is then endocytosed and the costimulatory ligand becomes degraded [61]. The Treg suppressive function strongly depends on CTLA-4 as mice with CTLA-4 deficient Treg cells show a severe autoimmunity phenotype that is similar to the one observed in Foxp3-deficient scurfy mice [62]. The induced deletion of CTLA-4 in Tregs shortly before immunization increased Tfr cell numbers and affected their suppressive capacity vs. GCB cells and Tfh cells [60]. Most probably transendocytosis plays a role rather in the T-cell zone and at the T-B-border, as CD80/CD86 was shown to be higher expressed on all B cells, but not on GCB cells, when Tregs were deficient in CTLA-4 [60]. Within the GC itself CTLA-4 might rather work in a Tfr intrinsic way as it counteracts the ICOS-signaling [63, 64]. It is hypothesized that Tfr cells physically disrupt the interaction of Tfh cells with GCB cells and that this disruption is supported via a “stop signal” being generated upon strong TCR signaling as it was shown in Tcon [65-68]. PD-1 counteracts the TCR-mediated stop signal, therefore this mechanism might be minor in the wildtypic situation and more pronounced in PD-1-deficient Tfr cells [65-67]. Tfr cells inhibit Tfh and GCB cells via the suppression of metabolic pathways and effector molecules. In the case of B cells, this suppression persists also in the absence of Tfr cells but can be overcome via the addition of IL-21, which also has a suppressive effect on Tfr cells [68]. Tfh cells express the IL-1R1 agonist receptor. In response to IL-1, Tfh cells expanded *in vivo* and produced more IL-4 and IL-21 *in vitro*. In contrary, Tfr cells express the IL-1 decoy receptor IL-1R2 and the IL-1 receptor antagonist IL-1Ra therewith counteracting IL-1-mediated activation of Tfh cells [55]. TGF-β signaling in Tfh cells controls Tfh cell numbers via rendering them susceptible to apoptosis [69]. It is proposed that Tfr cells also control Tfh cell numbers via a TGF-β-dependent mechanism, probably via the surface molecule GARP, which tethers latent TGF-β and is expressed on the surface of human Tfr cells [40, 69, 70]. Tfr cells are furthermore proposed to kill B cells directly via the production of perforin and granzymes

[13, 40, 71]. Tfr cells not only suppress the GCR, but also provide help via the secretion of IL-10 [40, 72]. The secretion of IL-10 by Tfr cells activates Foxo1, which facilitates the adoption of a dark zone phenotype of GCB cells and potentially enhances affinity maturation [72]. On the other side, Tfr cells seem to suppress the production of IL-10 and IL-21 in Tfh cells [73]. Tfr cells control the GCR mostly via keeping Tfh and GCB cell numbers in check, but might also have orchestrating roles that go beyond simple means of suppression [40].

5.9 Nuclear factor of activated T cells - NFAT

The Nuclear Factor of Activated T-cells (NFAT) family of transcription factors comprises in total five different family members. Due to different nomenclatures more than one name exists for every family member: NFATc1 (NFAT2 or NFATc), NFATc2 (NFAT1 or NFATp), NFATc3 (NFAT4 or NFATx), NFATc4 (NFAT3) and NFAT5. The first four of the mentioned NFATs are calcium-dependent in their activation (NFATc), whilst NFAT5 activation is regulated independently of calcium signaling and activated upon osmotic stress [74]. The four calcium-dependent NFAT family members (in the following only mentioned as NFATs) share a similar structure comprised of four domains. Starting from the N-terminus NFATs are build-up of a N-terminal transactivation domain (TAD-N), a regulatory domain, also known as NFAT-homology region (NHR), a DNA-binding domain, also known as Rel-homology domain (RHD) and a second transactivation domain at the C-terminus (TAD-C). Due to the usage of different promoters, polyadenylation sites and variations in the splicing, each NFAT occurs in multiple isoforms. In the following, we will discuss well described representatives. In resting cells, the NHR is highly phosphorylated and the nuclear localization signal is hidden, whilst the nuclear export signal is exposed, keeping NFAT in an inactive state in the cytoplasm. The RHD mediates the binding of NFAT to its consensus sequence GGAAA. The TADs are the least conserved between the different NFAT family members and are putative sites for different interaction partners. Still, there are conserved motifs within these domains, the N-terminus motif (NTM), the central motif (CM) and the C-terminus motif (CTM), which is comprised of two sub-motifs. The NTM is a potent inducer of transcriptional activation as it can act as an acidic activation domain (AAD) that is rich in acidic and hydrophobic residues. On the other side it can also be bound by the casein kinase 1, which phosphorylates the NHR leading to the nuclear export of NFAT. The inducible short isoform of NFATc1

(NFATc1/αA) is the only well-known NFAT, which does not comprise the NTM. The CM is present in most of the common NFATs except in the α- and β-form of NFATc1/A. The TAD-C of NFATc1 and NFATc2 each contain two lysine residues, which can be sumoylated [75, 76]. The sumoylation of NFATc1/C e.g. mediates the subnuclear relocalization and the interaction of NFAT1/C with histone deacetylases (HDACs). This interaction induces transcriptionally inactive chromatin leading to the transcriptional inactivation of the NFATc1 target gene *Il2* [76-78]. The TAD-C appears to mediate transcriptional activation [77].

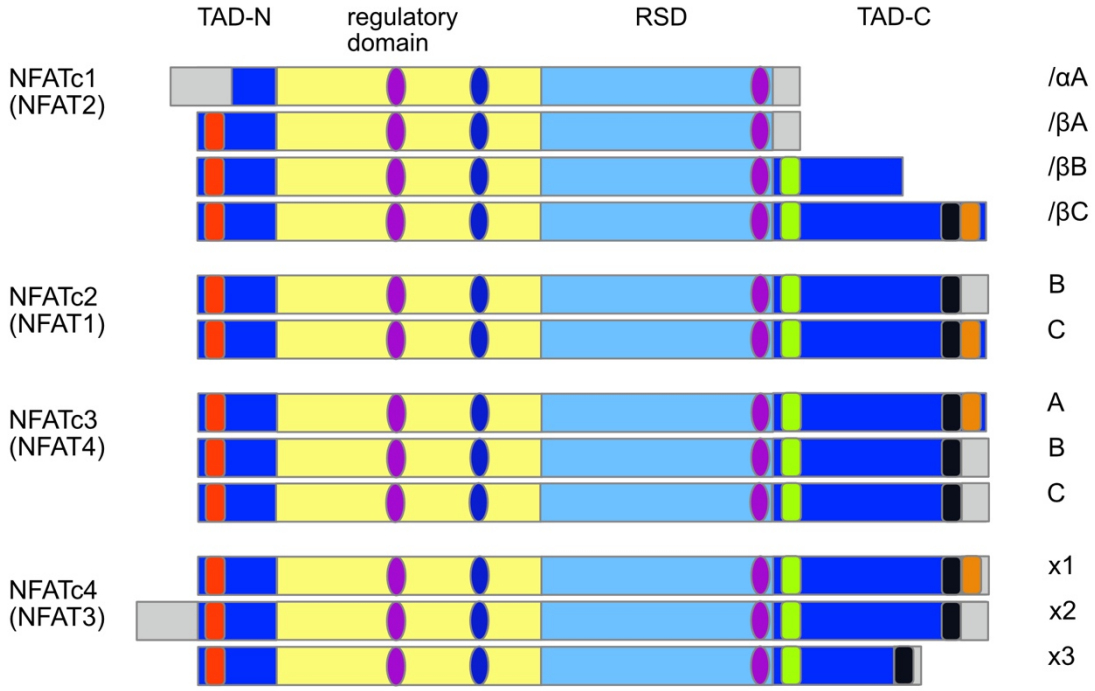

Figure 5.6: Scheme of the calcium dependent members of the NFAT family of transcription factors

Due to different nomenclatures more than one name per family member exists. The different names are indicated on the left-hand side. Well described isoforms of each family member are indicated on the right-hand side. The different domains are indicated via colored boxes as follows: TAD-N and TAD-C, both in dark blue; regulatory domain, yellow; RSD, light blue. The NTM is indicated as red box, the CM as green box and the CTM as black and orange box, symbolizing the two sub-motifs. The two NLS are indicated as purple ellipses and the NES as dark blue ellipse. This scheme was adapted from Mognol et al. [77].

5.10 The role of NFATs in T-cell activation and maintenance of tolerance

NFATs are expressed in multiple non-lymphoid tissues such as the heart, muscles, the brain, cartilage and fat. The knockout of NFATc1 in all cells is embryonic lethal due to a defect in cardiac valve development [74]. Within the immune system NFAT transcription factors play a special role. In resting cells, NFAT is maintained in the cytoplasm in a phosphorylated form via the action of constitutive kinases [79]. The stimulation of surface receptors, which are coupled to phospholipase C (PLC) leads to the production of inositol 1,4,5-triphosphate (IP_3), which opens IP_3 receptor channels in the endoplasmatic reticulum (ER) [78, 79]. The efflux of Ca^{2+} from the ER into the cytoplasm causes decreased Ca^{2+} levels in the ER, which activate the stromal interaction molecule 1 (STIM1) and STIM2. STIM1 and STIM2 subsequently bind to the Ca^{2+} release-activated Ca^{2+} (CRAC) channels, which are composed of ORAI1 and ORAI2 proteins in the plasma membrane and open them [78]. The subsequent Ca^{2+} influx into the cytoplasm activates calmodulin and the serine/threonine phosphatase calcineurin [78]. Phosphorylated NFAT in the cytoplasm becomes dephosphorylated at multiple serine/threonine residues within the transcriptional activation domain (TAD). This dephosphorylation causes a conformational change, which exposes nuclear localization signals (NLS), subsequently leading to the nuclear import of NFAT [74, 78]. The TCR of T cells is coupled to PLC-γ. Upon TCR signaling, NFAT localizes to the nucleus [80]. Depending on signals coming from costimulatory receptors, this translocation has different outcomes [80]. The co-stimulus induces the activation of other transcription factors, which form complexes with NFAT that can bind to their designated binding sites (consensus sites) within regulatory elements of genes such as promoters or enhancers. The binding of NFAT and its partner to the regulatory region of a gene either activates or blocks its transcription [77]. The combination of the TCR signal with a co-stimulus from CD28 or ICOS leads to the induction of the transcription from the inducible promoter P1 of NFATc1. Starting from the P1 promoter, the short isoform NFATc1/αA is transcribed and generates an autoregulatory feedback loop, resulting in a strong increase of NFATc1/αA transcripts [80]. NFATc1/αA differs in structure and function from other NFATs, as it is missing the CTM as well as the TAD-C. The high expression of NFATc1/αA is suggested to be important for the survival of the activated T cell and to act in an anti-apoptotic fashion [80]. This is supported by the report of NFATc1/αA mediated upregulation of c-Myc in pancreatic cancer [77, 81]. The activation of a T cell requires the TCR signal in combination with the CD28 co-stimulation [82]. The

signaling via these two surface receptors activates the activator protein 1 (AP-1) via a MAP-kinase (MAPK)-dependent pathway [80, 82]. AP-1 and NFAT cooperatively induce the expression of multiple cytokine genes, such as *Il2* (IL-2), *csf2* (GM-CSF), *Il3* (IL-3), *Il4* (IL-4) and *Ccl3* (MIP1α) as well as the surface molecule Fas-ligand [83]. Especially the production of IL-2 within effector T cells depends critically on NFAT-AP-1 signaling [80, 82]. The stimulation of the TCR without additional co-stimuli activates NFAT and other calcium dependent transcription factors, which cooperatively induce the transcription of genes being associated with anergy [82]. In the state of anergy, the TCR becomes uncoupled from its downstream signaling pathways, preventing the cell from proliferation and cytokine production in response to TCR signaling [84-88]. NFATc2 is especially important in anergy induction. NFATc2-deficient T cells are resistant to anergy induction and T cells expressing a constitutively active form of NFATc2 in the absence of AP-1 cooperation show increased expression of anergy associated genes [84]. In the absence of AP-1, NFATs can form either homodimers or complexes with Egr2 and Egr3, leading to the expression of anergy associated genes, such as caspase 3, diacylglycerol kinase α (DGKα) and the E3 ubiquitin ligases Cbl-b, Itch and GRAIL. Cbl-b, Itch and caspase 3 interfere with the TCR signaling via targeting of PLC-γ and PKCΘ for degradation, whilst DGKα and GRAIL hamper co-stimulatory pathways and CD40L signaling (reviewed in [89] and [78]). The short inducible isoform NFATc1/αA seems to play an opposing role and might even revert anergy [78, 90]. Anergy is rapidly induced in a naïve T cell at the time of first antigen stimulation. Another state of unresponsiveness to antigen stimulation is the exhaustion of T cells. In contrast to anergy, exhaustion develops over time in a progressive way usually in the setting of chronic inflammation, such as persistent virus infections [91]. Exhausted T cells express inhibitory receptors such as PD-1, CTLA-4, LAG-3, TIM-3, 2B4 and CD160 [91]. These inhibitory receptors counteract the stimulation coming from the TCR and co-stimulatory receptors [92]. A constitutive active variant of NFATc2 (CA-RIT-NFAT1), which cannot interact with AP-1, binds to regulatory regions of many exhaustion-associated genes, such as *Pdcd1* (PD-1) and *Havcr2* (TIM-3). In a two-step process, NFAT might first induce the transcription of *Egr2* and subsequently interact with Egr2 to induce LAG-3 expression [78, 93]. Besides the control of Tcons via the mechanisms of anergy and exhaustion, NFAT also plays a role in the induction of peripheral Tregs (iTregs). iTregs derive from Tcons and can be induced upon TCR- in combination with TGFβ signaling. The expression of the Foxp3 gene is regulated via

distinct conserved non-coding sequences (CNS). NFAT and Smad3 bind to the CNS1 of the *Foxp3* gene, therewith inducing the transcription of Foxp3 in a former Tcon, generating an iTreg [78, 94, 95]. This process is dependent on a threshold of NFAT rather than on a single family member. The capacity of Tcons to differentiate into iTregs reduces with the numbers of NFAT family members missing [95]. The induction of nTregs in the thymus is independent of NFATs. Mice carrying a deficiency in NFATc1, NFATc2 or NFATc3 in their T cells do not show reduced nTreg numbers. Finally, the suppression capacity of iTreg and nTregs is not affected by the deficiency of one or two of the mentioned NFAT family members [95, 96]. The transcriptional regulation mediated via the complex of AP-1 and NFAT is a main characteristic of effector Tcons [80]. In Tregs, NFAT forms transcriptional repressive complexes with other partners than AP-1, such as Foxp3 and inducible cAMP early repressor (ICER) (reviewed in [78]). Additionally, Foxp3 itself suppresses the expression of NFATc1/αA in Tregs, indicating that the NFAT-dependent transcriptional program of effector Tcons is prohibited in Tregs [78, 95, 97, 98].

5.11 NFAT in the induction and control of the humoral immune response

Follicular T cells (Tfoll), comprising Tfh and Tfr cells, express high levels of NFATc1 and especially NFATc1/αA. Mice carrying a NFATc1 deficiency in their T cells show expanded GCs and higher levels of antigen-specific antibodies. The reason for this dysregulation is the high dependency of Tregs on NFATc1. Whilst Tcons can differentiate into Tfh cells also in the absence of NFATc1, Tregs show a developmental defect due to their inability to upregulate CXCR5. This effect was Treg-intrinsic and could be rescued via the addition of CXCR5-competent nTregs [50]. Still, NFATc1 seems to be important in the induction of effector molecules that play a role in Tfh/Tfr development and function. NFATc1 deficiency in T cells reduces the expression of PD-1, ICOS, Ly108, CXCR5 and SLAM in activated T cells. This effect is even more pronounced in case of the double deficiency of NFATc1 and NFATc2. In the context of infection, NFATc1 and NFATc2 double-deficiency affects the GCB and overall Tfoll numbers, indicating that Tfh cells might also be affected by NFAT deficiency [99]. In line with this, the double-deficiency of STIM1 and STIM2 in T cells affects the expression of PD-1, ICOS and CD40L on the surface of Tfoll. Within the Tfoll population, IL-21-producing cells are drastically reduced, indicating a defect in Tfh function. On the RNA level the expression of even more genes associated with Tfr/Tfh function and development are shown to be affected. STIM-double

deficient Tfoll show reduced expression of *Icos*, *Cxcr5*, *Pdcd1*, *Cd40l*, *Btla*, *CD200* and *Ox40*, whereas *Il2ra* expression levels are increased. The double-deficiency extremely reduces the expression from the P1 promoter of *Nfatc1*, *Irf4*, *Batf* and *Bcl6* in Tfoll. The expression of IRF4 in Tfoll depends to a certain extend on NFATc1, as the retroviral expression of a constitutive active form of NFATc1 could almost restore the expression of IRF4 in STIM-double deficient T cells *in vitro.* Aged mice with a STIM double deficiency in T cells show signs of autoimmunity, indicating a Tfr-cell intrinsic defect [51]. The role of STIM in Tfr cells was further supported via the Treg-specific STIM double-knockout. Tregs isolated from this mouse show downregulation of many genes that are part of the Tfr-cell transcriptional signature, such as *Pdcd1* (PD-1), *Icos* (ICOS), *Irf4* (IRF4), *Batf* (BATF), *Prdm1* (Blimp-1) and *Ctla4* (CTLA-4) [52]. On the other hand, Tfh cells are also affected via the STIM double deficiency. This can be seen in the context of an LCMV infection, where these mice are unable to form a protective humoral immune response, leading to the death of these animals due to the inability to clear the infection [51]. In sum, NFATs regulate the expression of surface molecules and cytokines that are essential for the development of Tfh and Tfr cells. In Tregs, NFATc1 is essential for the upregulation of CXCR5, which is necessary for the differentiation into Tfr cells.

5.12 The transcriptional repressor Blimp-1

The human homologue of the transcriptional repressor Blimp-1 was first discovered in humans as a zinc finger protein, which binds to the positive regulatory domain I of the *IFNβ* promoter. The authors named it according to its function the positive regulatory domain I-binding factor I (PRDI-BF) [100]. Shortly after that Blimp-1 (B lymphocyte-induced maturation protein-1) was discovered in murine BCL1 lymphoma cells as a factor that contributes to the differentiation of Ig-secreting plasma cells [101]. The murine gene encoding Blimp-1 is given the name *prdm1* and contains eight exons. Due to the usage of different promoters and differential splicing, multiple isoforms of the Blimp-1 protein occur [102, 103]. The C-terminal region of the Blimp-1 protein contains five zinc fingers, which can bind DNA, therewith building the DNA-binding domain of Blimp-1. N-terminal from this DNA-binding domain, Blimp-1 harbors a proline-rich region. The proline-rich region and the DNA-binding domain mediates the binding to the transcriptional corepressor hGroucho and the histone deacetylases HDAC1 and HDAC2. HDACs mediate the deacetylation of lysine residues within histones. This deacetylation mediates a closer

binding of the DNA to the associated histones, leading to a structure, which represses the transcription of the gene. The N-terminal region of Blimp-1 contains a PR domain, which shows similarity to the SET domains of histone methyl transferases (HMT). The PR domain itself does not show HMT activity, but Blimp-1 recruits the H3 lysine methyltransferase G9a, which introduces a repressive histone modification (reviewed in [104]). The N- and the C-terminus of Blimp-1 contain acidic regions (Aci-N and Aci-C), both of which play a role in the suppressive function of Blimp-1 at the c-*myc* promoter [105]. Furthermore, Blimp-1 contains two proline glutamic acid, serine and threonine (PEST) sequences, one overlapping with the proline-rich region and one N-terminal of the zinc fingers [102]. PEST sequences are associated with a short half-life of proteins and render them prone to degradation [106]. The second zinc finger as well as portions of zinc fingers 1 and 3 are encoded in exon 7 [107, 108]. Due to differential splicing a variant without exon 7 occurs, giving rise to the protein Blimp-1Δexon7 [108, 109]. This variant is missing the zinc fingers 1-3, which are mediating the DNA binding [110]. Instead of binding to the DNA, Blimp-1Δexon7 builds homodimers and heterodimers with Blimp-1, therewith interfering with the endogenous Blimp-1 function [109].

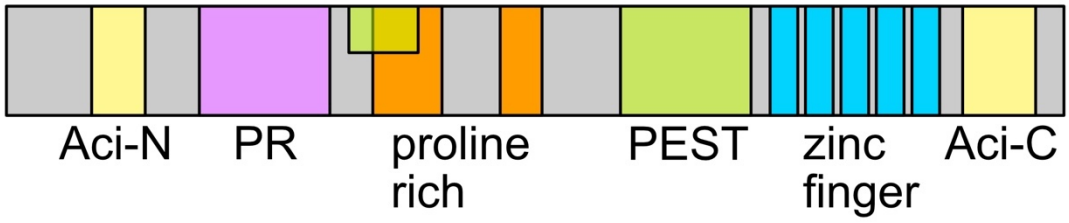

Figure 5.7: Scheme of Blimp-1 domains

The domain structure of Blimp-1 is indicated via colored boxes. The N- as well as the C-terminus of Blimp-1 harbor acidic regions named Aci-N and Aci-C, indicated as yellow boxes. Furthermore Blimp-1 is build-up of the PR domain (purple box), the proline-rich region (orange boxes), the PEST sequences (green boxes), one of which overlaps with one of the proline rich domains and the five zinc fingers (blue boxes). The scheme was adapted from [102].

5.13 The role of Blimp-1 in T cells

Blimp-1 is expressed in mice in multiple tissues such as the skin, forelimbs and the heart (reviewed in [102]). During the embryonic development in mice, Blimp-1 deficiency is

embryonic lethal at day 10.5 of gestation due to its role in primordial germ cells [111]. Blimp-1 is expressed in multiple cell types of the immune system, such as DC, macrophages, B and T cells [102, 112]. In B cells, Blimp-1 is upregulated during the differentiation into plasma cells and is sufficient for this process [113, 114]. In T cells, Blimp-1 is already expressed on a basal level in thymocytes, where it seems to be important for the survival of DP thymocytes [104, 115, 116]. In naïve T cells, *prdm1* is also transcribed at a basal level, but becomes strongly induced upon stimulation with anti-CD3, anti-CD28 and IL-2 [104, 115, 117]. However, the expression of Blimp-1 in thymocytes and naïve cells is not observed on the protein level as demonstrated with a *Prdm1*-GFP knock-in reporter mouse [117]. Within this reporter mouse, effector and memory $CD4^+$ and $CD8^+$ T cells, as well as $Foxp3^+$ Tregs express Blimp-1 [117]. The deletion of exon 6-8 ($prdm^{flox}$) [115] or the replacement of exon 7-8 with a green fluorescent protein [113] creates two types of Blimp-1 mutants, which are unable to bind to the DNA and therefore are considered as knockout proteins. Mice with a Blimp-1 deficiency in the myeloid lineage ($prdm^{gfp}$) [117] as well as mice with a Blimp-1 deficiency only in T cells ($prdm^{flox}$) [115] develop spontaneous auto-inflammatory diseases. This is due to the accumulation of effector T cells in multiple organs such as the colon, lungs and liver, the latter two being affected only via the Blimp-1 deficiency in the myeloid lineage. The reason for this loss of homeostasis in Blimp-1-deficient T cells is discussed in a model [104]. Blimp-1 deficiency only causes differences in the proliferation of cells under conditions of weak co-stimulation with CD28 and IL2 [104, 115, 117]. Therefore, Blimp-1 might be important in peripheral T cells to support the tolerance to self-antigens as presentation of these are usually linked with low or no co-stimulation [104]. The ectopic expression of Blimp-1 or also the induction of Blimp-1 expression via IL-4 decreases the proliferation of T cells and downregulates IL-2 expression [118-120]. Blimp-1 downregulates the expression of *bcl2a1*, a mechanism which could limit the numbers of Blimp-1-expressing effector cells [104]. The induction of Blimp-1 via the TCR and IL-2 signaling might therefore be important in limiting the population of effector T cells [104]. The repression of IL-2 signaling via Blimp-1 in effector T cells might be an important mechanism to end an immune response and to keep the state of homeostasis as Blimp-1 expression itself is induced via IL-2 signaling [104, 119].

5.14 Regulation of the transcriptional repressor Blimp-1

The regulation of Blimp-1 happens in multiple ways. The transcription of *prdm1* is induced via the TCR, CD28 and IL-2 signal [104, 115, 117]. The transcription factors NFAT, AP-1 and NF-κB are induced via the TCR and CD28 signaling. These transcription factors activate *prdm1* transcription in B cells and it is speculated that this is the same in T cells [104, 121, 122]. However, it is also reported that a constitutive active mutant of NFATc1/αA suppresses the expression of *prdm1* in murine splenic B cells *in vitro* [123]. The IL-2 signal induces the activation of *prdm1* transcription via STAT5 in T cells [104, 124]. Another interleukin which activates *prdm1* transcription is IL-21 via STAT3 in cooperation with IRF4 [125]. Furthermore, Blimp-1 can be induced under proinflammatory conditions in Th17 cells via IL-12-STAT4 and IL-27 (probably via STAT3) signaling [126]. The transcriptional repression of Blimp-1 happens in multiple ways. In naïve cells, Blimp-1 is dominantly repressed via the transcription factor Bach2 [127]. The function of this repression is discussed to maintain the state of naïve T cells and to suppress the expression of effector and memory-related genes [127]. In activated T cells, Blimp-1 downregulates itself via the suppression of IL-2 production via the transcriptional repression of *Il2* (IL-2) and and *fos* (AP-1) [107]. Blimp-1 and Bcl6 are reciprocally antagonistic repressors, which control antagonistic cell fate decisions. In a naïve $CD4^+$ T cell, Bcl6 induction leads to the differentiation of Tfh cells, suppressing the development of any other Th lineage [22, 24, 25]. Reciprocally, Blimp-1 suppresses Bcl6 expression in all the other Th fates. In differentiated Th lineages, Blimp-1 and Bcl6 finally make the decision between effector and memory cells. Whilst the expression of Blimp-1 enforces the development of effector cells, Bcl6 supports the development of memory cells (reviewed in [128]). The Blimp-1-Bcl6 axis in Tfh cells is regulated at a higher level. First of all, the presence of IL-2 induces STAT5 mediated transcription of Blimp-1, which in turn suppresses Bcl6 and therewith the Tfh fate [124, 129]. Second, the transcription factor Klf2 induces Blimp-1 expression therewith repressing Bcl6 expression [18]. Finally, the transcription factor TCF-1 promotes Bcl6 expression and inhibits Blimp-1 as well as CD25 expression. Similar to Blimp-1 and Bcl6 itself, Blimp-1 and TCF-1 are forming a negative circuit [130-133]. Besides the regulation of Blimp-1 at the transcriptional level also post-transcriptional and post-translational mechanisms exist. The post-transcriptional regulation of *prdm1* is mediated via the micro-RNA miR-9, which downregulates *PRDM1* expression

as shown in human $CD4^+$ T cells [134]. On the posttranslational level, the Blimp-1Δexon7 isoform can inhibit the function of Blimp-1 also [109].

5.15 Blimp-1 in Tregs and Tfr cells

One way how Tregs mediate their function especially at mucosal sites is the secretion of IL-10 [135]. Blimp-1 and IRF-4 jointly control the production of IL-10 in these Tregs, which might contribute to the inflammatory phenotype observed due to the Blimp-1 deficiency in T cells [115, 135]. *Bcl6* and *Prdm1* are mutually exclusive in their transcription [128]. However, Tfr cells are remarkably described as Bcl6 and Blimp-1 expressing cells [46, 136]. While Bcl6 is required for the formation of Tfr cells [46, 136], Blimp-1 restricts the numbers of Tfr cells [46]. Tfr cells successively downregulate the expression of CD25 during their development. Mature $CXCR5^{hi}PD\text{-}1^{hi}$ Tfr cells do not express CD25 on their surface anymore [55]. Blimp-1 might follow this downregulation as it is downstream of IL-2 signaling [56]. In contradiction to this, Tfr cells expressing Blimp-1 in the GC were described at the very beginning [46]. Post immunization with NP-Ova also the presence of $CD25^+Foxp3^+$ cells was reported in the GC, although only in a few GCs and at a percentage of max. 50% [137]. The IL-21 secreted by Tfh cells in the GC increases the expression of Bcl6 in Tfr cells via IL-21R signaling [58]. Bcl6 in turn downregulates CD25, therewith reducing IL-2-STAT5 signaling and probably also Blimp-1 expression [58]. $Bcl6^+$ Tfr cells express high amounts of CD122, which allows basal IL-2 STAT5 signaling to sustain Foxp3 expression even in the absence of CD25 [56]. High production of IL-2 as it occurs systemically during an influenza infection or the infection with an adeno-associated virus coding for IL-2 decreases Tfr-cell frequencies [41, 55, 56]. Upon decline of IL-2 levels towards the end of an influenza infection, Treg cells develop into Tfr cells to prevent the emergence of self-reactive B-cell clones [56].

5.16 Aim of this study

The aim of this work was to understand the role of the transcriptional activator NFATc1 and the transcriptional repressor Blimp-1 in T cell subsets of the GC. The functional role of these two transcriptional regulators in the function of Tfr and Tfh cells was evaluated in various mice models carrying loss or gain of function mutants of either transcriptional regulator within T cell subsets. The effects on the GCR and the humoral immune response

in these mice were monitored on a single cell level, in the context of the tissue, the serum and on the molecular level. This work can be subdivided into three parts:

Our group showed previously the dependency of Tfr cells on NFATc1 in order to migrate into the GC [50]. Mechanistically this migratory defect developed due to the essential role of NFATc1 in the expression of the chemokine receptor CXCR5 in Tfr cells [50]. Tfh cells were independent of NFATc1 in the expression of CXCR5 and did not show a defect in the homing to the GC [50]. This raised the question about a Tfr-cell intrinsic repression of CXCR5, which needed to be counter-regulated via NFATc1. Here we tested the hypothesis of a Blimp-1-mediated repression of *Cxcr5* and the counter regulation via NFATc1 on the molecular level and *in vivo*. Beyond *Cxcr5,* we were searching for genes regulated via NFATc1 and Blimp-1 in Tfr cells.

Follicular T cells vigorously express NFATc1 and especially NFATc1/αA [50]. If Tfr cells as a subset of Tfoll cells also express NFATc1/αA was not known, but it was known that the expression of NFATc1/αA in Tregs is suppressed via Foxp3 [78, 95, 97, 98]. We asked the question if the overexpression of a constitutive active mutant of NFATc1/αA (caNFATc1/αA) in Tregs changes their expression of CXCR5 *in vivo*. Additionally, we were interested in putative changes of the GCR due to the overexpression of caNFATc1/αA in Tfr cells.

NFATc1/αA has opposing roles compared to the other isoforms of NFATc1 [90]. It is important for the survival of activated T cells and acts in an anti-apoptotic and anti-anergic way [78, 80, 90]. We aimed to study the role of endogenous NFATc1 and ectopically overexpressed caNFATc1/αA in follicular T cells. Therefore, we combined a loss of function mutation of NFATc1 with the overexpression of caNFATc1/αA in all T cells. The changes in the GCR were monitored in order to deduce the function of these NFATc1 isoforms in Tfh and Tfr cells.

6 Material and Methods

6.1 Material

6.1.1 Chemicals and reagents

Chemical	Company
3,3′-5,5′-Tetramethylbenzidine (TMB)	Sigma-Aldrich
Acrylamid 30%	ROTH
Antibody Diluent with Background Reducing Components	Dako
APS	ROTH
Boric acid	ROTH
$CaCl_2$	Applichem
Calf thymus dsDNA	Sigma-Aldrich
Dextrose	ROTH
EDTA	ROTH
Formaldehyd 37%	ROTH
Formalin 4%	Pathologie Würzburg
HEPES	Applichem
Hoechst	Sigma-Aldrich
ImJect^{TM} Alum	ThermoScientific
KCl	ROTH
Mowiol supplemented with DABCO	ROTH
Na_2HPO_4	ROTH
NaCl	ROTH
Normal rat serum (NRS)	STEMCELL
NP-(14)-BSA	Biosearch
NP-(2)-BSA	Biosearch
NP-KLH (24-32)	Biosearch
Poly-L-lysin	Sigma-Aldrich

Polyethyleneimine (PEI)	Sigma-Aldrich
RLT buffer	QIAGEN
TEMED	ROTH
Tris	ROTH
Trypan blue	Sigma-Aldrich

6.1.2 Buffers

Anti-ds DNA ELISA	Blocking buffer	10 % FCS in PBS
	Wash buffer	0,01 % Tween in PBS
Anti-NP ELISA	Blocking buffer	1 % BSA in PBS
	Dilution buffer	0,1 % BSA in PBS
	Wash buffer	0,01 % Tween in PBS
FACS buffer	NaCl (pH 7,4)	137 mM
	Na_2HPO_4	10 mM
	KCl	2,6 mM
	KH_2PO_4	1,8 mM
	BSA	0,1 % (w/v)
	NaN_3	0,1 % (w/v)
MACS buffer	NaCl (pH 7,4)	137 mM
	Na_2HPO_4	10 mM
	KCl	2,6 mM
	KH_2PO_4	1,8 mM
	BSA	0,5 % (w/v)
	NaN_3	0,1 % (w/v)
	EDTA	2 mM

Phosphate buffered saline (PBS)	NaCl (pH 7,4)	137 mM
	Na_2HPO_4	10 mM
	KCl	2,6 mM
	KH_2PO_4	1,8 mM
Red blood cell lysis (RBC) buffer	NH_4Cl	150 mM
	$KHCO_3$	10 mM
	EDTA	1 mM
Tris Borat EDTA buffer (TBE) 5x	Tris	0,45 M
	EDTA	0,01 M
	Boric acid	0,45 M
	Distilled water up to	1 l
	Adjust to pH 8,3	

6.1.3 Media and cell culture supplements

2-mercaptoethanol
BSS/BSA
DMEM
FBS
HEPES
L-glutamine
Penicillin/Streptomycin
RPMI
Sodium pyruvate

All media and cell culture supplements were supplied by GIBCO, except BSS/BSA which we kindly received from the VIM, Wuerzburg

6.1.4 Cells

HEK 293T cells (DSMZ Nr. ACC305), human embryonic kidney cell line

6.1.5 Mice

The mice mentioned in the following were bred and kept in the "Zentrum für Experimentelle Molekulare Medizin" (ZEMM) in Wuerzburg. The mice were kept according to the German animal welfare laws for experimental animals either in the breeding facility of the ZEMM under SPF conditions or in an IVC-system at 22°C and at the humidity prescribed. The mice received water ad libitum and standard rodent chow. At the age of 4 weeks the mice were genotyped. Animals of at least 6 weeks of age were used for the experiments. The animals in one experiment were siblings if possible, but at least age and gender matched gathered from parallel breedings. The immunization experiments were performed according to the approved animal proposal AZ 55.2-2531.01-80/10 and AZ 55.2-2532-2-169. Offsprings of the following lines were used in the experiments:

Designated line	**Line according to reference**	**Reference**
Nc1$^{fl/fl}$	*Nfat2*$^{fl/fl}$	Vaeth, Schliesser et al. 2012, Martinez, Pereira et al. 2015 [93, 95]
Nc1^{caaA}	*c.n.Nfatc1*	Baumgart, Chen et al. 2014 [138]
Pr1$^{fl/fl}$	*Prdm1*$^{flox/flox}$	Martins, Cimmino et al. 2006 [115]
FIC	*Foxp3*-IRES-Cre	Wing, Onishi et al. 2008 [62]
dLckcre	dLck-icre	Zhang, Wang et al. 2005 [139]
Pr1$^{+/gfp}$	Blimp$^{gfp/+}$	Kallies, Hasbold et al. 2004 [113]
DEREG	DEREG	Lahl, Loddenkemper et al. 2007 [140]

6.1.6 Antibodies and Conjugates

6.1.6.1 Antibodies for super shifts in EMSA

Antibody-conjugate	Clone	Supplier	Concentration µg/ml
Anti-ER	MC-20	Santa Cruz Biotechnology	200 µg/0,1ml
Anti-Blimp-1-PE	5E7	Biolegend	200 µg/ml
Anti-NFATc1	7A6	Santa Cruz Biotechnology	200 µg/0,1ml

6.1.6.2 Antibody-conjugates for flow cytometry

Antibody-conjugate	Clone	Supplier	Dilution
Anti-B220-Percp	RA3-6B2	Biolegend	1:300
Anti-Bcl-2-PE/Cy7	BCL/10C4	Biolegend	1:200
Anti-CD16/anti-CD32	Clone 93	ThermoFisher	1:200
Anti-CD4-BV510	RM4-5	Biolegend	1:200
Anti-CD4-PacificBlue	GK1.5	Biolegend	1:300
Anti-CD44-FITC	IM7	eBioscience	1:200
Anti-CTLA-4-PE	UC10-4B9	Biolegend	1:50
Anti-CXCR5-BV421	L138D7	Biolegend	1:50
Anti-Fas-PE	Jo2	BD Pharmigen™	1:300
Anti-Foxp3-FITC	FJK-16s	eBioscience	1:200
Anti-Foxp3-PE	FJK-16s	Invitrogen	1:200
Anti-GITR-PE	DTA1	Biolegend	1:100
Anti-GL-7-FITC	GL-7	BD Pharmigen™	1:300
Anti-Ki-67-PE/Cy7	16A8	Biolegend	1:200

Anti-PD-1-APC	J43	eBioscience	1:160

6.1.6.3 Antibody-conjugates for ELISA

Antibody-conjugate	Cat. no.	Supplier	Dilution
Goat anti-mouse IgG3-HRP	1101-05	SouthernBiotech	1:10.000
Goat anti-mouse IgG1-HRP	1071-05	SouthernBiotech	1:10.000
Goat anti-mouse IgG2a-HRP	1081-05	SouthernBiotech	1:10.000
Goat anti-mouse IgG2b-HRP	1091-05	SouthernBiotech	1:10.000
Goat anti-mouse IgG2c-HRP	1078-05	SouthernBiotech	1:10.000
Goat anti-mouse IgM-HRP	1021-05	SouthernBiotech	1:10.000
Donkey anti-Mouse IgG-HRP	715-035-150	Jackson ImmunoResearch	1:10.000

6.1.6.4 Primary antibodies for the colocalization experiment

Antibody	Clone	Supplier	Species	Dilution
Anti-NFATc1	7A6	BD Pharmigen™	Mouse	1:50
Anti-Blimp-1	6D3	Santa Cruz	Rat	1:50
GFP-Booster Atto488	-	Chromotek	Alpaca	1:100

6.1.6.5 Secondary antibodies for the colocalization experiment

Antibody	Species	Supplier	Dilution
Anti-mouse AlexaFluor Plus 555	Goat	Invitrogen	1:400
Anti-rat AlexaFluor 594	Goat	Dianova	1:100

6.1.6.6 Primary antibodies/conjugates for immunofluorescence histology stainings

Antibody	Clone	Supplier	Species	Dilution
Anti-CD3	A0452	Dako	Rabbit	1:100
Anti-Foxp3	FJK-16s	ThermoFisher	Rat	1:100
PNA-biotin	B-1075	VECTOR	-	1:100

6.1.6.7 Antibody-conjugates for immunofluorescence histology stainings and corresponding EVOS LED Light Cubes

Antibody-conjugate	Clone	Supplier	Dilution	EVOS LED Light Cube
Anti-B220 AlexaFluor™ 594	RA3-6B2	Biolegend	1:400	Texas Red
Donkey anti-rat AlexaFluor™ 488	Polyclonal	ThermoFisher	1:400	GFP
Donkey anti-rabbit AlexaFluor™555	Polyclonal	ThermoFisher	1:400	RFP
Streptavidin AlexaFluor™ 647	-	ThermoFisher	1:400	Cy5

6.1.7 Plasmids

Plasmid	Reference
HA-Nfatc1-RSD	Klein-Hessling, Bopp et al. 2008, [141]
Prdm1-Flag	Schmidt, Nayak et al. 2008, [109]
Nfatc1/C-ER	Nayak, Glockner-Pagel et al. 2009, [76]
Prdm1-HA	Schmidt, Nayak et al. 2008, [109]

6.1.8 Ligands and chemicals for the stimulation of cells

Reagent	Company
Anti-CD28	BD Pharmigen™
Anti-CD3	BD Pharmigen™
Recombinant human IL-2	Peprotech
Ionomycin	CalBiochem
Tamoxifen	Sigma-Aldrich
TPA	Merck

6.1.9 DNA probes and competitors for EMSA

Oligonucleotides were synthesized by Eurofins. DNA-probes were biotinylated as indicated with a "B". Oligos used as competitors were left unbiotinylated.

6.1.9.1 DNA probes

Name of DNA probe	Sequence
Nfatc1-p1-tan_sB	5' GGAAGCGCTTTTCCAAATTTCCACAGCG
Nfatc1-p1-tan_aB	5' CGCTGTGGAAATTTGGAAAAGCGCTTCC
Myc-PRE_sB	5' CGCGTACAGAAAGGGAAAGGACTAG
Myc-PRE-aB	5' CTAGTCCTTTCCCTTTCTGTACGCG
Cxcr5-HS2-B_sB	5' GGGCAGCTGTGAGTGAAAGGTATG
Cxcr5-HS2-B_a	5' CATACCTTTCACTCACAGCTGCCC
Cxcr5-HS2-N1_sB	5' GGAGCTGAGGAAACGCAGGTGC
Cxcr5-HS2-N1_a	5' GCACCTGCGTTTCCTCAGCTCC
Cxcr5-HS2-N2_sB	5' GCCCCCTTCTTTTCCACTCAGAAAA
Cxcr5-HS2-N2_a	5' TTTTCTGAGTGGAAAAGAAGGGGGC
Cxcr5-HS2-N3_sB	5' TAGGAGGCCATTTCCTCAGTTTCAG
Cxcr5-HS2-N3_a	5' CTGAAACTGAGGAAATGGCCTCCTA

6.1.9.2 Competitors

Name of competitor	Sequence
Myc-PRE_s	5’ CGCGTACAGAAAGGGAAAGGACTAG
Myc-PRE_a	5’ CTAGTCCTTTCCCTTTCTGTACGCG
Il2Pubd_s	5’ CAAAGAGGAAAATTTGTTTCATACAG
Il2Pubd_a	5’ CTGTATGAAACAAATTTTCCTCTTTG

6.1.10 Kits

Item	Company
CD4 (L3T4) MicroBeads	Miltenyi Biotech
eBioscienceTM Foxp3/Transcription Factor Staining Buffer Set	ThermoFisher
GelshiftTM Chemiluminescent EMSA Kit	Active Motif
Mojo $CD4^+$ negative selection Kit	Biolegend
Mouse-IgG-Kit	Roche
Nuclear Extract Kit	Active Motif
OptEIATM Set for mouse IL-2	BD Pharmigen™
NE-PERTM Nuclear and Cytoplasmic Extraction reagents	ThermoFisher

6.1.11 Consumables

Item	Company
12-well slide	ibidi
5 ml round-bottom tubes	Falcon
70 µm Nylon filter	Falcon
Blood clotting tubes Micro tube 1.1ml Z-Gel	Sarstedt
Blood lancets (solofix from Braun)	Hartenstein Laborversand

Blotting paper	Laborhaus Scheller
Cannulas (27G)	BD Pharmigen™
Centrifuge tubes 15 ml and 50 ml	GBO
Cuvettes for photometer	ratiolab
Coverslips (18x18mm)	MENZEL Gläser
ELISA plates (Maxisorp Nunc)	ThermoFisher
ELISA plates half-area (costar flat bottom high binding non sterile polystyrene)	Hartenstein Laborversand
LS-colums	Miltenyi Biotech
Microscopy slides (SuperFrost plus)	Langenbrinck
Petri dishes (10cm diameter)	GBO
Reaction tube 1,5 and 2 ml	Eppendorf
Roti®-Nylon plus membrane	ROTH
Serological pipettes (5, 10, 25ml)	GBO
Sterile filter (0,2 and 0,45µm) Rotilabo	ROTH
Syringes (1ml, 5ml, 10ml)	BD Pharmigen™, Braun
Well-plates (6, 12, 24, 96-well)	GBO
X-ray films (Fuji Super RX/HR-E)	Hartenstein Laborversand

6.1.12 Machines

Machine	**Company**
Autoclave systec DX-45	Systec
Autoclave systec V-75	Systec
Balance KERN PFB	Kern und Sohn
BD FACSAriaII™, VIM Wuerzburg	BD
BD FACSCANTO™ II	BD
Centrifuge Eppendorf 5415C	Eppendorf
Centrifuge Eppendorf 5424	Eppendorf
Centrifuge Rotina 420R	Hettich Laborapparate

Confocal microscope Zeiss LSM 780	Zeiss
Fluorescence microscope Evos FL Auto 2	ThermoFisher
Freezer -20 °C	Liebherr, Privileg
Freezer -70 °C	Siemens
Fridges 4 °C	Liebherr, Privileg
Gel electrophoresis system Mini-PROTEAN System	Biorad
Heating block Liebisch 2099-DA	Liebisch
Ice machine Scotsmen AF100	Genheimer
Incubator	Heraeus
Light microscope LEICA DMIL	Leica
Magnetic stirrer	Heidolph
Microliter pipettes	Brand
Microplate reader Fluostar Omega	BMG Labtech
Microtome LEICA SM 2000R	Leica
Orbital shaker KS10 DIGI	Edmund Bühler
Paraffin-embedding center Leica Histocore Arcadia H	Leica
Ph meter	WTW
Photometer gene quant	Amersham Biosciences
Photometer nanodrop	PeqLab
Power pack 2009	Biorad
Scanner Kyocera TAS Kalfa 420i	A. Hofmann Nache GmbH
Sterile work bench	Heraeus
UV StratalinkerTM 1800	Strategene
Vortexer Reamix 2789	Hartenstein Laborversand

6.1.13 Data analysis software

AFFINITYPublisher 1.7.2

AFFINITYDesigner 1.7.3

BD FACSDiva 5.0

Endnote X9.3.2

FlowJo™ 10 software (BD)

GraphPad Prism 5

ImageJ

Microsoft ® Word for Mac

Microsoft ® Excel for Mac

Microsoft ® PowerPoint for Mac

6.2 Methods

6.2.1 Cellular and molecular methods

6.2.1.1 Cell culture Media

Cells were cultured at 37 °C and 5% CO_2 in an incubator. HEK 293T cells were cultured in DMEM and primary murine cells in RPMI as indicated.

DMEM supplemented with	10 % Fetal bovine serum (FBS) (v/v)
	2 mM L-glutamine
	1 mM Sodium pyruvate
	100 U/ml Penicillin/streptomycin

RPMI supplemented with	5 % FBS (v/v)
	2 mM L-glutamine
	1 mM Sodium pyruvate
	0,5 % Penicillin/streptomycin (v/v)
	0,1 mM 2-mercaptoethanol

6.2.1.2 Counting of cells

Depending on the density of the cell suspension, a 1:10 or 1:100 dilution of the cell suspension was generated in trypan blue. Trypan blue stains dead cells whilst leaving viable cells unstained. The dilution was applied onto a Neubauer counting chamber and the viable cells were counted in 4 fields and the average number per field was calculated. This number was multiplied with the dilution factor and 1 x 10^4 to calculate the concentration of the cells as cells/ml.

6.2.1.3 Cultivation of HEK 293T cells

The cells were cultivated in 10 cm petri dishes at 37 °C and 5 % CO_2. Once confluence was reached, the cells were washed with PBS and detached from the plate via 2 min incubation with Trypsin-EDTA for 2 min at room temperature (RT). In order to stop the reaction, cold DMEM supplemented with 10 % FCS was added. The cells were sedimented at 1300 rounds per minute (rpm) 4 °C for 3 min and seeded at a 1:10-1:20 dilution.

6.2.1.4 Calcium phosphate transfection

The principle of the transfection of cells via calcium phosphate is built on DNA-phosphate complexes, which are taken up by the cell probably via endocytosis. 2 x 10^6 HEK 293T cells were seeded in 10 cm petri dishes at a density of 2,5 x 10^5 cells/ml in DMEM supplemented with 10 % FBS and 1 % penicillin/streptomycin and grown for 24 h at 37 °C 5 % CO_2. Prior to transfection, the medium was changed to DMEM containing HEPES. The transfection mix was prepared as follows: 10 µg *HA-pEGZ-Nfatc1-RSD* or 15 µg *Flag-Prdm1* in 850 µl ultrapure water were mixed with 130 µl 2 M $CaCl_2$ in ultrapure water. 1000 µl of 2 x HBS buffer were added dropwise whilst vortexing. The transfection

mix was incubated for 20 min at RT, before it was added dropwise onto the cells. The transfected cells were incubated for 24 h at 5 % CO_2. Cells were stimulated with TPA (50 ng/ml) and ionomycin (0,5 µM) within the last 4 h.

2 x HBS buffer	Dextrose	0,012 M
	HEPES (pH 7,05)	0,05 M
	KCl	0,01 M
	NaCl	0,28 M
	Na_2HPO_4	0,0015 M

6.2.1.5 Polyethyleneimine (PEI) transfection

Similar to the transfection via calcium phosphate, polyethyleneimine (PEI) is building complexes with the DNA, which are taken up by the cell via endocytosis. PEI is a cationic polymer with nucleic acid binding and condensing properties. It works as a proton sponge, which counteracts intracellular degradation and might increase the transfection efficiency.

1 x 10^6 HEK 293T cells were seeded in 10 cm petri dishes at a density of 1 x 10^5 cells/ml in DMEM supplemented with 10 % FCS and grown for 24 h at 37 °C 5 % CO_2. The transfection mix was prepared as follows:

PEI solution	45 µg PEI
	1 ml DMEM
DNA solution	7,5 µg *Nfatc1/C-ER*
	7,5 µg *Prdm1-HA*
	1 ml DMEM

The PEI solution was added rapidly to the DNA solution and mixed well. The mixture was incubated for 30 min at RT. The medium was aspirated and 4 ml DMEM supplemented with 15 % FCS were added onto the cells. Subsequently, the transfection mix was added to the cells. The cells were grown for 24 h at 37 °C and 5 % CO2. After 24 h the transfection

mix was replaced with DMEM supplemented with 10 % FCS and the cells were grown for another 24 h at 37 °C and 5 % CO_2. Finally, the cells were stimulated for 4 h with 2 mM $CaCl_2$, 50 ng/ml TPA, 0,5 µM ionomycin and 0,4 nM tamoxifen.

6.2.1.6 Generation of single cell suspensions of spleen and mesenteric lymph nodes (mLN) for flow cytometry

On day 10 post immunization, the mice were euthanized via CO_2 intoxication. The spleen and mLN were taken out of the body. 70 µm cell strainers were placed on top of a 50 ml falcon and moistened with 3 ml BSS/BSA. The tissues were meshed through the cell strainer via the plunger of a syringe and washed through with 2 x 5 ml of BSS/BSA. The cell suspension was sedimented at 1300 rpm at 4 °C for 5 min and the supernatant was discarded. In order to remove the erythrocytes from the suspension generated from the spleen, the cells were resuspended in 1-2 ml RBC buffer and kept for 2 min at RT. The reaction was stopped via the addition of 9 ml BSS/BSA and the cells were sedimented again at 1300 rpm at 4 °C for 5 min. The supernatant was discarded, the cells were resuspended in FACS buffer and counted for further proceedings.

6.2.1.7 Negative isolation of $CD4^+$ T cells via a column-based protocol

Single cell suspensions were generated without erylysis and $CD4^+$ cells were isolated using a Mojosort $CD4^+$ negative selection kit from Biolegend in combination with a LS-column from Miltenyi Biotech. The reagents of the Mojo-kit were pre-diluted in MACS buffer according to their lot-number specific datasheet (biotin antibody cocktail 1:8, beads 1:9). The cells were taken into MACS buffer at a concentration of 1 x 10^8 cells/ml and the pre-diluted antibody cocktail was added at a ratio of 1:10 and incubated on ice for 15 min. After the incubation, the prediluted streptavidin nanobeads were added in a 1:10 ratio and incubated for another 15 min. The LS-column was equipped with a 70 µm filter. Only 1 x 10^8 cells were loaded onto one column. The filter and the column were moistened with 3 ml of MACS buffer, before the cells were added onto the column and washed afterwards also with 3 ml of MACS buffer.

6.2.1.8 Flow cytometry

Flow cytometry is a method to cluster cells according to different features, such as size, shape, granularity and expression of proteins. The detection of proteins via this method is based on the binding of fluorochrome-labeled antibodies to the protein of interest. This process will be called 'staining' in the following. Different pretreatments of the cell allow the staining of proteins in the cytoplasm and also the nucleus. The detection of these fluorochromes is based on an optical technique measuring the emission of light after the excitation via a laser of a distinct wavelength. Size and granularity are measured via the scattered light.

Depending on the analysis, 2,5 x 10^6 cells (GCB) or 5 x 10^6 cells (Tfoll cells) were washed in ice-cold FACS buffer. The supernatant was aspirated after centrifugation for 3 min at a speed of 8000 rpm. The cells were resuspended in 90 µl of an anti-CD16/anti-CD32-antibody mix, which was prediluted in FACS buffer 1:200. After an incubation of 20 min at 4 °C, 10 µl of a 10 x concentrated antibody mix were added to stain the molecules on the surface of the cell. The final concentration of the antibodies used varied due to manufacturers' recommendation and titration upon arrival of the antibodies. Individual dilutions are indicated in the material section. The cell suspension was mixed via vortexing and incubated for 15 min at RT in the dark. Exceeding antibodies were removed via the addition of 500 µl FACS buffer, followed via precipitation of the cells at 8000 rpm for 3 min. The supernatant was aspirated. Cells, which did not undergo intracellular stainings, were taken into 200 µl FACS buffer and acquired at the flow cytometer. In some cases, the cells were fixed via the addition of 100 µl 4 % formaldehyde in PBS and stored at 4 °C until acquisition.

Cells that were stained intracellularly for transcription factors were fixed and permeabilized with the eBioscienceTM Foxp3/Transcription Factor Staining Buffer Set according to manufacturer's instructions for 20 min at 4 °C in the dark. The cells were washed twice with 500 µl of 1 x Perm buffer and resuspended in 100 µl of antibody mix diluted in 1 x Perm. Again, the final concentration of the antibodies used varied as indicated in the material section. The cells were incubated overnight (O/N) at 4 °C in the dark. Exceeding antibodies were removed via the addition of 500 µl of 1 x Perm followed via precipitation of the cells at 8000 rpm for 3 min. The supernatant was aspirated and the cells were

resuspended in 400 µl FACS buffer. The cells were transferred into 5 ml round-bottom tubes and analyzed using a BD FACSCantoTM II flow cytometer (BD). The data was analyzed via the FlowJoTM 10 software (BD).

6.2.1.9 Evaluation of protein expression levels using flow cytometry

The level of protein expression in a cell can be evaluated using the median of the fluorescence intensity (MFI). The MFI is the fluorescence intensity measured at the point of a population, which is building the border of the 50 % upper and 50 % lower events of a population sorted according to their level of expression. Therefore, it is regarded as the protein expression level in the most representative cell of a population. Fluorescence Minus One Controls (FMOs) are useful to normalize variations found in the stainings from one day to the other. These controls are made from cells that were stained with all of the fluorochrome-labeled antibodies except the one targeting the protein of interest.

Protein expression = MFI / MFI of FMO

6.2.1.10 Sorting of Tfr cells

Mice were immunized with NP-KLH in ImJect^{TM} Alum for 10 days and boosted on day 7 as described in the following. On day 10 spleen and mLN were isolated and single cell suspensions were prepared. Without erylysis $CD4^+$ T cells were enriched with CD4 (L3T4) MicroBeads from Miltenyi according to the manufacturer's instructions.

6.2.1.10.1 Sorting of Blimp-1-GFP^+ Tfr cells

We sorted $B220^-CD4^+BlimpGFP^+CXCR5^+GITR^{hi}$ Tfr cells from spleen and mLN of NP-KLH-immunized mice 10 d p.i. via fluorescence-activated cell sorting (FACS) with a BD FACSAriaII^{TM} at the VIM Wuerzburg according to the sort strategy in Fig. 7.16. The Tfr cells were sorted in 350 µl RLT buffer supplemented with 2-mercaptoethanol (1:100) and immediately transferred to -20 °C. The lysates were shipped on dry ice to Dr. Matthias Klein at the Institute for Immunology University Medical Center of the Johannes Gutenberg University Mainz.

6.2.1.10.2 Sorting of Foxp3-eGFP$^+$ Tfr cells

We sorted B220$^-$CD4$^+$PD-1$^+$CXCR5$^+$eGFP$^+$CD44$^+$ Tfr cells from spleen and mLN of NP-KLH-immunized mice 10 days p.i. via FACS with a BD FACSAriaII^{TM} at the VIM Wuerzburg according to the sort strategy in Fig. 7.36. The Tfr cells were sorted in 350 µl RLT buffer supplemented with 2-mercaptoethanol (1:100). The lysates were immediately shipped on dry ice to Dr. Matthias Klein at the Institute for Immunology University Medical Center of the Johannes Gutenberg University Mainz.

6.2.2 *In vivo* experiments

6.2.2.1 Immunization of mice with NP-KLH

In order to generate a humoral answer, which could be measured specifically, we immunized the mice with 4-Hydroxy-3-Nitrophenylacetyl hapten, conjugated to the carrier Keyhole Limpet Hemocyanin (NP-KLH). KLH is a protein (carrier), which can be taken up by the B cell, which processes and presents it to the T cell. NP, on the other hand, is too small to be taken up by the B cell itself and needs to be conjugated to KLH to be processed and presented to a T cell via the MHCII. We generated a mixture of NP-KLH with the adjuvant Imject^{TM} Alum in order to generate a GCR and a humoral immune response against this hapten-carrier conjugate.

The immunization paste was prepared as a 1:1 mixture of NP-KLH (24-32) in PBS and Imject^{TM} Alum. The Imject^{TM} Alum was shaken thoroughly until the two phases of the reagent were mixed well and added dropwise to the NP-KLH whilst vortexing. In order to generate a good emulsion, the mixture was shaken on a vortexer at lowest speed for another 30 min at RT. The mice were immunized i.p. with 125 µg of NP-KLH emulsified in Imject^{TM} Alum on day 0 and boosted on day 7 the same way. On day 10 of the experiment, the mice were euthanized via CO_2 intoxication.

6.2.2.2 Generation of serum samples

Blood was drawn from the cheek of the mice on day 0, 7 and 10 of the experiment. The blood was collected into a Sarstedt Micro tube 1.1ml Z-Gel containing a clot activator and

left at RT for up to 1 h. The clotted fraction was sedimented for 5 min at 10.000 rpm. The serum was taken and stored at -20 °C.

6.2.3 Methods based on proteins

6.2.3.1 Generation of nuclear extracts

Two different types of kits were used for the preparation of nuclear extracts. Extracts from cells transfected via the calcium phosphate transfection method were prepared with the Nuclear Extract kit from Active Motif. Extracts from cells transfected via the PEI method were prepared using the NE-PER™ Nuclear and Cytoplasmic Extraction reagents from ThermoFisher. In both cases, the extracts were prepared according to the manufacturer's instructions.

6.2.3.2 Electro Mobility Shift Assay (EMSA)

The Electro Mobility Shift Assay (EMSA) is a method to study protein-DNA interactions. Oligonucleotides of a size of 20-35 bases were biotin-conjugated at their 3'ends and annealed to another oligonucleotide representing the complementary strand, which could also be biotinylated at the 3'end. These annealed oligonucleotides are called here 'DNA probes'. Generated in a very similar fashion, just without the labeling of the 3'end, are the so-called competitors. Putative binding sites of transcription factors in the genome can be synthesized as such DNA probes. The binding of the transcription factor to the DNA probe is then tested *in vitro*. Nuclear extracts containing the transcription factor of interest are incubated with the DNA probe. In a separate and parallel reaction, this interaction can be tested for its specificity via the addition of an unlabeled competitor, which is added in a 200 x molar excess, therewith competing for the binding of the transcription factor. The reaction mixture is run through a native polyacrylamide gel. The free DNA probe has a higher mobility within the gel and runs faster than the complex of DNA probe and transcription factor. Therefore, complexes of DNA probes and transcription factors "shift" within the gel. In case of a successful competition via the competitor, the DNA probe stays free and therefore the shift is competed. The complex of DNA probe and transcription factor can be even increased in molecular weight via the addition of an antibody, which

binds to the transcription factor. This leads to lower electromobility and a higher shift of the complex within the gel.

6.2.3.2.1 Annealing of oligonucleotides

The oligonucleotides were dissolved in nuclease-free water at a final concentration of 1 mM. One DNA probe or one competitor was generated from two complementary oligonucleotides. From each of the oligonucleotides, 1 µl was added into 998 µl annealing buffer, placed into a heating block at a temperature of 95 °C. After 5 min, the heating block was set to 37 °C. The DNA probes/competitors were left in the block for 2-3 h until the temperature of 37 °C was reached. Finally, the annealed DNA probes/competitors were transferred into a -20 °C freezer for long term storage.

Oligo annealing buffer	Tris	1 M	200 µl
	EDTA	0,5 M	40 µl
	NaCl	5 M	200 µl
	Ultrapure water	-	19,56 ml

6.2.3.2.2 Preparation of a TBE-polyacrylamide gel

The EMSA was run on a 6 %-polyacrylamide gel prepared with TBE buffer according to the following scheme:

6 %-polyacrylamide gel	Acrylamide 30 %	2 ml
	TBE buffer 5 x	1 ml
	Ultrapure water	7 ml
	APS	170 µl
	TEMED	14 µl

The gel was casted and run using the Mini-PROTEAN System from Biorad. The gel was pre-run in 0,5 x TBE buffer at 100 V until an amperage of 8 mA was reached.

EMSAs were performed using the GelshiftTM Chemiluminescent EMSA kit from Active Motif. The following pipetting scheme includes the volumes of all options that were applied:

Scheme for EMSA	Nuclear extract (2-2,5 µg/µl)	1 µl
	DNA probe (1:100)	2 µl
	Competitor	4 µl
	Antibody	1 µl
	Binding buffer	2 µl
	Poly (dI:dC)	1 µl
	Ultrapure water	Up to an EV of 20 µl

The reaction mix was pipetted on ice and then left at RT for 20 min. In case of a supershift the antibody was added 5 min prior to the end of the 20 min incubation. Supershifts were performed with an anti-ER (MC-20) or anti-NFATc1 (7A6) and anti-Blimp-1 (5E7). 5 µl of 5 x loading buffer were added to the reaction and 20 µl of the reaction mix were loaded onto the gel. The samples were run through the gel until the bromophenol band reached the lower end of the gel. The assays were blotted onto a Roti®-Nylon plus membrane. DNA-protein complexes were cross-linked onto the nylon membrane with an UV StratalinkerTM 1800 using the auto cross link function. The DNA-protein complex, which was crosslinked onto the nylon membrane, was incubated with a streptavidin-HRP conjugate according to the standard protocol of the manufacturer of the kit. Under red light, the membrane was overlaid with three consecutive X-ray films and left in a cassette O/N. The processing of the film was performed under red light. The X-ray film was developed for 2 min in developing solution, washed in water shortly and fixed 10 min in fixing solution. The X-ray film was washed and dried carefully before scans were acquired at the Kyocera TAS Kalfa 420i scanner.

6.2.4 Immunological methods

6.2.4.1 Standard sandwich ELISA

The humoral immune response to the antigen of immunization, as well as autoantigens, was measured via an Enzyme-linked Immunosorbent assay (ELISA). There are different principles of this assay. In either case, the concentration of antibodies was measured in murine serum samples. Depending on the question, protein, nucleic acid, or even antibodies were bound to the surface of a highly absorbing plastic plate in a process named coating. In order to avoid unspecific binding of the antibodies, the surface was saturated with a blocking agent. The coated surface was then incubated with serial dilutions of the serum samples containing the antibodies. Antibodies, specific for the plate coated protein or nucleic acid, bound their antigen according to their specificity. In case of an antibody-coated surface, the antibodies themselves were captured according to the specificity of the coated antibody. Differences in the affinity were measured via the coating with different concentrations of the antigen. In any case, the antibodies being captured from the serum were detected via an additional antibody being linked to an enzyme, which converts a substrate into a product, having a characteristic absorption character. This absorption was measured at the specific wavelength. All quantifications were done in a relative way with reference to a pool of sera.

6.2.4.1.1 Quantification of multiple isotypes of NP-specific-antibodies

Isotype quantification was performed via the standard sandwich ELISA method. Unless specified, all incubations were performed at 37 °C on an orbital shaker set at 300 rpm. The ELISA plates were coated with either 100 µl of NP-(14)-BSA (high) or NP-(2)-BSA diluted in PBS at a concentration of 1 µg/ml and incubated for 1 h. The plates were washed 3 x with 200 µl wash buffer to completely remove the coating solution. 100 µl blocking buffer was added and the plates were incubated for 1 h. During this incubation step, serial dilutions of the serum were made in a 96-well deep well plate. For this, an initial 1:500 dilution was prepared in dilution buffer, followed by a series of seven 1:5 dilutions also in dilution buffer. The blocking buffer was removed, and the wells were washed 3 x with 200 µl wash buffer. 100 µl of the diluted serum was transferred onto the blocked ELISA plates and incubated O/N at 4 °C. The serum was removed by washing the plates

3 x with 200 µl wash buffer. 100 µl of horseradish-peroxidase (HRP)-conjugated antibody, diluted 1:10.000 in dilution buffer was added to the plates and incubated for 1 h. The HRP antibody was removed by washing 3 x with 200 µl wash buffer. 100 µl of the HRP substrate 3,3′-5,5′-Tetramethylbenzidine (TMB) was added to each well and left at RT until measurement. The ELISA plates were read at 370 nm at the Fluostar Omega (BMG Labtech).

6.2.4.1.2 Quantification of total mouse-IgG

For total quantification of IgG, mouse-IgG-kit from Roche was used according to the manufacturer's instructions. The absorption at 405 nm was measured at the Fluostar Omega (BMG Labtech).

6.2.4.1.3 Quantification of anti-ds-DNA-antibodies

Anti-ds-DNA quantification was performed via the standard sandwich ELISA method. All incubations, unless specified, were performed at 37 °C on an orbital shaker set at 300 rpm. Corning half-area plates were coated with 50 µl of Poly-L-lysin for 1 h at RT. The Poly-L-lysin was removed and the plates were coated with 100 µl of calf thymus dsDNA (25 ng/ml in PBS) at 4 °C O/N. The plates were washed 3 x with 100 µl PBS. 100 µl of blocking buffer was added to each well. The plates were blocked for 2 h. During this incubation and in a separate 96-well-plate, an initial 1:10 dilution of the sera was prepared in blocking buffer followed by seven serial 1:2 dilutions. The blocking buffer was removed by washing 3 x with 100 µl wash buffer. 50 µl of the serum dilution was transferred onto the blocked plates and incubated O/N at 4 °C. The plates were washed 3 x with wash buffer. 50 µl of anti-mouse-IgG diluted 1:10.000 in blocking buffer was added into each well and plates were incubated at 37 °C for 2 h on an orbital shaker at 300 rpm. The plates were washed 3 x with wash buffer. 100 µl of the HRP substrate TMB was added to each well and incubated for approximately 30 min at 37 °C 300 rpm. The absorption was measured at 370 nm at the Fluostar Omega (BMG Labtech).

6.2.4.1.4 Cultivation of cells from mLN post immunization and IL-2 ELISA

Mice were immunized with NP-KLH in ImJect™ Alum as previously described. mLN were extracted on day 4 p.i., meshed through a 70 µm filter and kept in RPMI supplemented with 5 % FBS, 0,1 mM 2-mercaptoethanol, 0,5 % penicillin/streptomycin, 1 mM sodium pyruvate. Wells of a 24-well-plate were coated with anti-CD3 (5 µg/ml) and anti-CD28 (2 µg/ml) in PBS for 2 h at 37 °C. The cells were seeded in RPMI on the anti-CD3/anti-CD28-coated plates and kept for 48 h at 37 °C with 5 % CO_2. Samples of the supernatant were taken after 24 h and 48 h and analyzed for their IL-2 concentration via the OptEIATM Set for mouse IL-2 (BD) according to the standard protocol of the manufacturer.

6.2.5 Methods based on nucleic acids

6.2.5.1 Isolation of RNA from sorted cells

The lysates were shipped on dry ice to Dr. Matthias Klein at the Institute for Immunology University Medical Center of the Johannes Gutenberg University Mainz. Dr. Matthias Klein kindly performed the RNA isolation, the preparation of the cDNA libraries and the NGS-RNA-sequencing as follows:

The RNA was purified with the RNeasy Plus Micro kit from QIAGEN according to the manufacturer's protocol. The RNA was quantified with a Qubit 2.0 fluorometer from Invitrogen and the quality was assessed on a Bioanalyzer 2100 using an RNA 6000 Pico chip, both from Agilent.

6.2.5.2 Preparation of cDNA libraries and NGS-RNA-sequencing

For the cDNA library preparation only samples with an RNA integrity number (RIN) of > 8 were used. The results shown in Fig. 7.17 are an exception, as the ratio between the 28 S and the 18 S RNA needed to be relaxed in order to generate a RIN value of > 8. Barcoded mRNA-seq cDNA libraries were prepared from 10 ng (4-5 ng in Fig. 7.17) of total RNA using the NEBNext® Poly(A) mRNA Magnetic Isolation Module and NEBNext® Ultra™ II RNA Library Prep kit for Illumina® according to the manual with a final amplification of 15 PCR cycles. The quantity was assessed using Invitrogen's Qubit

HS assay kit and the library size was determined using Agilent's 2100 Bioanalyzer HS DNA assay. The barcoded RNA-Seq libraries were onboard clustered using the HiSeq® Rapid SR Cluster kit v2 and 8 pM of the cDNA library. 59 base pairs (bps) were sequenced on the Illumina HiSeq2500 using the HiSeq® Rapid SBS kit v2 (59 cycles). The raw output data of the HiSeq was preprocessed according to the Illumina standard protocol. Sequence reads were trimmed for adapter sequences and further processed using QIAGEN's software CLC Genomics Workbench (v12 with CLC's default settings for RNA-Seq analysis). The reads were aligned to the GRCm38 genome.

6.2.6 Bioinformatics

6.2.6.1 Identification of a Tfh-specific transcriptional signature

We made use of the RNA-seq data from Tfh and Tfr cells isolated from spleen and LN published by the Sage group [142] Omnibus database accession no. GSE124884. We calculated the mean of the expression data of Tfr- and Tfh cells, both from the spleen using Excel. The mean values were filtered for genes that were showing a mean expression value > 5 and were more than 2 x differentially regulated between the Tfr vs. Tfh. The same procedure was done for the Tfr vs. Tfh from the mLN. The two tables containing the genes and their expression values were uploaded to the Galaxy web platform [143]. We used the public server at usegalaxy.org to filter for the genes that were differentially regulated in spleen and lymph nodes using the tool "join two datasets". This gave us the Tfh signature, which we could compare to our own data.

6.2.6.2 Analysis of differentially expressed genes of Tfr cells from *Pr1$^{+/gfp}$.FIC*, *Pr1$^{+/gfp}$.Nc1$^{fl/fl}$.FIC* and *Pr1$^{fl/gfp}$.FIC*

The expression values, which we received from Matthias Klein were filtered for genes that showed an expression level > 5 (background set) in at least one group and differed at least twofold (target set) in Tfr cells between the *Pr1$^{+/gfp}$.FIC* and at least one of the knockouts using Excel. We searched for changes in the transcriptional signature via the online tool GORILLA [144, 145]. Additionally, we filtered the genes we previously subjected to the GO-analysis for their presence in the Tfh signature. The two tables containing the genes and their expression values were uploaded to the Galaxy web platform [143]. We used the

public server at usegalaxy.org to filter for the genes that were part of the Tfh signature using the tool "join two datasets". The expression values of these genes were visualized in a heatmap using the online tool Morpheus [146].

6.2.6.3 Analysis of differentially expressed genes of Tfr cells from *Nc1$^{fl/fl}$.Pr1$^{+/gfp}$.FIC*, *Nc1^{caaA}.Pr1$^{+/gfp}$.FIC* and *Nc1^{caaA}.Pr1$^{fl/gfp}$.FIC*

The expression values, which we received from Matthias Klein, were filtered for genes that showed an expression level > 5 (background set) in at least one of the groups and differed at least twofold (target set) in Tfr cells between the compared groups using Excel. We searched for enriched Gene Ontology (GO) terms within the genes that were differentially expressed via the online tool GORILLA [144, 145]. Additionally, the expression values of these genes were visualized in a heatmap using the online tool Morpheus [146].

6.2.6.4 Analysis of transcriptional changes in Foxp3-GFP$^+$ Tfr cells

Transcriptional changes in Foxp3-GFP$^+$ Tfr cells were kindly analyzed by Jun.-Prof. Dr. Florian Erhard (VIM, Wuerzburg). The acquired libraries were mapped with the help of the software STAR (Ensembl v90) [147]. The reads per gene and library were counted. One wt sample was excluded due to quality control issues. Genes that showed less than 10 reads in all libraries were also excluded. Genes that were significantly differentially regulated were defined with the help of DESeq2 [148]. Shown in the heatmap are log2-fold changes normalized to the mean of the wt libraries.

6.2.7 Imaging

6.2.7.1 Colocalization experiment

6.2.7.1.1 Isolation of CD4$^+$ T cells from spleen and mLN of a naïve mouse

Out of a naïve DEREG mouse mLN and spleen were isolated. Single cell suspensions were generated without erylysis and CD4$^+$ cells were isolated via the negative isolation for CD4$^+$ T cells via a column-based protocol mentioned earlier in this section.

6.2.7.1.2 Cultivation of $CD4^+$ T cells and stimulation with anti-CD3, anti-CD28 and IL-2

A well of a 24-well plate was coated with anti-CD3 (1:250) and anti-CD28 (1:500) in PBS for 2,5 h at 37 °C. Then, the coating solution was removed and the well was washed twice with PBS. The negatively selected cells were seeded at a density of 1 x 10^6 cells/ml in RPMI supplemented with IL-2 (1:3000) in a well of the precoated 24-well plate and cultivated for 22 h at 37 °C and 5 % CO_2. On the same day, the prepared coating solution was also added to the well of a 12-well ibidi slide and left O/N at 4 °C. On the next day, the coating solution was removed from the ibidi slide and the well was washed twice with PBS. The cells were harvested from the well of the 24-well plate and transferred into the well of the ibidi silde for the staining of the cells.

6.2.7.1.3 Staining of NFATc1 and Blimp-1 in $CD4^+$ T cells

Nora Müller (VIM, Wuerzburg) kindly performed the staining of NFATc1 and Blimp-1. The cells were fixed in 4 % formaldehyde in PBS for 20 min and permeabilized for 5 min in 0,2 % TX-100 in PBS. The cells were blocked for 1 h at RT in 5 % BSA in PBS. The primary antibodies anti-NFATc1 (1:50), anti-Blimp-1 (1:50) and GFP-Booster Atto488 (1:100) were diluted as indicated in 1 % BSA in PBS. The cells were stained with the primary antibodies at 4 °C O/N. Afterwards, the cells were washed 4 x with 1 % BSA in PBS and stained with the secondary-antibodies goat anti-mouse AlexaFluor Plus 555 (1:400) and goat anti-rat AlexaFluor 594 (1:100) for 45 min at RT. The cells were washed 4 x with PBS and stained with DRAQ5 (1:1000 in PBS) for another 15 min at RT. The cells were washed once with PBS.

6.2.7.1.4 Confocal microscopy

The pictures were kindly taken by Nora Müller at the Zeiss LSM 780 confocal microscope in the VIM, Wuerzburg. The data was further processed with the software ImageJ [149].

6.2.8 Histology

In order to visualize the structure of the GC and the position of Foxp3$^+$ cells within the tissue, we performed immunofluorescence stainings of sections from mLN of immunized mice. The principle for staining structures of a tissue is similar to the staining of single cells for flow cytometry. The tissue needs to be conserved, stabilized and cut into very fine slices. The process of conservation and stabilization can mask certain structures, which need to be retrieved in order to become accessible for the staining with antibodies. First, the tissue is blocked to prevent unspecific binding of antibodies. During the initial step of staining, the tissue is incubated with primary antibodies against the structures of interest. These antibodies are either biotin-conjugated or unconjugated and had to be generated in different species. In a second step, secondary antibodies directed against the different species in which the primary antibodies were generated or streptavidin, conjugated to a fluorochrome are added onto the tissue. These fluorochrome-labeled antibodies/streptavidin will bind to the primary antibodies of the species they are directed against, or the biotin. Therefore, the primary antibodies need to be generated all in different species. The use of a tertiary antibody out of a species, which was already used, in order to generate a primary antibody, is possible. This requires the blocking of the tissue with serum from the species, in which the tertiary and one of the primary antibodies were generated in. Afterwards, the tertiary antibody directed against a structure of interest will be added to the tissue. It is recommended that this antibody is directly conjugated to a fluorochrome in order to avoid cross-reactivities.

6.2.8.1 Preparation of mouse tissue for paraffin sections

The draining LN (mesenterial) and the spleen were taken from euthanized mice. The spleen was cut longitudinally in two halves and the mLN were cleaned from fat. The tissue was kept for 3 days in formalin to fix the tissue. The formalin was changed every 24 h. Fixed tissues were stored in PBS at 4 °C until further processing. The tissue was dehydrated and paraffinized by the routine laboratory of the Institute of Pathology. The tissues were embedded at a Leica Histocore Arcadia H paraffin embedding center and stored at RT until cutting.

6.2.8.2 Paraffin sections

Sections were performed by Tabea Steinmüller using a LEICA SM 2000R microtome. The sections had a thickness of 3 µm and were added onto SuperFrost plus slides manufactured by Langenbrinck. The slides were stored in dust free cassettes at RT until further processing.

6.2.8.3 Immunofluorescence stainings

The sections were deparaffinized via the immunohistochemistry laboratory of the Institute of Pathology using a citrate buffer at a pH of 6.0 (20 mM) and a H_2O_2 block. All following staining steps were performed in a humid chamber at RT in the dark. Tissues were circled with a pap pen and blocked with antibody diluent with background reducing components (AbDil) for 1 h. The primary antibodies or conjugates were diluted 1:100 in AbDil and incubated with the tissue for 1 h. The following primary antibodies/conjugates were used: rabbit anti-CD3, PNA-biotin and rat anti-Foxp3. Exceeding amounts of antibody were washed off with PBS in a glass cuvette on an orbital shaker 3 x for 5 min. Secondary antibodies were diluted 1:400 in AbDil and incubated for 1 h on the tissue. The following antibodies/conjugates were used: donkey anti-rat Alexa Fluor™ 488, donkey anti-rabbit Alexa Fluor™ 555, streptavidin Alexa Fluor™ 647. Exceeding amounts of antibody were washed off with PBS in a glass cuvette on an orbital shaker 3 x for 5 min. The tissue was blocked for 1 h at RT with normal rat serum (NRS) and further stained with rat anti-B220 Alexa Fluor™ 594 diluted 1:400 as well as Höchst diluted 1:2000 in NRS for 1 h at RT. Exceeding amounts of antibody were washed off with PBS in a glass cuvette on an orbital shaker 3 x for 5 min. The stained tissues were mounted with Mowiol containing DABCO.

6.2.8.4 Immunofluorescence microscopy

Pictures were taken at the Evos FL Auto 2 fluorescence microscope manufactured by Invitrogen. The EVOS LED Light Cubes used for acquisition are named with their corresponding fluorochromes in the material section. The pictures were first processed via the Invitrogen EVOS FL Auto 2.0 Imaging system and further processed via ImageJ [149].

Overlays of the single channels were generated with ImageJ, the B-cell follicle and the GC were marked as regions of interest and $CD3^+Foxp3^+$ cells were counted by eye.

6.2.9 Statistical analysis

All results are shown as median with interquartile range. The statistical significance of the differences between the groups was determined via a Mann-Whitney test. Results were calculated with the software Prism 5 (GraphPad). Differences for p-values > 0.05 were considered not significant, but still were indicated as numbers. Differences in p-values ≤ 0.05 were considered significant and indicated in figures as $p \leq 0.05$ (*), $p \leq 0.01$ (**), $p \leq 0.001$ (***), $p \leq 0.0001$ (****).

7 Results

7.1 The role of NFATc1 and Blimp-1 in Tfr cells

7.1.1 NFATc1 and Blimp-1 cooperate to allow CXCR5 expression

We evaluated the repressive function of Blimp-1 on CXCR5 expression in Tregs. First, a short hairpin RNA knockdown of *Prdm1* (encoding Blimp-1) was examined in Tregs (Fig. S1). The reduction of Blimp-1-encoding RNA led to a remarkable increase of *Cxcr5* RNA as well as CXCR5 protein on the surface. It seems likely that Blimp-1 also has a repressing effect on CXCR5 expression in Tfr cells and that NFATc1 is needed to overcome this repression.

The CXCR5 expression is regulated via the *Cxcr5* promoter as well as the hypersensitivity region 2 (*HS2*) representing an enhancer located in the first intron of the *Cxcr5* gene [150] (Fig. 7.1). Our previous findings revealed one NFAT binding site (*Cxcr5-pro-N1*) [50], as well as one site, which is similar to a Blimp-1 consensus site (*Cxcr5-pro-B1*) in the *Cxcr5* promoter (Fig. 7.1). We could prove the binding of NFATc1 to *Cxcr5-pro-N1*, as well as the binding of Blimp-1 to *Cxcr5-pro-B1* via an Electro Mobility Shift Assay (EMSA) (Fig. S2).

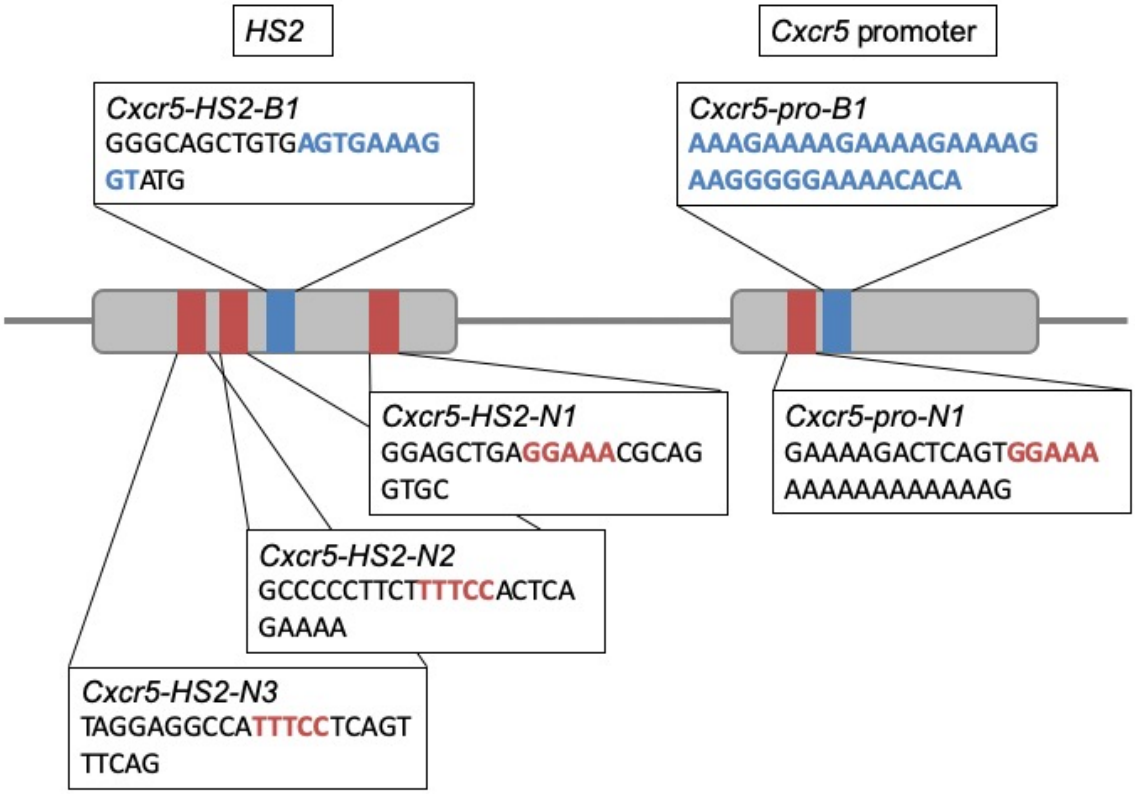

Figure 7.1: Blimp-1 and NFATc1 binding sites in the *Cxcr5* promoter and enhancer

Scheme of putative Blimp-1 and NFATc1 binding sites in the *Cxcr5* promoter and enhancer (*HS2*). Blimp-1 consensus sites are indicated in blue, NFATc1 consensus sites are indicated in red. DNA probes tested via EMSA for their binding by NFATc1 and Blimp-1 are shown in boxes. Scheme was modified from [151].

Further, we recognized five different NFAT consensus sites in the murine *HS2* region, of which three are conserved between men and mice (Fig. S3A and Fig. 7.1). The *HS2* region furthermore contains one binding site for Blimp-1 and the transcription factor E2A (Fig. S3A and Fig. 7.1). As shown by others, Blimp-1 and E2A control the CXCR5 expression in follicular $CD8^+$ T cells [150]. We were interested in the influence of Blimp-1 and NFATc1 on the CXCR5 expression in follicular $CD4^+$ T cells. Therefore, we created oligonucleotides in order to test the binding of NFATc1 and to verify the binding of Blimp-1 to their conserved consensus sites in the *HS2* region. We named these oligonucleotides *Cxcr5-HS2-B1, Cxcr5-HS2-N1*, *Cxcr5-HS2-N2* and *Cxcr5-HS2-N3* (Fig. 7.1 and Fig. S3B). The binding capacity of a fusion protein, consisting of the DNA

binding domain of NFATc1 (rel similarity domain – RSD) with a n-terminal hemagglutinin (HA) -tag to each of these regions was tested via EMSA (Fig. 7.2A). As a positive control for the binding of HA-NFATc1-RSD, we used a DNA-probe coding for the published NFATc1 binding site in the *Nfatc1* promoter P1, named *Nfatc1-P1-tan* [152]. We could verify a weak binding of HA-NFATc1-RSD to *Cxcr5-HS2-N1*, but a strong one to *Cxcr5-HS2-N2*. *Cxcr5-HS2-N3* was showing a shift that was even weaker than the one with *Cxcr5-HS2-N1.* The binding of HA-NFATc1-RSD to the three DNA-probes was competed via the known NFAT binding site *Il2-Pubd* [153], confirming that these are true NFAT binding sites. Next, we wanted to know if NFATc1 could recruit Blimp-1 to bind cooperatively to the NFAT binding sites in the *HS2* (Fig. 7.2B). Therefore, we ectopically overexpressed a fusion protein of NFATc1/C with a c-terminal estrogen-receptor tag (NFATc1/C-ER) and a fusion protein of Blimp-1 with a c-terminal HA-tag (Blimp-1-HA) in HEK 293T cells and prepared nuclear extracts. The binding of the fusion proteins to the conserved binding sites in the *HS2* was tested via EMSA. NFATc1/C-ER only interacted with *Cxcr5-HS2-N2*. We did not observe the binding of the whole NFATc1/C-ER to *Cxcr5-HS2-N1* or *Cxcr5-HS2-N3* site as this was the case before with HA-NFATc1-RSD. In order to check if the visible shift was caused by NFATc1/C-ER and/or Blimp-1-HA, we included the competitors *Il2-Pubd* and *Myc-PRE*, the latter resembling a known Blimp-1 response element [154]. Only *Il2-Pubd* was competing with the shift giving a first indication that only NFATc1/C-ER interacts with the designated response elements in the *HS2* region.

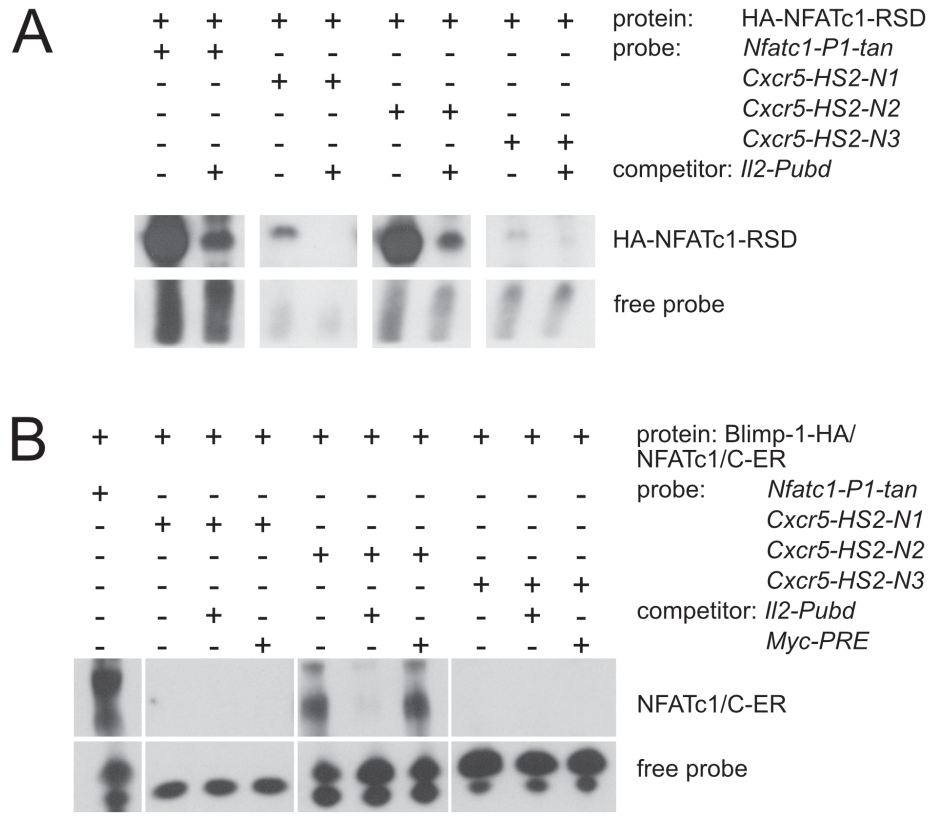

Figure 7.2: NFATc1 binds in the *Cxcr5* enhancer

(A) The binding of HA-NFATc1-RSD to the conserved NFAT consensus sites in *HS2* was tested via EMSA. HA-NFATc1-RSD was ectopically overexpressed in HEK 293T cells. Nuclear extracts were tested for their binding to DNA-probes via EMSA. *Nfatc1-P1-tan* was used as a positive control for the HA-NFATc1-RSD binding to the DNA-probes. The binding of HA-NFATc1-RSD to the DNA-probe was competed with *Il2-Pubd*. (B) NFATc1/C-ER and Blimp-1-HA were tested for their binding to the conserved consensus sites in *HS2*. NFATc1/C-ER as well as Blimp-1-HA were ectopically overexpressed in HEK 293T cells. The binding of NFATc1/C-ER to the DNA-probe was competed with *Il2-Pubd* and the putative binding of Blimp-1-HA to the DNA-probe was competed via the competitor *Myc-PRE*.

Since binding sites of Blimp-1 and NFAT (c1) are in close neighborhood at the promoter as well as at the *HS2* enhancer, we evaluated if the two transcriptional regulators interact on the protein level. Both, Tcon and Treg expressed NFATc1 in the nucleus upon activation, but Blimp-1 was only prominent in Tregs (Fig. S4). In line, immunoprecipitation of Blimp-1 pulled down NFATc1 from nuclear extracts of Tregs, indeed representing

protein interactions of Blimp-1 and NFATc1 in Tregs (Fig. S4). We tested once more if NFATc1/C-ER could recruit Blimp-1-HA to the *Cxcr5-HS2-N2* binding site via EMSA. This time, we tested if the shifted complex of protein and probe could be super shifted via an anti-NFATc1/anti-ER and/or an anti-Blimp-1 antibody. The binding of NFATc1/C-ER to *Cxcr5-HS2-N2* was confirmed, however, we could not shift the protein-DNA complex with the anti-Blimp1 antibody (Fig. 7.3A). We furthermore tested if Blimp-1-HA could recruit NFATc1/C-ER to the *Cxcr5-HS2-B* binding site (Fig. 7.3B). This time the protein-DNA complex could only be shifted via the anti-Blimp-1 antibody.

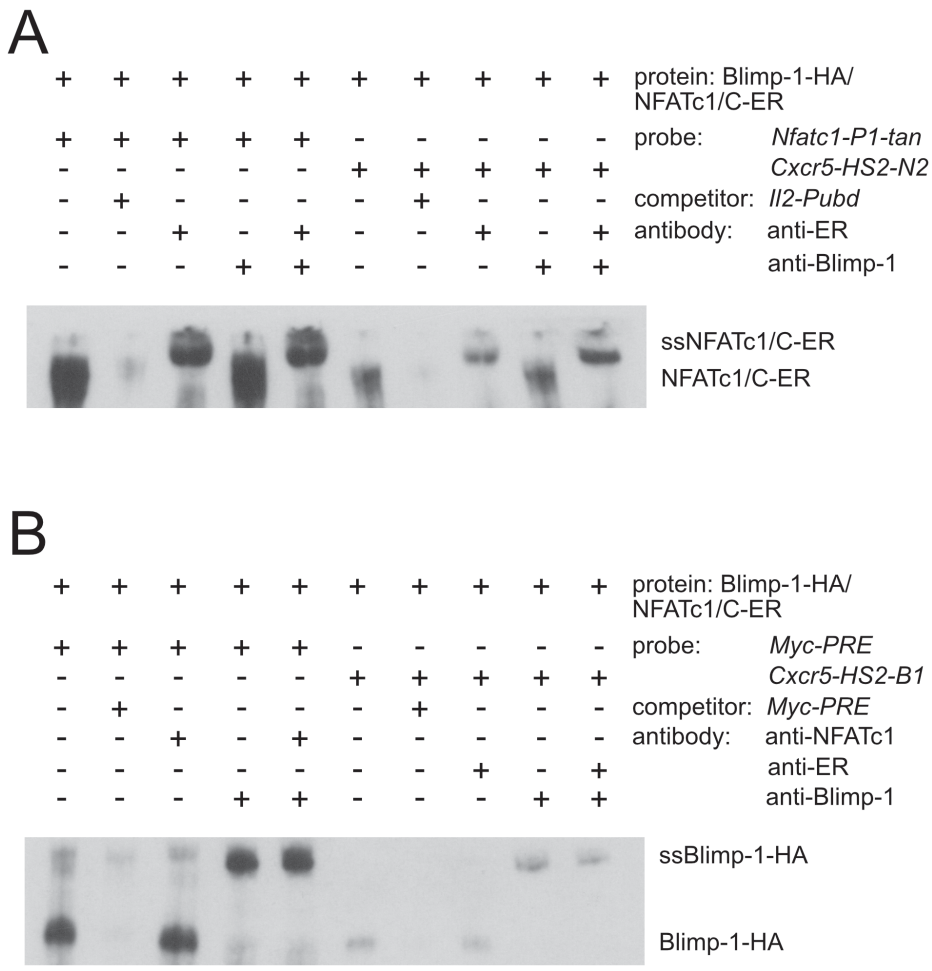

Figure 7.3: Blimp-1 and NFATc1 bind to sites in the *Cxcr5* enhancer

(A) The NFATc1 binding site *Cxcr5-HS2-N2* was tested for the binding of NFATc1/C-ER and Blimp-1-HA. (B) The Blimp-1 binding site *Cxcr5-HS2-B1* was tested for the binding of NFATc1/C-ER and Blimp-1-HA. (A and B) NFATc1/C-ER as well as Blimp-1-HA were ectopically overexpressed in HEK 293T cells. The binding of

NFATc1/C-ER to the DNA-probe was competed with *Il2-Pubd* and the binding of Blimp-1-HA to the DNA-probe was competed via the competitor *Myc-PRE*. NFATc1/C-ER bound to the probes was super shifted via an anti-NFATc1 or anti-ER-antibody, Blimp-1 bound to the probes was super shifted via an anti-Blimp-1-antibody. The DNA-probes *Myc-PRE* and *Nfatc1-P1-tan* were diluted 1:200 instead of 1:100 as usual.

In sum, this shows that NFATc1 and Blimp-1 can bind to the *Cxcr5* promoter at *Cxcr5-pro-N1* [50] and *Cxcr5-pro-B1* (Fig. S2), as well as to the *Cxcr5-HS2* enhancer at *Cxcr5-HS2-N2* and *Cxcr5-HS2-B1* (Fig. 7.3A and B). Although we could not prove the cooperative binding of NFATc1/C-ER and Blimp-1-HA to the *HS2*-enhancer *in vitro*, NFATc1 and Blimp-1 co-immunoprecipitated in nuclear extracts prepared from Tregs (Fig. S4). This could mean that in Blimp-1-expressing Tregs, especially Tfr cells, a combined regulation of CXCR5 expression takes place via NFATc1 and Blimp-1.

NFATc1 and Blimp-1 need to translocate to the nucleus to be functionally active, therefore the localization within the cell plays an important role. In order to verify the subcellular distribution in activated Tregs – as we had seen it in nuclear extracts before (Fig. S4), and to evaluate if this occurs in one cell, we isolated $CD4^+$ T cells out of an unchallenged DEREG mouse [140], stimulated these cells with anti-CD3/anti-CD28-antibodies and IL-2 for 24 h and stained for NFATc1 as well as Blimp-1. Tregs were identified via the GFP reporter, which is expressed under the control of the Foxp3 regulator elements in DEREG mice. Consistent with our former results [95], we observed a higher NFATc1 expression and translocation into the nucleus in $CD4^+GFP^-$ Tcon than in $CD4^+GFP^+$ Tregs. Within the Treg population most of the cells were Blimp-1^+. The NFATc1 expression within the Blimp-1^+ Treg population varied, ranging from Blimp-1^+ Tregs that showed almost no NFATc1 expression (Treg $Nc1^{lo}$) to Blimp-1^+ Tregs that showed at least intermediate expression and translocation to the nucleus (Treg $Nc1^{int}$). Interestingly, NFATc1 expression appeared stronger in the cytoplasm than in the nucleus in the presence of Blimp-1 (Fig. 7.4).

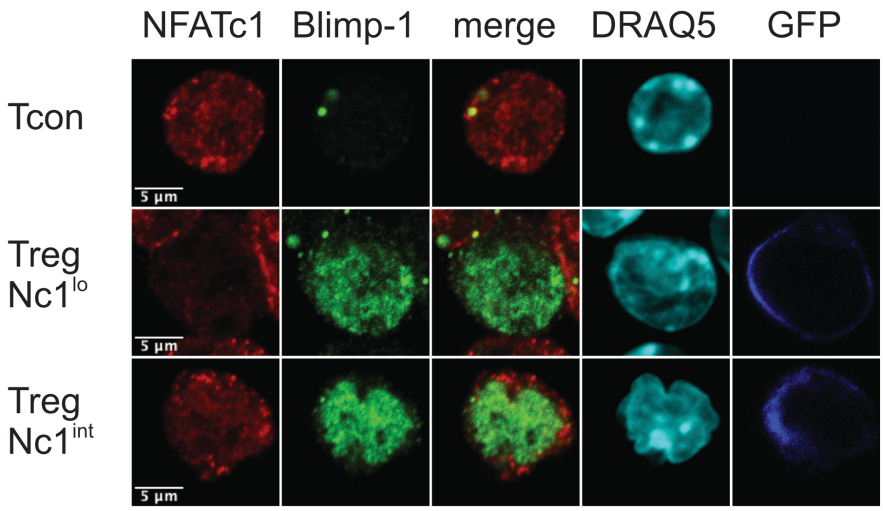

Figure 7.4: Blimp-1 and NFATc1 colocalize in the nuclei of Tregs

$CD4^+$ T cells were isolated from LNs and spleen of naive DEREG mice and stimulated for 24 h with anti-CD3/anti-CD28 and IL-2. The GFP reporter, which is expressed under the control of the Foxp3 regulator elements, was used to identify Tregs within the $CD4^+$ T cells. Cells were stained for NFATc1 (red) and Blimp-1 (green). Stainings and confocal microscopy were performed in cooperation with Nora Müller at the VIM Wuerzburg.

Having assessed the co-expression and nuclear coappearance of the two transcriptional regulators in Tregs, the influence of NFATc1 and Blimp-1 on the expression of CXCR5 was examined via a reporter gene assay. The luciferase reporter gene stood under the control of the full *Cxcr5* promoter as well as the *HS2* and was transfected together with expression plasmids for murine Blimp-1 and human NFATc1/C into HEK 293T cells. Expectedly, the presence of NFATc1 supported the expression of the *Cxcr5*-driven luciferase reporter gene (Fig. S5) [50]. This was dependent on the binding of NFATc1/C to the *Cxcr5* promoter, as the mutation of the NFAT binding site in the promoter reduced the reporter gene activity (Fig. 7.5 and Fig. S5). Unexpected, however, was that co-expression of NFATc1 and Blimp-1 further increased measurable luciferase activity, pointing to a possible cooperation of NFATc1 and Blimp-1 at the *Cxcr5* regulatory elements (Fig. S5).

We created a reporter construct containing the proximal 329 bp fragment of the *Cxcr5* promoter as well as the *HS2* (Fig. 7.5 and S6). The functional role of NFATc1 and Blimp-1

for the proximal promoter and the *HS2* enhancer was examined via transfection of EL-4 cells in various combinations and with luciferase constructs (Fig. S6), which carried mutations of the identified binding sites in these two regions with one exception (Fig. 7.5). The region of Blimp-1 binding in the promoter comprises a 34 bp long region with multiple repetitions of a Blimp-1-like binding motif, which makes it difficult to accurately mutate. Consequently, we had to focus on the manipulation of the Blimp-1 binding site in the *HS2* and found that the eradication of the Blimp-1 binding site in *HS2* increased the transcriptional activity remarkably, giving proof for Blimp-1 as a transcriptional repressor of *Cxcr5* (Fig. S6A). Both NFAT sites, which were bound strongly by NFATc1 *in vitro* and mutated individually, contributed to transactivation of *Cxcr5* by NFATc1 (Fig. S6A, Fig. S6B). Luciferase constructs with a mutation in both mapped NFAT sites, one in the promoter, one in the enhancer of *Cxcr5* and the mutation of the Blimp-1 binding site in the enhancer, fell down to very low expression and could not be transactivated by NFATc1 and/or Blimp-1 anymore. This marks *Cxcr5-pro-N1* and *Cxcr5-HS2-N2* as the essential NFAT binding sites within the *Cxcr5* locus and indicates the cooperation of NFATc1 with Blimp-1 in the transactivation of the *Cxcr5*-expression (Fig. S6B).

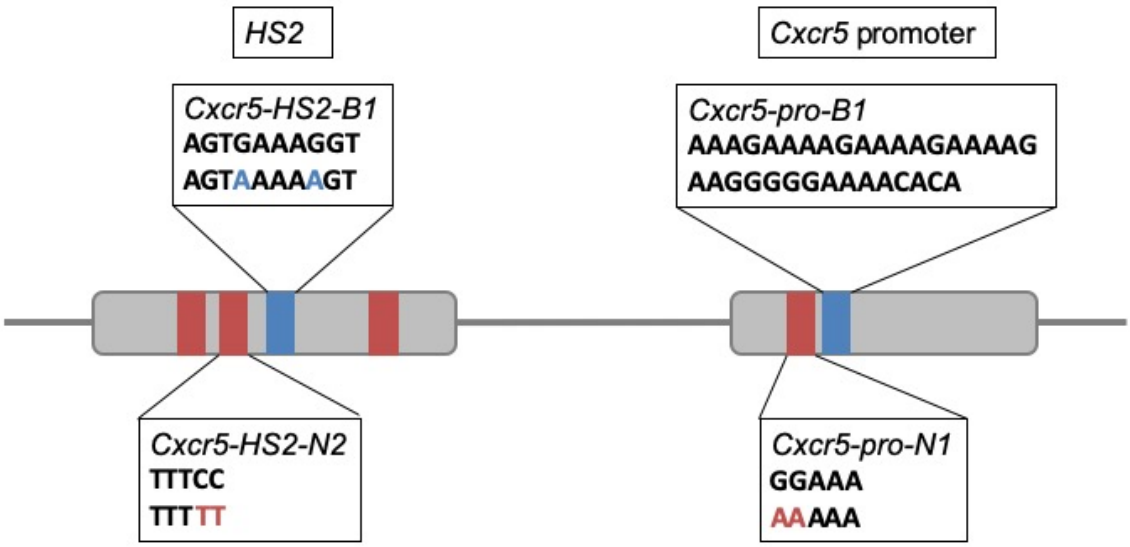

Figure 7.5: Mutations of Blimp-1 and NFATc1 binding sites in the *Cxcr5* promoter and *HS2*

Scheme of putative Blimp-1 and NFATc1 binding sites in the *Cxcr5* promoter and *HS2*. Blimp-1 binding sites are indicated in blue, NFATc1 binding sites are indicated in red. Comparison of the wildtypic and the mutated NFATc1 and Blimp-1 binding sites are shown in boxes. Mutations

inserted into the Blimp-1 binding sites are indicated in blue and mutations in the NFAT binding sites are indicated in red. Scheme was modified from [151].

Overall, we hypothesized that, while NFATc1 has to overcome Blimp-1-mediated repression, Blimp-1 then cooperates with NFATc1 in CXCR5 expression in Tregs and that this cooperation might be essential for Tfr-cell differentiation.

7.1.2 The role of NFATc1 and Blimp-1 in Tfr cells *in vivo*

We have shown that NFATc1 and Blimp-1 are both expressed in Tregs, colocalize in their nuclei and contribute to the regulation of the homing receptor for GCs, CXCR5. Therefore, we wanted to elicit the *in vivo* role of NFATc1 and Blimp-1 in Tfr cells for the GCR.

7.1.3 Increased Tfr-cell frequencies in adult *Pr1$^{fl/fl}$.FIC* mice in the steady state

In order to understand more about the function of NFATc1 and Blimp-1 in Tfr cells, we made use of Treg-specific [62] conditional NFATc1-[93, 95] and Blimp-1 deficient [115] mice, namely *Nc1$^{fl/fl}$.FIC*, *Pr1$^{fl/fl}$.FIC*, *Nc1$^{fl/fl}$.Pr1$^{fl/fl}$.FIC* and *FIC* only (Foxp3-IRES-Cre).

We recorded the basal level of GCR in naive adult mice having 2-3 months of age. GCB cells were defined as CD4$^-$B220$^+$PNA$^+$Fas$^+$ cells and detected via flow cytometry (Fig. 7.6A). A small population of GCB cells was detected in the mesenteric LNs (mLNs), while GCB cells were almost absent in the spleen of all individuals. This difference might be caused via a constant supply of antigen draining from the intestinal flora to mLNs. We could not see differences in the relative GCB-cell numbers of mice of the tested genotypes. Tfr cells were defined as B220$^-$CD4$^+$CD44$^+$Foxp3$^+$PD-1$^+$CXCR5$^+$. A small population of these cells could be detected already in the steady state (Fig. 7.6B). The *Pr1$^{fl/fl}$.FIC* mouse exhibited elevated frequencies of Tfr cells in the mLN and the spleen, while the *Nc1$^{fl/fl}$.Pr1$^{fl/fl}$.FIC* mouse showed this increase in the spleen only. Although Tfr cells should restrain Tfh cells, the relative number of B220$^-$CD4$^+$CD44$^+$Foxp3$^-$PD-1$^+$CXCR5$^+$ Tfh cells was elevated by 35% in the *Pr1$^{fl/fl}$.FIC* mouse and by 25% in *Nc1$^{fl/fl}$.Pr1$^{fl/fl}$.FIC* mouse compared to the *FIC* mouse in the mLN. In conclusion, specific ablation of Blimp-1 in

Tregs had a positive effect on the number of Tfr cells in unchallenged mice, which did not reduce the number of present Tfh cells.

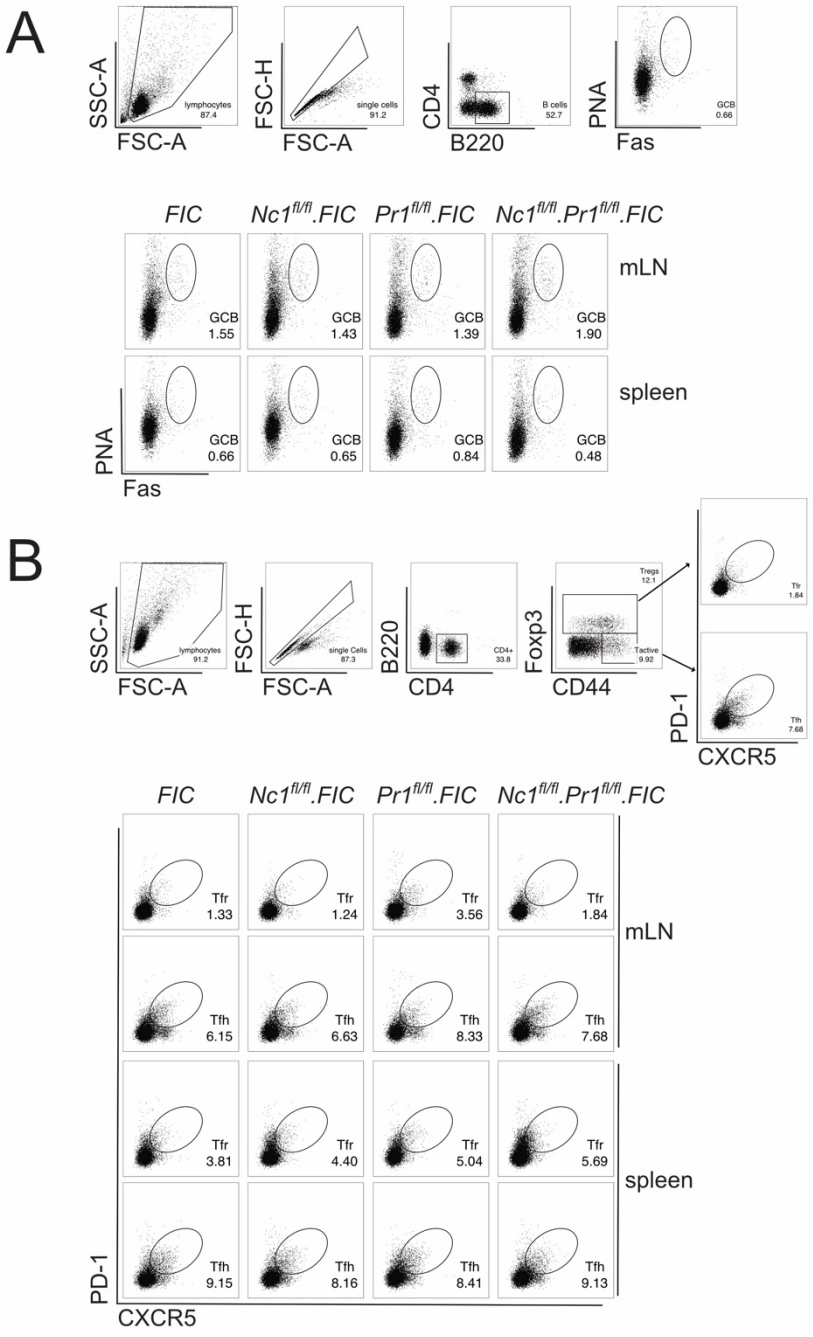

Figure 7.6: *Pr1$^{fl/fl}$.FIC* mice show increased Tfr-cell frequencies in the steady state

Spleen and mLN of 2-3 months old *FIC*, *Nc1$^{fl/fl}$.FIC*, *Pr1$^{fl/fl}$.FIC* and *Nc1$^{fl/fl}$.Pr1$^{fl/fl}$.FIC* mice were harvested. Cells were taken into suspension and stained for GCB cells, Tfr cells and Tfh cells. (A, upper) Gating strategy of GCB cells. (A, lower) Representative flow cytometry of GCB cell

numbers in spleen and mLN in the steady state. (B, upper) Gating strategy of Tfr cells and Tfh cells (B, lower) Representative flow cytometry of Tfr and Tfh cell numbers in spleen and mLN in the steady state.

7.1.4 NFATc1 enhances CXCR5 expression in Tfr cells

Next, we challenged *Nc1$^{fl/fl}$.FIC*, *Pr1$^{fl/fl}$.FIC*, *Nc1$^{fl/fl}$.Pr1$^{fl/fl}$.FIC* and *FIC* mice via the intraperitoneal injection of NP-KLH in ImJect Alum, followed by a second injection on day 7 (boost) (Fig. 7.7). The mice were sacrificed on day 10 and the numbers of Tfr cells were determined in the mLNs as well as in the spleen using flow cytometry.

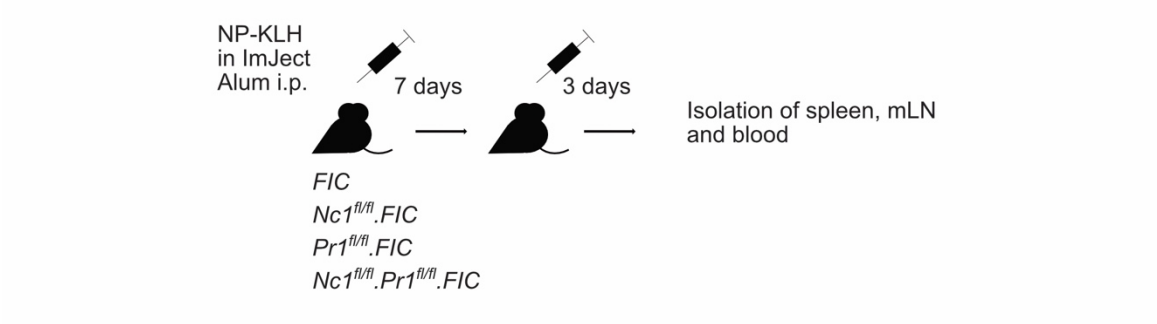

Figure 7.7: Induction of a GCR in mice with NFATc1 and Blimp-1 deficient Tregs

FIC, *Nc1$^{fl/fl}$.FIC*, *Pr1$^{fl/fl}$.FIC* and *Nc1$^{fl/fl}$.Pr1$^{fl/fl}$.FIC* mice were immunized with NP-KLH in ImJect Alum i.p. for 10 days and boosted on day 7. Spleen and mLN were harvested and stained for flow cytometry.

Nc1$^{fl/fl}$.FIC mice showed reduced frequencies of Tfr cells in both organs, as previously reported by us for *Nc1$^{fl/fl}$.Cd4cre* and *Nc1$^{fl/fl}$.FIC* mice [50] (Fig. 7.8A and B). *Pr1$^{fl/fl}$.FIC* mice were high in relative Tfr-cell numbers within the Treg population, while the relative Tfr-cell numbers of *Nc1$^{fl/fl}$.Pr1$^{fl/fl}$.FIC* mice compared to *FIC* only were still, but less significantly increased (Fig. 7.8A and B). Since our primary hypothesis was that Tfr cells need NFATc1 to overcome Blimp-1-mediated repression of CXCR5 expression, we checked the median of fluorescence intensity (MFI) of CXCR5 as a measurement of CXCR5 expression on the surface of Tregs (Fig. 7.8C). Of course, this excludes all Tregs, which could not upregulate CXCR5 at all due to NFATc1 deficiency. Nevertheless and in line with former data [50], *Nc1$^{fl/fl}$.FIC* mice showed reduced levels of CXCR5 on the surface of Tregs, which explains the reduction of Tfr-cell frequencies. However, the strong

increase of relative Tfr-cell numbers in the *Pr1*$^{fl/fl}$*.FIC* mice was not reflected by higher CXCR5 expression per cell. Only Tregs from mLN of *Pr1*$^{fl/fl}$*.FIC* mice elicited a slight increase in the CXCR5 MFI compared to wildtypic *FIC* mice. In comparison to Tregs from *Nc1*$^{fl/fl}$*.FIC* mice, however, the additional loss of Blimp-1 in Tregs of *Nc1*$^{fl/fl}$*.Pr1*$^{fl/fl}$*.FIC* rescued the detectable amount of CXCR5 per Treg in the spleen. Together, this implies that NFATc1 has indeed an important role in CXCR5 expression, when Blimp-1 is present.

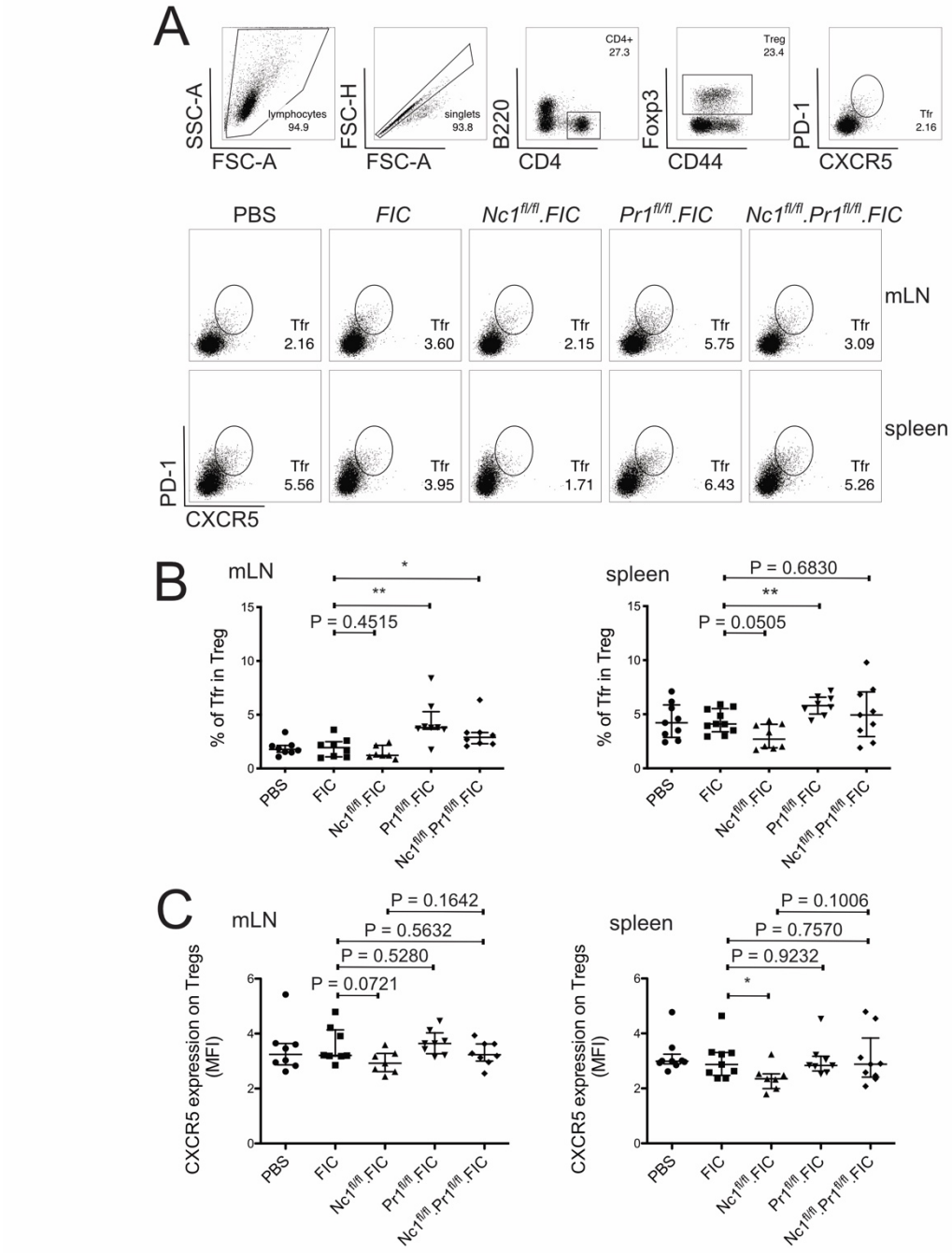

Figure 7.8: NFATc1 enhances CXCR5 expression in Tfr cells

(A, upper) Gating strategy of $B220^{-}CD4^{+}CD44^{+}Foxp3^{+}PD\text{-}1^{+}CXCR5^{+}$ Tfr cells. (A, lower) Representative flow cytometry of Tfr-cell frequencies in spleen and mLN 10 d after NP-KLH immunization. (B) Tfr-cell frequencies shown as percentage of Tregs. (C) CXCR5 expression on Tregs, MFI normalized via the FMO of CXCR5. (B and C) Compilation of 7 independent experiments, Mann-Whitney-test: $n \geq 7$; *, $P \leq 0.05$; **, $P \leq 0.01$

7.1.5 Blimp-1 controls Tfr-cell homeostasis

Compared to the *FIC* mice, Tfr-cell frequencies were augmented in *Prdm1*$^{fl/fl}$*.FIC* mice as well as in *Nfatc1*$^{fl/fl}$*.Prdm1*$^{fl/fl}$*.FIC* mice (Fig. 7.8A and B). Remarkably, the percentages of Tregs in $CD4^{+}$ cells were also higher in mLNs, although not in the spleen (Fig. 7.9A). There was a previous report on the loss of effector Treg (eTreg) homeostasis due to Blimp-1 deficiency in a mouse model of mixed bone marrow chimeras generated half from wt and half from Blimp-1 deficient mice [135]. The authors mention more Bcl-2-expressing Tregs as a cause of the loss of homeostasis [135]. We therefore checked the level of Bcl-2 expression per cell via flow cytometry, but the Tfr cells of *Prdm1*$^{fl/fl}$*.FIC* mice did not show remarkably higher levels of Bcl-2 per cell compared to the ones of *FIC* mice (Fig. 7.9B). The Treg population (Fig. 7.9A) was not augmented to the same extend as the Tfr-cell population in *Prdm1*$^{fl/fl}$*.FIC* mice (Fig. 7.8B) compared to the *FIC* mice. We claim that the rise in relative numbers caused via the Blimp-1 deficiency is associated with an eTreg phenotype. Dissimilarly, we observed the tendency of an increased Bcl-2-expression in the Tfr cells of mLN from *Nfatc1*$^{fl/fl}$*.FIC* mice compared to the ones from the *FIC* mice, indicating that those Tfr cells might survive longer in the GC. This even pronounces the role of NFATc1 in the CXCR5 expression of Tregs, leading to reduced Tfr-cell frequencies. We stained Tfr cells for Ki-67, as we suspected the Tfr cells to proliferate more in the absence of Blimp-1 (Fig. 7.9C). In fact, both NFATc1 and Blimp-1-deficient Tfr cells demonstrated higher Ki-67 expression in mLNs. This effect seemed to add up by combined NFATc1 and Blimp-1 deletion in Tregs. However, it was not observed in the spleen. We therefore claim that Blimp-1 controls Tfr-cell homeostasis via an additional mechanism besides Ki-67-indicated proliferation.

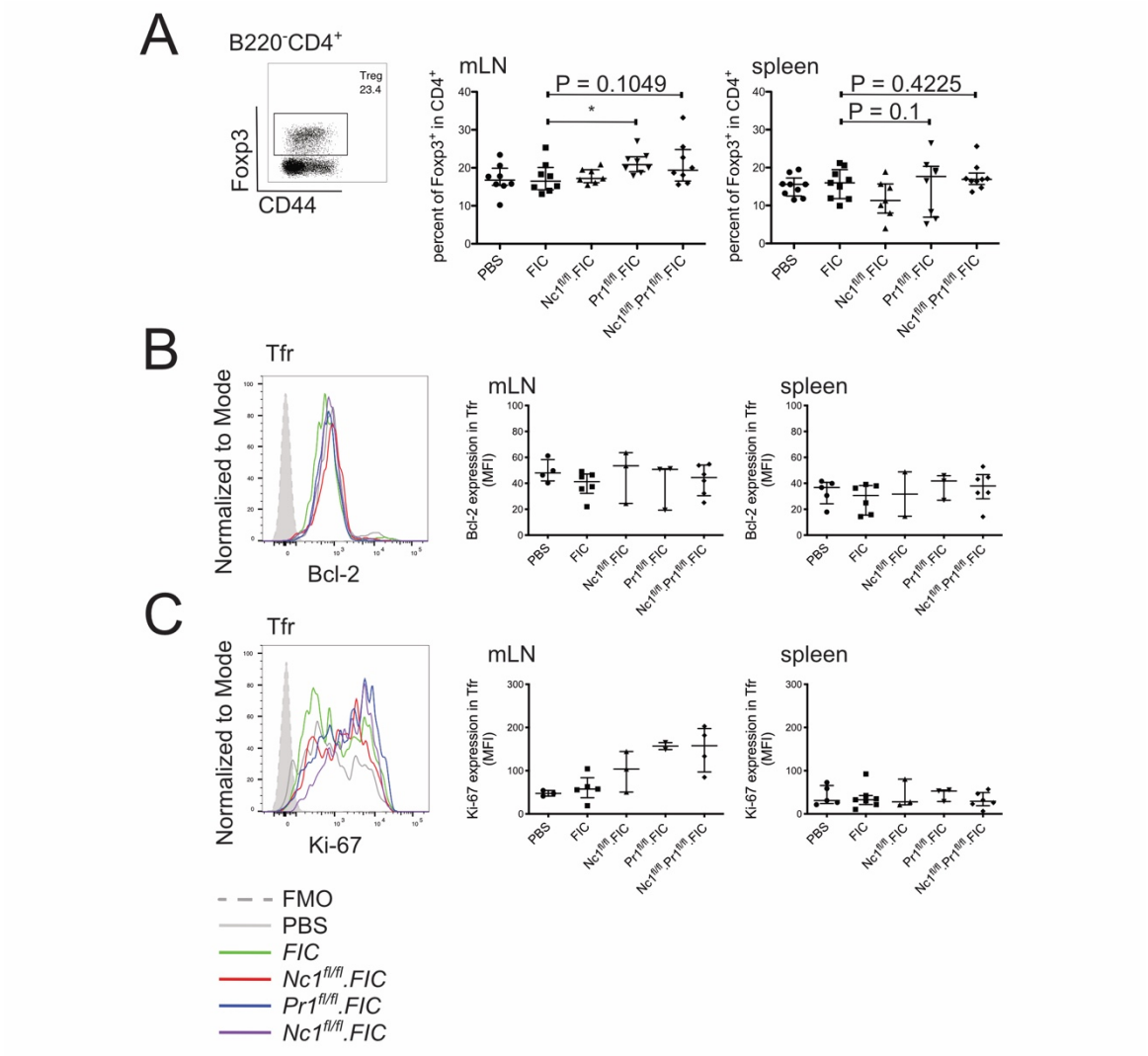

Figure 7.9: Blimp-1 controls Tfr-cell homeostasis

(A-C) Mice were immunized with NP-KLH in ImJect Alum i.p. for 10 days and boosted on day 7. Spleen and mLN were harvested and stained for flow cytometry. (A, left) Representative dot blot of the Treg gating strategy (A, right) Tregs in relative numbers, compilation of 7 independent experiments, Mann-Whitney-test: $n \geq 7$; *, $P \leq 0.05$; **, $P \leq 0.01$. (B, left) Representative histogram showing the Bcl-2 expression in Tfr cells. (B, right) MFI of Bcl-2 normalized to the FMO of Bcl-2. (C, left) Representative histogram showing the Ki67 expression in Tfr cells. (C, right) MFI of Ki-67 normalized to the FMO of Ki-67, (B and C) Compilation of three independent experiments, $n \geq 2$

7.1.6 Blimp-1 deficiency affects Tfr-cell function

Tfr cells control the GC by keeping the numbers of Tfh cells and GCB cells in check. High numbers of Tfr cells should therefore suppress the proliferation of Tfh cells and GCB cells

better than low numbers. We analyzed the frequency of $B220^{-}CD4^{+}CD44^{+}Foxp3^{-}CXCR5^{+}PD\text{-}1^{+}$ Tfh cells via flow cytometry on day 10 p.i. (Fig. 7.10A-C). The *Nc1*$^{fl/fl}$*.FIC* exhibited increased relative Tfh-cell numbers compared to the *FIC* mice, which was especially evident in the spleen and correlated well with the reduced Tfr-cell frequencies (Fig. 7.8B), presumably providing less control on the proliferation of Tfh cells. On the other hand, Blimp-1 deficiency raised relative Tfr-cell numbers significantly (Fig. 7.8B), but Tfh-cell frequencies were not reduced as expected in the respective animals (Fig. 7.10C). Quite the contrary, *Pr1*$^{fl/fl}$*.FIC* and even *Nc1*$^{fl/fl}$*.Pr1*$^{fl/fl}$*.FIC* mice showed a trend towards more Tfh cells compared to the *FIC* mice. We therefore analyzed the Ki-67 expression in Tfh cells (Fig. 7.10D). While the Ki-67 expression increases in Tfh cells of the mLN of *Nc1*$^{fl/fl}$*.FIC, Pr1*$^{fl/fl}$*.FIC* and *Nc1*$^{fl/fl}$*.Pr1*$^{fl/fl}$*.FIC* mice, this effect was not observed in the spleen. However, the tendencies seen in the Ki-67 expression do resemble the tendencies in the relative numbers of Tfh cells in both organs as Blimp-1- and NFATc1.Blimp-1-deficient Tfr cells controlled the proliferation of Tfh cells less in the mLN than in the spleen.

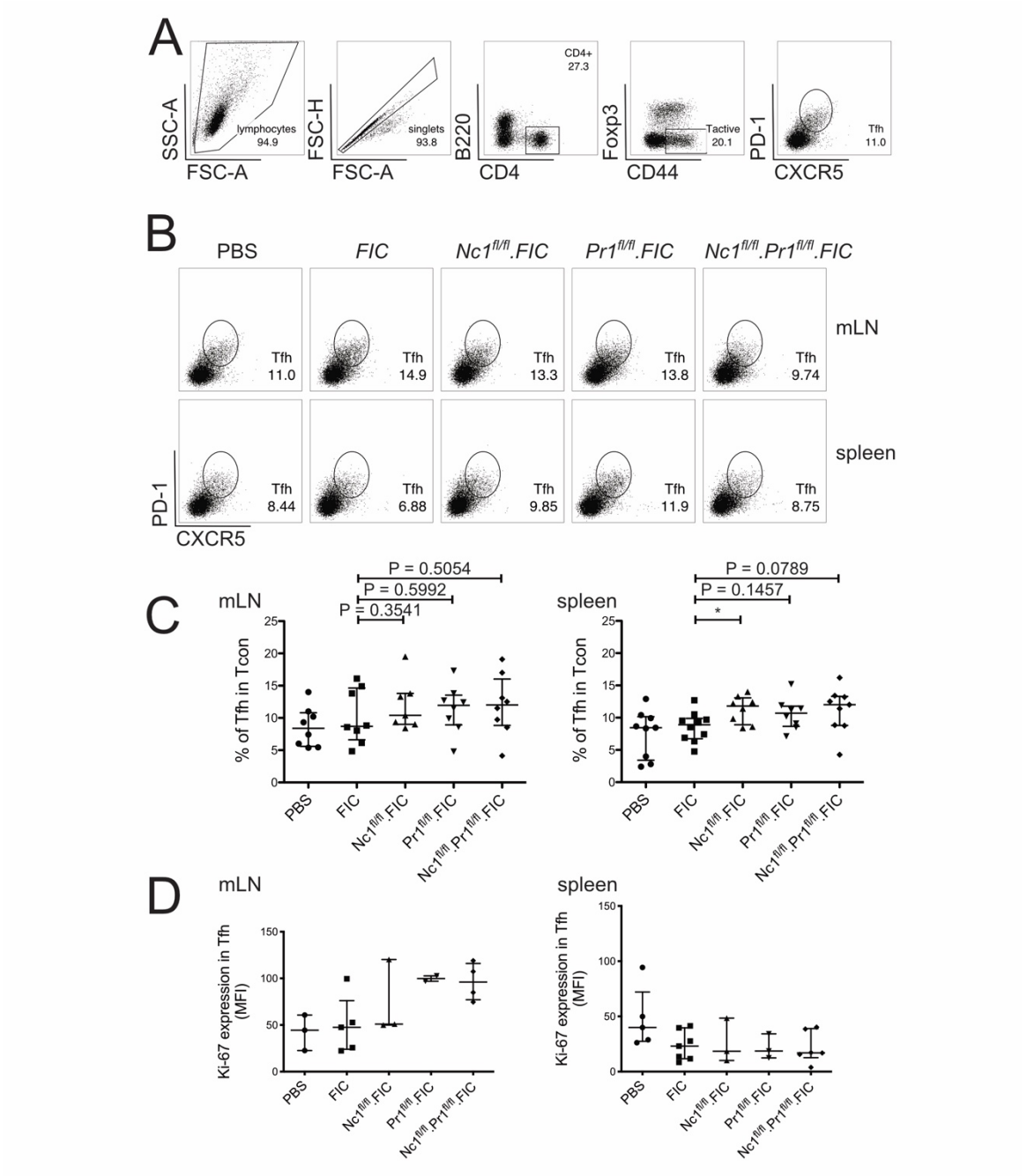

Figure 7.10: Blimp-1 deficiency affects Tfr-cell function - less control of Tfh-cell proliferation

(A-D) Mice were immunized with NP-KLH in ImJect Alum i.p. for 10 days and boosted on day 7. Spleen and mLN were harvested and stained for flow cytometry. (A) Gating strategy of Tfh cells. (B) Representative experiment, relative Tfh cell numbers of mLN and spleen are shown as dot blots. (C) Relative numbers of Tfh cells in mLN and spleen, compilation of 7 independent experiments, Mann-Whitney-test: $n \geq 7$; *, $P \leq 0.05$; **, $P \leq 0.01$. (D) MFI of Ki-67 normalized to the FMO of Ki-67, compilation of three independent experiments, $n \geq 2$

The proportions of Tfr to Tfh cells in the GC and their functional capacity should influence GCB-cell frequencies. In the mLN of *Nc1*$^{fl/fl}$*.FIC*, Tfr cells declined in proportion to Tfh cells compared to the ratio in *FIC* mice, while in the mLN of *Pr1*$^{fl/fl}$*.FIC* and *Nc1*$^{fl/fl}$*.Pr1*$^{fl/fl}$*.FIC* mice Tfr cells were higher in proportion to Tfh cells compared to the situation in the *FIC* mouse (Fig. 7.11A). In spleens of *Nc1*$^{fl/fl}$*.FIC*, the ratio of Tfh to Tfr again changed significantly in favor of Tfh cells. Splenic Tfh cells and Tfr cells from *Pr1*$^{fl/fl}$*.FIC* and *Nc1*$^{fl/fl}$*.Pr1*$^{fl/fl}$*.FIC* mice, however, were similar in their Tfr/Tfh ratio compared to the *FIC* mice.

Next, we analyzed GCB cells (Fig. 7.11B-D). In mLN and spleen of *Nc1*$^{fl/fl}$*.FIC* and *Nc1*$^{fl/fl}$*.Pr1*$^{fl/fl}$*.FIC* mice, more GCB cells could be detected compared to the *FIC*, whereas in the *Pr1*$^{fl/fl}$*.FIC* mice, this increase was only a tendency. The rise of GCB cells in *Nc1*$^{fl/fl}$*.FIC* mice is in line with less Tfr cells as well as a tilted ratio of Tfr to Tfh, while the overall tendency to more GCB cells in *Pr1*$^{fl/fl}$*.FIC* mice and *Nc1*$^{fl/fl}$*.Pr1*$^{fl/fl}$*.FIC* mice was in contradiction to more Tfr cells in proportion to Tfh in the mLN. The latter implies a loss of Blimp-1-ablated Tfrs' capacity to suppress the proliferation of GCB cells. Overall, we claim Blimp-1-deficient Tfr cells to home better to GC, but to lose their suppressive capacity.

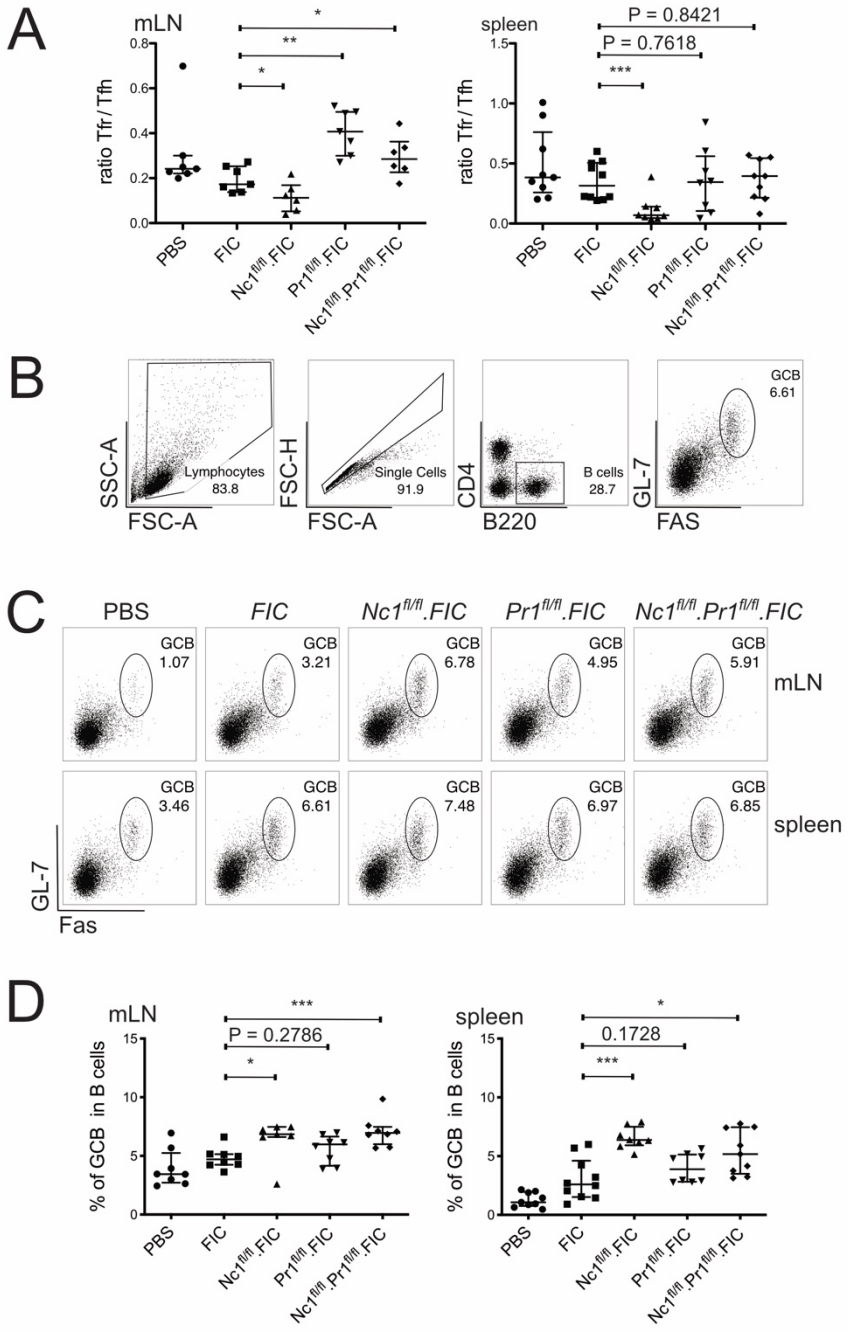

Figure 7.11: Blimp-1 deficiency affects Tfr-cell function - less control of GCB-cell proliferation

(A-D) Mice were immunized with NP-KLH in ImJect Alum i.p. for 10 days and boosted on day 7. Spleen and mLN were harvested and stained for flow cytometry. (A) Tfr/Tfh ratio of absolute numbers. (B) Gating strategy of GCB. (C) Representative experiment, relative GCB-cell numbers of mLN and spleen are shown as dot blots. (D) Relative numbers of GCB cells in mLN and spleen, Compilation of 7 independent experiments, Mann-Whitney-test: $n \geq 7$; *, $P \leq 0.05$; **, $P \leq 0.01$.

7.1.7 NFATc1 and Blimp-1 deficiencies in Tregs add up in the loss of control over humoral immune response

We measured the titers of different anti-NP-isotypes in the serum of NP-KLH immunized *Nc1$^{fl/fl}$.FIC*, *Pr1$^{fl/fl}$.FIC*, *Nc1$^{fl/fl}$.Pr1$^{fl/fl}$.FIC* and *FIC* mice on day 10 p.i. The NP-specific IgG titers were slightly increased in *Nc1$^{fl/fl}$.FIC* and *Pr1$^{fl/fl}$.FIC* mice. However, the highest titers of antibodies directed vs. the antigen of immunization were observed in the *Nc1$^{fl/fl}$.Pr1$^{fl/fl}$.FIC* mice, indicating that the loss of NFATc1 and Blimp-1 in Treg adds up in the functional loss of Tfr cells to control the humoral immune response (Fig. 7.12A). This effect of higher antibody titers similarly holds true in the subclasses IgG1, IgG2b, IgG2c and IgG3 (Fig. 7.13). Similar to NP-specific IgG, NP-specific IgM titers were heightened in the *Nc1$^{fl/fl}$.FIC* and especially in the *Nc1$^{fl/fl}$.Pr1$^{fl/fl}$.FIC* mice (Fig. 7.12B). We measured the ratio of NP-specific antibodies of high affinity vs. the ones of low affinity (Fig. 7.12C). Both NFATc1 and Blimp-1 ablation in Tregs, but especially double-deficiency led to an enhanced affinity maturation, although the data did not reach significance. In order to evaluate if the overall humoral immune response was changed, we checked the levels of overall IgG independent of their specificity in the sera of immunized mice 10 days p.i. (Fig. 7.12D). The amount of IgG was elevated in *Nc1$^{fl/fl}$.FIC* and even more in *Nc1$^{fl/fl}$.Pr1$^{fl/fl}$.FIC* mice compared to wildtypic *FIC*, indicating that NFATc1 in Tregs plays a major function in the overall control of humoral immune responses. The buildup of total IgG in the sera of immunized mice suggested an autoreactive phenotype. We therefore checked the levels of double-stranded (ds) DNA-specific IgG in the sera of NP-KLH-immunized mice before immunization and on day 10 p.i. (Fig. 7.12E). We observed slightly increased anti-ds DNA IgG titers in the *Nc1$^{fl/fl}$.FIC* mice prior to immunization and on day 10 p.i.. Some *Nc1$^{fl/fl}$.Pr1$^{fl/fl}$.FIC* mice also showed high levels of anti-ds DNA IgG titers 10 days p.i.. It seems that the loss of NFATc1 in Tregs provokes an overall increase of antibodies in the blood irrespective of antigen specificity, while Blimp-1-deficient Tregs specifically lose the control over the antigen-specific immune response.

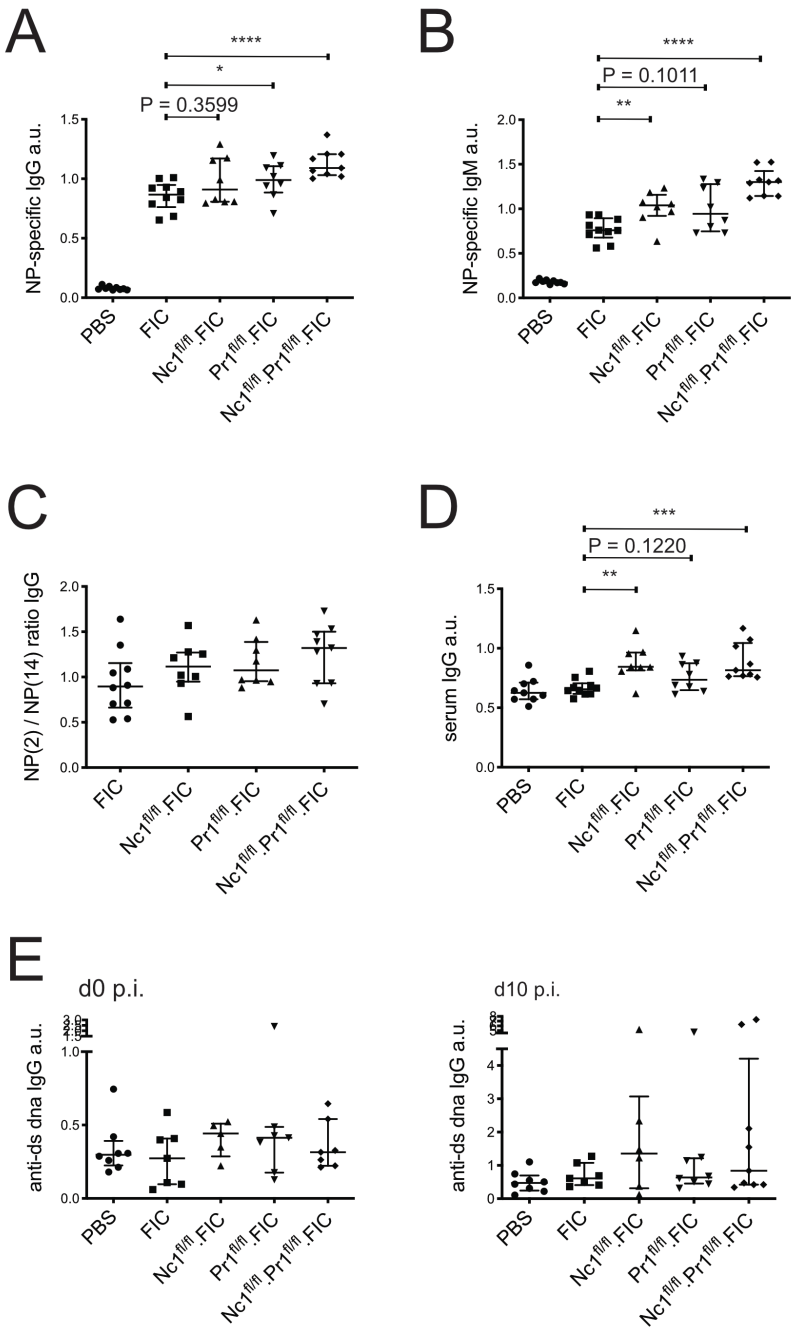

Figure 7.12: NFATc1 and Blimp-1 deficiencies in Tregs add up to the loss of control of humoral immune response

(A-D, E, left) Mice were immunized with NP-KLH in ImJect Alum i.p. for 10 days and boosted on day 7. (A-E) Antibodies in the serum of the mice were measured via ELISA. Sera were carefully titrated and set in reference to a reference serum (pool of sera from NP-immunized mice, arbitrary units (a.u.)). (A) NP-specific IgG. (B) NP-specific IgM. (C) Ratio of NP-specific antibody titers of high affinity (NP-2) vs. low affinity (NP-14). (D) Serum IgG quantification (E, left) Anti-ds DNA IgG measured in serum prior to immunization. (E, right) Anti-ds DNA IgG measured in serum on day 10

p.i. (A-E) Compilation of 7 independent experiments, Mann-Whitney-test: n ≥ 8; *, P ≤ 0.05; **, P ≤0.01.

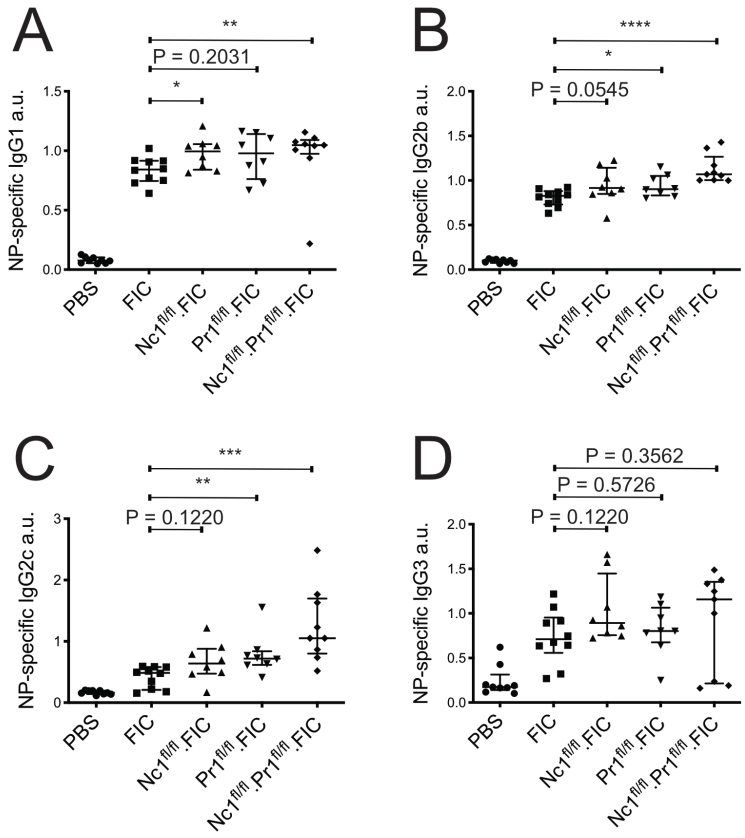

Figure 7.13: NFATc1 and Blimp-1 deficiencies in Tregs add up to the loss of control of the humoral immune response

(A-D) Mice were immunized with NP-KLH in ImJect Alum i.p. for 10 days and boosted on day 7. Antibodies in the serum of the mice were measured via ELISA. Sera were carefully titrated and set in reference to a reference serum (pool of sera from NP-immunized mice, (a.u.). (A) NP-specific IgG1. (B) NP-specific IgG2b. (C) NP-specific IgG2c. (D) NP-specific IgG3. (A-D) Compilation of 7 independent experiments, Mann-Whitney-test: n ≥ 8; *, P ≤ 0.05; **, P ≤ 0.01.

7.1.8 NFATc1 and Blimp-1 influence the migration of Foxp3$^+$ cells into the GC and therewith control Tfr-cell differentiation

We suspected the Tfr cells, which we previously analyzed via flow cytometry to be impaired in their migration capacity to the B-cell follicle and the GC and it seemed to be worthwhile to determine the numbers of Foxp3$^+$ cells that localize to the GC itself.

Therefore, we counted the Foxp3$^+$ cells in the B-cell follicle vs. those in the GC. We immunized *Nc1$^{fl/fl}$.FIC*, *Pr1$^{fl/fl}$.FIC*, *Nc1$^{fl/fl}$.Pr1$^{fl/fl}$.FIC* and *FIC* as described (Fig. 7.7). Immune histology fluorescent (IHF) stainings were performed on sections of mLNs (Fig. 7.14A). The B220$^+$ area indicates the B-cell zone, the CD3$^+$ area marks the T-cell zone, the PNA$^+$ area equals the GC and Tregs are defined as Foxp3$^+$ cells. The ligand for CXCR5, namely CXCL13 is secreted by FDCs and shapes the B-cell zone as B cells express CXCR5. We found reduced numbers of Foxp3$^+$ cells in the B-cell follicle as well as in the GC in *Nc1$^{fl/fl}$.FIC* mice (Fig. 7.14B and C), confirming the reduction of Tfr-cell frequencies described via surface markers and flow cytometry. Foxp3$^+$ cells were enriched in the B-cell zone and the GC in *Pr1$^{fl/fl}$.FIC* mice correlating with high Tfr-cell frequencies detected by flow cytometry. Enrichment of Blimp-1-deficient Tfr cells was more pronounced in the B-cell zone than in the GC itself. Interestingly, *Nc1$^{fl/fl}$.Pr1$^{fl/fl}$.FIC* mice revealed similar numbers of Foxp3$^+$ cells as *FIC* mice in these areas. In conclusion, the reduction of Tfr cell numbers caused by a Treg-specific NFATc1 knockout could be to a certain extend reversed via the Blimp-1 knockout. *Vice versa*, the loss of homeostasis caused by a Blimp-1 deficiency was compensated via the NFATc1 knockout.

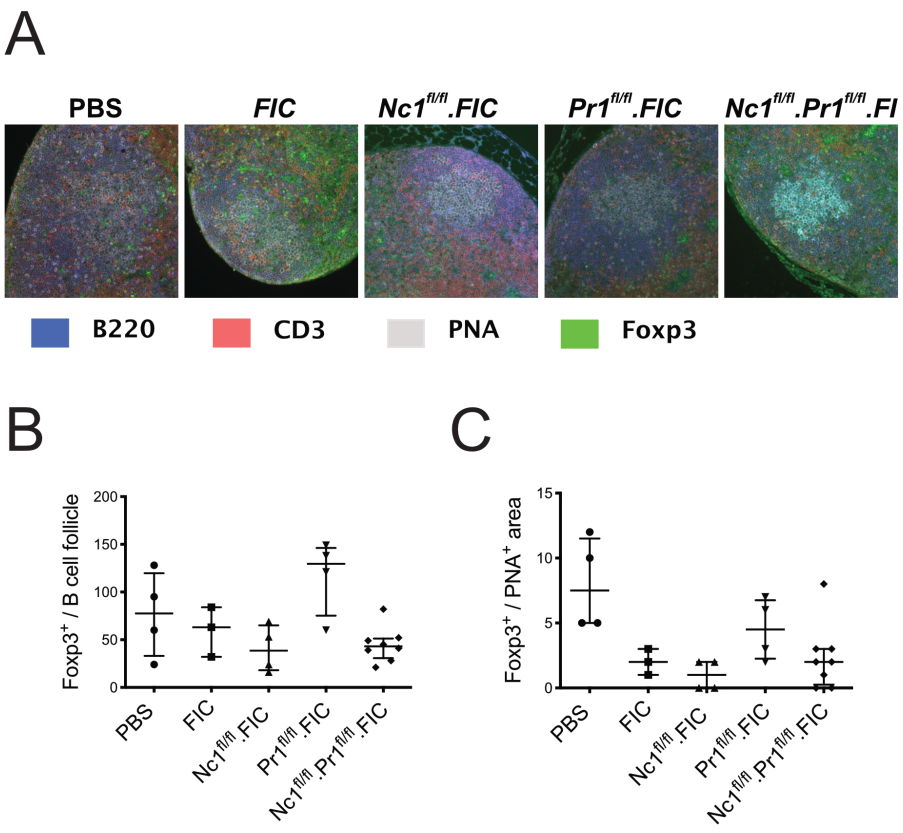

Figure 7.14: NFATc1 and Blimp-1 influence the migration of Foxp3$^+$ cells into the GC and therewith control Tfr-cell differentiation

(A-C) Mice were immunized with NP-KLH in ImJect Alum i.p. for 10 days and boosted on day 7. MLN were extracted and IHF stainings were performed. (A) Representative pictures of stained GC: blue: B220, red: CD3, grey: PNA, green: Foxp3. (B) Numbers of Foxp3$^+$ per follicle. (C) Numbers of Foxp3$^+$ per GC.

7.1.9 NFATc1 knockout affects the effector molecule CTLA-4

We were interested in the loss of function in Blimp-1-deficient Tfr cells. A central mechanism of Treg/Tfr cell exerted suppression is mediated by the coinhibitory receptor CTLA-4. To this end, we evaluated the expression of CTLA-4 on the surface and intracellularly via flow cytometry. We observed a slight decrease in CTLA-4 expression in the Tfr cells of *Nc1$^{fl/fl}$.FIC* mice compared to *FIC* mice in spleen as well as mLN. *Pr1$^{fl/fl}$.FIC* mice did not show a change in CTLA-4 expression, neither in the mLN nor in the spleen. A weak decline was also observed in the *Nc1$^{fl/fl}$.Pr1$^{fl/fl}$.FIC* mice in the spleen, indicating that NFATc1 deficiency results in less CTLA-4 expression irrespective of the presence of Blimp-1 (Fig. 7.15).

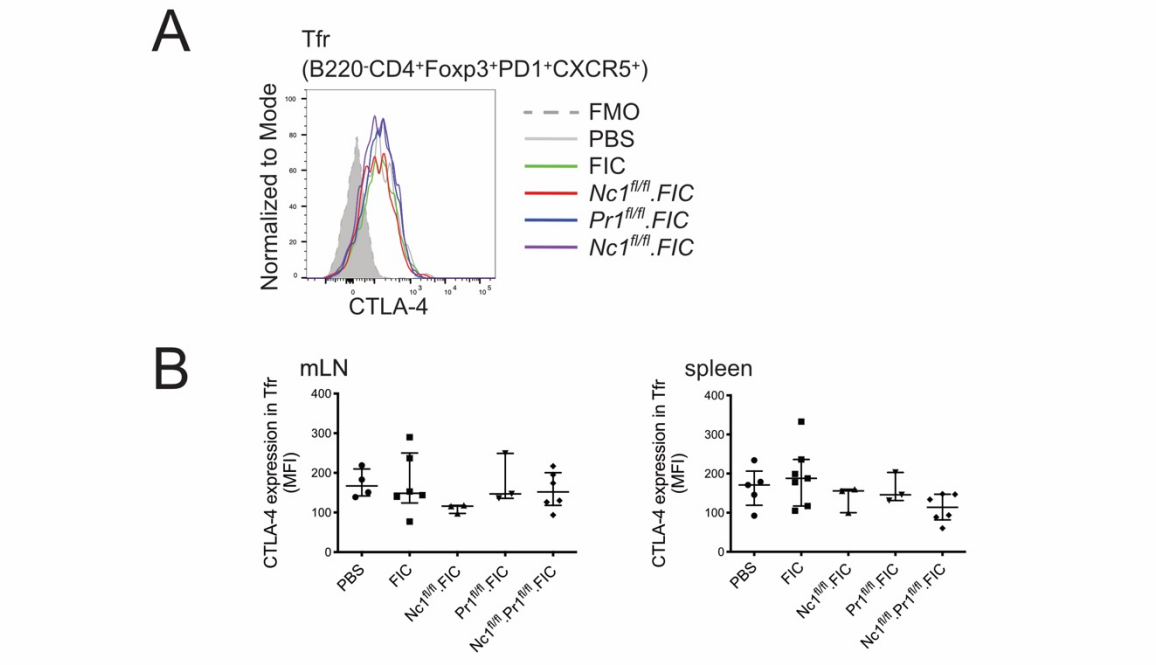

Figure 7.15: NFATc1 deficiency in Tregs reduces CTLA-4 expression

Mice were immunized with NP-KLH in ImJect Alum i.p. for 10 days and boosted on day 7. Spleen and mLN were harvested and stained for flow cytometry. (A) Representative histogram showing the CTLA-4 expression in Tfr cells. (B) MFI of CTLA-4 in Tfr cells, compilation of three independent experiments, $n \geq 2$

7.1.10 NFATc1 and Blimp-1 change the expression of Tfh signature genes involved in posttranslational modification and signal transduction

In order to understand the role of Blimp-1 for the function of Tfr cells, we isolated Blimp-1$^+$ Tfr cells via fluorescence-activated cell sorting (FACS). We took advantage of the Blimp-1 reporter strain *Pr1^{gfp}* and crossed it into the *Nfatc1* and *Prdm1* Treg-specific conditional knockouts. *Pr1$^{+/gfp}$.FIC*, *Nc1$^{fl/fl}$.Pr1$^{+/gfp}$.FIC* and *Pr1$^{fl/gfp}$.FIC* mice were immunized for 10 days with NP-KLH in ImJectAlum and boosted on day 7 p.i. (Fig. 7.16A). On day 10 p.i. we isolated the CD4$^+$B220$^-$GFP$^+$CXCR5$^+$GITR^{hi} cells (Fig. 7.16B), extracted the RNA and performed next generation RNA sequencing.

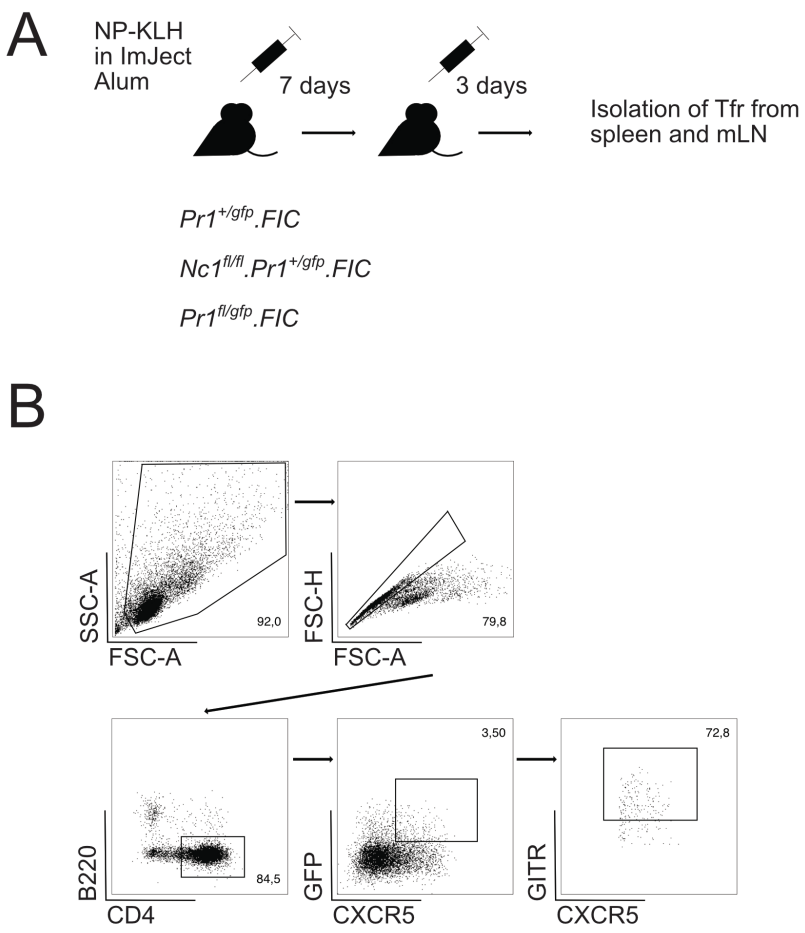

Figure 7.16: Isolation of Blimp-1-expressing Tfr cells after immunization with NP-KLH

(A) Mice were immunized with NP-KLH i.p. and boosted on day 7. Spleen and mLN were isolated on day 10. (B) $CD4^+$ T cells were preselected and stained for Tfr-cell markers. Tfr cells defined as $B220^-$ $CD4^+BlimpGFP^+CXCR5^+GITR^{hi}$ were isolated via FACS.

We were searching for enriched gene ontology terms (GO-terms) within the gene sets that were at least twofold differentially expressed between the *FIC* and the *Nc1$^{fl/fl}$.FIC* mice or the *FIC* and the *Pr1$^{fl/fl}$.FIC* mice using the Gene Ontology enRIchment anaLysis and visuaLizAtion tool (Gorilla) [144, 145]. The gene sets being differentially regulated between *FIC* and *Nc1$^{fl/fl}$.FIC* (Tab. S1) as well as *Pr1$^{fl/fl}$.FIC* and *FIC* (Tab. S2) did show no enrichment of GO-terms with a p-value less than 10^{-7}, which is considered to be a rather low probability. None of the GO-terms that were enriched in this gene sets were considered to be associated with a loss of function in Tfr-cell suppressive capacity. We wanted to delimit the genes that are of importance for the Tfr-cell function and phenotype from the

whole set of differentially expressed genes. Therefore, we took advantage of RNA-seq data published by the Sage lab [142]. We defined a set of genes that are differentially expressed between Tfh cells and Tfr cells in draining LNs and the spleen (Fig. 7.17A) using the RNA-seq data publicly available. The gene sets differing between *FIC* and either conditional knockout were filtered for genes that are differentially expressed between Tfh cells and Tfr cells (Tfh-cell signature). We suspected the loss of function in Tfr cells due to the conditional knockout of NFATc1 and Blimp-1 in Tregs to originate from a shift in the transcriptional profile into the direction of Tfh cells. Therefore, we filtered the RNA-seq data generated from sorted Tfr cells from *FIC*, $Nc1^{fl/fl}$*.FIC* and $Pr1^{fl/fl}$*.FIC* for differentially expressed genes that were part of the Tfh-cell signature and visualized the change in gene expression between *FIC* and either conditional knockout within two heat maps (Fig. 7.17B). One heat map represented the genes that were upregulated in Tfh cells and the other one the genes, which were downregulated in Tfh cells. Unfortunately, we were only able to generate a duplicate of RNA-seq data from $Pr1^{fl/fl}$*.FIC*. Looking at the differences between these two individuals, one can tell that a higher n-size might be necessary to understand more about the changes between all of the groups. Nevertheless, we observed differentially regulated genes coding for enzymes that play a role within posttranslational modifications. We found three genes coding for proteins that are involved in ubiquitylation, a posttranslational modification that marks proteins for their proteasomal degradation or influences signal transduction pathways by altered protein-protein interaction [155, 156]. The gene *Rnf103* e.g. codes for the E3 ubiquitin-protein ligase RNF103. *Rnf103* is slightly upregulated due to the deletion of NFATc1 and highly upregulated in one of the Blimp-1-deficient individuals. Another E3 ubiquitin-protein ligase named SIAH1A is highly upregulated in Tfr cells of one of the $Pr1^{fl/fl}$*.FIC. Arrdc4* is coding for the Arrestin domain-containing protein 4. This protein functions as an adapter that is recruiting ubiquitin protein ligases to their substrates [157]. A few genes coding for signal transducing proteins were also differentially expressed due to the NFATc1 or Blimp-1 deletion in Tregs. The gene *Tnfsf9* is coding for the Tumor necrosis factor ligand super family member 9 (TNFSF9 / 4-1BBL / CD137L), which is the ligand to the receptor TNFRSF9 (4-1BB / CD137). *Tnfsf9* is lower expressed in NFATc1-deficient Tfr cells and lowest in Blimp-1 deficient Tfr cells. The gene *Pmepa1* was down regulated in NFATc1 as well as Blimp-1-deficient Tfr cells. *Pmepa1* codes for Prostate transmembrane protein, androgen induced 1 (PMEPA1). PMEPA1 is shown to block TGF-β signaling in prostate

cancer cells [158]. NFATc1, as well as Blimp-1-deficient Tfr cells showed increased expression of *Myd88*, coding for Myeloid differentiation primary response protein 88 (MyD88), an adapter protein that is involved in multiple signal transduction pathways. Blimp-1-deficient Tfr cells showed elevated expression of *Ikzf4*. The gene *Ikzf4* codes for the zinc finger protein Eos, which is involved in the transcriptional regulation in Tregs. Surprisingly, we found an elevated expression of *Il10* in Blimp-1-deficient Tfr cells. This was unexpected, as Blimp-1 is known for its transactivating function on the *Il10* gene [159].

7.1.11 Blimp-1 deficiency supports Tfr-cell survival via enhanced *Bcl2a1a* expression

We observed enhanced levels of *Bcl2a1a* expression (Fig. 7.17B). *Bcl2a1* – itself expressed in three functional isoforms Bcl2A1α, β and δ - is a family member of the *Bcl-2* family belonging to the subgroup of anti-apoptotic members. It was reported previously that Blimp-1 limits the expression of the pro-survival molecule Bcl-2, the eponymous member of the family of anti- and pro-apoptotic molecules [135], while our group has plenty indications for Blimp-mediated repression of Bcl2a1 isoforms (Xiao, Qureischi, Dietz et al., in revision). Therefore, the increase of *Bcl2a1a* expression might explain the high frequencies of Tfr cells observed in the $Prdm1^{fl/fl}$.*FIC*.

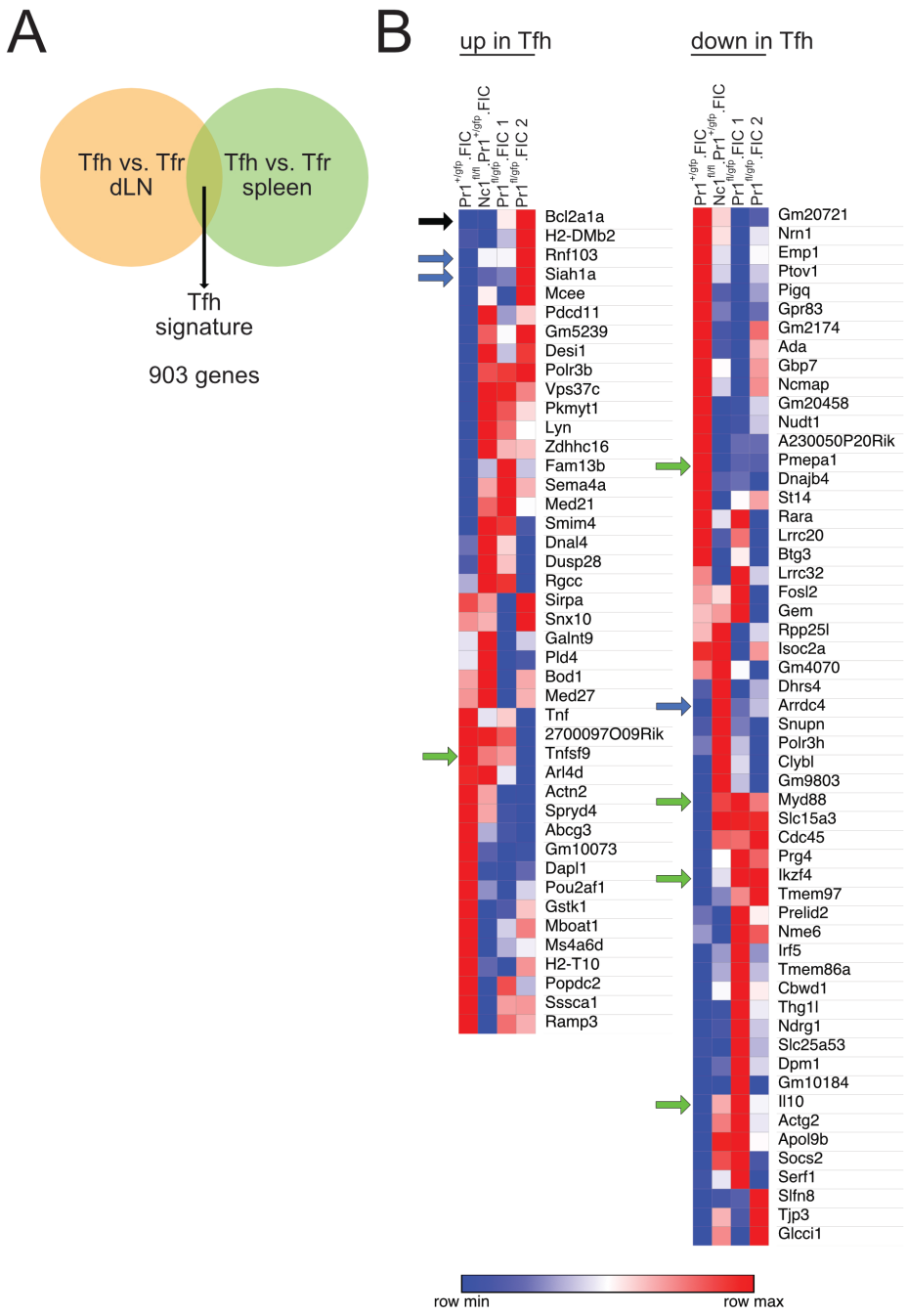

Figure 7.17: Changes in the Tfh-cell signature of Tfr cells due to NFATc1 and Blimp1-knockout

(A) The Tfh-cell signature was deduced from RNA-Seq-Data of sorted Tfh and Tfr cells from draining LNs and spleen of three mice that were immunized with NP-Ova. The gene sets were filtered for genes that differed at least twofold in expression between the groups, showing a mean expression level of at least five in at least one of the groups. The data was published by the Sage group and found at Gene Expression Omnibus database (accession no.GSE124884) (B) Tfr cells were sorted from *Pr1*$^{+/gfp}$*.FIC*, *Nc1*$^{fl/fl}$*.Pr1*$^{+/gfp}$*.FIC* and *Pr1*$^{fl/gfp}$*.FIC* mice as described in

Fig. 7.16 and subjected to RNA-seq analysis. Heatmap showing the expression of genes of the Tfh-cell signature that differed at least twofold in Tfr cells between *Pr1*$^{+/gfp}$*.FIC* and at least one of the knockouts. Arrows indicate genes that show trends of differential regulation due to the knockouts, black: apoptosis regulating protein, blue: posttranslational modifying protein, green: protein involved in signal transduction

7.2 Overexpression of caNFATc1/αA in Tregs and its influence on the GCR

7.2.1 Overexpression of a constitutive active form of NFATc1/αA increases CXCR5 expression on Tregs, but not Tfr-cell frequencies

NFATc1 deficiency in Tregs limited Tfr-cell numbers via halted CXCR5 expression. Therefore, we decided to test if the overexpression of a constitutive active form of NFATc1/αA (caNFATc1/αA) has an impact on CXCR5 expression on Tregs. We used mice, in which the transgene coding for caNFATc1/αA was preceded by a loxP-flanked stop cassette, all placed into the *Rosa-26* locus (*R26-caNfatc1aA-Stop*$^{fl/fl}$: designated thereafter *Nc1*^{caaA}). In order to generate Treg-specific caNFATc1/αA-overexpressing mice, we bred them with *FIC* mice (*Nc1*^{caaA}*.FIC*). We observed an increase of the CXCR5 expression on Tregs especially in the spleen, but also in mLN in the steady state of four months old mice (Fig. 7.18A).Relative Tfr-cell numbers were slightly reduced in the spleen but did not change in mLN (Fig. 7.18C, upper and 7.18D, upper). However, Tfh-cell frequencies were drastically reduced due to the overexpression of caNFATc1/αA in Tregs (Fig. 7.18C, lower and Fig. 7.18D, lower).

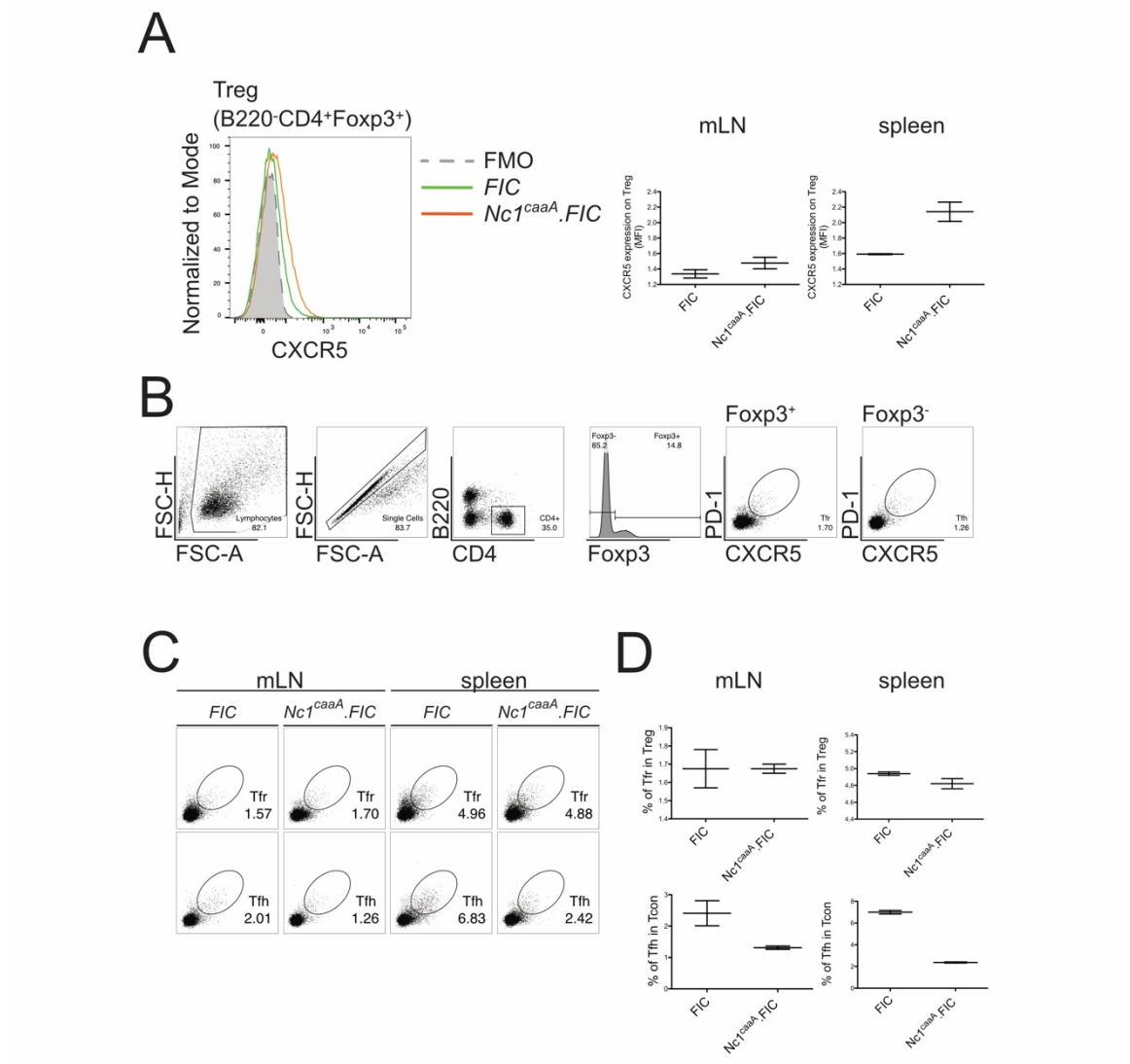

Figure 7.18: Overexpression of caNFATc1/αA enhances CXCR5 expression in Tregs and reduces Tfh-cell frequencies in the steady state

(A) CXCR5 expression on Tregs, MFI normalized via the FMO of CXCR5. (B) Gating strategy of $B220^{-}CD4^{+}Foxp3^{+}PD\text{-}1^{+}CXCR5^{+}$ Tfr cells and $B220^{-}CD4^{+}Foxp3^{-}PD\text{-}1^{+}CXCR5^{+}$ Tfh cells (C) Representative flow cytometry of relative Tfr and Tfh-cell numbers in mLN and spleen in the steady state. (D, upper) Tfr-cell frequencies shown as percentage of Tregs. (D, lower) Tfh-cell frequencies shown as percentage of Tcon.

We immunized these mice, boosted on day 7 and checked the CXCR5 expression on Tregs via the MFI of CXCR5 on day 10 (Fig. 7.19A). *Nc1^{caaA}.FIC* mice elicited an almost twofold higher CXCR5 expression on Tregs in mLN compared to wildtypic *FIC* mice. In the spleen the expression was increased even 3,5-fold (Fig. 7.19B). Surprisingly, this elevated CXCR5 expression was not reflected by abundant Tfr-cell frequencies. On the contrary,

the *Nc1^{caaA}.FIC* mice responded with even less Tfr cells in mLN than the *FIC* mice (Fig. 7.19C and D). Taken together, NFATc1 is necessary for and efficient in transactivation of *Cxcr5* in Tregs.

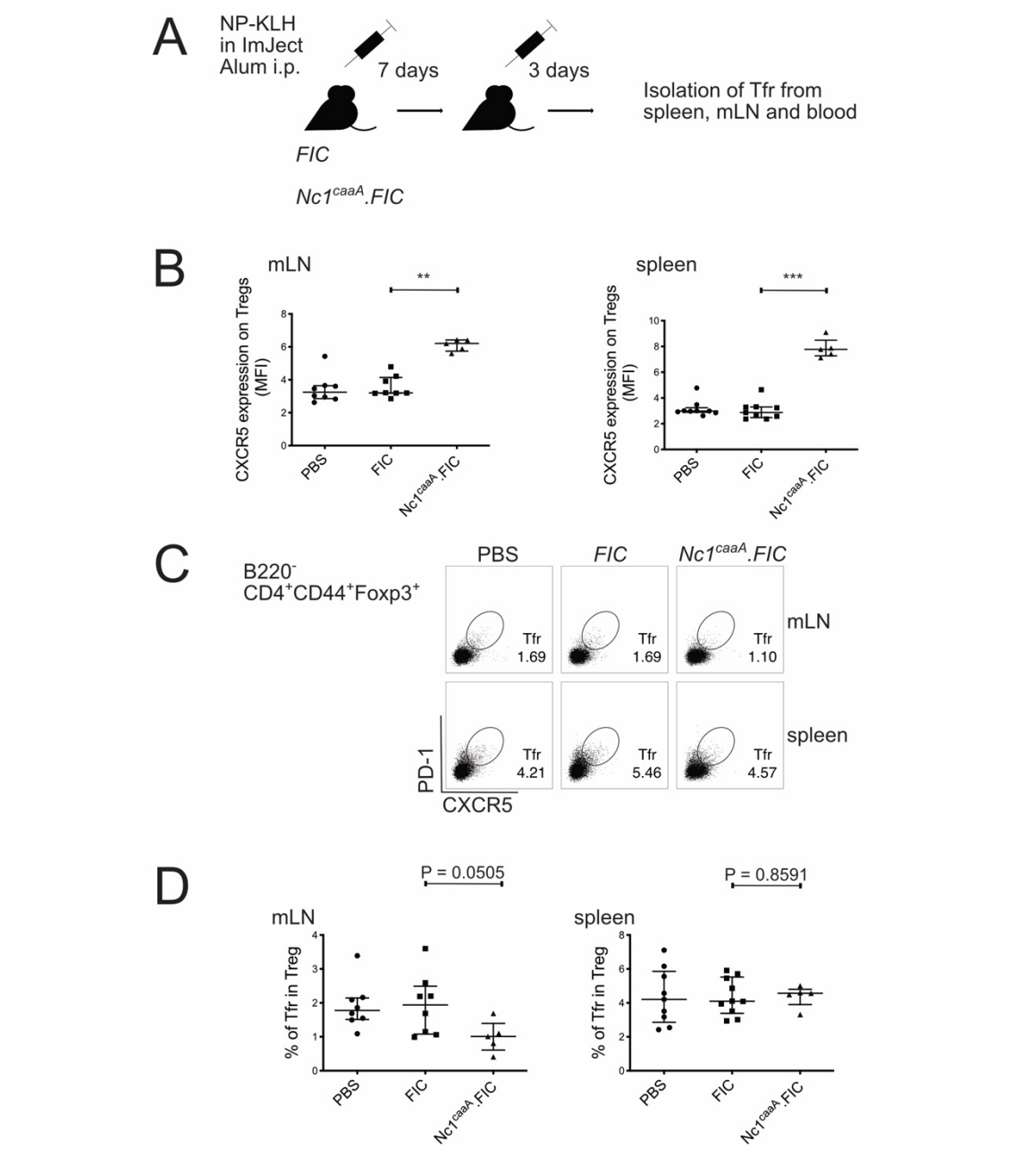

Figure 7.19: Overexpression of caNFATc1/αA increases CXCR5 expression, but not Tfr-cell frequencies

Mice were immunized with NP-KLH in ImJect Alum i.p. for 10 days and boosted on day 7. Spleen and mLN were harvested and stained for flow cytometry. Blood was taken for serological analyses. (A) Scheme of experiment (B) CXCR5 expression on Tregs, MFI normalized via the FMO of CXCR5. (C) Representative flow cytometry of Tfr-cell frequencies in

spleen and mLN 10 d after NP-KLH immunization. (D) Tfr-cell frequencies shown as percentage of Tregs. (B-D) Compilation of 7 independent experiments, PBS and *FIC* control groups also shown in Fig. 7.8 - Fig. 7.13 and Fig. 7.15, Mann-Whitney-test: $n \geq 5$; *, $P \leq 0.05$; **, $P \leq 0.01$

7.2.2 Overexpression of caNFATc1/αA increases Tfr-cell numbers especially in the GC

We observed a tendency towards less relative *Nc1^{caaA}* Tfr-cell numbers in mLN via flow cytometry (Fig. 7.19D), but flow cytometry cannot distinguish between a Tfr cell that is localized in the B-cell zone and one that is localized directly in the GC. We immunized mice according to the scheme in Fig. 7.19A and recorded the localization of Foxp3$^+$ cells in the mLN via IHF staining of sections made from mLN (Fig. 7.20A). In general, most of the Tfr cells were confined to the overall B-cell zone and rather few numbers were found in the GC themselves (Fig. 7.20B and C). Intriguingly though, overexpression of caNFATc1/αA in Tregs increased the numbers of Foxp3$^+$ cells in the GC itself, while it raised the numbers of Foxp3$^+$ cells in the B-cell zone only slightly. Therefore, the level of CXCR5 on the surface determines the distribution between B-cell zone and GC.

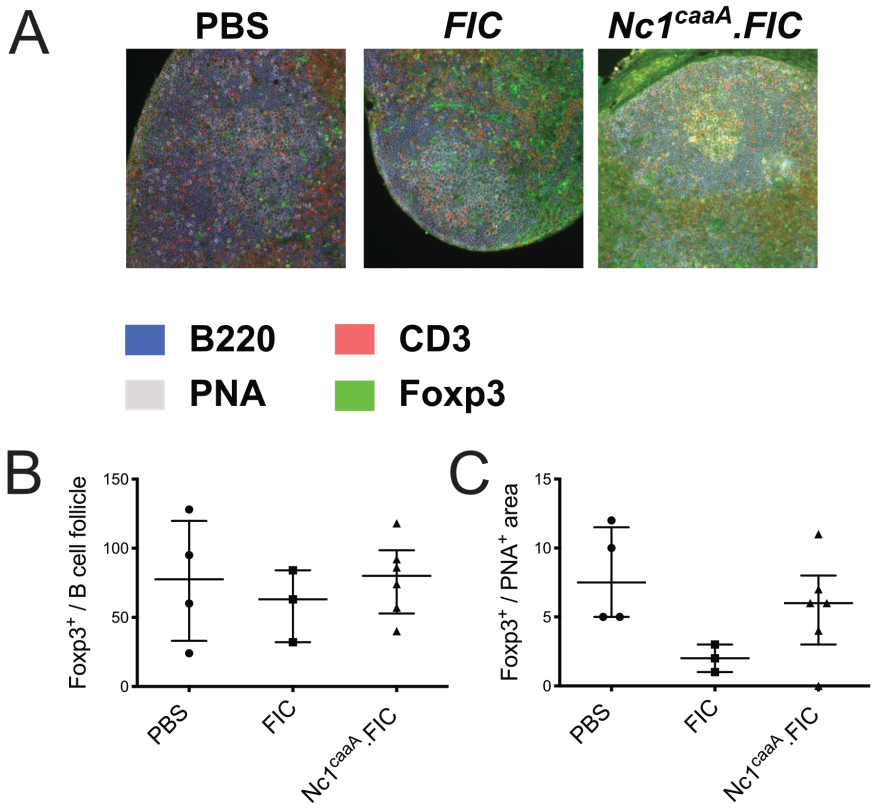

Figure 7.20: Overexpression of caNFATc1/αA increases the number of Tfr cells especially in the GC

Mice were immunized with NP-KLH in ImJect Alum i.p. for 10 days and boosted on day 7. mLN were extracted and IHF stainings were performed. (A) Representative pictures of stained GCs: blue: B220, red: CD3, grey: PNA, green: Foxp3. (B) Numbers of $Foxp3^+$ per B cell follicle. (C) Numbers of $Foxp3^+$ per GC. (B and C) PBS and *FIC* control groups also shown in Fig 7.14

7.2.3 The antigen-specific humoral immune response is reduced in *Nc1^{caaA}.FIC* mice

Immunized *Nc1^{caaA}.FIC* mice did not show changes in relative Tfh-cell numbers (Fig. 7.21A), while there was a tendency to less GCB cells especially in the spleen (Fig. 7.21B). In the steady state, even Tfh-cell frequencies had been severely reduced due to overexpression of caNFATc1αA (Fig. 7.18D, lower). This indicates at least that the overexpression of caNFATc1/αA in Tregs did not hamper the suppressive capacity of Tfr cells.

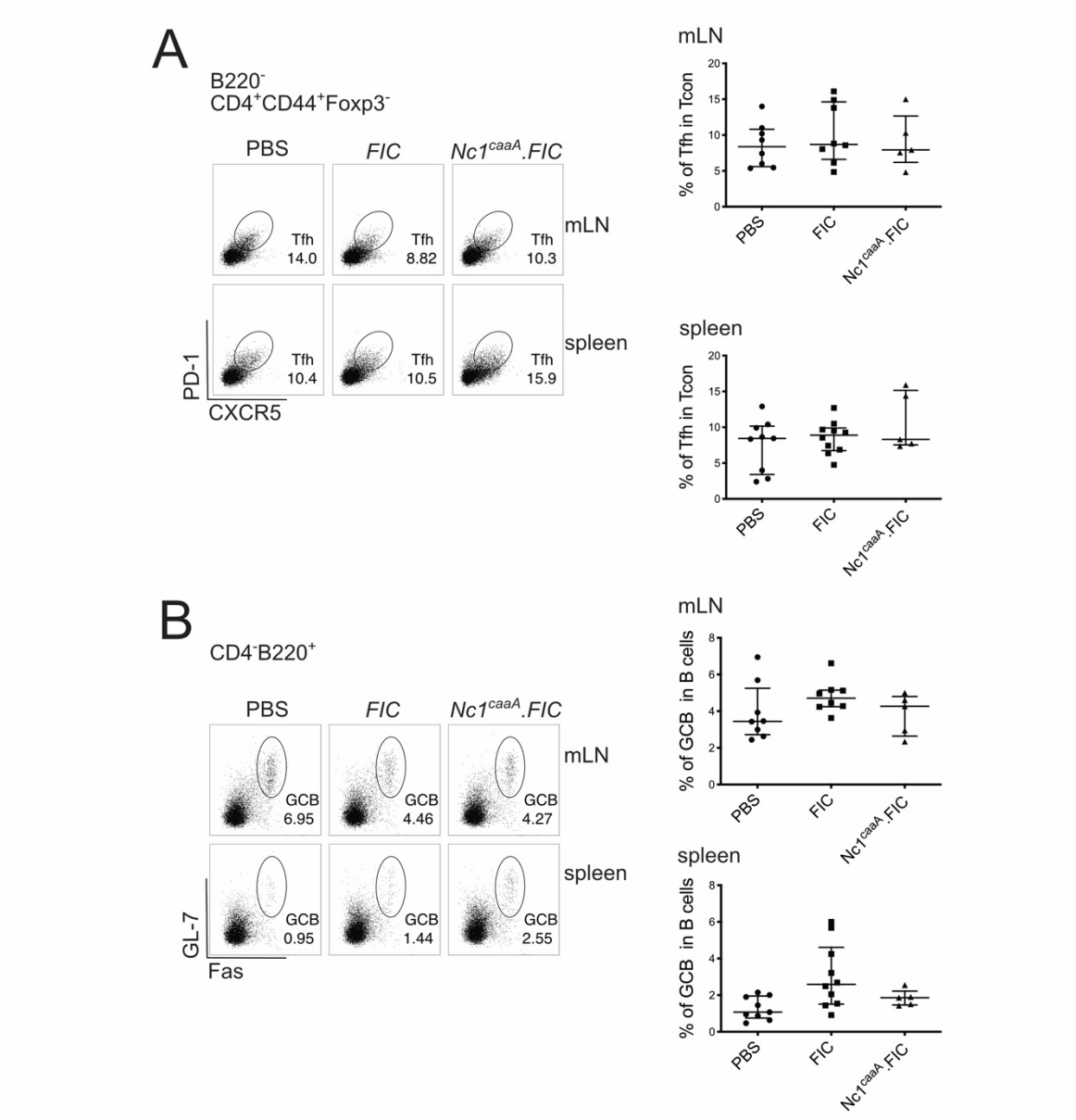

Figure 7.21: Overexpression of caNFATc1/αA does not affect relative Tfh-cell numbers, but slightly reduces GCB-cell frequencies

Mice were immunized with NP-KLH in ImJect Alum i.p. for 10 days and boosted on day 7. Spleen and mLN were harvested and stained for flow cytometry. (A, left) Representative flow cytometry of Tfh-cell frequencies in spleen and mLN 10 d after NP-KLH immunization. (A, right) Frequencies of Tfh cells in mLN and spleen. (B, left) Representative flow cytometry of GCB-cell frequencies in spleen and mLN 10 d after NP-KLH immunization. (B, right) Frequencies of GCB cells in mLN and spleen. (A and B) Compilation of 7 independent experiments, PBS and *FIC* control groups also shown in Fig. 7.8 - Fig. 7.13 and Fig. 7.15

The final product of the GCR are plasma cells, which have undergone SHM and CSR. If one of these processes is affected in *Nc1^{caaA}.FIC* mice, the amount of NP-specific IgG as well as the affinity of the same should be different compared to *FIC* mice. Indeed, the titer of NP-specific IgG was significantly lower in *Nc1^{caaA}.FIC* mice compared to *FIC* mice (Fig. 7.22A). The subclasses IgG1, IgG2b, IgG2c and IgG3 showed trends similar to total Ag-specific IgG (Fig. 7.23). NP-specific IgM was also reduced in *Nc1^{caaA}.FIC* mice compared to *FIC* mice indicating that the overall antigen-specific humoral immune response decreased in these mice (Fig. 7.22B). Nonetheless, the affinity of NP-specific antibodies did not change in *Nc1^{caaA}.FIC* mice (Fig. 7.22C). Overall IgG titers were not affected in *Nc1^{caaA}.FIC* mice (Fig. 7.22D). This indicated that the overexpression of caNFATc1/αA in Tregs specifically reduced the humoral immune response for the antigen of immunization. We furthermore recorded the IgG titers vs. dsDNA in the serum prior to immunization and on day 10 p. i. (Fig. 7.22E). *Nc1^{caaA}.FIC* mice tended to show less anti-dsDNA IgG in the serum compared to *FIC* mice, in line with a tighter control of the GCR.

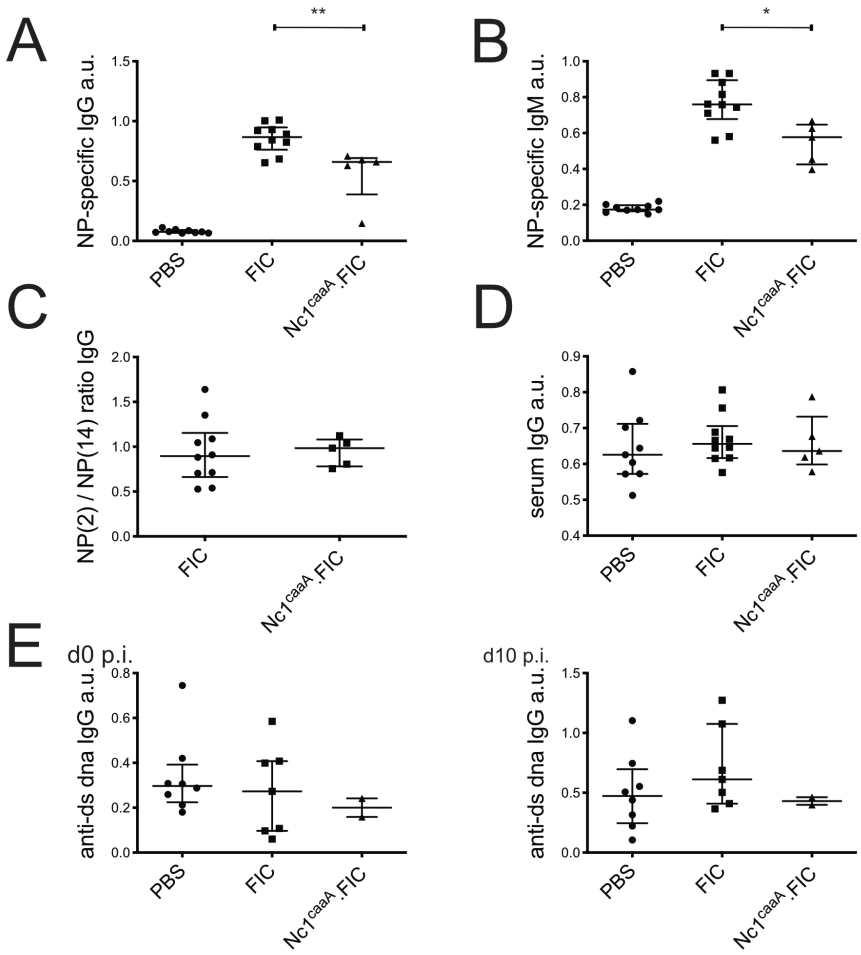

Figure 7.22: Overexpression of caNFATc1/αA in Tregs reduces antigen-specific humoral immune response

Mice were immunized with NP-KLH in ImJect Alum i.p. for 10 days and boosted on day 7. Antibodies in the serum of the mice were measured via ELISA. Sera were carefully titrated and set in reference to a reference serum (pool of sera from NP-immunized mice), (a.u.). (A) NP-specific IgG. (B) NP-specific IgM. (C) Ratio of NP-specific antibody titers of high affinity (NP-2) vs. low affinity (NP-14). (D) IgG titer in the serum of immunized mice. (E, left) Anti-dsDNA IgG titers in the serum of mice prior to immunization. (E, right) Anti-dsDNA IgG titers in serum of immunized mice, 10d p.i. (A-E) Compilation of 7 independent experiments; $n \geq 2$, PBS and *FIC* control groups also shown in Fig. 7.8 - Fig. 7.13 and Fig. 7.15, (A and B) Mann-Whitney-test: *, $P \leq 0.05$; **, $P \leq 0.01$.

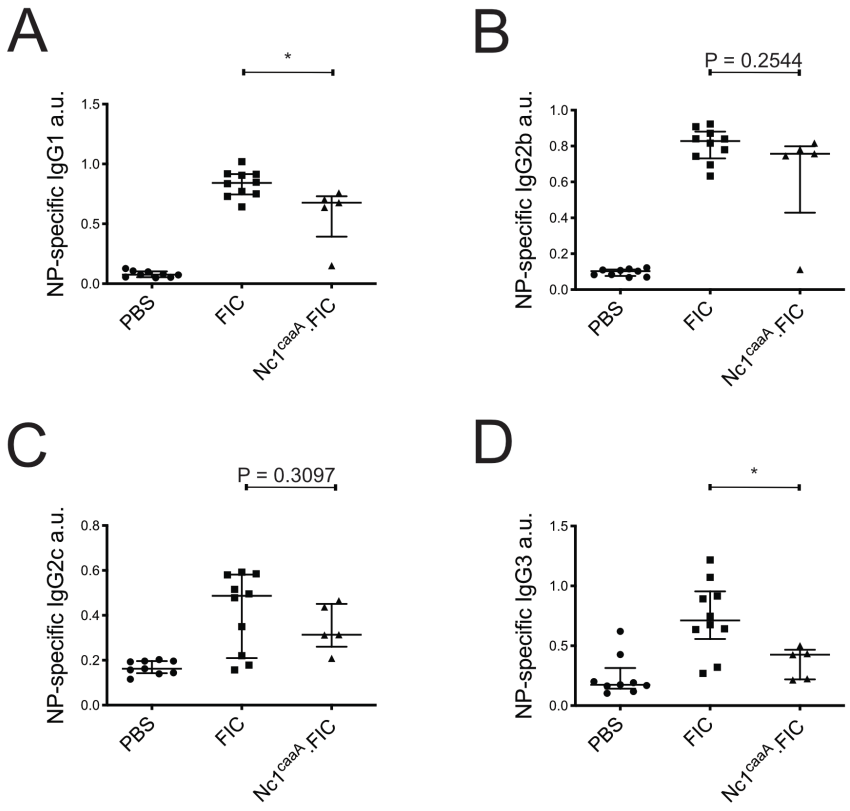

Figure 7.23: Overexpression of caNFATc1/αA in Tregs reduces antigen-specific IgG isotypes

Mice were immunized with NP-KLH in ImJect Alum i.p. for 10 days and boosted on day 7. Antibodies in the serum of the mice were measured via ELISA. Sera were carefully titrated and set in reference to a reference serum (pool of sera from NP-immunized mice), (a.u.). (A) NP-specific IgG1. (B) NP-specific IgG2b. (C) NP-specific IgG2c. (D) NP-specific IgG3. (A-D) Compilation of 7 independent experiments, PBS and *FIC* control groups also shown in Fig. 7.8 - Fig. 7.13 and Fig. 7.15, Mann-Whitney-test: $n \geq 5$; *, $P \leq 0.05$; **, $P \leq 0.01$.

7.2.4 caNFATc1/αA-overexpressing Tfr cells elicit a different transcriptional profile than NFATc1-ablated ones, affecting immune-cell function

The overexpression of caNFATc1/αA in Tregs is mimicking parts of a constant TCR signal. The high expression of NFATc1/αA occurs dominantly in effector T cells [152]. We were interested in the provoked consequence of such a TCR signal for the transcriptome of a Tfr cell. In order to pinpoint any influence of NFATc1 expression better, the two extremes, i.e. NFATc1 deletion and caNFATc1/αA overexpression, were compared.

(Fig. 7.24). We bred *Nc1^{caaA}.Pr1$^{+/gfp}$.FIC* mice which are overexpressing caNFATc1/αA in Tregs. The breeding itself proved difficult. We received only minor numbers of offsprings, additionally predisposed to die within the first weeks of age. We immunized healthy *Nc1$^{fl/fl}$.Pr1$^{+/gfp}$.FIC* and *Nc1^{caaA}.Pr1$^{+/gfp}$.FIC* mice with NP-KLH for 10 days and sorted the Tfr cells according to the scheme in Fig. 7.24. The RNA isolated from three individuals of *Nc1^{caaA}.Pr1$^{+/gfp}$.FIC* was pooled and compared to the one of the *Nc1$^{fl/fl}$.Pr1$^{+/gfp}$.FIC* mouse within an RNA-seq analysis.

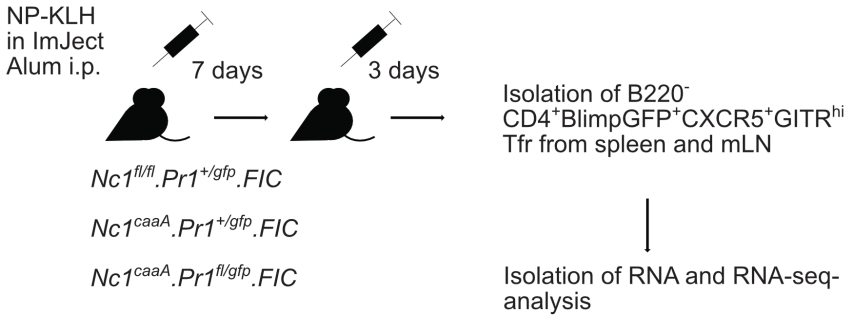

Figure 7.24: Comparison of the Tfr-cell transcriptional profile of *Nc1^{caaA}.Pr1$^{+/gfp}$.FIC* mice with the *Nc1$^{fl/fl}$. Pr1$^{+/gfp}$.FIC* mouse and *Nc1^{caaA}.Pr1$^{fl/gfp}$.FIC* mice

Mice were immunized with NP-KLH i.p. and boosted on day 7. Spleen and mLN were isolated on day 10. CD4$^+$ T cells were preselected and stained for Tfr-cell markers. Tfr cells defined as B220$^-$ CD4$^+$BlimpGFP$^+$CXCR5$^+$GITR^{hi} were isolated via FACS. The RNA was isolated and subjected to RNA-Seq-analysis.

We subjected the set of genes that differed at least twofold between these two groups to a GO-analysis performed with the GORILLA-tool [144, 145]. Seven GO-terms concerning a change in a process were enriched in this gene set with a p-value of at least 10^{-7} (Tab. 7.1). No GO-term describing a function was enriched with a p-value below 10^{-6} pointing to subtle alterations only. Still, the processes that were changed were associated with the function of immune cells or the inflammatory response, indicating that presence or absence of NFATc1 and therefore the quality and/or strength of the TCR signal influenced the function of Tfr cells.

Table 7.1: Comparison of the Tfr-cell transcriptional profile of *Nc1^{caaA}.Pr1$^{+/gfp}$.FIC* mice with the *Nc1$^{fl/fl}$. Pr1$^{+/gfp}$.FIC* mouse

Tfr cells were isolated and subjected to RNA-seq-analysis according to the scheme in Fig. 7.24. Enriched GO-terms in the set of genes being differentially regulated between *Nc1$^{fl/fl}$.Pr1$^{+/gfp}$.FIC* and *Nc1^{caaA}.Pr1$^{+/gfp}$.FIC*. The target set was defined as the set of genes differing at least twofold in their expression between the compared groups. The background set was defined as genes showing an expression level of at least five in at least one of the groups. Ontologies are described in terms of biological process and function. The p-value threshold was defined as $p \leq 10^{-7}$. The GO-analysis was performed via the help of the GORILLA-tool[144, 145].

process

GO term	Description	P-value
GO:0006952	defense response	4.97E-9
GO:0032101	regulation of response to external stimulus	7.08E-8
GO:0031347	regulation of defense response	1.61E-7
GO:0006954	inflammatory response	1.86E-7
GO:0006955	immune response	1.87E-7
GO:0050727	regulation of inflammatory response	4.87E-7
GO:0031349	positive regulation of defense response	9.53E-7

7.2.5 Blimp-1-ablation in NFATc1/αA overexpressing Tfr cells influences the expression of genes associated with migration

Overexpression of caNFATc1/αA altered the transcriptional profile of Tfr cells in a way that indicated a change in the inflammatory response. Tfh-cell frequencies were similar (Fig. 7.21A), but overexpression of caNFATc1/αA enabled Tfr cells to a tighter control of the GCR being reflected by lowered GCB-cell frequencies (Fig. 7.21B) and clearly reduced NP-specific antibody titers (Fig. 7.22 and 7.23). On the contrary, deficiency in Blimp-1 increased Tfr-cell frequencies (Fig. 7.8A and B), while it seemed to reduce Tfr-cell suppressive capacity (Fig. 7.10 and 7.11). Therefore, we wanted to reveal in what way the gain of immune function by caNFATc1/αA overexpression was dependent on Blimp-1. We bred *Nc1^{caaA}.FIC* mice with *Pr1$^{fl/gfp}$.FIC* mice to receive a conditional *Prdm1* knockout that overexpresses caNFATc1/αA specifically in Tregs and named the combined mouse line *Nc1^{caaA}.Pr1$^{fl/gfp}$.FIC*. The breeding proved similarly difficult as the one of the *Nc1^{caaA}.Pr1$^{+/gfp}$.FIC* mice. Three healthy individuals were immunized according to the scheme in Fig. 7.24. Tfr cells were isolated via FACS. We pooled the RNA isolated from

three individuals of *Nc1^{caaA}.Pr1$^{fl/gfp}$.FIC* and compared it to the pool of *Nc1^{caaA}.Pr1$^{+/gfp}$.FIC* mice within an RNA-seq analysis. The set of genes that differed at least twofold between these two groups was subjected to a GO-analysis done with the GORILLA-tool [144, 145]. 33 GO-terms describing a process were enriched with a p-value smaller or equal to 10^{-7} (Tab. 7.2). The highest enrichment was found in the G protein-coupled receptor-signaling pathway and signal transduction. Screening through the GO-terms, many of them were associated with cell motility. Eleven GO-terms describing a function were enriched with a p-value smaller or equal to 10^{-7} (Tab. 7.2). Most of these terms were describing receptor-ligand binding and signal transduction. Summarizing the results found in the GO-analysis, we conclude that the deletion of Blimp-1 primarily influenced the expression of genes associated with cell migration in caNFATc1/αA-overexpressing Tfr cells.

Table 7.2: Comparison of the Tfr-cell transcriptional profile of *Nc1^{caaA}.Pr1$^{+/gfp}$.FIC* mice with the one of *Nc1^{caaA}. Pr1$^{fl/gfp}$.FIC* mice

Tfr cells were isolated and subjected to RNA-seq-analysis according to the scheme in Fig. 7.24. Enriched GO-terms in the set of genes being differentially regulated between *Nc1^{caaA}.Pr1$^{+/gfp}$.FIC* and *Nc1^{caaA}.Pr1$^{fl/gfp}$.FIC* concerning processes and function. The target set was defined as the set of genes differing at least twofold in their expression between the compared groups. The background set was defined as genes showing an expression level of at least five in at least one of the groups. The p-value threshold was defined as $p \leq 10^{-7}$. The GO-analysis was performed via the help of the GORILLA-tool [144, 145].

process

GO term	Description	P-value
GO:0007186	G protein-coupled receptor signaling pathway	8.38E-14
GO:0007165	signal transduction	4.92E-10
GO:0051239	regulation of multicellular organismal process	1.22E-9
GO:0051480	regulation of cytosolic calcium ion concentration	2.95E-9
GO:0006935	chemotaxis	5.42E-9
GO:0042330	taxis	8.01E-9
GO:0006954	inflammatory response	8.84E-9
GO:0006928	movement of cell or subcellular component	1.26E-8
GO:0072503	cellular divalent inorganic cation homeostasis	3.29E-8
GO:0006874	cellular calcium ion homeostasis	3.64E-8
GO:0051240	positive regulation of multicellular organismal process	4.55E-8
GO:0032879	regulation of localization	5.84E-8
GO:0055074	calcium ion homeostasis	6.44E-8
GO:0072507	divalent inorganic cation homeostasis	6.49E-8
GO:0030334	regulation of cell migration	7.65E-8
GO:0060326	cell chemotaxis	7.73E-8
GO:0007204	positive regulation of cytosolic calcium ion concentration	7.79E-8
GO:2000145	regulation of cell motility	7.99E-8
GO:0030003	cellular cation homeostasis	9.98E-8
GO:0006873	cellular ion homeostasis	1.51E-7
GO:0055080	cation homeostasis	1.59E-7
GO:0098771	inorganic ion homeostasis	2.35E-7
GO:0050900	leukocyte migration	2.62E-7
GO:0051094	positive regulation of developmental process	3.34E-7
GO:0006875	cellular metal ion homeostasis	3.39E-7
GO:0051270	regulation of cellular component movement	3.56E-7
GO:0048870	cell motility	3.76E-7
GO:0016477	cell migration	3.79E-7
GO:0002376	immune system process	3.85E-7
GO:0055065	metal ion homeostasis	5.55E-7
GO:0040011	locomotion	7.75E-7
GO:0040012	regulation of locomotion	9.17E-7
GO:2000026	regulation of multicellular organismal development	9.48E-7

function

GO term	Description	P-value
GO:0004888	transmembrane signaling receptor activity	1.72E-12
GO:0038023	signaling receptor activity	1.82E-11
GO:0019955	cytokine binding	6.71E-11
GO:0004930	G protein-coupled receptor activity	1.32E-10
GO:0060089	molecular transducer activity	4.88E-10
GO:0001653	peptide receptor activity	3.21E-9
GO:0008528	G protein-coupled peptide receptor activity	3.21E-9
GO:0030545	receptor regulator activity	5.04E-9
GO:0004896	cytokine receptor activity	5.07E-9
GO:0048018	receptor ligand activity	6.97E-9
GO:0019838	growth factor binding	4.96E-8

7.2.6 Investigation of the influence of NFATc1 on transcriptional profiles and the dependence of these changes on Blimp-1 in Tfr cells

The overexpression of caNFATc1/αA changed the transcriptional profile in a way that GO-terms associated with the immune response were enriched. The deletion of *Prdm1* in Tregs changed the transcriptional profile in Tfr cells in a way that GO-terms associated with locomotion and chemotaxis were changed. We wanted to know if changes that are

influenced by NFATc1 are reverted, modulated or enhanced via the deletion of *Prdm1*. The RNA-Seq data was filtered for genes that differed at least twofold in their expression between $Nc1^{fl/fl}.Pr1^{+/gfp}.FIC$ and $Nc1^{caaA}.Pr1^{+/gfp}.FIC$, as well as $Nc1^{caaA}.Pr1^{+/gfp}.FIC$ and $Nc1^{caaA}.Pr1^{fl/gfp}.FIC$. The expression levels of these genes are summarized in a hierarchically clustered heatmap (Fig. 7.25). For reasons of clarity, the heatmap was split into six consecutive parts, while clusters were preserved.

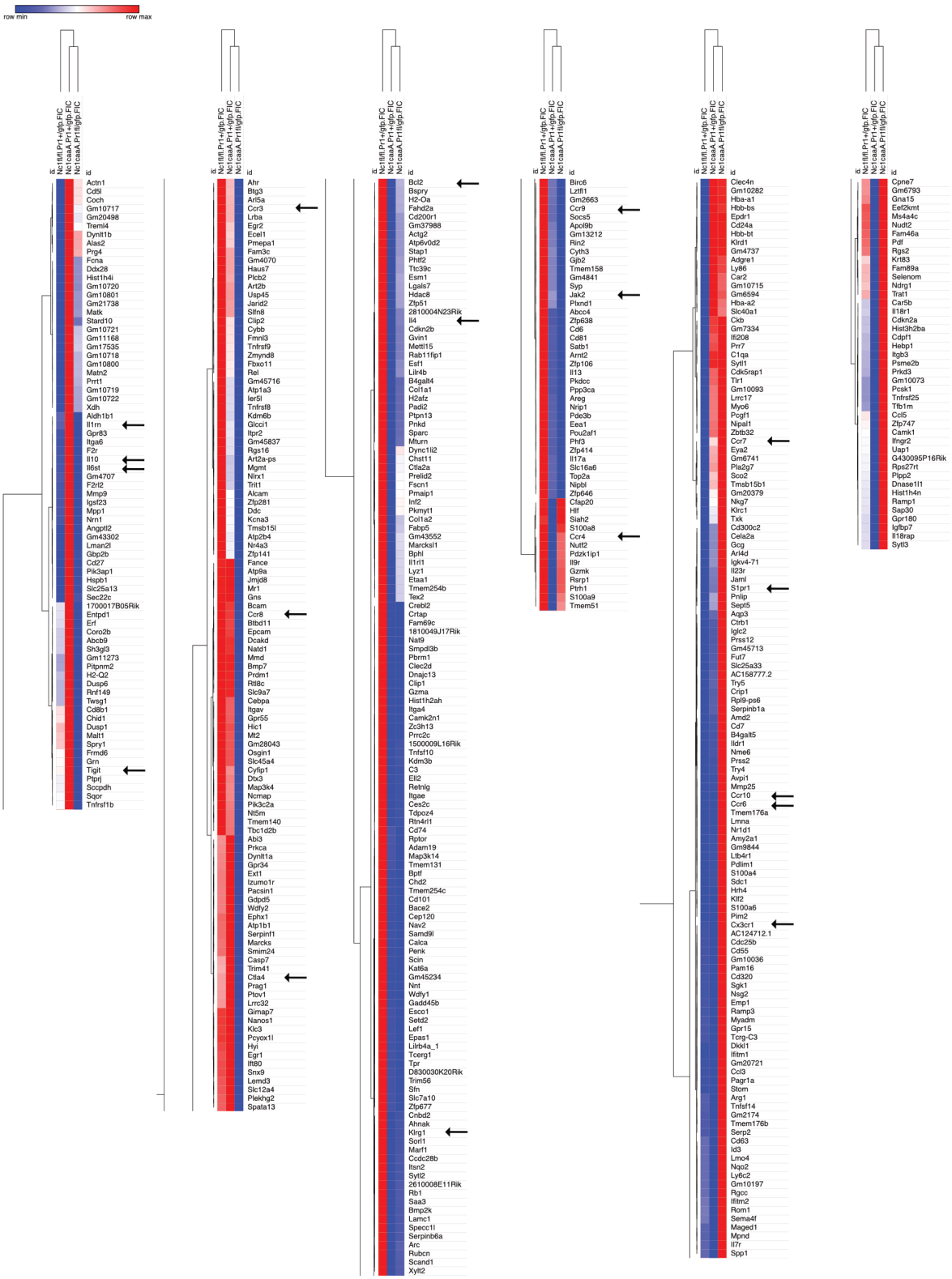
row min
row max
Nc1fl/fl.Pr1+/gfp.FIC
Nc1caaA.Pr1+/gfp.FIC
Nc1caaA.Pr1fl/gfp.FIC
id
Actn1
Cd5l
Coch
Gm10717
Gm20498
Trem14
Dynlt1b
Alas2
Prg4
Fcna
Ddx28
Hist1h4i
Gm10720
Gm10801
Gm21738
Matk
Stard10
Gm10721
Gm11168
Gm17535
Gm10718
Gm10800
Matn2
Prrt1
Gm10719
Gm10722
Xdh
Aldh1b1
Il1rn
Gpr83
Itga6
F2r
Il10
Il6st
Gm4707
F2rl2
Mmp9
Igsf23
Mpp1
Nrn1
Angptl2
Gm43302
Lman2l
Gbp2b
Cd27
Pik3ap1
Hspb1
Slc25a13
Sec22c
1700017B05Rik
Entpd1
Erf
Coro2b
Abcb9
Sh3gl3
Gm11273
Pitpnm2
H2-Q2
Dusp6
Rnf149
Twsg1
Cd8b1
Chid1
Dusp1
Malt1
Spry1
Frmd6
Grn
Tigit
Ptprj
Sccpdh
Sqor
Tnfrsf1b
Ahr
Btg3
Ari5a
Ccr3
Lrba
Egr2
Ecel1
Pmepa1
Fam3c
Gm4070
Haus7
Plcb2
Art2b
Usp45
Jarid2
Slfn8
Clip2
Cybb
Fmnl3
Tnfrsf9
Zmynd8
Fbxo11
Rel
Gm45716
Atp1a3
Ier5l
Tnfrsf8
Kdm6b
Glcci1
Itpr2
Gm45837
Rgs16
Art2a-ps
Mgmt
Nlrx1
Trit1
Alcam
Zfp281
Ddc
Kcna3
Tmsb15l
Atp2b4
Nr4a3
Zfp141
Fance
Atp9a
Jmjd8
Mr1
Gns
Bcam
Ccr8
Btbd11
Epcam
Dcakd
Natd1
Mmd
Bmp7
Prdm1
Rtl8c
Slc9a7
Cebpa
Itgav
Gpr55
Hic1
Mt2
Gm28043
Osgin1
Slc45a4
Cyfip1
Dtx3
Map3k4
Ncmap
Pik3c2a
Nt5m
Tmem140
Tbc1d2b
Abi3
Prkca
Dynlt1a
Gpr34
Ext1
Izumo1r
Pacsin1
Gdpd5
Wdfy2
Ephx1
Atp1b1
Serpinf1
Marcks
Smim24
Casp7
Trim41
Ctla4
Prag1
Ptov1
Lrrc32
Gimap7
Nanos1
Klc3
Pcyox1l
Hyi
Egr1
Ifit80
Snx9
Lemd3
Slc12a4
Plekhg2
Spata13
Bcl2
Bspry
H2-Oa
Fahd2a
Cd200r1
Gm37988
Actg2
Atp6v0d2
Stap1
Phtf2
Ttc39c
Esm1
Lgals7
Hdac8
Zfp51
2810004N23Rik
Il4
Cdkn2b
Gvin1
Mettl15
Rab11fip1
Eaf1
Lilr4b
B4galt4
Col1a1
H2afz
Padi2
Ptpn13
Pnkd
Sparc
Mturn
Dync1li2
Chst11
Ctla2a
Prelid2
Fscn1
Pmaip1
Inf2
Pkmyt1
Col1a2
Fabp5
Gm43552
Marcksl1
Bphl
Il1rl1
Lyz1
Etaa1
Tmem254b
Tex2
Crebl2
Crtap
Fam69c
1810049J17Rik
Nat9
Smpdl3b
Pbrm1
Clec2d
Dnajc13
Clip1
Gzma
Hist1h2ah
Itga4
Camk2n1
Zc3h13
Prrc2c
1500009L16Rik
Tnfsf10
Kdm3b
C3
Ell2
Retnlg
Itgae
Ces2c
Tdpoz4
Rtn4rl1
Cd74
Rptor
Adam19
Map3k14
Tmem131
Bptf
Chd2
Tmem254c
Cd101
Bace2
Cep120
Nav2
Samd9l
Calca
Penk
Scin
Kat6a
Gm45234
Nnt
Wdfy1
Gadd45b
Esco1
Setd2
Lef1
Epas1
Lilrb4a_1
Tcerg1
Tpr
D830030K20Rik
Trim56
Sfn
Slc7a10
Zfp677
Cnbd2
Ahnak
Klrg1
Sorl1
Marf1
Ccdc28b
Itsn2
Sytl2
2610008E11Rik
Rb1
Saa3
Bmp2k
Lamc1
Specc1l
Serpinb6a
Arc
Rubcn
Scand1
Xylt2
Birc6
Lztfl1
Gm2663
Ccr9
Socs5
Apol9b
Gm13212
Rin2
Cyth3
Gjb2
Tmem158
Gm4841
Syp
Jak2
Plxnd1
Abcc4
Zfp638
Cd6
Cd81
Satb1
Arnt2
Zfp106
Il13
Pkdcc
Ppp3ca
Areg
Nrip1
Pde3b
Eea1
Pou2af1
Pht3
Zfp414
Il17a
Slc16a6
Top2a
Nipbl
Zfp646
Ctap20
Htf
Siah2
S100a8
Ccr4
Nutf2
Pdzk1ip1
Il9r
Gzmk
Rsrp1
Ptrh1
S100a9
Tmem51
Clec4n
Gm10282
Hba-a1
Hbb-bs
Epdr1
Cd24a
Hbb-bt
Klrd1
Gm4737
Adgre1
Ly86
Car2
Gm10715
Gm6594
Hba-a2
Slc40a1
Ckb
Gm7334
Ifi208
Prr7
C1qa
Sytl1
Cdk5rap1
Tlr1
Gm10093
Lrrc17
Myo6
Pcgf1
Nipal1
Zbtb32
Ccr7
Eya2
Gm6741
Pla2g7
Sco2
Tmsb15b1
Gm20379
Nkg7
Klrc1
Txk
Cd300c2
Cela2a
Gcg
Arl4d
Igkv4-71
Il23r
Jaml
S1pr1
Pnlip
Sept5
Aqp3
Ctrb1
Iglc2
Prss12
Gm45713
Fut7
Slc25a33
AC158777.2
Try5
Crip1
Rpl9-ps6
Serpinb1a
Amd2
Cd7
B4galt5
Ildr1
Nme6
Prss2
Try4
Avpi1
Mmp25
Ccr10
Ccr6
Tmem176a
Lmna
Nr1d1
Amy2a1
Gm9844
Ltb4r1
Pdlim1
S100a4
Sdc1
Hrh4
Klf2
S100a6
Pim2
Cx3cr1
AC124712.1
Cdc25b
Cd55
Gm10036
Pam16
Cd320
Sgk1
Nsg2
Emp1
Ramp3
Myadm
Gpr15
Tcrg-C3
Dkkl1
Ifitm1
Gm20721
Ccl3
Pagr1a
Stom
Arg1
Tnfsf14
Gm2174
Tmem176b
Serp2
Cd63
Id3
Lmo4
Nqo2
Ly6c2
Gm10197
Rgcc
Ifitm2
Rom1
Sema4f
Maged1
Mpnd
Il7r
Spp1
Cpne7
Gm6793
Gna15
Eef2kmt
Ms4a4c
Nudt2
Fam46a
Pdf
Rgs2
Krt83
Fam89a
Selenom
Ndrg1
Trat1
Car5b
Il18r1
Cdkn2a
Hist3h2ba
Cdpf1
Hebp1
Itgb3
Psme2b
Prkd3
Gm10073
Pcsk1
Tnfrsf25
Tfb1m
Ccl5
Zfp747
Camk1
Ifngr2
Uap1
G430095P16Rik
Rps27rt
Plpp2
Dnase1l1
Hist1h4n
Ramp1
Sap30
Gpr180
Igfbp7
Il18rap
Sytl3

Figure 7.25: Heatmap visualizing the differential gene expression in Tfr cells between *Nc1$^{fl/fl}$.Pr1$^{+/gfp}$.FIC*, *Nc1^{caaA}.Pr1$^{+/gfp}$.FIC* and *Nc1^{caaA}.Pr1$^{fl/gfp}$.FIC*

Tfr cells were isolated and subjected to RNA-seq-analysis according to the scheme in Fig. 7.24. RNA-seq results were filtered for genes that showed an expression level of at least five in at least one of the groups and were more than twofold differentially expressed either between *Nc1$^{fl/fl}$.Pr1$^{+/gfp}$.FIC* and *Nc1^{caaA}.Pr1$^{+/gfp}$.FIC* or *Nc1^{caaA}.Pr1$^{+/gfp}$.FIC* and *Nc1^{caaA}.Pr1$^{fl/gfp}$.FIC*. Results were clustered hierarchically and plotted using the online tool Morpheus [146]. Genes considered to be especially relevant within the enriched GO-terms are marked with an arrow.

We pinpointed genes of the differentially expressed genes in Fig. 7.25, which we considered to be especially relevant in the function and the migration of Tfr cells (Fig. 7.26). Overexpression of caNFATc1/αA reduced *Jak2, Bcl2, Klrg1* and *Il4* expression (Fig 7.26A). In contrary, the expression of *Il6st*, *Il1rn*, *Il10*, *Tigit* and *Ctla4* was enhanced. All of these genes were rather low expressed in the additionally Blimp-1-deficient Tfr cells. *Jak2,* coding for the Tyrosine-protein kinase JAK2, is involved in the STAT5 signaling, which is supporting Treg identity and survival [160]. *Bcl2* codes for the apoptosis regulator Bcl-2, which supports survival [161]. *Klrg1* is encoding the killer cell lectin-like receptor subfamily G member 1 (KLRG1). The expression of KLRG1 is associated with a highly differentiated phenotype and a loss of effector function [162]. *Il4* encodes the cytokine IL-4, which is usually secreted by Th2 and Tfh cells and supports the GCR [163]. *Il6st,* coding for the Interleukin-6 receptor subunit beta is involved in the STAT3 signaling pathway. STAT3 supports the transcription of Tfh-cell signature genes [164]. *Il1rn* is the gene coding for the IL-1 receptor antagonist, which is expressed on Tfr cells and suppresses the production of IL-4 and IL21 in Tfh cells [55]. *Tigit* is encoding the T-cell immunoreceptor with Ig and ITIM domains (TIGIT). TIGIT induces IL-10 secretion from DCs [165]. IL-10 itself is secreted by Tfr cells in order to support the GCR [72]. CTLA-4, as discussed before is an important mediator of Tfr-cell effector function [60, 166].

The deletion of Blimp-1 on the background of caNFATc1/αA overexpression changed the expression of multiple chemokine receptors. Blimp-1-deficient Tfr cells – on the background of NFATc1/αA overexpression – showed enhanced expression of *Ccr7*, *S1pr1*, *Ccr4*, *Ccr10*, *Ccr6*, *Cx3cr1*, while *Ccr3*, *Ccr8*, and *Ccr9* were reduced. CCR7 mediates the

trafficking in lymphoid tissues to the T-cell zone and therewith CCR7 could cause the Tfr cells to remain within the same instead of migrating to the T-B border. *S1pr1* encodes the Sphingosine 1-phosphate receptor 1 (S1PR1). S1PR1 signaling mediates the migration out of the secondary lymphoid organs into the blood via following the Sphingosine-1-Phosphate (S1P) gradient. CCR4 and CCR10 mediate the homing to the skin. CCR4 additionally mediates migration into the lung [167]. CX3CR1 is shown to be associated with an effector memory phenotype in $CD8^+$ T cells, which reside in the LN [168]. Within the LN, these cells were found in the peripheral paracortex and the subcapsular sinus area. In a model of EAE, CCR6 on Tregs and Th17 cells is important for the homing to inflamed tissues [169].

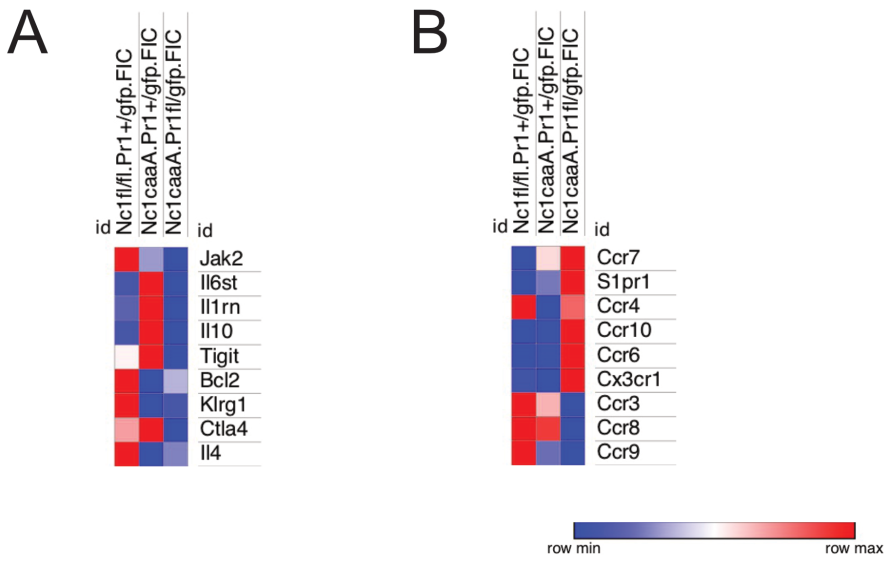

Figure 7.26: NFATc1 and Blimp-1 regulate genes putatively influencing Tfr-cell function and migration

Extraction of candidate genes from Fig. 7.25. (A) Genes being differentially regulated especially via the deletion of NFATc1 vs. overexpression of caNFATc1/αA in Tfr cells. (B) Chemotaxis regulating receptors being affected via the deletion of Blimp-1 in Tregs.

7.3 Overexpression of caNFATc1/αA in T cells and its influence on the GCR

7.3.1 Enforced NFATc1 expression in all T cells downsizes the GCR

The overexpression of caNFATc1/αA in Tregs increased the expression of CXCR5 drastically (Fig. 7.19B). Next, we enabled the expression of caNFATc1/αA in all post-thymic T cells. In order to separate the effects of the endogenously expressed NFATc1 and the ectopically overexpressed caNFATc1/αA, we bred *Nc1*$^{fl/fl}$ with *Nc1*^{caaA} and *dLckcre* mice. All transgenic combinations of this mating were examined (Fig. 7.27). The *Nc1*$^{fl/fl}$*.dLckcre* was devoid of all endogenous (mostly long) isoforms of NFATc1 in all post-thymic T cells, while *Nc1*^{caaA}*.dLckcre* was overexpressing caNFATc1/αA (short isoform) and *Nc1*$^{fl/fl}$*.Nc1*^{caaA}*.dLckcre* doing so on the background of total NFATc1 ablation. This enabled us to study the effects of the short isoform NFATc1/αA separately from the long isoforms of NFATc1. In contrast to *Nc1*^{caaA}*.FIC*, *Nc1*^{caaA}*.dLckcre* and *Nc1*$^{fl/fl}$*.Nc1*^{caaA}*.dLckcre* mice bred with normal litter size and offsprings with normal lifespan.

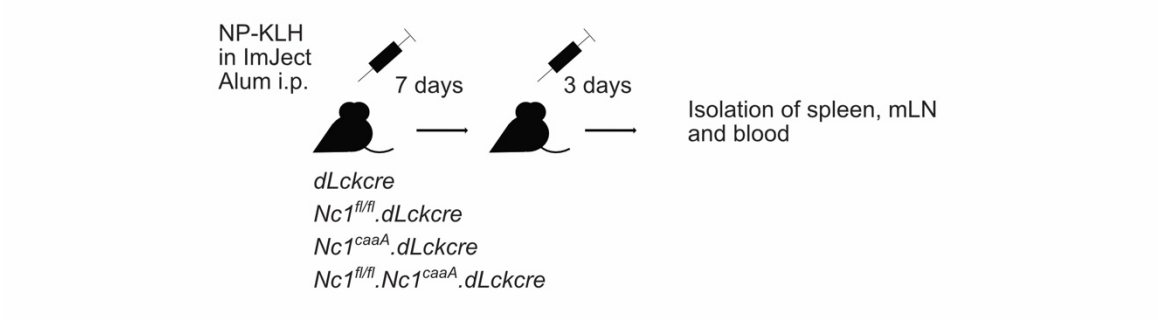

Figure 7.27: Influence of the long and short isoform of NFATc1 in T cells on the GCR

dLckcre, Nc1$^{fl/fl}$*.dLckcre, Nc1*^{caaA}*.dLckcre and Nfatc1*$^{fl/fl}$*.Nc1*^{caaA}*.dLckcre* mice were immunized with NP-KLH in ImJect Alum i.p. for 10 days and boosted on day 7. Spleen and mLN were harvested and stained for flow cytometry.

7.3.2 Overexpression of caNFATc1/αA in T cells decreases Tfh-cell frequencies drastically

We immunized mice of all those genotypes for 10 days according to the scheme in Fig. 7.27. Spleen and mLN were extracted and cells were stained for flow cytometry. We

observed a drastic reduction in Tfh cells in the *Nc1^{caaA}.dLckcre* compared to *dLckcre* (Fig. 7.28). In contrast, deletion of NFATc1 increased Tfh-cell frequencies as seen in the comparison between the *dLckcre* and *Nc1$^{fl/fl}$.dLckcre* as well as *Nc1^{caaA}.dLckcre* and *Nc1$^{fl/fl}$.Nc1^{caaA}.dLckcre.* This resembles the phenotype of *Nc1$^{fl/fl}$.Cd4cre* [50], which we resolved as a consequence of abolished upregulation of CXCR5 on Tregs and unleashed Tfh-cell proliferation. Therefore, the new data, i.e. a strong decrease in Tfh cells in mice overexpressing caNFATc1/αA in all T cells, could resemble the other side of the picture. Contradictory was that in immunized *Nc1^{caaA}.FIC* mice relative Tfh-cell numbers had stayed the same (Fig. 7.21A).

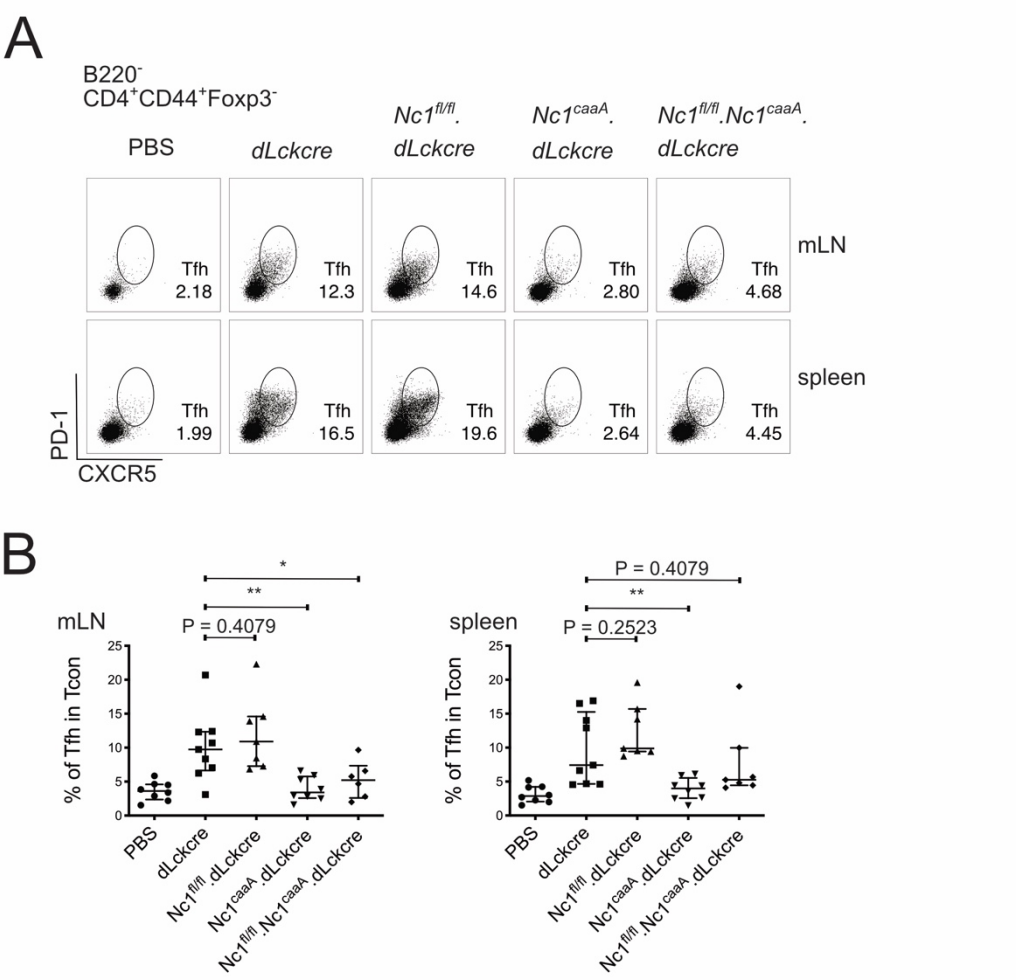

Figure 7.28: Overexpression of caNFATc1/αA in T cells reduces Tfh-cell frequencies and counteracts NFATc1 deficiency

(A-B) Mice were immunized with NP-KLH in ImJect Alum i.p. for 10 days and boosted on day 7. Spleen and mLN were harvested and stained for flow cytometry. (A) Representative flow cytometry of Tfh-cell frequencies in spleen and mLN 10 d after NP-KLH immunization. (B) Frequencies of Tfh

cells in mLN and spleen. Compilation of 4 independent experiments, Mann-Whitney-test: n ≥ 6; *, P ≤ 0.05; **, P ≤0.01.

7.3.3 Tfh-cell numbers decrease in proportion to Tfr cells when caNFATc1/αA is overexpressed in T cells

Similar to *Nc1^{caaA}.FIC* mice, relative Tfr-cell numbers did not vary significantly within the Treg population, when caNFATc1/αA was overexpressed in all T cells (Fig. 7.29A and B). In detail, while the Tfr-cell frequencies in *Nc1$^{fl/fl}$.dLckcre* and *Nc1^{caaA}.dLckcre* were reduced in mLN compared to the *dLckcre*, they were increased in the spleen. Relative Tfr-cell numbers of *Nc1$^{fl/fl}$.Nc1^{caaA}.dLckcre* were increased in the spleen only. In total, alterations in Tfr-cell frequency never reached significance and, importantly, the reduction in relative Tfh-cell numbers cannot be explained via increased Tfr-cell frequencies. Nevertheless, for the control of the GCR, the proportion of Tfr to Tfh cells is more important than the absolute numbers of the same. Because of the low Tfh-cell numbers, overexpression of caNFATc1/αA shifted the balance between Tfr cells and Tfh cells in favor of Tfr cells (Fig. 7.29C). This was especially evident in spleen, but also in mLN. Remarkably, the loss of Tfh cells and the concurring dominance of Tfr cells was most significant in the *Nc1^{caaA}.dLckcre* mice, i.e. in presence of endogenous NFATc1.

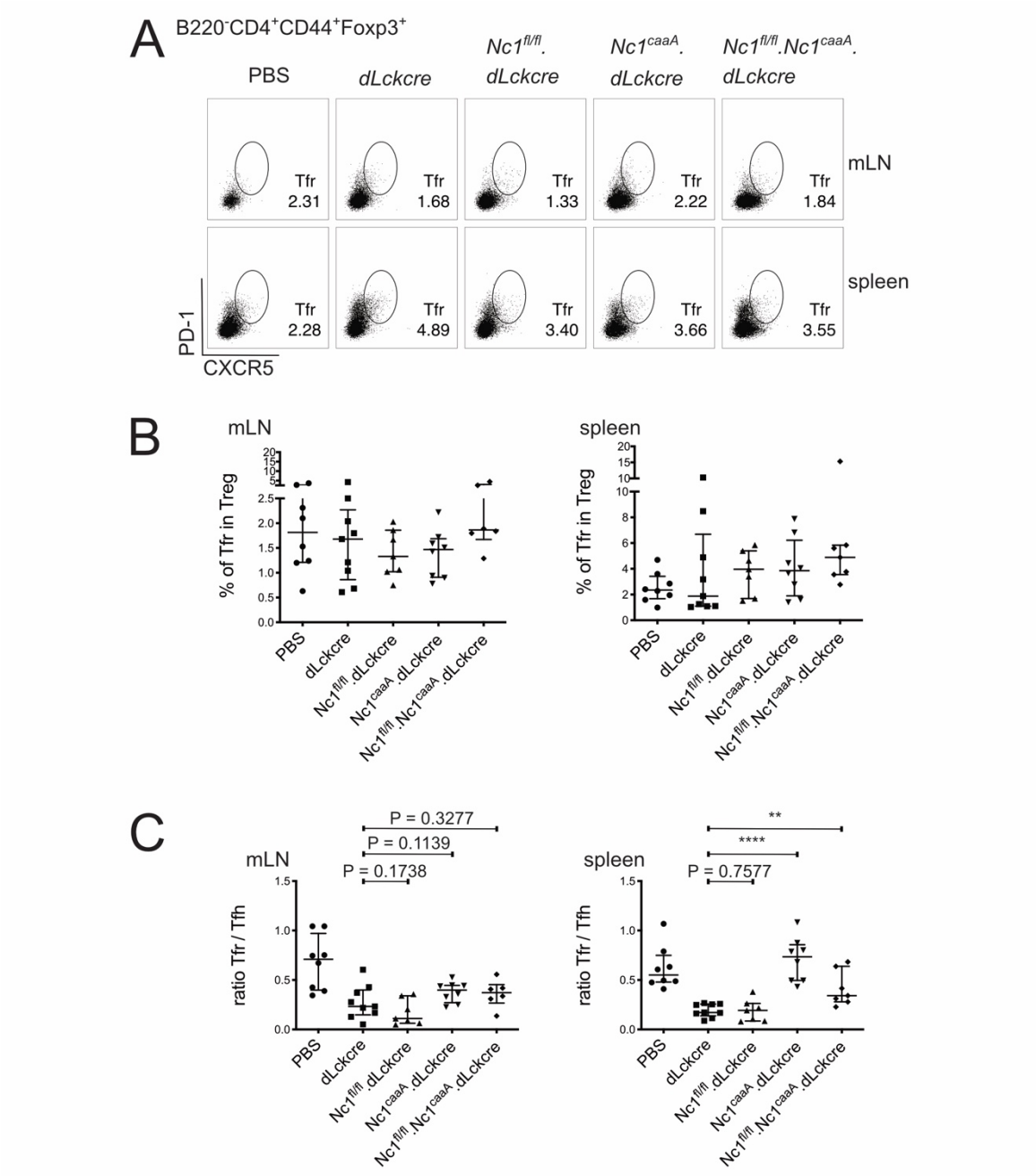

Figure 7.29: Overexpression of caNFAT1/αA in T cells has no consistent effect on Tfr-cell frequencies, still Tfr cells increase in proportion to Tfh cells

(A-C) Mice were immunized with NP-KLH in ImJect Alum i.p. for 10 days and boosted on day 7. Spleen and mLN were harvested and stained for flow cytometry. (A) Representative flow cytometry of relative Tfr-cell numbers in spleen and mLN 10 d after NP-KLH immunization. (B) Frequencies of Tfr cells in mLN and spleen. (C) The ratio of Tfr cells to Tfh cells was calculated via the absolute numbers of each population. (B-C) Compilation of 4 independent experiments, (C) Mann-Whitney-test: $n \geq 6$; *, $P \leq 0.05$; **, $P \leq 0.01$.

7.3.4 Overexpression of caNFATc1/αA in T cells increases Tfr-cell numbers in the B-cell follicle and the GC

We measured the expression level of CXCR5 on the surface of Tregs from immunized mice that were NFATc1 deficient and/or overexpressing caNFATc1/αA in T cells (Fig. 7.30A). Unexpectedly, CXCR5 MFIs on Tregs were almost unaffected via the overexpression of caNFATc1/αA in T cells, completely dissimilar to the effect observed in *Nc1*^{caaA}*.FIC* (Fig. 7.19A). In line with previous results, NFATc1 deficiency reduced CXCR5 expression, however, only in mLN this reduction was considered to be significant. Overexpression of caNFATc1/αA showed the tendency to raise the level of CXCR5 expression on the background of NFATc1 deletion, but only in the spleen this increase was significant (Fig. 7.30A).

At this point, we performed IHF stainings on sections of mLN from mice immunized for 10 days with NP-KLH (Fig. 7.30B). The numbers of Foxp3$^+$ cells in the B-cell follicle and the GC were counted (Fig. 7.30C and D). The numbers of Foxp3$^+$ cells in the B-cell follicle were drastically overrepresented due to caNFATc1/αA in all post-thymic T cells. One reason for this could be the increase in absolute numbers of Tfr cells as this would take into account a putative increase in organ size as well as total Treg numbers. Actually, this was not the case (Fig. 7.30E). In sum, although frequencies of Tfr cells were not different and CXCR5 levels were only provably enhanced on Tregs of *Nc1*$^{fl/fl}$*.Nc1*^{caaA}*.dLckcre* in the spleen, overexpression of caNFATc1/αA enabled them to home better to the B-cell follicle.

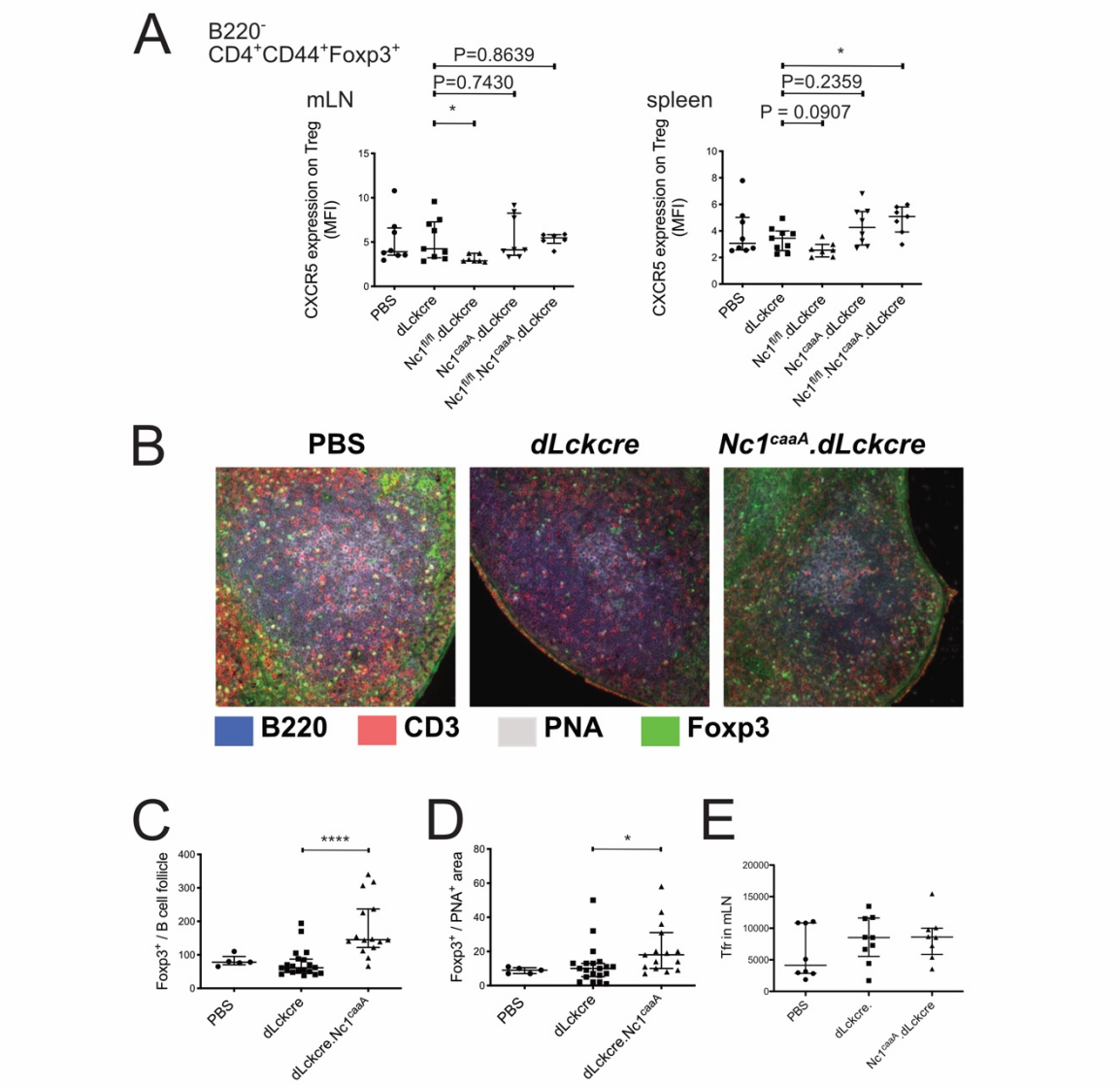

Figure 7.30: Overexpression of caNFATc1/αA increases Tfr cells in the B cell follicle and the GC

Mice were immunized with NP-KLH in ImJect Alum i.p. for 10 days and boosted on day 7. (A) mLN and spleen were extracted and cells were stained for flow cytometry. CXCR5 expression on Tregs, MFI normalized via the FMO of CXCR5. Compilation of 4 independent experiments, Mann-Whitney-test: $n \geq 6$; *, $P \leq 0.05$; **, $P \leq 0.01$. (B) mLN were extracted and IHF stainings were performed. Representative pictures of stained GC: blue: B220, red: CD3, grey: PNA, green: Foxp3. (C) Numbers of $Foxp3^+$ per follicle. (D) Numbers of $Foxp3^+$ per GC. Five follicles per mouse, 1-4 mice, Mann-Whitney-test: $n \geq 5$; *, $P \leq 0.05$; **, $P \leq 0.01$ (E) Absolute numbers of Tfr cells in mLN. Compilation of 4 independent experiments, $n \geq 6$

7.3.5 Overexpression of caNFATc1/αA in T cells reduces relative GCB-cell numbers

In line with the clearly reduced Tfh-cell frequencies in caNFATc1/αA overexpressing mice, also relative GCB-cell numbers of *Nc1^{caaA}.dLckcre* and *Nc1$^{fl/fl}$.Nc1^{caaA}.dLckcre* were severely reduced in both organs (Fig. 7.31). The cause of this reduction can be both direct and indirect, i.e. due to the limited help provided by low Tfh-cell numbers as well as enforced direct suppression by more frequent and/or more suppressive Tfr cells.

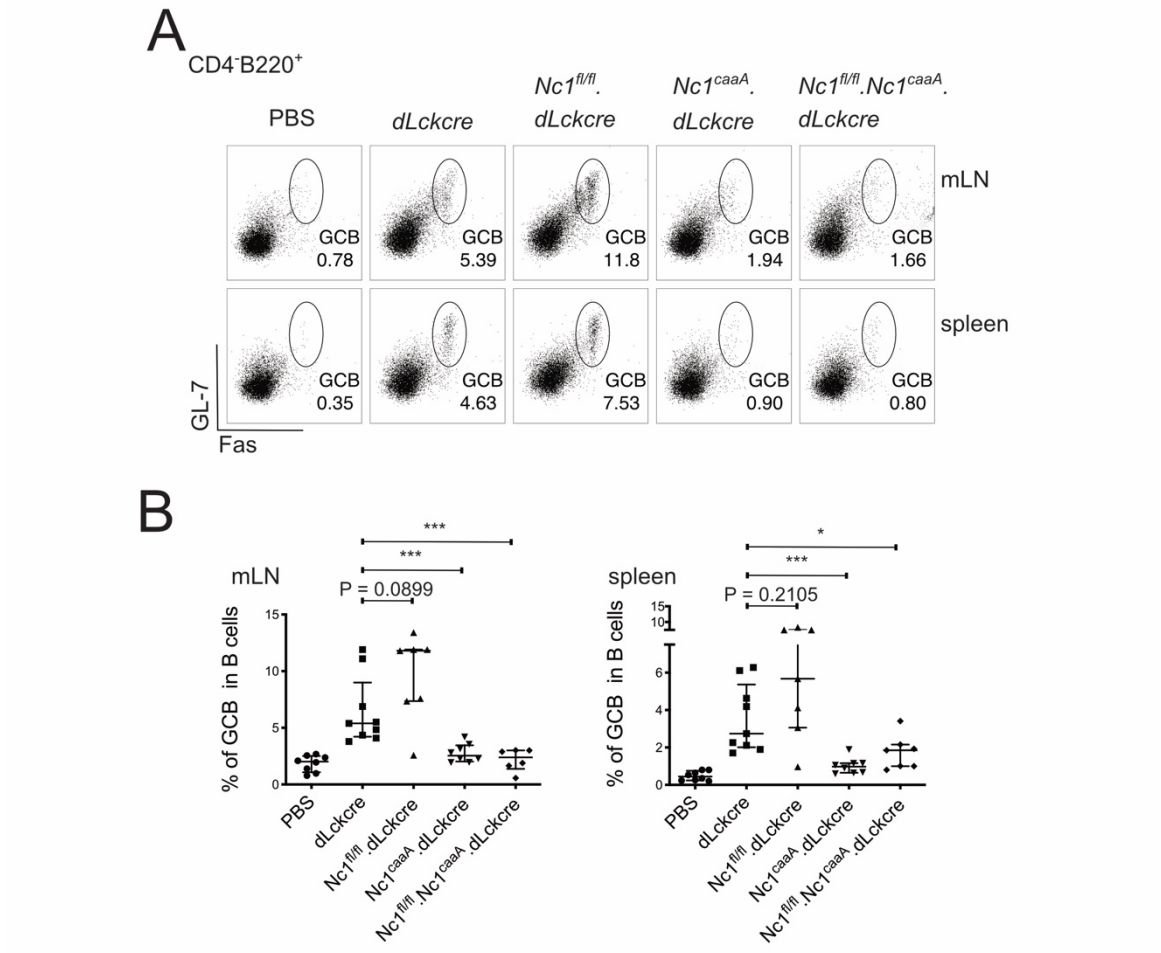

Figure 7.31: Overexpression of caNFATc1/αA in T cells reduces GCB-cell frequencies and counteracts NFATc1 deletion

(A and B) Mice were immunized with NP-KLH in ImJect Alum i.p. for 10 days and boosted on day 7. Spleen and mLN were harvested and stained for flow cytometry. (A) Representative flow cytometry of GCB-cell frequencies in spleen and mLN 10 d after NP-KLH immunization. (B) Relative numbers of GCB cells in mLN and spleen. Compilation of 4 independent experiments, Mann-Whitney-test: n ≥ 6; *, P ≤ 0.05; **, P ≤0.01.

7.3.6 Overexpression of caNFATc1/αA in T cells reduces the antigen-specific humoral immune response

Since GCB cells were less in immunized mice, which constitutively overexpress NFATc1/αA in post-thymic T cells, antigen-specific antibody titers were measured in the serum after immunization for 10 days (Fig. 7.32). *Nc1$^{fl/fl}$.dLckcre* mice served as control and revealed a tendency to lower NP-specific IgG titers compared to *dLckcre* mice (Fig. 7.32A). This was especially the case for the IgG1-isotype (Fig. 7.32B), while the titers of IgG2b, IgG2c and IgG3 were elevated when compared to the *dLckcre* (Fig. 7.32C-E). The general NP-specific IgG titers in *Nc1^{caaA}.dLckcre* and *Nc1$^{fl/fl}$.Nc1^{caaA}.dLckcre* mice, however, were significantly less compared to the *dLckcre* (Fig. 32A), which hold true for all isotypes, i.e. IgG1, IgG2b, IgG2c and IgG3, although this was not significant in all of the cases (Fig. 32B-E). This indicated that the overexpression of caNFATc1/αA in all post-thymic T cells delimits the antigen-specific humoral immune response. The concurrent deletion of endogenous NFATc1 even strengthened this effect as the NP-specific titers were lower in the *Nc1$^{fl/fl}$.Nc1^{caaA}.dLckcre* as compared to the *Nc1^{caaA}.dLckcre*.

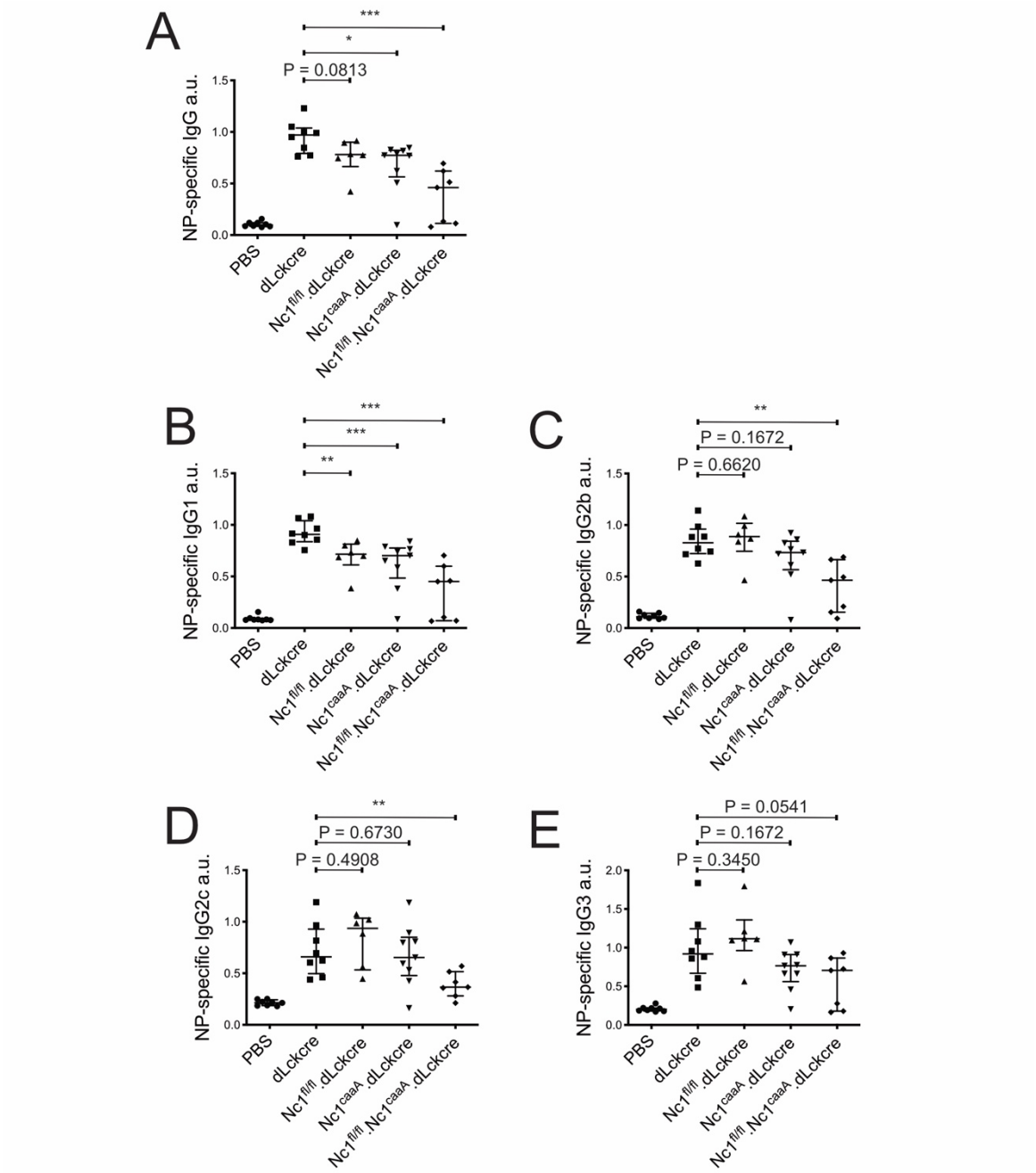

Figure 7.32: Overexpression of caNFATc1/αA in T cells reduces antigen specific humoral immune response

(A-E) Mice were immunized with NP-KLH in ImJect Alum i.p. for 10 days and boosted on day 7. Antibodies in the serum of the mice were measured via ELISA. Sera were carefully titrated and set in reference to a reference serum (pool of sera from NP-immunized mice, (a.u.). (A) NP-specific IgG. (B) NP-specific IgG1, (C) NP-specific IgG2b, (D) NP-specific IgG2c, (E) NP-specific IgG3, (A-E) Compilation of 7 independent experiments, Mann-Whitney-test: $n \geq 6$; *, $P \leq 0.05$; **, $P \leq 0.01$.

Although the production of IgM does not require a class switch, NP-specific IgM-titers were reduced in the *Nc1*$^{fl/fl}$.*Nc1*^{caaA}.*dLckcre* and the *Nc1*^{caaA}.*dLckcre* as well (Fig. 7.33A). There was no significant difference between the *dLckcre* and any of the knockouts in serum IgG titers irrespective of antigen specificity (Fig. 7.33B). Further, we checked the titers of anti-dsDNA to evaluate if there was a significant change in the recognition of autoantigens; this was not the case, neither before nor after immunization (Fig. 7.33C). Finally, we checked the affinity of NP-specific IgG to see if the process of affinity maturation was changed. The deletion of NFATc1 significantly cut-down NP-specific IgG-titers with a high affinity for the antigen, whilst the overexpression of caNFATc1/αA only lowered the high affinity NP-specific IgG-titers. However, the overexpression of caNFATc1/αA even seemed to raise the NP-specific IgG-titers with a high affinity on the background of NFATc1 deletion (Fig. 7.33D). In sum, while NFATc1 deficiency in all T cells or specifically in Tregs leads to an exaggerated immune response, caNFATc1/αA overexpression in T cells restricts the GCR leading to less antigen-specific antibodies.

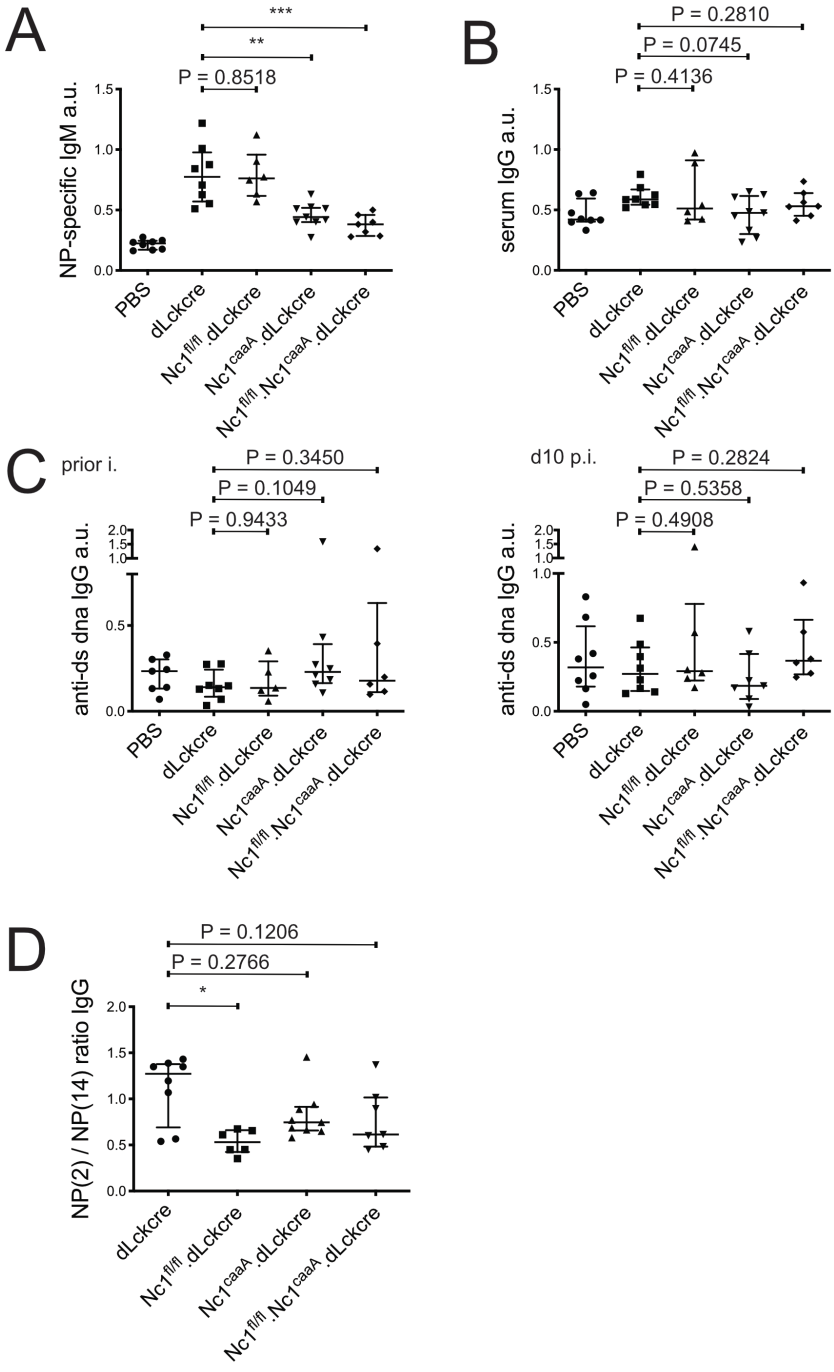

Figure 7.33: Overexpression of caNFATc1/αA in T cells has no effect on the titers of antibodies that are not specific for the antigen of immunization

(A, B, C, right, D) Mice were immunized with NP-KLH in ImJect Alum i.p. for 10 days and boosted on day 7. Antibodies in the serum of the mice were measured via ELISA. Sera were carefully titrated and set in reference to a reference serum (pool of sera from NP-immunized mice, (a.u.). (A) NP-specific IgM titers. (B) Overall IgG titers in the serum of immunized mice (C, left) Anti-dsDNA antibody titers prior to immunization with NP-KLH. (C, right) Anti-dsDNA antibody titers on day 10 p.i. with NP-KLH (D) Ratio

of NP-specific antibody titers of high affinity (NP-2) vs. low affinity (NP-14). (A-D) Compilation of 7 independent experiments, Mann-Whitney-test: $n \geq 6$; *, $P \leq 0.05$; **, $P \leq 0.01$.

7.3.7 Overexpression of caNFATc1/αA in T cells activates $CD4^+$ T cells and raises $CD4^+$ T-cell frequencies

In effector T cells, NFATc1/αA is highly expressed [152], therefore, we suspected the overexpression of caNFATc1/αA in T cells to cause an activated phenotype in the same. There are multiple markers for the evaluation of T-cell activation. Here we defined activated T-helper cells as $CD4^+CD44^+Foxp3^-$ (Tactive). Only in the spleen of *Nc1$^{fl/fl}$.Nc1^{caaA}.dLckcre* mice, Tactive were significantly enhanced in frequency (Fig. 7.34A). Likewise, NFATc1/αA supports antigen-mediated proliferation and protects lymphocytes against rapid Activation-Induced Cell Death (AICD) [90]. In line with this, frequencies of $CD4^+$ T cells were enhanced in mice overexpressing caNFATc1/αA in T cells (Fig. 7.34B). Interestingly, the total cell numbers in mLN and spleen of *Nc1^{caaA}.dLckcre* and *Nc1$^{fl/fl}$.Nc1^{caaA}.dLckcre* mice were slightly reduced, indicating no lymphoproliferative disorder that could be associated with high numbers of $CD4^+$ T cells (Fig. 7.34C).

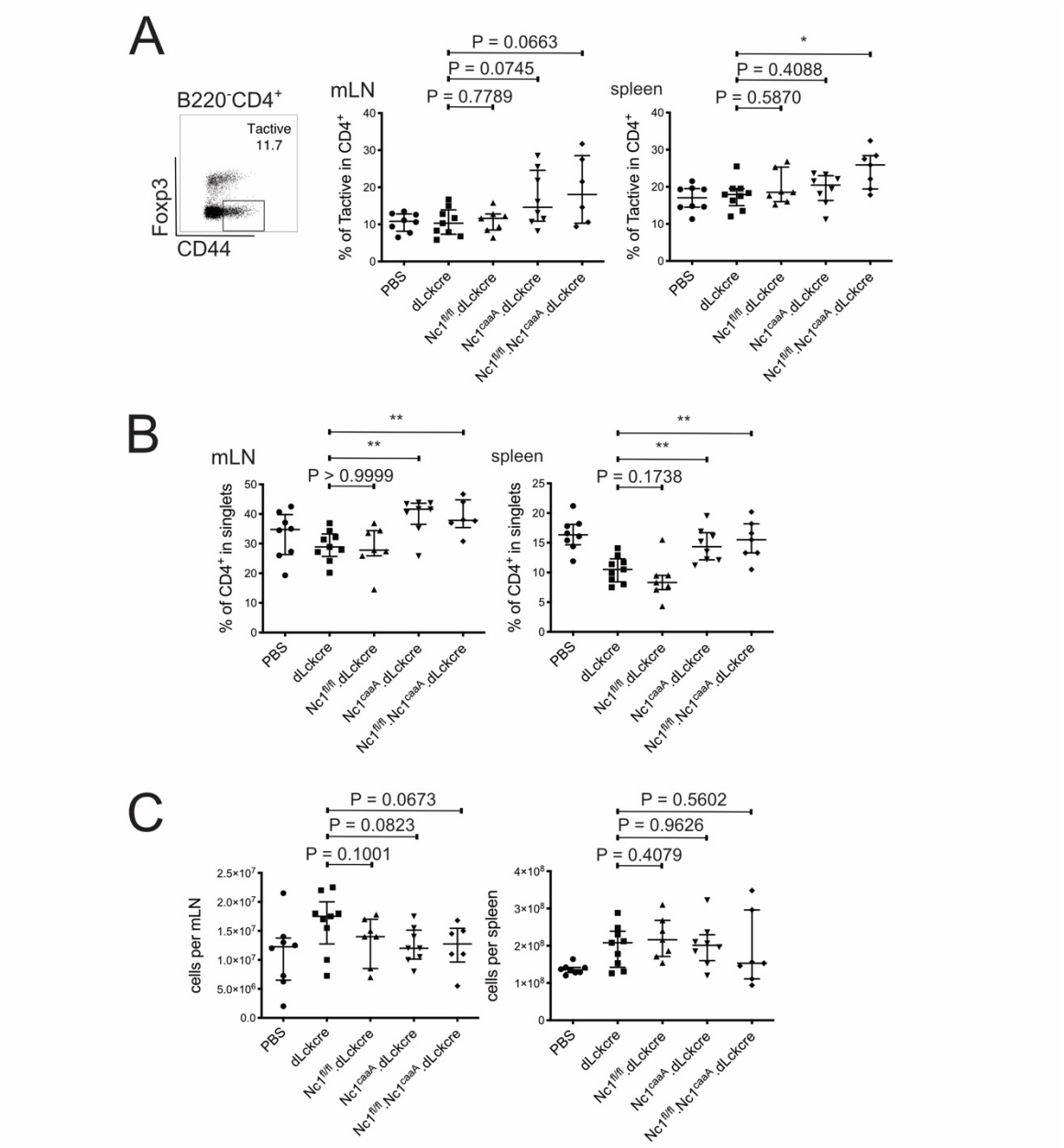

Figure 7.34: Overexpression of caNFATc1/αA in T cells activates CD4$^+$ T cells and raises CD4$^+$ T-cell frequencies

(A, B, C) Mice were immunized with NP-KLH in ImJect Alum i.p. for 10 days and boosted on day 7. (A, left) Representative flow cytometry of Tactive frequencies in spleen and mLN 10 days after NP-KLH immunization. (A, right) Frequencies of Tactive in mLN and spleen. (B) Frequencies of CD4$^+$ T cells in mLN and spleen. (C) Cell numbers of mLN and spleen (A-C) Compilation of 7 independent experiments, (A and C) Mann-Whitney-test: $n \geq 6$; *, $P \leq 0.05$; **, $P \leq 0.01$.

7.3.8 Overexpression of caNFATc1/αA in T cells increases IL-2 secretion after TCR-stimulation

We suspected the high numbers of $CD4^+$ T cells in the caNFATc1/αA overexpressing mice to stem from a higher production of IL-2. NFAT proteins are known to activate the transcription of IL-2 [153]. IL-2 functions as a major growth factor for T cells [170]. To get an idea, how much IL-2 is secreted by NFATc1-deficient or caNFATc1/αA-overexpressing T cells during immunization, we performed a pilot experiment (Fig. 7.35A). The frequencies of IL-2 producing $CD4^+$ T cells were not changed in the mLN of *Nc1*$^{fl/fl}$*.dLckcre* and *Nc1*$^{fl/fl}$*.Nc1*^{caaA}*.dLckcre* mice four days post immunization compared to the wild type (wt) (Fig. 7.35B, left). The frequencies of IL-2 producing $CD8^+$ T cells in the mLN of *Nc1*$^{fl/fl}$*.Nc1*^{caaA}*.dLckcre* mice were even reduced, whilst remaining unchanged in *Nc1*$^{fl/fl}$*.dLckcre* mice compared to the wt (Fig. 7.35B, right). Thus, single cell suspensions from mLN of immunized mice were stimulated with αCD3/αCD28 for 24h and as expected, we observed reduced IL-2 levels in the supernatant of NFATc1-ablated T cells (Fig. 7.35C, left). This effect was compensated when T cells additionally overexpressed caNFATc1/αA. After 48h of stimulation with αCD3/αCD28, IL-2 titers were still lower in the supernatants from *Nc1*$^{fl/fl}$*.dLckcre* cultures compared to the wt, while IL-2 titers in the supernatants from *Nc1*$^{fl/fl}$*.Nc1*^{caaA}*.dLckcre* cultures were even higher than the ones from the wt (Fig. 7.35C, right), indicating that caNFATc1/αA indeed influences IL-2 expression positively. A surplus of IL-2 should influence Tregs including Tfr cells. To get an unbiased idea, how the transcriptome of Tfr cells is altered, when caNFATc1/αA is overexpressed in T cells, we performed another RNA-seq experiment (see below).

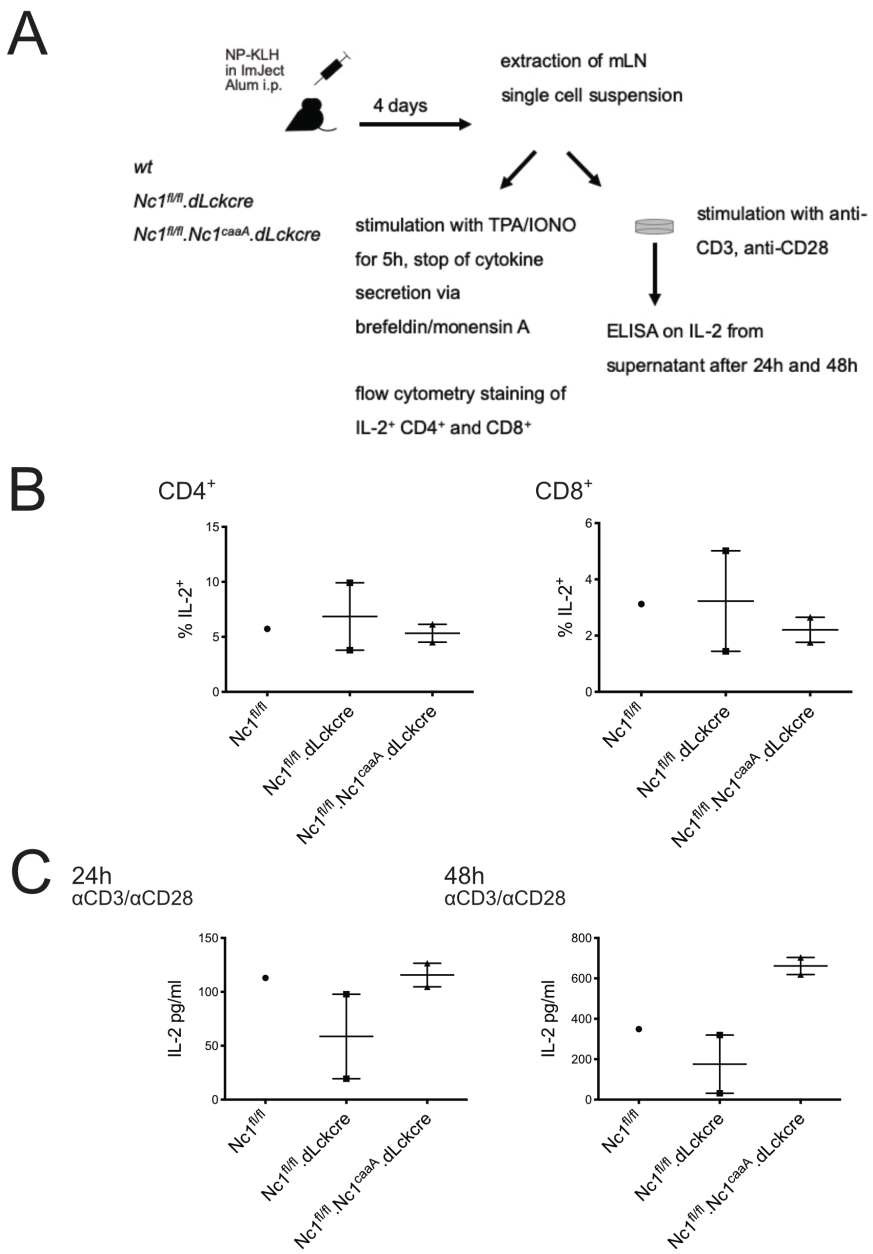

Figure 7.35: Overexpression of caNFATc1/αA increases IL-2 secretion after 48h stimulation with αCD3/αCD28

(A) Experimental setup. (B) Frequencies of IL-2 producing $CD4^+$/$CD8^+$ T cells within the mLN on day 4 p.i.. Cells were stimulated with TPA/ionomycin for 5h. Secretion was blocked via brefeldin/monensin A. (C) Concentration of IL-2 in the supernatant after 24h and 48h stimulation with αCD3/αCD28.

7.3.9 Isolation of Tfr cells via the marker Foxp3

Tfr cells are a specialized type of Foxp3$^+$ Tregs, wherefore Foxp3 can be used to distinguish them within the follicular T-cell population. Before, our sorting strategy was based on the *Pr1^{gfp}* reporter mouse, as it was described that Blimp-1 is highly expressed in Tfr cells [46]. It seemed to be the perfect choice to isolate Tfr cells from secondary lymphoid organs out of an immunized mouse. Regrettably, Blimp-gfp proved to be expressed rather weakly in CD4$^+$CXCR5$^+$ cells (Fig. 7.16B). To circumvent this problem, we decided to make use of DEREG mice. The DEREG mouse expresses a simian diphteria toxin receptor-enhanced green fluorescent (DTR-eGFP) fusion protein under the control of the endogenous *Foxp3* promoter/enhancer regions on the BAC transgene [140]. Therefore, GFP expression allows sorting of Tfr cells similar to the gating strategy, which was applied previously to record the frequencies of B220$^-$CD4$^+$PD-1$^+$CXCR5$^+$CD44$^+$Foxp3$^+$ Tfr cells via flow cytometry (Fig. 7.29). We bred DEREG mice with *dLckcre* and *Nfatc1$^{fl/fl}$*, as well as *Nfatc1^{caaA}* mice. We sorted B220$^-$CD4$^+$CXCR5$^+$PD-1$^+$CD44$^+$eGFP$^+$ cells and subjected these to RNA-seq analysis (Fig. 7.36).

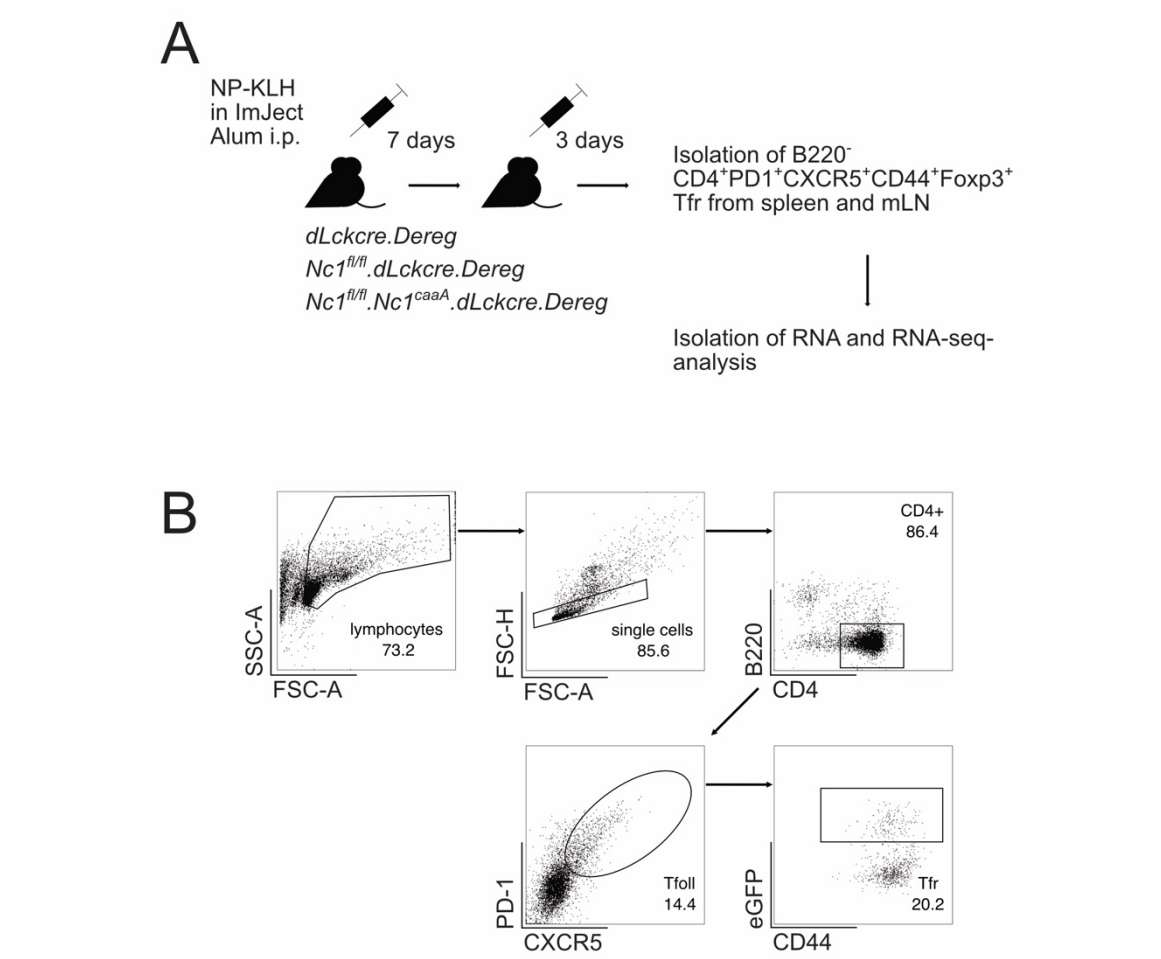

Figure 7.36: Strategy to examine the influence of NFATc1 isoforms on Tfr-cell transcriptional profile, i.e. the isolation of Tfr cells via the marker Foxp3

(A) Mice were immunized with NP-KLH i.p. and boosted on day 7. Spleen and mLN were isolated on day 10. $CD4^+$ T cells were preselected and stained for Tfr-cell markers. Tfr cells defined as $B220^-$ $CD4^+PD\text{-}1^+CXCR5^+CD44^+Foxp3^+$ were isolated via FACS. The RNA was isolated and subjected to RNA-seq analysis, (B) Sorting strategy of $Foxp3^+$ Tfr cells.

7.3.10 caNFATc1/αA upregulates *Il6st* and stabilizes Tfr-cell identity

The RNA-seq results were filtered for genes that were reproducibly changed between the groups (Fig. 7.37). This filter generated a list of 28 genes showing the characteristic changes between the groups. We checked this list carefully for genes, which could influence the Tfr-cell function positively or negatively. *Il6st* caught our special interest. *Il6st* upregulation due to overexpression of caNFATc1/A was also observed in the Tfr cells

from *Nc1*^{caaA}*.FIC* compared to the *Nc1*$^{fl/fl}$*.FIC*. Higher levels of IL6ST could strengthen the expression of Tfh-cell associated genes via a STAT3 dependent pathway. This could be a reason for the constant frequencies of Tfr cells in mice overexpressing caNFATc1/αA also in the presence of higher IL-2 titers produced by the overexpressing caNFATc1/αA Tcons.

The NFATc1 deficient Tfr cells showed higher levels of expression from multiple gene loci coding for parts of the MHCII molecule, namely *H2-Eb1* (H-2 class II histocompatibility antigen, I-A beta chain), *H2-Ab1* (H-2 class II histocompatibility antigen, A-F beta chain), *H2-Aa* (H-2 class II histocompatibility antigen, A-B alpha chain) and *Cd74* (H-2 class II histocompatibility antigen gamma chain). The majority of murine T cells usually does not express MHCII genes [171]. The upregulation of MHCII genes could indicate a loss of Tfr-cell identity. Interestingly, additional overexpression of caNFATc1/αA downregulated the expression of the mentioned MHCII genes, indicating that it could stabilize the Tfr-cell identity.

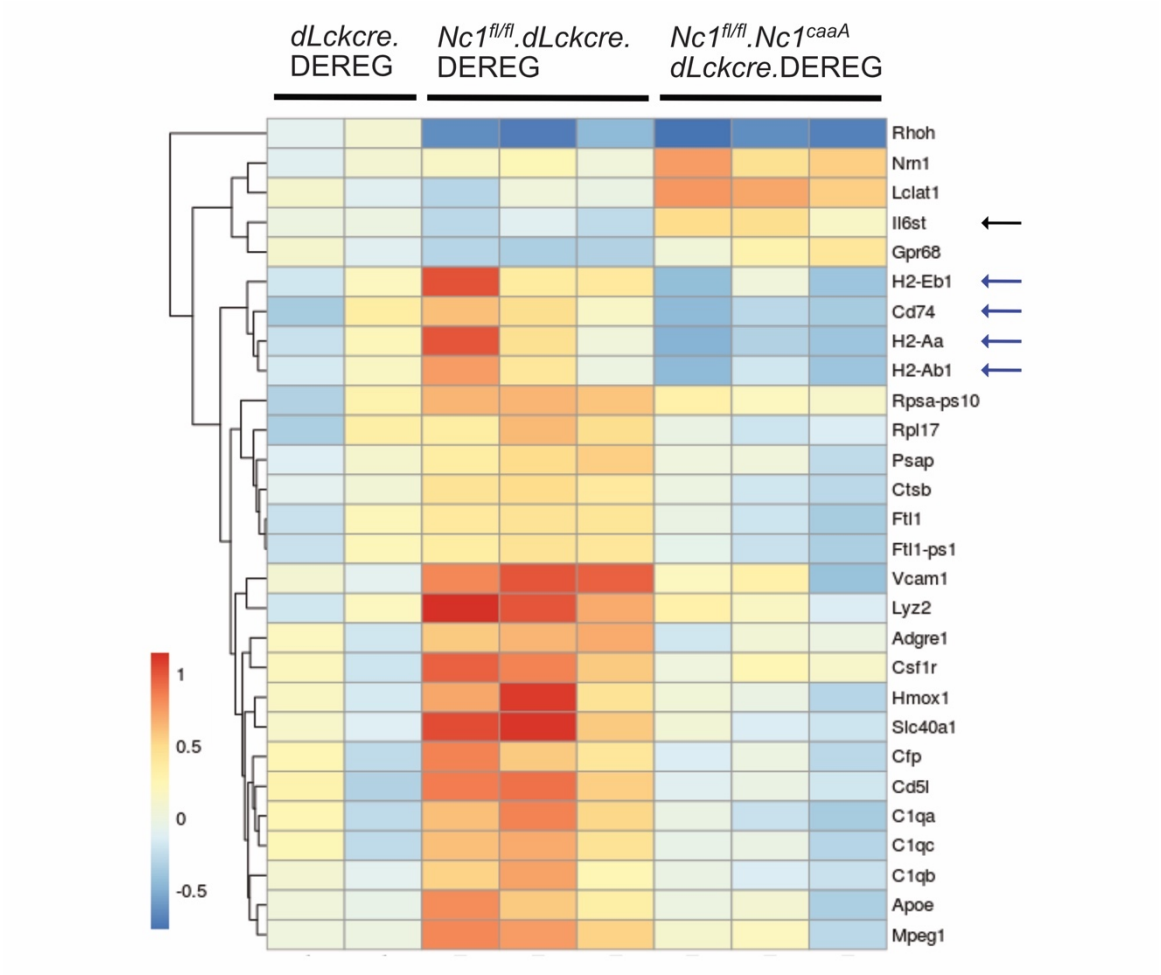

Figure 7.37: Heatmap visualizing the differential gene expression between *dLckcre.*DEREG, *Nc1$^{fl/fl}$.dLckcre.*DEREG and *Nc1^{caaA}.dLckcre.*DEREG

Tfr cells were isolated and subjected to RNA-seq-analysis according to the scheme in Fig. 7.36. The following analysis was done by Jun.-Prof. Dr. Florian Erhard, VIM Wuerzburg: RNA-seq libraries were mapped using the bioinformatics tool STAR (Ensembl v90) [147]. The reads per gene and library were counted and genes giving less then 10 reads in all libraries were excluded. Significantly regulated genes were defined via a Likelihood ratio test undergoing multiple testing corrected p-value <0.01 using the package DESEq2 [148]. Here shown are log2 fold changes normalized to the mean of the two *dLckcre.*DEREG libraries. Genes of special interest are indicated with arrows. Blue arrows mark genes coding for parts of the MHCII molecule.

This heatmap was kindly provided by Jun.-Prof. Dr. Florian Erhard, VIM Wuerzburg

8 Discussion

8.1 The role of NFATc1 and Blimp-1 in Tfr cells

8.1.1 NFATc1 and Blimp-1 cooperate to allow CXCR5 expression

It was shown by us that the deletion of NFATc1 in T cells leads to a defect in CXCR5 expression in Tregs. However, Tcons were not affected in their CXCR5 expression via the NFATc1 knockout [50]. This observation raised the question of the difference in the transcriptional regulation of CXCR5 expression in Tfr cells and Tfh cells. It is known that in difference to Tfh cells, Tfr cells express the transcriptional repressor Blimp-1 [46]. For long it was known that Blimp-1 inhibits CXCR5 expression in plasma cells and now that Blimp-1 represses the expression of CXCR5 in follicular cytotoxic T cells (Tfc) [150, 172]. In Tfcs, the repression can be overcome via an E2A-dependent mechanism. Blimp-1 and E2A both bind to the *Cxcr5* enhancer *HS2* [150]. We suspected NFATc1 to take over a similar role as E2A in Tfr cells. The deletion of NFATc1 in Tregs increases the frequency of GCB cells. This phenotype can be rescued via the transduction of Tregs with a CXCR5-expressing construct. The reconstitution of the CXCR5 expression therefore was sufficient to reestablish Tfr-cell functionality after NFATc1 deletion [50]. The knockdown of *Prdm1* expression in nTregs via shRNA increased CXCR5 expression, indicating that also in Tregs Blimp-1 might suppress CXCR5 expression. Interestingly, NFATc1 and Blimp-1 coprecipitated in nuclear extracts generated from Tregs and colocalized to the nucleus of Tregs after stimulation with αCD3/αCD28 and IL-2. In line, the promoter of *Cxcr5* as well as the enhancer *HS2* are bound by NFATc1 and Blimp-1. Different from expectation that NFATc1 transactivates, while Blimp-1 represses CXCR5 expression, at least in reporter gene assays, the simultaneous presence and thus possible interaction of NFATc1 and Blimp-1 amplifies the expression of *Cxcr5* in comparison to NFATc1 transactivation alone. This distinguishes the regulation of *Cxcr5* expression via NFATc1 and Blimp-1 from the one via E2A and Blimp-1, where E2A was counteracting Blimp-1-mediated repression. Nevertheless, in Tfr cells the transactivation of *Cxcr5* is dependent primarily on NFATc1, as mutations of the NFAT binding sites in the *Cxcr5* promoter and/or enhancer always reduced the transactivation of the reporter construct. On the other hand, transactivation increased when the Blimp-1 binding site in the *HS2* was mutated in the presence of

NFATc1. Finally, the cooperation of NFATc1 and Blimp-1 to allow *Cxcr5* expression was observed again in the reporter gene assay; the combined mutation of both dominant identified NFAT binding sites in the *Cxcr5*-promoter and *HS2* with the mutation of the Blimp-1 responsive element in the *HS2* ablated the transactivation of the reporter construct. With this, we assign now also a transactivating role to the combined binding to NFATc1 and Blimp-1 to the regulatory region, namely the enhancer *HS2* for CXCR5 expression. The difference between NFATc1 and E2A might lie in the fact that NFATc1 interacts with Blimp-1 on the protein level. Thereby, Blimp-1 could support NFATc1 recruitment to the *Cxcr5* locus. Secondly, preliminary studies demonstrated that Blimp-1 interacts via a domain known to employ HDAC2 [105], for which NFATc1 could compete and prevent deacetylation leading to more CXCR5 expression.

8.1.2 NFATc1-deficient Tregs fail to develop into Tfr cells due to the inability to upregulate CXCR5

Tfr cells ordinarily originate from nTregs [46, 136, 173]. Under circumstances that promote plasticity, Tfr cells can also derive from peripheral induced Tregs (iTregs) [44]. NFATc1 plays different roles for these two subtypes of Tregs [95]. nTreg frequencies do not change due to the deletion of NFATc1, NFATc2 or NFATc3 alone or in combination of two. On the other hand, iTregs, which develop from Tcons, diminish with the number of NFAT family members missing [95]. Neither nTregs nor iTregs are affected in their suppressive function due to NFATc1 deletion *in vitro* and *in vivo* [95]. Here we intercrossed $Nc1^{fl/fl}$ and $Pr1^{fl/fl}$ with a Foxp3-regulated Cre. The deletion of NFATc1 and Blimp-1 therefore only occurs after the induction of Foxp3 expression, leaving the nTreg and iTreg development untouched. We therefore claim that the here studied Tfr cells are a subtype of Tregs especially dependent on NFATc1 and that the functional loss caused via NFATc1 deficiency in these cells is reflected via the inability to upregulate CXCR5 [50].

This is also reproduced by the low numbers of Tregs in the overall B-cell follicle of $Nc1^{fl/fl}$*.FIC* and $Nc1^{fl/fl}.Pr1^{fl/fl}$*.FIC* mice. Tfr cells do control the GC in a way different from Tregs and cannot simply be replaced by the same [38, 68]. Tregs might also control the GCR outside of the B cell follicle. The shared labor between Tfr cells and Tregs in the control of the humoral immune response is a matter of debate. A model that only harbors Tfr cells and no Tregs was not examined till now and needs to be addressed in future studies

[166]. However, such a model will presumably suffer from high inflammation, making it almost impossible to understand the role of Tfr cells in controlling the humoral immune response. There are many models that examine the specific deletion of Tfr cells, therewith shedding light on the role of Tfr cells in controlling the humoral immune response different from Tregs [46, 73, 136, 173, 174]. These studies used different strategies to deplete Tfr cells and reported different outcomes on the GCR due to Tfr-cell deficiency. Two models were based on the deletion of CXCR5 in Tregs and therefore are to mention particularly. Chung et al. adoptively transferred *Cxcr5*$^{-/-}$ Treg and wt naïve CD4^{+} T cells at a 1:9 ratio into *Tcrb*$^{-/-}$ mice i.e. in mice without αβ T cells, immunized subcutaneously (s.c.) with KLH in Complete Freund's Adjuvant (CFA) [136]. Wollenberg et al. also transferred *Cxcr5*$^{-/-}$ Treg, but OVA-specific T cells at a 1:1 ratio into TCR-α$^{-/-}$ mice, missing αβ T cells and immunized i.p. with Ova-alum [173]. Both models work with adoptive transfers of *Cxcr5*-deficient Tregs into αβ T cell deficient mice. The usage of a transgenic TCR for the antigen of immunization in transferred T cells favors the development of Tfh cells in comparison to Tfr cells in the setting of Wollenberg et al.. Chung et al. established this disbalance to the favor of Tfh via the ratio of 1:9. The routes of injection, as well as the adjuvants also were different. Nevertheless, both models report a migratory defect of *Cxcr5*$^{-/-}$ Tregs into the GC. In the case of Chung et al. this correlated with a statistically significant increase of GL-7^{+}CD95^{+} GCB cells within the B-cell population and a small increase of CXCR5^{+}BTLA-4^{+}CD4^{+} Tfh cells within the population of transferred naïve T cells. Wollenberg et al. report similar effects via different means, as they observed increased GC volumes and serum titers of Ova-specific antibodies on day 12 post immunization. Therefore, both models show that CXCR5 is needed for Tregs to migrate into the GC and that the absence of Tregs in this region leads to less control of the GCR. In our model the upregulation of CXCR5 in Tregs is affected via the deficiency of NFATc1 [50]. In line with the *Cxcr5*$^{-/-}$ Treg models mentioned, we observed the expansion of the GCR in *Nc1*$^{fl/fl}$*.FIC* mice. Therefore, we claim the low numbers of Tregs that upregulate CXCR5 and develop into Tfr cells while migrating into the B-cell follicle to be the cause of the GCR-expansion as it is reflected in the rise of GCB-cell frequencies.

8.1.3 NFATc1 and Blimp-1 control Tfr-cell frequencies via regulation of CXCR5 expression

NFATc1 is highly expressed in follicular T cells and translocated to the nucleus [50]. It is essential for the CXCR5 expression in Tfr cells, determining the homing of Tfr cells into the B-cell follicle and therewith to the GC [50]. Blimp-1 is highly expressed in Tfr cells, whilst almost absent in Tfh cells [46]. Blimp-1 is known as a dominant repressor of *Cxcr5*-expression in multiple cell types, such as Tfcs or plasma cells [150, 172]. On a molecule per cell basis, the regulation of the CXCR5 expression via NFATc1 and Blimp-1 was only slightly observable. CXCR5 MFIs on Tregs tended to be low due to NFATc1 deletion and higher due to Blimp-1 deletion. Conversely, ablation of Blimp-1 rather raised the frequency of Tfr cells and therewith CXCR5-expressing Tregs. Interestingly, NFATc1 and Blimp-1 double-deficient Tregs showed higher frequencies in Tfr cells compared to the wt. Blimp-1 and NFATc1 might therefore regulate rather the number of CXCR5-expressing cells with a similar level of CXCR5 expression, making a certain threshold of transcription factors necessary for a binary regulation of induction or repression.

Blimp-1-deficient Tregs loose homeostasis via a Bcl-2-dependent mechanism [135]. This is especially the case for eTregs in peripheral organs such as Peyer's patches, intestinal epithelium and the lung [135]. In our experiments, Treg frequencies were increased in mLN of *Prdm1*$^{fl/fl}$*.FIC* mice, but not in the spleen, which is in line with the observation of eTregs being more abundant close to sites rich in presentation of microbial antigens [135]. Different from the report, however, Tfr cells did not rise in their Bcl-2 expression on the protein level when Blimp-1 had been ablated. The reason for this difference could lie in the experimental set up. The published data was based on the increase in frequencies of CD103$^+$ Bcl-2$^+$ Tregs isolated from the compartment of *Prdm1*$^{gfp/gfp}$ cells from mixed bone marrow chimeras. Here we used the *Prdm1*$^{fl/fl}$ mouse combined with the *FIC* deleter strain to generate a Treg specific conditional knockout, which we immunized. Most probably the difference might stem from the Tfr cell being different from a CD103$^+$ Treg. An alternative for the advantage of *Prdm1*$^{fl/fl}$ Tfr cells could be that Blimp-1-deficient T cells are less prone to cell death by cytokine deprivation, can produce IL-2 and proliferate more upon antigen stimulation [107]. In line, the proliferation marker Ki-67 was higher expressed in Tfr cells of mLN due to NFATc1 and Blimp-1 deletion, although this effect was not observed in the spleen and did not follow the dynamics observed in Tfr-cell frequencies. Therefore, it might

rather reflect a strong proliferation due to pronounced antigen presentation near the intestine, as Tfh cells that are wildtypic in this conditional knockout show the same effect. Therefore, high Tfr-cell frequencies due to Blimp-1 deficiency might originate from extended Treg numbers expressing CXCR5 at a level sufficient to become a Tfr cell.

8.1.4 Blimp-1-deficient Tfr cells show reduced suppressive capacity

Under healthy conditions, Tfr cells regulate the GCR via limiting Tfh- and GCB-cell numbers [46, 136]. In aged mice, Tfr cells even increase in proportion to Tfh cells compared to young mice, and since Tfh cells additionally attenuate in their effector function, providing less help to GCB cells, this leads to defective antibody production associated with aging [175]. Overall, a high abundance of Tfr cells should be correlated with low numbers of Tfh- and GCB cells. Tfr-cell frequencies in *Prdm1*$^{fl/fl}$*.FIC* mice were boosted compared to *FIC* mice and lifted in *Prdm1*$^{fl/fl}$*.Nc1*$^{fl/fl}$*.FIC* mice compared to *Nc1*$^{fl/fl}$*.FIC* mice. Nevertheless, this surplus in Tfr-cell frequency was not reflected in a reduction of Tfh- or GCB-cell frequency. Blimp-1 deficiency therefore seems to cause a defect in the suppressive capacity of Tfr cells. A previous study on the role of Blimp-1 in Tfr cells was performed in mixed fetal liver chimeras being reconstituted in a 1:1 ratio with Blimp-1-deficient and Blimp-1-competent fetal liver cells. In line with our results, the loss of Blimp-1 doubled Tfr-cell frequencies, whilst leaving relative Tfh-cell numbers unaffected [46]. Of note, these fetal liver chimeras still harbored Blimp-1 competent Tfr cells, which could control Tfh-cell frequencies. This made our Treg-specific conditional *Prdm1* knockout mice (*Prdm1*$^{fl/fl}$*.FIC*) superior in eliciting the suppressive capacity of Blimp-1-deficient Tfr cells *in vivo*, especially since Blimp-1-deficient Tregs are fully suppressive in culture [115, 117]. In our *in vivo* model, all Tregs, including Tfr cells are Blimp-1-deficient, whilst Tfh cells remain wildtypic and we can conclude that Blimp-1-ablated Tregs – although upregulating CXCR5 – loose function. The suppressive capacity of Blimp-1-deficient Tregs *in vivo* has been discussed for different situations before: In two colitis models based on the adoptive transfer of T cells into Rag1-deficient mice, Blimp-1-deficient Tregs showed similar functionality compared to their wildtypic counterparts [115, 117]. In contrast, in a chemically induced colitis model Blimp-1-deficient Tregs failed to control the disease [115]. The authors hold the reduced expression of IL-10 accountable for this phenotype [115]. In the context of the GCR, however, IL-10 might rather play a supportive role, as IL-10 supports the survival of GCB cells via the induction of Bcl-2 in

humans [176]. In mice subpopulations of Tfr cells are shown to express IL-10 and to support via these means a DZ-GCB-cell phenotype in the context of an acute LCMV infection [72]. Besides Tfr cells, Tfh cells themselves express IL-10 under certain circumstances during a viral infection, supporting the GCB cells via IL-10R signaling and helping therewith to clear the antigen [177]. Furthermore, GCB cells develop into plasma cells rather than into memory cells under the influence of IL-10 [178]. Here we report the expression of *Il10* to be increased in sorted Tfr cells of $Prdm1^{fl/gfp}$ mice compared to the ones from $Prdm1^{+/gfp}$ mice on the day 10 after immunization. This is unexpected as Blimp-1 is shown to support the secretion of IL-10 in Tregs [135]. However, in view of the role of IL-10 in the GCR this increase in *Il10* would rather support GCB cells and might explain to a certain extend why Blimp-1 deficient Tfr cells are less suppressive vs. GCB cells.

How exactly Tfr cells suppress the proliferation of GCB- and Tfh cells is discussed. One important mediator of Treg effector function is CTLA-4 [62]. The deletion of CTLA-4 on Tregs increases overall GC responses whilst decreasing the proportion of antigen-specific B cells [166]. Tfr cells express the inhibitory coreceptor CTLA-4 higher than Tregs [46]. The deletion of CTLA-4 on Tfr cells themselves actually enhanced the antigen specific B-cell response in GCs [60]. We did not observe major differences in the expression of CTLA-4 on Tfr cells due to Blimp-1 deletion, also NFATc1 deletion did not change CTLA-4 expression on Tfr cells. We claim therefore, that Blimp-1 is necessary for the suppressive function of Tfr cells in a mechanism different from CTLA-4 mediated suppression.

8.1.5 NFATc1 and Blimp-1 cooperate to control the antigen specific humoral immune response

We observed higher frequencies of GCB cells due to NFATc1 deficiency in Tregs. NFATc1/Blimp-1 double-deficient Tregs similarly boosted GCB-cell frequencies after immunization with NP-KLH. The overall IgG titers in the sera of NP-KLH immunized mice also rose when Tregs were NFATc1-deficient. This effect was even more pronounced when Blimp-1 was additionally missing in Tregs. Blimp-1-deficient Tregs did not cause an overall increase of GCB-cell frequencies or IgG titers in the serum of immunized mice. Still, as GCB-cell frequencies and IgG titers were not reduced due to the increase in Tfr cells in these mice, this indicates a loss of function in Blimp-1-deficient Tfr cells. Differently from the overall IgG titers, NP-specific IgG especially rose in mice with

NFATc1/Blimp-1 double-deficient Tregs. It seems that the deficiency of NFATc1 affects the control of the overall GCR irrespective of the antigen specificity. Therefore, the overall GCR is less controlled. The double deficiency of NFATc1 and Blimp-1 in Tregs might especially affect the control of the antigen-specific GCB cells. This can be a hint for the way, how the Tfr-cell suppressive capacity is affected via the double deficiency of NFATc1 and Blimp-1. Tfr cells need to be in close contact to GCB cells specifically to suppress the single cell. It is likely that the expression of a surface molecule or the time of interaction between the Tfr cell and the GCB cell might be modulated via the double deficiency. CTLA-4 deletion on Tfr cells was shown to increase antigen-specific GCB-cells [60]. We show here that it is actually not CTLA-4 that is changed in its expression on Tfr cells due to the double knockout, but it might be another surface molecule.

8.1.6 NFATc1 and/or Blimp-1 deletion change the expression of posttranslational modifying enzymes in Tfr cells

In order to find changes in Tfr cells that lead to the loss of their suppressive capacity, we sorted Tfr cells from immunized mice and performed RNA-seq analyses. The deletion of NFATc1 in Tregs changed the gene expression in Tfr cells in a way similar as Blimp-1 deletion did. The gene sets that were enriched in these two cases were indicating a change in nucleosome organization and chromatin assembly/disassembly. This similarity could be an indication for a failure during the experiment. The difference observed in the control of the GCR between the *FIC, Nc1$^{fl/fl}$.FIC* and *Pr1$^{fl/fl}$.FIC* mice could not be explained with the change in these GO-terms. We assumed that changes in RNA levels of GCR relevant genes might be masked by this artefact, therefore we filtered for genes that are part of the gene set that differs between Tfh- and Tfr cells [142] and are substantially changed in their expression either due to the deletion of NFATc1 or Blimp-1 in Tregs. Within this gene set, we searched especially for genes encoding costimulatory/repressive surface molecules or messengers, such as cytokines. We did not find a gene coding for a surface molecule that was differentially expressed due to the knockout of NFATc1 or Blimp-1 in Tregs within this set of genes. Interestingly, many genes being differentially expressed due to NFATc1 or Blimp-1 deficiency are involved in posttranslational modifications of proteins, such as ubiquitination. Therefore, the Tfr-cell function could be affected due to the degradation of proteins being involved in the interaction between Tfr- and Tfh cells or Tfr- and GCB-cells.

Those effects would be beyond RNA expression and not reflected in differentially expressed transcripts.

8.1.7 NFATc1 and Blimp-1 deletion impact the expression of genes involved in Tfr-cell function and stability

We furthermore found differentially regulated genes being involved in the signal transduction. One gene which caught our interest was *Tnfsf9.* We found *Tnfsf9* to be lower expressed in NFATc1-deficient Tfr cells and lowest in Blimp-1-deficient Tfr cells. *Tnfsf9* codes for CD137, which is found on FDCs. The ligand for CD137, named CD137L is expressed on GCB cells [179]. Mice being deficient in CD137L are predisposed to develop B-cell lymphoma with an incidence of approximately 60% at an age of 12 months [179]. CD137L deficiency increased the expression of multiple GC regulators in B cells, amongst other things Bcl6 [179]. Tfr cells could putatively suppress GCB cells via CD137-CD137L interaction. The low expression of *Tnfsf9* would then lead to a loss of this putative mechanism of Tfr-cell mediated suppression, which would be in line with the reduced suppressive capacity in Blimp-1 deficient Tfr cells. The gene *Pmepa1*, coding for PMEPA1 was down regulated in NFATc1 as well as Blimp-1-deficient Tfr cells. PMEPA1 blocks TGF-β signaling and is part of a negative feedback loop to shut down TGF-β signaling in prostate cancer cells [158]. TGF-β is shown to expand Tfr cells from human tonsils *in vitro* [180] and the combined deficiency of TGF-β and CD25 in T cells increases the GCR in mice [181]. If TGF-β is necessary for Tfr-cell function is not known, but increased levels of TGF-β due to less PMEPA1 might support Tfr-cell numbers as seen in the $Pr1^{fl/fl}$*.FIC* mice. NFATc1, as well as Blimp-1-deficient Tfr cells showed increased expression of *Myd88*, coding for Myeloid differentiation primary response protein 88 (MyD88). MyD88 functions as an adapter protein involved in the IL-18 and IL-1 receptor-signaling pathway in T cells [182]. The overexpression of MyD88 induces the activation of the c-Jun N-terminal kinase (JNK), as well as NF-κB *in vitro*, which is downstream of the IL-1 signaling pathway [183]. IL-1 signaling expands Tfh cells, whilst Tfr cells suppress the IL-1 mediated activation of Tfh cells [55]. Overexpression of MyD88 in Tfr cells therefore could intervene with the Tfr-cell program in a way changing it into the direction of Tfh cells. We observed this upregulation in NFATc1 as well as Blimp-1-deficient Tfr cells, therefore it might not explain the difference observed between the NFATc1 and Blimp-1 conditional

knockout mice, but it might add up in the double-deficient mice, which are also showing especially high IgG titers in the serum of immunized mice independent of antigen specificity. Blimp-1-deficient Tfr cells exhibited increased levels of *Ikzf4* RNA. *Ikzf4* codes for the zinc finger protein Eos. Eos interacts with Foxp3 and mediates Foxp3 -dependent gene silencing in Tregs [184]. Eos therewith supports Treg stability. High levels of Eos in Blimp-1-deficient Tfr cells would rather support Tfr stability and function and can therefore not explain the loss of suppressive capacity. Although we report here changes in the signal transduction within Tfr cells due to NFATc1 and/or Blimp-1 deletion, such as TGF-β and IL-1 receptor signaling as well as Treg stability, no major changes in the overall transcriptional program were observed that were pointing towards the differentiation of Tfr cells into another cell type. For that reason, we assume rather small changes due to NFATc1 or Blimp-1 knockout affecting single genes or proteins via posttranslational changes rather than whole gene signatures.

8.1.8 Blimp-1 deficiency upregulates *Bcl-2a1a*

We found *Bcl2a1a* to be upregulated in Blimp-1-deficient Tfr cells. *Bcl2a1a* codes for the Bcl-2-related protein A1 (formerly named A1 or BFL-1 in humans) and is a pro-survival protein of the Bcl-2 family of apoptosis regulating proteins [161]. In mice, *Bcl2a1* is quadruplicated with *Bcl2a1a*, *-b* and *–d* being functional genes. They harbor similar regulatory regions, but individual Bcl2A1 proteins dominate differentially in different cell types. As mentioned, Blimp-1 deficiency leads to upregulation of the pro-survival guardian Bcl-2 in eTregs [135]. Since we could not detect higher amounts of Bcl-2 in Tfr cells, when Blimp-1 had been ablated, we now conclude that the elevated frequencies of Blimp-1-deficient Tfr cells stem from increased levels of A1-A. The observation of upregulated *Bcl2a1a* is very well in line with our detailed molecular analyses of Blimp-1-mediated *Bcl2a1* repression (Xiao, Qureischi, Dietz…Koenig et al., in revision).

8.1.9 Experimental difficulties

NFATc1 or Blimp-1 deficiency upregulated the expression of *Il10* in Tfr cells. Blimp-1 is noted for the positive regulation of *Il10* expression [159]. The observation of increased levels of *Il10* RNA in Blimp-1-deficient Tfr cells is not in line with the literature. Either the regulation of *Il10* expression in Tfr cells is different from the ones in Tregs, as we

discussed it earlier, or we do observe a different result due to contaminating cells expressing high levels of *Il10* within our sorted Tfr-cell population. In principle, this could be the case as Blimp-1 was used as a marker for the sort of Tfr cells. Due to the conditional deletion of Blimp-1 in Tregs only, Tcons are still Blimp-1-competent and could be sorted as a Blimp-1-GFP^{+} cell. This problem could be circumvented in future experiments via the breeding of NFATc1 and/or Blimp-1 conditional knockout combined with a Foxp3-reporter strain. This would enable us to sort Foxp3-positive Tfr cells.

8.2 Overexpression of caNFATc1/αA in Tregs and its influence on the GCR

8.2.1 Overexpression of caNFATc1/αA increases CXCR5 expression on Tregs, but not Tfr-cell frequencies

In line with an NFATc1 dependence for CXCR5 expression in Tfr cells, caNFATc1/αA enhanced CXCR5 expression on Tregs. However, the relative number of Tfr cells did not increase. Thus, this is the other side of the coin of having a higher number of Blimp-1-deficient Tfr cells without increased CXCR5 expression levels. It seems that it is only the ability to express CXCR5, which defines the number of Tfr cells. Higher levels of CXCR5 expression do not increase the Tfr-cell frequencies.

The overexpression of caNFATc1/αA in Tregs even slightly reduced Tfr-cell frequencies in mLN after immunization. We cannot exclude that a more of caNFATc1/αA in Tregs affects Tfr cells in a way different from CXCR5 expression e.g. affecting proliferation or survival, however, after immunization neither Bcl-2 nor Ki-67 levels were reduced in Tfr cells due to caNFATc1/αA overexpression in Tregs (Fig. S7) and the reduction in Tfr cells did not reach significance anyhow.

In the steady state, the frequencies of Tfh cells were reduced due to the overexpression of caNFATc1/αA and subsequently CXCR5 in Tregs. This effect was lost after immunization, when Tfh-cell frequencies in *Nc1^{caaA}.FIC* resembled the ones observed in the *FIC* mouse. The immunization breaks the state of homeostasis. This is primarily achieved via the addition of an adjuvant to the antigen of immunization. The exact way how the adjuvant used operates, is discussed [185]. Studies on aluminum-containing adjuvants report a

limited amount of necrosis of tissue cells, which may lead to the limited release of danger associated molecular patterns (DAMP) that recruit and activate inflammatory cells [186]. This might overcome the Tfr-cell mediated suppression of Tfh cells as we see it in the *Nc1^{caaA}.FIC* mouse in the steady state.

8.2.2 Higher CXCR5 expression facilitates the migration into the GC in *Nc1^{caaA}.FIC* mice

The overexpression of caNFATc1/αA drastically increased the expression of CXCR5 on Tregs before and after immunization. In an *in vitro* chemotaxis assay, naïve murine T cells migrated into the direction of CXCL13 with the magnitude of the migration response corresponding to the CXCR5 expression level [187]. Similarly, the dependence on NFATc1-induced CXCR5 expression for following a CXCL13 gradient was demonstrated in the lab by a transwell assay before [50]. Thus, the increased CXCR5 expression on Tregs might change the migration behavior and therewith the positioning of the Tregs within the follicle rather than the Tfr-cell frequencies. CXCL13 is produced in the light zone of the GC mainly by FDCs and CXCR5 is suggested to be involved in the coordination of the appropriate positioning of antigen responding T cells into the LZ of the GC [187, 188]. Indeed, we observed an enrichment of Tregs that overexpress caNFATc1/αA within the B-cell follicle and especially within the GC. This observation is new, as the overexpression of CXCR5 in naïve T cells only promoted the migration into the B-cell follicle in the absence of the CCR7 ligand [187]. Therefore, the level of CXCR5 expression, which was especially high due to caNFATc1/αA, seems to dictate the depth of migration into the GC. Only if Tregs overexpressing caNFATc1/αA really concentrate within the light zone of the GC needs to be addressed in future experiments.

Furthermore, we observed less Tregs within the B-cell follicle after immunization with NP-KLH in ImJect Alum in the *FIC* mouse compared to the PBS control. It seems that our treatment causes Tfr cells to migrate out of the follicle. This effect was only observed within the *FIC*, but not within the *dLckcre* mice and needs further investigation.

Intriguingly, enhanced CXCR5 expression on Tfr cells and deeper migration into GCs via the overexpression of caNFATc1/αA in Tregs did not impact relative Tfh-cell numbers and reduced GCB-cell frequencies only slightly. Still, CXCR5^{hi} Tfr cells were functionally

augmented as the influence of caNFATc1/αA overexpression in Tregs became visible in the humoral immune response vs. the antigen of immunization. NP-specific IgG and IgM titers were lowered in *Nc1^{caaA}.FIC* mice compared to *FIC*, whilst the overall serum IgG-titers were not changed. This indicates that additional Tregs within the B-cell follicle, and especially within the GC, control the development of antigen-specific plasma cells more strictly. The control of the GCR might also take place extra follicular or at the T-B-border. This might be the locations where the establishment of the GCR irrespective of antigen specificity is controlled. The antigen-specific-GCB cells and therewith the development of plasma cells producing antigen specific antibodies might be controlled in the GC itself. Here, the CXCR5^{hi} Tfr cells of *Nc1^{caaA}.FIC* mice, which migrate deeper into the GC might control the antigen-specific humoral immune response better, just because of the reason of better accessibility. However, the affinity of NP-specific IgG was not changed, giving the hint that the process of affinity maturation was unaffected via overexpression of caNFATc1/αA.

8.2.3 Overexpression of caNFATc1/αA creates a Tfr-cell signature that is associated with an effector phenotype which is Blimp-1-dependent

Overall, the overexpression of caNFATc1/αA showed a beneficial influence on the suppressive function of Tfr cells, i.e. on the antigen-specific humoral immune response. In peripheral Tregs, the expression level of NFATc1 is by default suppressed via the binding of Foxp3 to its inducible *P1* promoter, which drives NFATc1/αA expression via an auto-regulatory loop in T-effector cells [98, 152]. Nevertheless, Tfr cells showed *P1* activity, which is less than in Tfh cells, but still evident (Martin Vaeth, unpublished data). Consequently, NFATc1/αA distinguishes Tfr cells from peripheral Tregs, something which might also be true for other types of eTregs. Data from the lab further indicated that not only Foxp3, but also Blimp-1 could suppress transactivation of the inducible *P1* promoter of NFATc1. This explains why Blimp-1^{+} Tfr cells engage the *P1* to a lesser extent than Tfh cells, but not how this type of Treg can overcome the complete repression of *P1*. We assume that T-cell receptor signals are of such high affinity and avidity in Tfr cells that the auto-regulatory loop of NFAT activation is re-installed in spite of Foxp3. The inherent danger is unleashed cytokine expression, wherefore Foxp3 and probably Blimp-1 further guard repression. In this context, it is noteworthy that Blimp-1 is known to inhibit IL-2 and

Fos as well as T-bet and IFN-γ expression in T cells or IL-17 in intestinal pTregs [107, 189, 190]. Not only in plasma cells, but also in T cells, Blimp-1 also represses Bcl6, a puzzle for Tfr cells since their description as Foxp3$^+$Bcl6$^+$Blimp-1$^+$ follicular T cells [46, 136]. Intriguingly, however, Bcl6 can be robustly induced by NFATc1/αA [123], pointing to a delicate balance between NFATc1/αA-mediated transactivation and Blimp-1-mediated repression in Tfr cells.

To understand this balance, we compared the transcriptional profiles of Tfr cells that were expressing caNFATc1/αA with that of Tfr cells, which were depleted of endogenous NFATc1. Further, we included caNFATc1/αA$^+$Blimp-1$^-$ Tfr cells in our transcriptome analyses. The Gene Ontology term "defense response" was mostly enriched in the comparison of NFATc1-deficient vs. caNFATc1/αA$^+$ Tfr cells. Within this set of genes, we discovered *Jak2* coding for the tyrosine-protein kinase JAK2 to be downregulated due to overexpression of caNFATc1/αA and even further downregulated when Blimp-1 was missing in addition. JAK2 activates STAT5 [191], which activates Blimp-1 [104] and inhibits Bcl6 expression [124, 129], therewith allowing less differentiation into follicular T cells. If on the contrary the presence of caNFATc1/αA and the deficiency of Blimp-1 limit *Jak2*, this should be beneficial for Tfr-cell differentiation of Tregs. This is in line with – now direct and indirect – boosted Bcl6 expression by NFATc1/αA [123]. However, the expression levels of *Bcl6* in Tfr cells of the different genotypes were not twofold differentially regulated, this is the reason why *Bcl6* also does not appear in the heat map.

In addition, we observed *Il6st*, the gene coding for the Interleukin-6 receptor subunit beta (IL6ST) to be upregulated due to the overexpression of caNFATc1/αA. IL6ST is the signal-transducing chain of the Interleukin-6 receptor system. IL-6 signaling activates STAT3 [192]. Here again, the Tfr-cell differentiation program is a delicate balance as STAT3 - via the induction of Bcl6 [164] - supports the transcriptional program for follicular T cell, whereas STAT5-mediated transcription ensures Treg identity [160]. Higher expression of IL6ST could therefore shift the STAT5/STAT3 balance in favor of STAT3 and therewith strengthen the Tfh-cell like features on the expense of the Treg phenotype. Contra-intuitively, this effect was lost with the additional Blimp-1 deficiency.

Nevertheless, the shift towards less Tfr-cell like and thus maybe more Tfh-cell like gives rise to the risk that NFATc1/αA$^+$ Tfr cells acquire helping capacities for GCB cells. One way, Tfh cells provide help to GCB cells is the secretion of IL-4 and IL-21 [16]. *Il21* was not changed considerably and therefore not unleashed in its expression due to caNFATc1/αA overexpression, whereas *Il4* RNA was even reduced. Thus, at least the major cytokines released by Tfh cells, did not de-repress due to caNFATc1/αA overexpression.

IL-1 receptor signaling activates Tfh cells to secrete IL-4 and IL-21 in response [55]. This is blocked by Tfr cells, which express the decoy receptor for IL-1, IL-1R2 as well as the IL-1 receptor antagonist IL-1Ra [55]. caNFATc1/αA$^+$ Tfr cells exhibited increased RNA levels of *Il1rn*, the gene coding for the IL-1 receptor antagonist, and therewith are predicted to suppress Tfh-secreted IL-21 and IL-4 more efficiently. This plus in *Il1rn* expression was depending on Blimp-1 and might therefore be a mechanism of suppression controlled via the cooperation of Blimp-1 and NFATc1. This mechanism of suppression is especially important in the GC itself as IL-1R2 and IL-1Ra are expressed on CD25$^-$ Tfr cells [55].

caNFATc1/αA in Tfr cells increased the expression of *Il10.* This effect was lost due to Blimp-1 deletion in Tfr cells, in line with Blimp-1 being essential for IL-10 expression in eTregs [135]. However, loss of NFATc1 can also lead to enhanced IL-10 expression as documented for B cells [193]. In B cells, all NFATc1 isoforms were deleted and it is not known, if the short NFATc1/αA and the long NFATc1/βC act differentially on IL-10 like it was reported for IL-2 and some effector cytokines [76]. On the other hand, IL-10 expression in Th2 and eTregs depends on IRF4 [135, 194], which is induced by T-cell receptor mediated NFATc1 transactivation. [51, 195]. Therefore, if NFATc1/αA does not transactivate IL-10 directly in Tfr cells, it would do so by inducing IRF4, which together with Blimp-1 leads to IL-10 expression in eTregs. At last, the overexpression of caNFATc1/αA in Tfr cells upregulated the expression of the gene *Tigit*, coding for the immunoreceptor TIGIT. TIGIT$^+$ cells interact with dendritic cells, therewith increasing their IL-10 secretion [165], which of course can induce further IL-10 expression in IL-10R$^+$ cells via STAT3 activation [196, 197]. TIGIT is even found on Tfh cells, where it interacts with CD155 on FDCs [198]. The authors discuss, that this interaction is important to keep

the Tfh cells within the GC. Here, the expression of TIGIT on Tfr cells could guide them to the FDC, exerting regulatory functions.

The effects of IL-10 on the GCR are divers. It is reported that IL-10 derived from mast cells in the skin after UV-radiation suppresses the development of GC [199]. On the other hand, the survival of GCB cells [176], as well as the differentiation into plasma cells [178] is supported by IL-10. Only recently, Tfr cells themselves were reported to secrete IL-10 in order to promote the GCR in the context of a LCMV infection [72]. If at all, we observed a reduction of GCB-cell frequencies and for sure lower NP-specific IgG and IgM titers. Therefore, a pronounced survival of GCB cells due to IL-10 signaling seems unlikely. Secondly, the affinity maturation of the plasma cells secreting NP-specific antibodies was not affected, therefore a premature differentiation into plasma cells is not indicated. In the context of the experiments performed here, an increase in IL-10 expression correlated with a reduced GCR, thus more the classical role of IL-10 in limiting an immune response.

In line with elevated levels of *Tigit* mRNA, we observed reduced levels of *Bcl2* [200] in caNFATc1/αA$^+$ Tfr cells, indicating that these cells comprise a stronger effector phenotype and are therefore more susceptible to die. In line with this, also *Klrg1* –RNA was less upon caNFATc1/αA expression. The gene *Klrg1* codes for the co-inhibitory receptor killer-cell lectin like receptor G1 (KLRG1). Its expression on T cells is associated with a highly differentiated phenotype and a reduction in effector function [162]. A reduced expression of *Klrg1* in Tfr cells might therefore be associated with an increase in effector function. This effect did not depend on the presence of Blimp-1. To our knowledge, there are no reports on any direct influence of NFAT on KLRG1 expression and the lessened expression in presence of caNFATc1/αA could hence be indirect.

On the contrary, CTLA-4 has long been described as an NFAT target gene [93, 201]. Not surprisingly, *Ctla4* RNA was increased in the presence of overexpressed caNFATc1αA. Expression was lost in the absence of Blimp-1, again in line with data defining CTLA-4 as Blimp-1-regulated [130]. Unfortunately, we could not observe higher levels of CTLA-4 on the surface of Tfr cells overexpressing caNFATc1/αA by flow cytometry (Fig. S8), but this could be due to multifactorial regulation of CTLA-4 surface expression [202]. CTLA-4 is an important mediator of the Tfr-cell effector function [60, 166]. High levels of CTLA-4 could potentially strengthen the suppressive capacity of Tfr cells. Taken together, Tfr cells

expressing caNFATc1/αA showed upregulation of genes that are important for T-follicular differentiation, at the same time strengthening expression of genes that are particularly important for Tfr-cell effector function. This differential regulation of genes depended on Blimp-1, indicating an interaction of NFATc1 and Blimp-1 at multiple regulatory sites important for Tfr-cell identity and function.

8.2.4 Blimp-1 deficiency in Tregs weakens homing of Tfr cells to the GC

We compared the transcriptional signature of Tfr cells that overexpressed caNFATc1/αA with that one of Tfr cells which were additionally Blimp-1-deficient. Most of the enriched GO-terms were reflecting a change in the migration of the Tfr cells. Blimp-1 deficiency changed the expression of many chemokine receptors on the background of caNFATc1/αA overexpression. *Ccr7* as well as *S1pr1* were already slightly upregulated due to overexpression of caNFATc1/αA in Tfr cells, but highly upregulated under the additional absence of Blimp-1. With focus on the GCR, the upregulation of *Ccr7* and *S1pr1* are especially relevant. An upregulation of S1PR1 on Tfh cells leads to the relocation into the T cell zone [17]. Thus, higher expression of *Ccr7* on Tfr cells should force their migration into the T-cell zone rather than to the B cell follicle of secondary lymphoid organs. It might even counteract the higher expression of CXCR5, which we observed on the surface of caNFATc1/αA overexpressing Tregs (Fig. 7.19B). This would be in line with a report that overexpression of CXCR5 in naïve T cells only promotes the migration into the B-cell follicle in the absence of the CCR7 ligand [187]. So far, we did not observe less Foxp3$^+$ cells in the B-cell follicle of mice that harbored Blimp-1-deficient Tregs. Compared to the wt, these mice showed even higher numbers of Foxp3$^+$ cells within the B cell zone (Fig. 7.14B). It remains to be tested if the additional Blimp-1 deficiency in caNFATc1/αA overexpressing Tregs can revert the pronounced migration into the B-cell zone and the GC caused via the increased CXCR5 expression on Tfr cells. Besides these chemokine receptors that are known to directly influence the positioning of Tregs in the T-cell or B-cell zone, Blimp-1 deficiency in Tfr cells raised the expression levels of *Ccr4*, *Ccr10*, *Ccr6* and *Cx3cr1*, whilst downregulating *Ccr3*, *Ccr8* and *Ccr9*. This could change the migratory behavior of Tregs in general, recruiting them to different tissues like lung, skin and gut [167]. It might be of interest to address this issue within future experiments.

8.3 Overexpression of caNFATc1/αA in T cells and its influence on the GCR

8.3.1 The restriction of the GCR in mice overexpressing caNFATc1/αA in T cells is a Tcon-intrinsic effect

NFATc1/αA is highly expressed and activated in Tfoll, comprising both Tfr- and Tfh cells [50]. Therefore, we included *Nc1^{caaA}.dLckcre* and *Nc1$^{fl/fl}$.Nc1^{caaA}.dLckcre* mice in our analyses, the latter being devoid of endogenous NFATc1 and hence the longer isoforms NFATc1/βB and NFATc1/βC. The overexpression of caNFATc1/αA in T cells reduced Tfh-cell frequencies drastically. It shifted the Tfr-/Tfh-cell ratio to the favor of Tfr cells. This happened mainly due to the lower numbers of Tfh cells, as Tfr-cell frequencies were almost unaffected. When caNFATc1/αA was overexpressed in Tregs only, IgG and IgM titers were significantly lower against the antigen of immunization, GCB-cell frequencies were maybe slightly reduced, and Tfh-cell frequencies were not affected at all. The strong reduction in Tfh- and GCB-cell frequencies observed due to the overexpression of caNFATc1/αA in all T cells might therefore be an effect coming from the Tcon side. The overexpression of caNFATc1/αA in Tregs only enhanced the level of CXCR5 expression on the surface of Tregs significantly, but this effect was not seen as drastic, when caNFATc1/αA was overexpressed in all T cells. Accordingly, the reason for this could be secondary effects coming from the side of the Tcons, having an influence on the Tregs. Of note, cells from the mLN of immunized *Nc1$^{fl/fl}$.Nc1^{caaA}.dLckcre* mice secreted more IL-2, upon stimulation with CD3/CD28 *in vitro* compared to the wildtypic mouse (see below). IL-2 is not only inhibiting Tfh-cell differentiation, but can also halt that of Tfr cells. [56]. Interestingly, the authors report that high IL-2 induced Blimp-1, which we know to repress CXCR5 expression. Therefore, we interpret that caNFATc1/αA-mediated unrestrained IL-2 expression in Tcon might have supported Treg survival and proliferation but prevented overshooting CXCR5 expression on Tfr cells albeit the Treg themselves were caNFATc1/αA$^+$.

Although the CXCR5 expression on Tregs was not as drastically increased, Foxp3$^+$ cells enriched in the B-cell follicle and the GC, when caNFATc1/αA was overexpressed in T cells. Nonetheless, the enrichment of Foxp3$^+$ cells in the GC was less significant, indicating that the expression level of CXCR5 dictates the migration capacity into the GC.

8.3.2 Overexpression of caNFATc1/αA might suppress Tfh-cell development via an IL-2 -dependent mechanism

Comparing the small frequencies of Tfh- and GCB-cells in *Nc1^{caaA}.dLckcre* with the almost unaffected levels in the *Nc1^{caaA}.FIC*, the major impact of caNFATc1/αA in all T cells on the GCR should stem from the Tcon side. It was shown before that the expression of an NFATc1 mutant, which is constantly localized in the nucleus of T cells, leads to signs of autoimmunity in 4-6 weak old mice [203]. This phenotype is associated with increased levels of Th1 and Th2 cytokines, as well as high IgG2a levels in the serum of mice and increased numbers of CD4$^+$CD25$^+$CD40L$^+$CD69$^+$ T cells in LN and spleen [203]. The overexpression of caNFATc1/αA in T cells enhanced Tcons with an activated phenotype only significantly on the background of NFATc1 deletion in the spleen. Mice overexpressing caNFATc1/αA did not show any signs of sickness at the age of three months. Spleen and mLN elicited even the tendency to smaller organ size indicating that the overexpression of caNFATc1/αA in T cells might be beneficial to keep the state of homeostasis within the secondary lymphoid organs. Nevertheless, we observed a higher frequency of CD4$^+$ T cells in spleen and mLN, when caNFATc1/αA was overexpressed in T cells. We suspected this increase to stem from a higher production of IL-2, since NFAT factors are known to activate the transcription of IL-2 [153] and IL-2 functions as a major growth factor for T cells [170]. Interestingly, overexpression of caNFATc1/αA had no influence on the frequencies of IL-2 producing CD4$^+$ and CD8$^+$ T cells in mLN four days post immunization. Still, as mentioned, additional *ex vivo* stimulation with αCD3/αCD28 for 48 h revealed enhanced IL-2 secretion due to overexpression of caNFATc1/αA even on the background of NFATc1 deficiency. As expected, the deletion of NFATc1 itself limited IL-2 secretion. In sum, caNFATc1/αA enhanced IL-2 expression, although this was not an uncontrolled situation, but needed additional T-cell activation. IL-2 signaling counteracts Tfh-cell development via a STAT5 -dependent mechanism [124]. Therefore, high concentrations of IL-2 produced by caNFATc1/αA$^+$ Tcons presumably interfered with the development of Tfh cells already during the priming, possibly leading to the differentiation into another subtype of T-helper cells. This would be in line with previously published data demonstrating increased levels of Th1 and Th2 cytokines in mice with an NFATc1 mutant, giving rise to all NFATc1 isoforms, which then constantly localize to the nucleus of T cells [203]. However, NFATc1/αA primarily drives IL-2 induction, whereas

the other isoforms are more decisive for effector cytokine expression [76], which could account for the prevention of an autoimmune phenotype of our *Nc1^{caaA}.dLckcre* and *Nc1$^{fl/fl}$.Nc1^{caaA}.dLckcre* mice. Besides, a surplus in IL-2 supports Tregs, preventing autoimmunity on their own.

8.3.3 NFATc1/βC in T cells plays a role separately from caNFATc1/αA concerning the GCR

In accordance with a differential influence of the NFATc1 isoforms, caNFATc1/αA^{+} Tfh-cell frequencies were higher in the absence of endogenous NFATc1. The endogenous NFATc1 comprises the long isoform NFATc1/βC with a long C-terminus that harbors sumoylation sites. The sumoylation of NFATc1 turns NFATc1 into a repressor for IL-2 and enables effector cytokine expression [76]. However, the slight increase in Tfh cells in *Nc1$^{fl/fl}$.Nc1^{caaA}.dLckcre* compared to *Nc1^{caaA}.dLckcre* stands in contradiction to the hypothesis that sumoylated NFATc1/βC could play a major role, when the short isoform is constitutively active and surely dominating NFATc1 expression in these mice. On the other hand, in this model also the Tregs are sufficient vs. deficient for endogenous NFATc1 and therewith the long isoforms. Since the expression level of CXCR5 slightly rised on caNFATc1/αA^{+} Tregs when they were additionally devoid of endogenous NFATc1, the difference between the two genotypes might stem from the Tregs. The major difference between the *Nc1^{caaA}.dLckcre* and the *Nc1$^{fl/fl}$.Nc1^{caaA}.dLckcre* became visible in the antigen-specific humoral immune response. *Nc1$^{fl/fl}$.Nc1^{caaA}.dLckcre* showed the lowest titers of class switched antibodies vs. the antigen of immunization compared to their wildtypic littermates. This indicated a specific reduction of the antigen specific humoral immune response and correlated well with enhanced CXCR5 expression on Tfr cells.

8.3.4 Overexpression of caNFATc1/αA in T cells strengthens IL-6 receptor signaling in Tfr cells

Lastly, the transcriptional signature of Tfr cells isolated from immunized *dLckcre*, *Nc1$^{fl/fl}$.dLckcre* and *Nc1$^{fl/fl}$.Nc1^{caaA}.dLckcre* was examined. In line with Tfr cells from *Nc1^{caaA}.FIC,* the overexpression of caNFATc1/αA enhanced the expression of *Il6st* coding for the Interleukin-6 receptor subunit beta (IL6ST). Again, higher levels of IL6ST could

strengthen the STAT3 signaling and therewith the expression of T follicular-associated genes. MHCII genes were upregulated upon loss of NFATc1 expression, which could be restored by caNFATc1/αA (here on the background of NFATc1 deletion). *H2-Eb1* and *H2-Ab1* are encoding the β-chains of MHCII, whereas *H2-Aa* the α-chain and *Cd74* for the γ-chain of MHCII. Now, it might be surprising to see MHCII expression on Tregs, but this has been reported for mice with Gata3 or Bcl6-ablated Tregs and those Tregs were coined 'Antigen-Presenting Cell (APC)-Like Treg' [204].

Taken together, in Tfr cells NFATc1 expression is not only necessary to allow CXCR5 expression and home deep into the GC, but to support the effector phenotype of follicular T cells and avoid plasticity towards untypical Tregs. Blimp-1 ensures the effector phenotype of Tfr cells, for instance by *Il10* and *Ctla4* expression and represses all kinds of homing receptors. Here, NFATc1 is needed to counteract CXCR5 repression, which then maybe driven in conjunction, i.e. an NFATc1 and Blimp-1 complex.

9 Annex

9.1 Supplementary Data

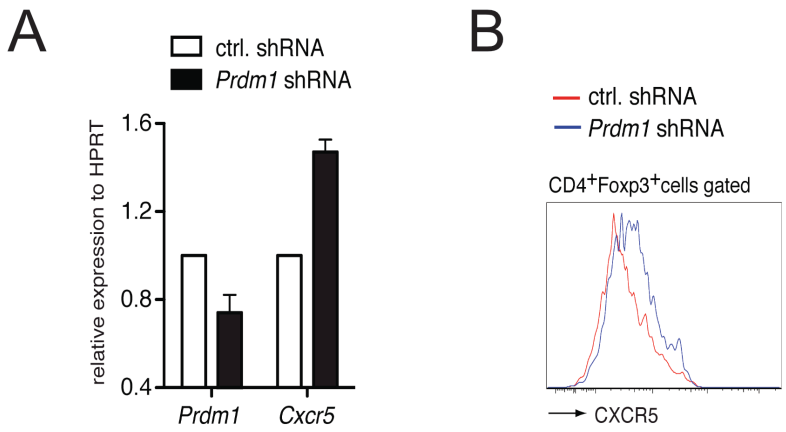

Figure S1: *Prdm1* shRNA knockdown increases CXCR5 expression

(A) shRNA-mediated knock down of *Prdm1* in primary Foxp3$^+$ nTregs. RNA levels of *Prdm1* and *Cxcr5* were monitored by qRT-PCR (B) CXCR5 protein expression was analyzed by flow cytometry. The experiment was performed by Martin Vaeth.

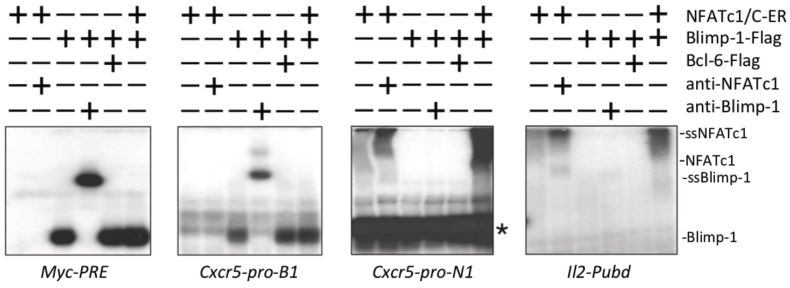

Figure S2: Blimp-1 and NFATc1/C bind to the *Cxcr5*-promoter

EMSA with nuclear extracts from HEK 293T cells transiently transfected with NFATc1/C-ER, Blimp-1-Flag, and/or Bcl6-Flag. *Myc-PRE*, *Cxcr5-pro-B1*, *Cxcr5-pro-N1*, or *Il2-Pubd* were used as probes and anti-Blimp-1 or anti-NFATc1 super shifts (*, unidentified band). The experiment was performed by Friederike Berberich-Siebelt.

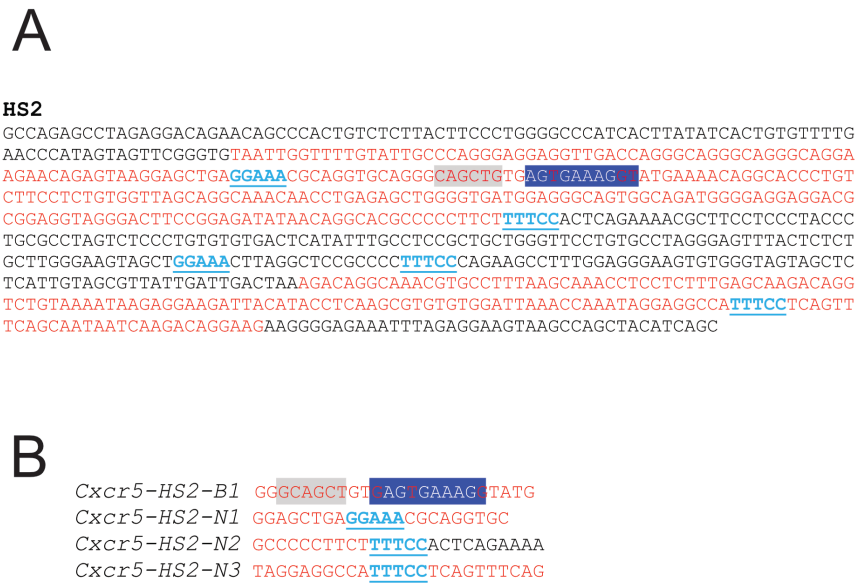

Figure S3: The *Cxcr5*-promoter harbors conserved NFAT and Blimp-1 binding sites

(A) Murine sequence of *HS2*. Conserved areas between mouse and men are marked in red. NFAT-consensus sites are marked in light blue. The binding site for the E-box-factor E2A is marked in gray and the binding site for Blimp-1 in dark blue. (B) Sequences of the sense strand of oligonucleotides containing the conserved E2A and Blimp-1 binding sites (*Cxcr5-HS2-B1*), as well as the three conserved NFAT binding sites (*Cxcr5-HS2-N1*, *Cxcr5-HS2-N2* and *Cxcr5-HS2-N3*). (A and B) modified from Friederike Berberich-Siebelt

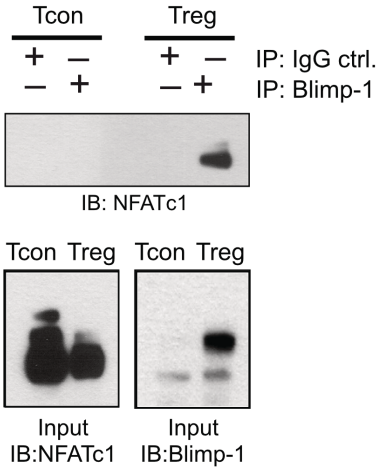

Figure S4: Blimp-1 and NFATc1 interact with each other

CoIP of NFATc1 with Blimp-1 using nuclear protein extracts from activated primary Tcon and Treg cells. Experiment was performed by Martin Vaeth.

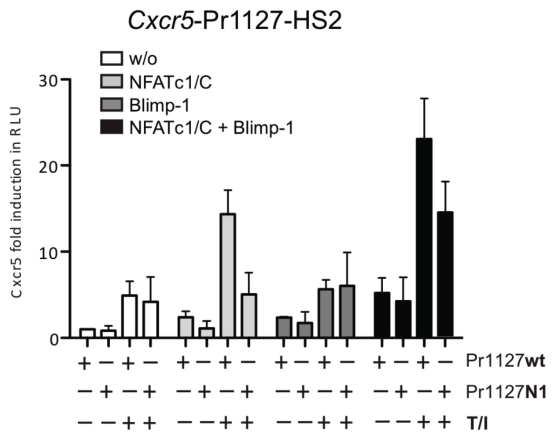

Figure S5: Blimp-1 and NFATc1 transactivate CXCR5 expression

Luciferase assays of full length *Cxcr5*-promoter (-1127) of wildtypic or mutated proximal *Cxcr5-pro-N1* NFAT motif (NFAT-mutated). HEK 293T cells were transiently transfected with plasmids encoding for NFATc1/C and/or Blimp-1 and left unstimulated or stimulated with TPA/ionomycin; data from 2 independent experiments are shown. The experiment was performed by Friederike Berberich-Siebelt

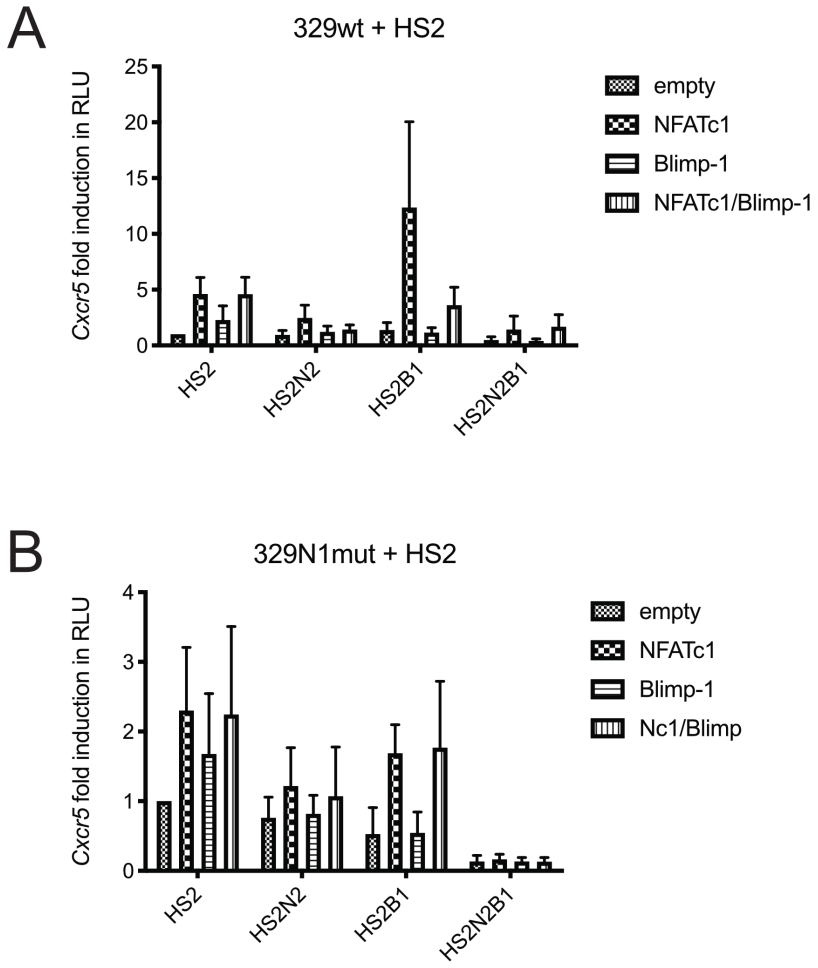

Figure S6: NFATc1 and Blimp-1 mediated CXCR5-expression is transactivated via NFATc1 binding sites and repressed via Blimp-1 binding sites

(A and B) Luciferase assay of the proximal part of the *Cxcr5* promoter (-329) and the *HS2* region. NFATc1 and Blimp-1-dependent expression is mediated via NFATc1 and Blimp-1 responsive elements. The *Cxcr5-HS2-N2* and/or *Cxcr5-HS2-B1* sites were mutated as indicated. The reporter construct was cotransfected with NFATc1 and/or Blimp-1 into EL-4 cells as indicated. Levels of transactivation are shown as normalized RLU relative to the *HS2*, empty (A) The promoter remained wildtypic. Data from 5 independent experiments are shown. (B) The *Cxcr5-pro-N1* site was mutated. Data from 3 independent experiments are shown. Experiments were performed by Felix Schüssler.

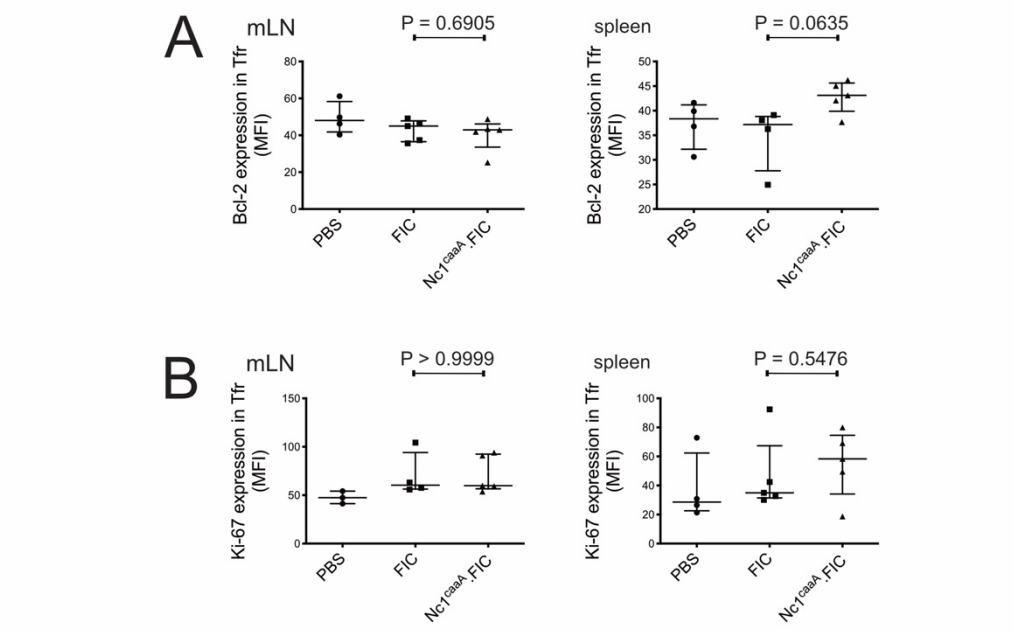

Figure S7: Overexpression of caNFATc1/αA in Tregs has no significant impact on Bcl-2 or Ki-67 expression in Tfr cells

Mice were immunized with NP-KLH in ImJect Alum i.p. for 10 days and boosted on day 7. Spleen and mLN were harvested and stained for flow cytometry. Tfr cells were gated according to the strategy in Fig. 7.19C. (A) Bcl-2 expression on Tfr cells, MFI normalized to the FMO of Bcl-2 (B) Ki-67 expression on Tfr cells, MFI normalized to the FMO of Ki-67. (A and B) Compilation of 5 independent experiments, PBS and *FIC* control groups also shown in Fig. 7.8 - Fig. 7.13 and Fig. 7.15, Mann-Whitney-test: n ≥ 3; *, P ≤ 0.05; **, P ≤0.01

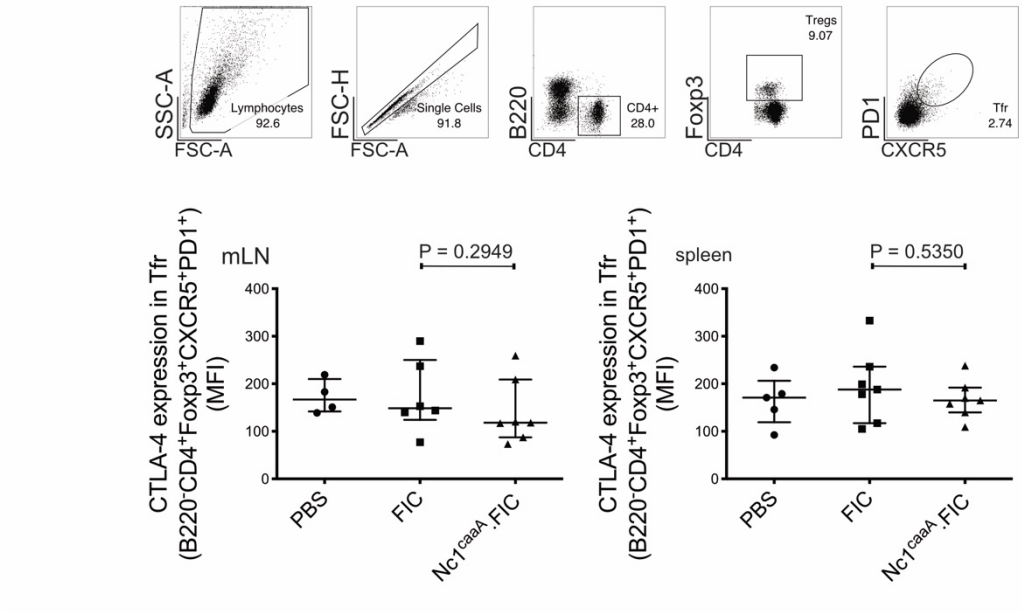

Figure S8: Overexpression of caNFATc1/αA in Tregs does not increase CTLA-4 expression on the surface of Tfr cells

Mice were immunized with NP-KLH in ImJect Alum i.p. for 10 days and boosted on day 7. Spleen and mLN were harvested and stained for flow cytometry. Tfr cells were gated as shown here. CTLA-4 expression on Tfr cells are shown as MFI. Compilation of 7 independent experiments, PBS and *FIC* control groups also shown in Fig. 7.8 - Fig. 7.13 and Fig. 7.15, Mann-Whitney-test: $n \geq 4$

Table S1: Enriched GO-terms differentially regulated in Tfr cells from *Pr1$^{+/gfp}$.FIC* vs. *Nc1$^{fl/fl}$.Pr1$^{+/gfp}$.FIC* mice

Enriched GO-terms in the set of genes being differentially regulated in Tfr cells of *Pr1$^{+/gfp}$.FIC* and *Nc1$^{fl/fl}$.Pr1$^{+/gfp}$.FIC* mice. The target set was defined as the set of genes differing at least twofold in their expression between the compared groups. The background set was defined as genes showing an expression level of at least five in at least one of the groups. Ontologies are described in terms of biological process, function and component. The p-value threshold was defined as $p \leq 10^{-4}$. The GO-analysis was performed via the help of the GORILLA-tool [144, 145].

process

GO term	Description	P-value	FDR q-value	Enrichment (N, B, n, b)	Genes
GO:0034723	DNA replication-dependent nucleosome organization	1.68E-6	2E-2	6.18 (6544,14,681,9)	[+] Show genes
GO:0006335	DNA replication-dependent nucleosome assembly	1.68E-6	9.98E-3	6.18 (6544,14,681,9)	[+] Show genes
GO:0006336	DNA replication-independent nucleosome assembly	4.79E-5	1.9E-1	4.55 (6544,19,681,9)	[+] Show genes
GO:0034724	DNA replication-independent nucleosome organization	7.92E-5	2.35E-1	4.32 (6544,20,681,9)	[+] Show genes
GO:0006333	chromatin assembly or disassembly	1.66E-4	3.94E-1	3.05 (6544,41,681,13)	[+] Show genes
GO:0010954	positive regulation of protein processing	1.81E-4	3.57E-1	5.77 (6544,10,681,6)	[+] Show genes
GO:1903319	positive regulation of protein maturation	1.81E-4	3.06E-1	5.77 (6544,10,681,6)	[+] Show genes
GO:0006334	nucleosome assembly	5.87E-4	8.71E-1	2.72 (6544,46,681,13)	[+] Show genes

function

GO term	Description	P-value	FDR q-value	Enrichment (N, B, n, b)	Genes
GO:0004252	serine-type endopeptidase activity	1.27E-4	4.16E-1	3.29 (6544,35,681,12)	[+] Show genes

component

GO term	Description	P-value	FDR q-value	Enrichment (N, B, n, b)	Genes
GO:0000788	nuclear nucleosome	6.31E-4	1E0	4.20 (6544,16,681,7)	[+] Show genes

Table S2: Enriched GO-terms differentially regulated in Tfr cells from *Pr1$^{+/gfp}$.FIC* vs. *Pr1$^{fl/gfp}$.FIC mice*

Enriched GO-terms in the set of genes being differentially regulated in Tfr cells of *Pr1$^{+/gfp}$.FIC* and *Pr1$^{fl/gfp}$.FIC* mice. The target set was defined as the set of genes differing at least twofold in their expression between the compared groups. The background set was defined as genes showing an expression level of at least five in at least one of the groups. Ontologies are described in terms of biological process, function and component. The p-value threshold was defined as $p \leq 10^{-4}$. The GO-analysis was performed via the help of the GORILLA-tool [144, 145].

process

GO term	Description	P-value	FDR q-value	Enrichment (N, B, n, b)	Genes
GO:0006336	DNA replication-independent nucleosome assembly	4.5E-7	5.34E-3	6.61 (6544,19,521,10)	[+] Show genes
GO:0034724	DNA replication-independent nucleosome organization	8.36E-7	4.96E-3	6.28 (6544,20,521,10)	[+] Show genes
GO:0034723	DNA replication-dependent nucleosome organization	2.99E-6	1.18E-2	7.18 (6544,14,521,8)	[+] Show genes
GO:0006335	DNA replication-dependent nucleosome assembly	2.99E-6	8.87E-3	7.18 (6544,14,521,8)	[+] Show genes
GO:0006334	nucleosome assembly	7.62E-6	1.81E-2	3.82 (6544,46,521,14)	[+] Show genes
GO:0045653	negative regulation of megakaryocyte differentiation	1.69E-5	3.34E-2	8.37 (6544,9,521,6)	[+] Show genes
GO:0006333	chromatin assembly or disassembly	5.29E-5	8.96E-2	3.68 (6544,41,521,12)	[+] Show genes
GO:0034728	nucleosome organization	6.18E-5	9.16E-2	2.96 (6544,68,521,16)	[+] Show genes
GO:0065004	protein-DNA complex assembly	1.52E-4	2.01E-1	2.75 (6544,73,521,16)	[+] Show genes
GO:0045652	regulation of megakaryocyte differentiation	4.27E-4	5.06E-1	5.38 (6544,14,521,6)	[+] Show genes
GO:0002740	negative regulation of cytokine secretion involved in immune response	5.02E-4	5.41E-1	12.56 (6544,3,521,3)	[+] Show genes
GO:0009240	isopentenyl diphosphate biosynthetic process	5.02E-4	4.96E-1	12.56 (6544,3,521,3)	[+] Show genes
GO:0046490	isopentenyl diphosphate metabolic process	5.02E-4	4.58E-1	12.56 (6544,3,521,3)	[+] Show genes
GO:0071824	protein-DNA complex subunit organization	6.19E-4	5.25E-1	2.31 (6544,98,521,18)	[+] Show genes

function

n.a. p>0,001

component

GO term	Description	P-value	FDR q-value	Enrichment (N, B, n, b)	Genes
GO:0000788	nuclear nucleosome	1.11E-5	1.82E-2	6.28 (6544,16,521,8)	[+] Show genes
GO:0000786	nucleosome	1.43E-5	1.17E-2	4.46 (6544,31,521,11)	[+] Show genes
GO:0044815	DNA packaging complex	3.86E-5	2.11E-2	4.06 (6544,34,521,11)	[+] Show genes

9.2 Curriculum Vitae

9.3 Participation in international conferences

2018	September 2nd-5th, 5th European Congress of Immunology (ECI), Amsterdam, **talk**: "In follicular regulatory T cells NFATc1 is essential for homing to germinal centers"
	June 21st-22nd, T Cells: Subsets and Functions, Marburg, **talk**: "NFATc1 and Blimp-1 cooperate in follicular regulatory T cells"
2017	November 8th-10th, 21st Joint Meeting Signal Transduction – Receptors, Mediators and Genes, Weimar, **poster**: "In follicular regulatory T cells NFATc1 is essential for homing to germinal centers"- 1st poster prize
	Mai 4th-5th, "Translational Immunology - From Target to Therapy IV", Würzburg
2016	November 9th -11th, 20th Joint Meeting Signal Transduction – Receptors, Mediators and Genes, Weimar, **poster**: "In follicular regulatory T cells NFAT2 is essential for homing to germinal centers"
	October 12th-13th, 11th International Student Symposium, Eureka!, Würzburg, **talk**: "NFATc1 and BLIMP-1 cooperate in follicular regulatory T-cells"
	August 21st-26th, ICI – International Congress of Immunology, Melbourne, Australia, **poster**: "In follicular regulatory T cells NFAT2 is essential for homing to germinal centers"
	June 27th -28th, T Cells: Subsets and Functions, Marburg

2015	October 14th -15th, International Student Symposium, Eureka!, Würzburg, **poster**: "NFAT2 is essential in follicular regulatory T cells to control humoral immunity"
	June 29th -30th, T Cells: Subsets and Functions, Marburg
2014	June 30th -July 1st, T Cells: Subsets and Functions, Marburg
	April 11th-12th, "Translational Immunology - From Target to Therapy II", Würzburg

9.4 Publications

Lucia Campos Carrascosa*, Matthias Klein*, Yohko Kitagawa, Christina Lückel, Federico Marini, Anika König, Anna Guralnik, Hartmann Raifer, Stefanie Hagner-Benes, Diana Rädler, Andreas Böck, Cholho Kang, Michael Lohoff, Holger Garn, Bianca Schaub, Friederike Berberich-Siebelt, Shimon Sakaguchi, Tobias Bopp and Magdalena Huber** (2017). **Reciprocal regulation of the Il9 locus by counteracting activities of transcription factors IRF1 and IRF4**, Nature Communications 8:15366

Yin Xiao*, Musga Qureischi*, Lena Dietz*, Martin Vaeth, Subrahmanya D. Vallabhapurapu, Stefan Klein-Hessling, Matthias Klein, Anika König, Edgar Serfling, Anja Mottok, Tobias Bopp, Andreas Rosenwald, Mathias Buttmann, Ingolf Berberich, Andreas Beilhack, Friederike Berberich-Siebelt**. **Lack of NFATc1 SUMOylation prevents autoimmunity and alloreactivity**, Journal of Experimental Medicine, in revision

Anika Koenig, Martin Vaeth, Raghu Erapaneedi, Stefan Klein-Hessling, Matthias Klein, Lena Dietz, Felix Schuessler, Katharina Schwarz, Tobias Bopp, Nora Mueller, Florian Erhard, Andreas Rosenwald, Ingolf Berberich, Friederike Berberich-Siebelt**, **NFATc1/αA and Blimp-1 support the follicular and effector phenotype of Tregs**, in preparation

* These authors contributed equally to the work. **Corresponding author

9.5 List of abbreviations

9.5.1 General abbreviations

a.u.	arbitrary units
AAD	acidic activation domain
AbDil	antibody diluent with background reducing components
Aci-C	c-terminal acidic region
Aci-N	n-terminal acidic region
AICD	activation-induced cell death
AID	activation-induced deaminase
Akt	protein kinase B
AP-1	activator protein 1
APC	antigen presenting cell
BCR	B-cell receptor
Blimp-1	B lymphocyte-induced maturation protein-1
bp	base pair
BSA	bovine serum albumin
caNFATc1/aA	constitutively active NFATc1/αA
CD	cluster of differentiation
CFA	Complete Freund's Adjuvant
CM	central motif
CNS	conserved non-coding sequence
CRAC	Ca2+ release-acticated Ca2+
CRC	CXCL-12 producing reticular cells
CSR	class switch recombination
cTfr	circulating Tfr
CTM	C-terminus motif
DAMP	damage-associated molecular pattern

DC	dendritic cell
DGKα	diacylglycerol kinase α
DN	double negative Thymocyte
DP	double positive Thymocyte
DTR	diphteria toxin receptor
DZ	dark zone
ELISA	enzyme-linked Immunosorbent assay
EMSA	electro mobility shift assay
ER	endoplasmatic reticulum
EV	end volume
FACS	fluorescence activated cell sorting
FBS	fetal bovine serum
FIC	Foxp3-IHRES-Cre)
Fig	figure
FMO	fluorescence minus one (control)
GC	germinal center B cell
GCB	germinal center B cell
GCR	germinal center reaction
GFP	green fluorescent protein
GO	gene ontology-(term)
HA	hemagglutinin (tag)
HDAC	histone deacetylase
HEV	high endothelial venules
HMT	histone methyl transferase
HRP	horseradish-peroxidase
HS2	hypersensitivity region 2
ICER	inducible cAMP early repressor
IHF	immune histology fluorescent (stainings)
IL	interleukin
ILC	innate lymphoid cell

IP3	inositol 1,4,5-triphosphate
iTfr	intermediate Tfr
iTreg	induced Treg
LN	lymph node
LZ	light zone
MFI	median of the fluorescence intensity
MHC	Major Histocompatibility Complex
mLN	mesenteric lymph node
mTfr	mature Tfr
mTORC1	mTOR complex 1
NFAT	nuclear factor of activated T cells
NK	natural killer cell
NLS	nuclear localization signal
NP-KLH	4-Hydroxy-3-Nitrophenylacetyl-Keyhole Limpet Hemocyanin
NRS	normal rat serum
NTM	N-terminus motif
nTreg	natural Treg
O/N	over night
OPN	osteoponin
PAMP	pathogen-associated molecular pattern
PBS	phosphate buffered saline
PD-1	programmed death-1
PEI	Polyethyleneimine
PEST	proline glutamic acid, serine and threonine (sequence)
PI3K	phosphatidylinositol-3-kinase
PLC	phospholipase C
PNA	peanut agglutinin
PNAd	peripheral node addressin
PRR	pattern recognition receptor

RBC	red blood cell lysis (buffer)
RIN	RNA integrity number
RSD	rel similarity domain
s.c.	subcutaneously
S1P	sphingosine-1-phosphate (gradient)
S1PR1	sphingosine 1-phosphate receptor 1
SHM	somatic hypermutation
STIM	stromal interaction molecule
TAD-C	C-terminal transactivation domain
TAD-N	N-terminal transactivation domain
TBE	Tris Borat EDTA (buffer)
Tcon	conventional T cell
TCR	T-cell receptor
Tfc	follicular cytotoxic T cells
Tfh	T follicular helper (cell)
Tfoll	follicular T cells
Tfr	T follicular regulatory (cell)
Th	T helper
TMB	3,3'-5,5'-Tetramethylbenzidine
TR	transcriptional regulators
Treg	regulatory T cell
u.a.	unter anderem
v/v	volume per volume
vs.	versus
w/v	weight per volume
wt	wild type
TMB	3,3'-5,5'-Tetramethylbenzidine
NRS	normal rat serum
PEI	Polyethyleneimine
w/v	weight per volume

v/v	volume per volume
PBS	phosphate buffered saline
RBC	red blood cell lysis (buffer)
TBE	Tris Borat EDTA (buffer)
FBS	fetal bovine serum
O/N	over night
MFI	median of the fluorescence intensity
FMO	fluorescence minus one (control)
FACS	fluorescence activated cell sorting
NP-KLH	4-Hydroxy-3-Nitrophenylacetyl-Keyhole Limpet Hemocyanin
EMSA	electro mobility shift assay
EV	end volume
ELISA	enzyme-linked Immunosorbent assay
BSA	bovine serum albumin
HRP	horseradish-peroxidase
RIN	RNA integrity number
bp	base pair

9.5.2 Units

A	ampere
°C	degrees celsius
d	day
g	gram
h	hour
l	liter
M	mol per liter
min	minutes
rpm	rounds per minute

RT	room temperature

9.5.3 Physical prefixes

k	kilo (10^{3})
m	milli (10^{-3})
µ	micro (10^{-6})
n	nano (10^{-9})
p	pico (10^{-12})

10 Bibliography

1. Abbas, A.K., Lichtman, A.H. and Pillai, S., *Properties and Overview of Immune Responses*, in *Cellular and Molecular Immunology*. 2015, Elsevier Saunders: Philadelphia. p. 1-12.
2. Abbas, A.K., Lichtman, A.H. and Pillai, S., *Innate Immunity*, in *Cellular and Molecular Immunology*. 2015, Elsevier Saunders: Philadelphia. p. 51-84.
3. Abbas, A.K., Lichtman, A.H. and Pillai, S., *Cells and Tissues of the Immune System*, in *Cellular and Molecular Immunology*. 2015, Elsevier Saunders: Philadelphia. p. 13-32.
4. Abbas, A.K., Lichtman, A.H. and Pillai, S., *Immune Receptors and Signal Transduction*, in *Cellular and Molecular Immunology*. 2015, Elsevier Saunders: Philadelphia. p. 138-167.
5. Germain, R.N., *T-cell development and the CD4-CD8 lineage decision.* Nat Rev Immunol, 2002. **2**(5): p. 309-22.
6. Hogquist, K.A., T.A. Baldwin, and S.C. Jameson, *Central tolerance: learning self-control in the thymus.* Nature Reviews Immunology, 2005. **5**(10): p. 772-782.
7. Zhu, J., H. Yamane, and W.E. Paul, *Differentiation of effector CD4 T cell populations (*).* Annu Rev Immunol, 2010. **28**: p. 445-89.
8. Kaplan, M.H., M.M. Hufford, and M.R. Olson, *The development and in vivo function of T helper 9 cells.* Nature Reviews Immunology, 2015. **15**: p. 295.
9. Abbas, A.K., Lichtman, A.H. and Pillai, S., *Activation of T Lymphocytes*, in *Cellular and Molecular Immunology*. 2015, Elsevier Saunders: Philadelphia. p. 199-212.
10. Nurieva, R.I. and Y. Chung, *Understanding the development and function of T follicular helper cells.* Cellular & Molecular Immunology, 2010. **7**(3): p. 190-197.
11. Drayton, D.L., et al., *Lymphoid organ development: from ontogeny to neogenesis.* Nature Immunology, 2006. **7**(4): p. 344-353.
12. Mebius, R.E. and G. Kraal, *Structure and function of the spleen.* Nature Reviews Immunology, 2005. **5**(8): p. 606-616.
13. Stebegg, M., et al., *Regulation of the Germinal Center Response.* Front Immunol, 2018. **9**: p. 2469.
14. *T Cell-Dependent Antigen*, in *Encyclopedic Reference of Immunotoxicology*, H.-W. Vohr, Editor. 2005, Springer Berlin Heidelberg: Berlin, Heidelberg. p. 626-626.
15. Victora, G.D. and M.C. Nussenzweig, *Germinal centers.* Annu Rev Immunol, 2012. **30**: p. 429-57.
16. Vinuesa, C.G., et al., *Follicular Helper T Cells.* Annual Review of Immunology, 2016. **34**(1): p. 335-368.
17. Weber, J.P., et al., *ICOS maintains the T follicular helper cell phenotype by down-regulating Krüppel-like factor 2.* The Journal of Experimental Medicine, 2015. **212**(2): p. 217-233.
18. Lee, J.Y., et al., *The transcription factor KLF2 restrains CD4(+) T follicular helper cell differentiation.* Immunity, 2015. **42**(2): p. 252-264.
19. Stone, E.L., et al., *ICOS coreceptor signaling inactivates the transcription factor FOXO1 to promote Tfh cell differentiation.* Immunity, 2015. **42**(2): p. 239-251.
20. Bauquet, A.T., et al., *The costimulatory molecule ICOS regulates the expression of c-Maf and IL-21 in the development of follicular T helper cells and TH-17 cells.* Nat Immunol, 2009. **10**(2): p. 167-75.

21. Bélanger, S. and S. Crotty, *Dances with cytokines, featuring TFH cells, IL-21, IL-4 and B cells.* Nature Immunology, 2016. **17**: p. 1135.
22. Crotty, S., *Follicular Helper CD4 T Cells (TFH).* Annual Review of Immunology, 2011. **29**(1): p. 621-663.
23. van Essen, D., H. Kikutani, and D. Gray, *CD40 ligand-transduced co-stimulation of T cells in the development of helper function.* Nature, 1995. **378**(6557): p. 620-3.
24. Liu, X., R.I. Nurieva, and C. Dong, *Transcriptional regulation of follicular T-helper (Tfh) cells.* Immunological Reviews, 2013. **252**(1): p. 139-145.
25. Nurieva, R.I., et al., *Bcl6 Mediates the Development of T Follicular Helper Cells.* Science, 2009. **325**(5943): p. 1001-1005.
26. Choi, Y.S., J.A. Yang, and S. Crotty, *Dynamic regulation of Bcl6 in follicular helper CD4 T (Tfh) cells.* Curr Opin Immunol, 2013. **25**(3): p. 366-72.
27. Liu, X., et al., *Transcription factor achaete-scute homologue 2 initiates follicular T-helper-cell development.* Nature, 2014. **507**: p. 513.
28. Hatzi, K., et al., *BCL6 orchestrates Tfh cell differentiation via multiple distinct mechanisms.* The Journal of Experimental Medicine, 2015. **212**(4): p. 539-553.
29. MacLennan, I.C., et al., *Extrafollicular antibody responses.* Immunol Rev, 2003. **194**: p. 8-18.
30. Qi, H., *From SAP-less T cells to helpless B cells and back: dynamic T-B cell interactions underlie germinal center development and function.* Immunol Rev, 2012. **247**(1): p. 24-35.
31. Victora, G.D., et al., *Germinal center dynamics revealed by multiphoton microscopy with a photoactivatable fluorescent reporter.* Cell, 2010. **143**(4): p. 592-605.
32. Abbas, A.K., Lichtman, A.H. and Pillai, S., *B Cell Activation and Antibody Production*, in *Cellular and Molecular Immunology*. 2015, Elsevier Saunders: Philadelphia. p. 239-261.
33. Geha, R.S., H.H. Jabara, and S.R. Brodeur, *The regulation of immunoglobulin E class-switch recombination.* Nature Reviews Immunology, 2003. **3**(9): p. 721-732.
34. Crotty, S., *T follicular helper cell differentiation, function, and roles in disease.* Immunity, 2014. **41**(4): p. 529-42.
35. Good-Jacobson, K.L., et al., *PD-1 regulates germinal center B cell survival and the formation and affinity of long-lived plasma cells.* Nature Immunology, 2010. **11**(6): p. 535-542.
36. Cyster, J.G. and C.D.C. Allen, *B Cell Responses: Cell Interaction Dynamics and Decisions.* Cell, 2019. **177**(3): p. 524-540.
37. Hale, J.S. and R. Ahmed, *Memory T Follicular Helper CD4 T Cells.* Frontiers in Immunology, 2015. **6**(16).
38. Sage, P.T., et al., *Circulating T follicular regulatory and helper cells have memory-like properties.* J Clin Invest, 2014. **124**(12): p. 5191-204.
39. Weber, J.P., F. Fuhrmann, and A. Hutloff, *T-follicular helper cells survive as long-term memory cells.* European Journal of Immunology, 2012. **42**(8): p. 1981-1988.
40. Wing, J.B., M. Tekguc, and S. Sakaguchi, *Control of Germinal Center Responses by T-Follicular Regulatory Cells.* Front Immunol, 2018. **9**: p. 1910.
41. Fonseca, V.R., F. Ribeiro, and L. Graca, *T follicular regulatory (Tfr) cells: Dissecting the complexity of Tfr-cell compartments.* Immunological Reviews, 2019. **288**(1): p. 112-127.

42. Maceiras, A.R., et al., *T follicular helper and T follicular regulatory cells have different TCR specificity.* Nature Communications, 2017. **8**(1): p. 15067.
43. Maceiras, A.R., et al., *T follicular regulatory cells in mice and men.* Immunology, 2017. **152**(1): p. 25-35.
44. Aloulou, M., et al., *Follicular regulatory T cells can be specific for the immunizing antigen and derive from naive T cells.* Nat Commun, 2016. **7**: p. 10579.
45. Fazilleau, N. and M. Aloulou, *Several Follicular Regulatory T Cell Subsets With Distinct Phenotype and Function Emerge During Germinal Center Reactions.* Front Immunol, 2018. **9**: p. 1792.
46. Linterman, M.A., et al., *Foxp3+ follicular regulatory T cells control the germinal center response.* Nat Med, 2011. **17**(8): p. 975-82.
47. Linterman, M.A., et al., *CD28 expression is required after T cell priming for helper T cell responses and protective immunity to infection.* Elife, 2014. **3**.
48. Sage, P.T., et al., *The receptor PD-1 controls follicular regulatory T cells in the lymph nodes and blood.* Nat Immunol, 2013. **14**(2): p. 152-61.
49. Fonseca, V.R., et al., *Human blood Tfr cells are indicators of ongoing humoral activity not fully licensed with suppressive function.* Sci Immunol, 2017. **2**(14).
50. Vaeth, M., et al., *Follicular regulatory T cells control humoral autoimmunity via NFAT2-regulated CXCR5 expression.* 2014. **211**(3): p. 545-561.
51. Vaeth, M., et al., *Store-Operated Ca(2+) Entry in Follicular T Cells Controls Humoral Immune Responses and Autoimmunity.* Immunity, 2016. **44**(6): p. 1350-64.
52. Vaeth, M., et al., *Tissue resident and follicular Treg cell differentiation is regulated by CRAC channels.* Nature Communications, 2019. **10**(1): p. 1183.
53. Ritvo, P.-G., et al., *High-resolution repertoire analysis reveals a major bystander activation of Tfh and Tfr cells.* Proceedings of the National Academy of Sciences, 2018. **115**(38): p. 9604-9609.
54. Xu, L., et al., *The Kinase mTORC1 Promotes the Generation and Suppressive Function of Follicular Regulatory T Cells.* Immunity, 2017. **47**(3): p. 538-551.e5.
55. Ritvo, P.G., et al., *Tfr cells lack IL-2Ralpha but express decoy IL-1R2 and IL-1Ra and suppress the IL-1-dependent activation of Tfh cells.* Sci Immunol, 2017. **2**(15).
56. Botta, D., et al., *Dynamic regulation of T follicular regulatory cell responses by interleukin 2 during influenza infection.* Nature Immunology, 2017. **18**: p. 1249.
57. Leavenworth, J.W., et al., *A p85alpha-osteopontin axis couples the receptor ICOS to sustained Bcl-6 expression by follicular helper and regulatory T cells.* Nat Immunol, 2015. **16**(1): p. 96-106.
58. Jandl, C., et al., *IL-21 restricts T follicular regulatory T cell proliferation through Bcl-6 mediated inhibition of responsiveness to IL-2.* Nature Communications, 2017. **8**(1): p. 14647.
59. Miyazaki, M., et al., *Id2 and Id3 maintain the regulatory T cell pool to suppress inflammatory disease.* Nat Immunol, 2014. **15**(8): p. 767-76.
60. Sage, P.T., et al., *The coinhibitory receptor CTLA-4 controls B cell responses by modulating T follicular helper, T follicular regulatory, and T regulatory cells.* Immunity, 2014. **41**(6): p. 1026-39.
61. Qureshi, O.S., et al., *Trans-Endocytosis of CD80 and CD86: A Molecular Basis for the Cell-Extrinsic Function of CTLA-4.* Science, 2011. **332**(6029): p. 600-603.
62. Wing, K., et al., *CTLA-4 control over Foxp3+ regulatory T cell function.* Science, 2008. **322**(5899): p. 271-5.

63. Walker, L.S., et al., *Established T cell-driven germinal center B cell proliferation is independent of CD28 signaling but is tightly regulated through CTLA-4.* J Immunol, 2003. **170**(1): p. 91-8.
64. Riley, J.L., et al., *ICOS costimulation requires IL-2 and can be prevented by CTLA-4 engagement.* J Immunol, 2001. **166**(8): p. 4943-8.
65. Sage, P.T. and A.H. Sharpe, *T follicular regulatory cells in the regulation of B cell responses.* Trends Immunol, 2015. **36**(7): p. 410-8.
66. Sage, P.T. and A.H. Sharpe, *T follicular regulatory cells.* Immunological Reviews, 2016. **271**(1): p. 246-259.
67. Fife, B.T., et al., *Interactions between PD-1 and PD-L1 promote tolerance by blocking the TCR-induced stop signal.* Nat Immunol, 2009. **10**(11): p. 1185-92.
68. Sage, P.T., et al., *Suppression by TFR cells leads to durable and selective inhibition of B cell effector function.* Nat Immunol, 2016. **17**(12): p. 1436-1446.
69. McCarron, M.J. and J.C. Marie, *TGF-beta prevents T follicular helper cell accumulation and B cell autoreactivity.* J Clin Invest, 2014. **124**(10): p. 4375-86.
70. Sun, L., H. Jin, and H. Li, *GARP: a surface molecule of regulatory T cells that is involved in the regulatory function and TGF-beta releasing.* Oncotarget, 2016. **7**(27): p. 42826-42836.
71. Zhao, D.-M., et al., *Activated CD4+CD25+ T cells selectively kill B lymphocytes.* Blood, 2006. **107**(10): p. 3925-3932.
72. Laidlaw, B.J., et al., *Interleukin-10 from CD4⁺ follicular regulatory T cells promotes the germinal center response.* Science Immunology, 2017. **2**(16): p. eaan4767.
73. Wu, H., et al., *Follicular regulatory T cells repress cytokine production by follicular helper T cells and optimize IgG responses in mice.* Eur J Immunol, 2016. **46**(5): p. 1152-61.
74. Macián, F., C. López-Rodríguez, and A. Rao, *Partners in transcription: NFAT and AP-1.* Oncogene, 2001. **20**(19): p. 2476-2489.
75. Terui, Y., et al., *Dual role of sumoylation in the nuclear localization and transcriptional activation of NFAT1.* J Biol Chem, 2004. **279**(27): p. 28257-65.
76. Nayak, A., et al., *Sumoylation of the transcription factor NFATc1 leads to its subnuclear relocalization and interleukin-2 repression by histone deacetylase.* J Biol Chem, 2009. **284**(16): p. 10935-46.
77. Mognol, G.P., et al., *Cell cycle and apoptosis regulation by NFAT transcription factors: new roles for an old player.* Cell Death & Disease, 2016. **7**(4): p. e2199-e2199.
78. Vaeth, M. and S. Feske, *NFAT control of immune function: New Frontiers for an Abiding Trooper.* F1000Research, 2018. **7**: p. 260.
79. Kiani, A., A. Rao, and J. Aramburu, *Manipulating immune responses with immunosuppressive agents that target NFAT.* Immunity, 2000. **12**(4): p. 359-72.
80. Serfling, E., F. Berberich-Siebelt, and A. Avots, *NFAT in Lymphocytes: A Factor for All Events?* 2007. **2007**(398): p. pe42-pe42.
81. Buchholz, M., et al., *Overexpression of c-myc in pancreatic cancer caused by ectopic activation of NFATc1 and the Ca2+/calcineurin signaling pathway.* Embo j, 2006. **25**(15): p. 3714-24.
82. Macian, F., *NFAT proteins: key regulators of T-cell development and function.* Nature Reviews Immunology, 2005. **5**(6): p. 472-484.

83. Macian, F., C. Garcia-Rodriguez, and A. Rao, *Gene expression elicited by NFAT in the presence or absence of cooperative recruitment of Fos and Jun.* Embo j, 2000. **19**(17): p. 4783-95.
84. Macian, F., et al., *Transcriptional mechanisms underlying lymphocyte tolerance.* Cell, 2002. **109**(6): p. 719-31.
85. Fields, P.E., T.F. Gajewski, and F.W. Fitch, *Blocked Ras activation in anergic CD4+ T cells.* Science, 1996. **271**(5253): p. 1276-8.
86. Li, W., et al., *Blocked signal transduction to the ERK and JNK protein kinases in anergic CD4+ T cells.* Science, 1996. **271**(5253): p. 1272-6.
87. Boussiotis, V.A., et al., *Maintenance of human T cell anergy: blocking of IL-2 gene transcription by activated Rap1.* Science, 1997. **278**(5335): p. 124-8.
88. Fathman, C.G. and N.B. Lineberry, *Molecular mechanisms of CD4+ T-cell anergy.* Nat Rev Immunol, 2007. **7**(8): p. 599-609.
89. Serfling, E., et al., *NFAT transcription factors in control of peripheral T cell tolerance.* European Journal of Immunology, 2006. **36**(11): p. 2837-2843.
90. Serfling, E., et al., *NFATc1/αA: The other Face of NFAT Factors in Lymphocytes.* 2012. **10**(1): p. 16.
91. Wherry, E.J., *T cell exhaustion.* Nat Immunol, 2011. **12**(6): p. 492-9.
92. Crawford, A. and E.J. Wherry, *The diversity of costimulatory and inhibitory receptor pathways and the regulation of antiviral T cell responses.* Curr Opin Immunol, 2009. **21**(2): p. 179-86.
93. Martinez, G.J., et al., *The transcription factor NFAT promotes exhaustion of activated CD8(+) T cells.* Immunity, 2015. **42**(2): p. 265-278.
94. Tone, Y., et al., *Smad3 and NFAT cooperate to induce Foxp3 expression through its enhancer.* Nat Immunol, 2008. **9**(2): p. 194-202.
95. Vaeth, M., et al., *Dependence on nuclear factor of activated T-cells (NFAT) levels discriminates conventional T cells from Foxp3+ regulatory T cells.* 2012. **109**(40): p. 16258-16263.
96. Bopp, T., et al., *NFATc2 and NFATc3 transcription factors play a crucial role in suppression of CD4+ T lymphocytes by CD4+ CD25+ regulatory T cells.* J Exp Med, 2005. **201**(2): p. 181-7.
97. Hock, M., et al., *NFATc1 induction in peripheral T and B lymphocytes.* J Immunol, 2013. **190**(5): p. 2345-53.
98. Torgerson, T.R., et al., *FOXP3 inhibits activation-induced NFAT2 expression in T cells thereby limiting effector cytokine expression.* J Immunol, 2009. **183**(2): p. 907-15.
99. Martinez, G.J., et al., *Cutting Edge: NFAT Transcription Factors Promote the Generation of Follicular Helper T Cells in Response to Acute Viral Infection.* The Journal of Immunology, 2016. **196**(5): p. 2015-2019.
100. Keller, A.D. and T. Maniatis, *Identification and characterization of a novel repressor of beta-interferon gene expression.* Genes Dev, 1991. **5**(5): p. 868-79.
101. Turner, C.A., Jr., D.H. Mack, and M.M. Davis, *Blimp-1, a novel zinc finger-containing protein that can drive the maturation of B lymphocytes into immunoglobulin-secreting cells.* Cell, 1994. **77**(2): p. 297-306.
102. John, S.A. and L.A. Garrett-Sinha, *Blimp1: A conserved transcriptional repressor critical for differentiation of many tissues.* Experimental Cell Research, 2009. **315**(7): p. 1077-1084.

103. Morgan, M.A., et al., *Blimp-1/Prdm1 alternative promoter usage during mouse development and plasma cell differentiation.* Mol Cell Biol, 2009. **29**(21): p. 5813-27.
104. Martins, G. and K. Calame, *Regulation and Functions of Blimp-1 in T and B Lymphocytes.* Annual Review of Immunology, 2008. **26**(1): p. 133-169.
105. Yu, J., et al., *Transcriptional repression by blimp-1 (PRDI-BF1) involves recruitment of histone deacetylase.* Mol Cell Biol, 2000. **20**(7): p. 2592-603.
106. Rogers, S., R. Wells, and M. Rechsteiner, *Amino acid sequences common to rapidly degraded proteins: the PEST hypothesis.* Science, 1986. **234**(4774): p. 364-8.
107. Martins, G.A., et al., *Blimp-1 directly represses Il2 and the Il2 activator Fos , attenuating T cell proliferation and survival.* 2008. **205**(9): p. 1959-1965.
108. Tunyaplin, C., M.A. Shapiro, and K.L. Calame, *Characterization of the B lymphocyte-induced maturation protein-1 (Blimp-1) gene, mRNA isoforms and basal promoter.* Nucleic Acids Res, 2000. **28**(24): p. 4846-55.
109. Schmidt, D., et al., *Blimp-1Deltaexon7: a naturally occurring Blimp-1 deletion mutant with auto-regulatory potential.* Exp Cell Res, 2008. **314**(20): p. 3614-27.
110. Keller, A.D. and T. Maniatis, *Only two of the five zinc fingers of the eukaryotic transcriptional repressor PRDI-BF1 are required for sequence-specific DNA binding.* Mol Cell Biol, 1992. **12**(5): p. 1940-9.
111. Vincent, S.D., et al., *The zinc finger transcriptional repressor Blimp1/Prdm1 is dispensable for early axis formation but is required for specification of primordial germ cells in the mouse.* Development, 2005. **132**(6): p. 1315-25.
112. Kim, S.J., *Immunological function of Blimp-1 in dendritic cells and relevance to autoimmune diseases.* Immunol Res, 2015. **63**(1-3): p. 113-20.
113. Kallies, A., et al., *Plasma cell ontogeny defined by quantitative changes in blimp-1 expression.* J Exp Med, 2004. **200**(8): p. 967-77.
114. Shapiro-Shelef, M., et al., *Blimp-1 is required for the formation of immunoglobulin secreting plasma cells and pre-plasma memory B cells.* Immunity, 2003. **19**(4): p. 607-20.
115. Martins, G.A., et al., *Transcriptional repressor Blimp-1 regulates T cell homeostasis and function.* Nat Immunol, 2006. **7**(5): p. 457-65.
116. Tabrizifard, S., et al., *Analysis of transcription factor expression during discrete stages of postnatal thymocyte differentiation.* J Immunol, 2004. **173**(2): p. 1094-102.
117. Kallies, A., et al., *Transcriptional repressor Blimp-1 is essential for T cell homeostasis and self-tolerance.* Nat Immunol, 2006. **7**(5): p. 466-74.
118. Santner-Nanan, B., et al., *Blimp-1 is expressed in human and mouse T cell subsets and leads to loss of IL-2 production and to defective proliferation.* Signal Transduction, 2006. **6**(4): p. 268-279.
119. Gong, D. and T.R. Malek, *Cytokine-dependent Blimp-1 expression in activated T cells inhibits IL-2 production.* J Immunol, 2007. **178**(1): p. 242-52.
120. Wang, L., et al., *Blimp-1 induced by IL-4 plays a critical role in suppressing IL-2 production in activated CD4 T cells.* J Immunol, 2008. **181**(8): p. 5249-56.
121. Vasanwala, F.H., et al., *Repression of AP-1 function: a mechanism for the regulation of Blimp-1 expression and B lymphocyte differentiation by the B cell lymphoma-6 protooncogene.* J Immunol, 2002. **169**(4): p. 1922-9.

122. Winslow, M.M., et al., *The calcineurin phosphatase complex modulates immunogenic B cell responses.* Immunity, 2006. **24**(2): p. 141-52.
123. Muhammad, K., et al., *Induction of Short NFATc1/αA Isoform Interferes with Peripheral B Cell Differentiation.* Frontiers in Immunology, 2018. **9**(32).
124. Nurieva, R.I., et al., *STAT5 protein negatively regulates T follicular helper (Tfh) cell generation and function.* J Biol Chem, 2012. **287**(14): p. 11234-9.
125. Kwon, H., et al., *Analysis of interleukin-21-induced Prdm1 gene regulation reveals functional cooperation of STAT3 and IRF4 transcription factors.* Immunity, 2009. **31**(6): p. 941-52.
126. Heinemann, C., et al., *IL-27 and IL-12 oppose pro-inflammatory IL-23 in CD4+ T cells by inducing Blimp1.* Nature Communications, 2014. **5**(1): p. 3770.
127. Tsukumo, S., et al., *Bach2 maintains T cells in a naive state by suppressing effector memory-related genes.* Proc Natl Acad Sci U S A, 2013. **110**(26): p. 10735-40.
128. Crotty, S., R.J. Johnston, and S.P. Schoenberger, *Effectors and memories: Bcl-6 and Blimp-1 in T and B lymphocyte differentiation.* Nature Immunology, 2010. **11**: p. 114.
129. Johnston, R.J., et al., *STAT5 is a potent negative regulator of TFH cell differentiation.* J Exp Med, 2012. **209**(2): p. 243-50.
130. Fu, S.H., et al., *New insights into Blimp-1 in T lymphocytes: a divergent regulator of cell destiny and effector function.* J Biomed Sci, 2017. **24**(1): p. 49.
131. Choi, Y.S., et al., *LEF-1 and TCF-1 orchestrate T(FH) differentiation by regulating differentiation circuits upstream of the transcriptional repressor Bcl6.* Nat Immunol, 2015. **16**(9): p. 980-90.
132. Wu, T., et al., *TCF1 Is Required for the T Follicular Helper Cell Response to Viral Infection.* Cell Rep, 2015. **12**(12): p. 2099-110.
133. Xu, L., et al., *The transcription factor TCF-1 initiates the differentiation of T(FH) cells during acute viral infection.* Nat Immunol, 2015. **16**(9): p. 991-9.
134. Thiele, S., et al., *miR-9 enhances IL-2 production in activated human CD4(+) T cells by repressing Blimp-1.* Eur J Immunol, 2012. **42**(8): p. 2100-8.
135. Cretney, E., et al., *The transcription factors Blimp-1 and IRF4 jointly control the differentiation and function of effector regulatory T cells.* Nature Immunology, 2011. **12**: p. 304.
136. Chung, Y., et al., *Follicular regulatory T cells expressing Foxp3 and Bcl-6 suppress germinal center reactions.* Nature Medicine, 2011. **17**(8): p. 983-988.
137. Wing, J.B., et al., *A distinct subpopulation of CD25(-) T-follicular regulatory cells localizes in the germinal centers.* Proc Natl Acad Sci U S A, 2017. **114**(31): p. E6400-e6409.
138. Baumgart, S., et al., *Inflammation-induced NFATc1-STAT3 transcription complex promotes pancreatic cancer initiation by KrasG12D.* Cancer Discov, 2014. **4**(6): p. 688-701.
139. Zhang, D.J., et al., *Selective expression of the Cre recombinase in late-stage thymocytes using the distal promoter of the Lck gene.* J Immunol, 2005. **174**(11): p. 6725-31.
140. Lahl, K., et al., *Selective depletion of Foxp3⁺ regulatory T cells induces a scurfy-like disease.* The Journal of Experimental Medicine, 2007. **204**(1): p. 57-63.

141. Klein-Hessling, S., et al., *Cyclic AMP-induced chromatin changes support the NFATc-mediated recruitment of GATA-3 to the interleukin 5 promoter.* J Biol Chem, 2008. **283**(45): p. 31030-7.
142. Hou, S., et al., *FoxP3 and Ezh2 regulate Tfr cell suppressive function and transcriptional program.* The Journal of Experimental Medicine, 2019. **216**(3): p. 605-620.
143. Afgan, E., et al., *The Galaxy platform for accessible, reproducible and collaborative biomedical analyses: 2018 update.* Nucleic Acids Research, 2018. **46**(W1): p. W537-W544.
144. Eden, E., et al., *Discovering motifs in ranked lists of DNA sequences.* PLoS Comput Biol, 2007. **3**(3): p. e39.
145. Eden, E., et al., *GOrilla: a tool for discovery and visualization of enriched GO terms in ranked gene lists.* BMC Bioinformatics, 2009. **10**: p. 48.
146. Morpheus, h.s.b.o.m.
147. Dobin, A., et al., *STAR: ultrafast universal RNA-seq aligner.* Bioinformatics, 2013. **29**(1): p. 15-21.
148. Love, M.I., W. Huber, and S. Anders, *Moderated estimation of fold change and dispersion for RNA-seq data with DESeq2.* Genome Biology, 2014. **15**(12): p. 550.
149. Schindelin, J., et al., *Fiji: an open-source platform for biological-image analysis.* Nature Methods, 2012. **9**(7): p. 676-682.
150. Leong, Y.A., et al., *CXCR5+ follicular cytotoxic T cells control viral infection in B cell follicles.* Nature Immunology, 2016. **17**(10): p. 1187-1196.
151. Schwarz, K., *Untersuchung der Interaktion verschiedener Transkriptionsfaktoren an Zielpromotoren follikulär regulatorischer T-Zellen* in *Institute of Pathology*. 2017, JMU Wuerzburg.
152. Chuvpilo, S., et al., *Autoregulation of NFATc1/A Expression Facilitates Effector T Cells to Escape from Rapid Apoptosis.* 2002. **16**(6): p. 881-895.
153. Serfling, E., A. Avots, and M. Neumann, *The architecture of the interleukin-2 promoter: a reflection of T lymphocyte activation.* Biochim Biophys Acta, 1995. **1263**(3): p. 181-200.
154. Kuo, T.C. and K.L. Calame, *B lymphocyte-induced maturation protein (Blimp)-1, IFN regulatory factor (IRF)-1, and IRF-2 can bind to the same regulatory sites.* J Immunol, 2004. **173**(9): p. 5556-63.
155. Isaksson, A., A.M. Musti, and D. Bohmann, *Ubiquitin in signal transduction and cell transformation.* Biochim Biophys Acta, 1996. **1288**(1): p. F21-9.
156. Schwartz, D.C. and M. Hochstrasser, *A superfamily of protein tags: ubiquitin, SUMO and related modifiers.* Trends Biochem Sci, 2003. **28**(6): p. 321-8.
157. Mackenzie, K., et al., *Regulation of the divalent metal ion transporter via membrane budding.* Cell Discov, 2016. **2**: p. 16011.
158. Fournier, P.G., et al., *The TGF-beta Signaling Regulator PMEPA1 Suppresses Prostate Cancer Metastases to Bone.* Cancer Cell, 2015. **27**(6): p. 809-21.
159. Cretney, E., A. Kallies, and S.L. Nutt, *Differentiation and function of Foxp3(+) effector regulatory T cells.* Trends Immunol, 2013. **34**(2): p. 74-80.
160. Feng, Y., et al., *Control of the inheritance of regulatory T cell identity by a cis element in the Foxp3 locus.* Cell, 2014. **158**(4): p. 749-763.
161. and, D.T.C. and S.J. Korsmeyer, *BCL-2 FAMILY: Regulators of Cell Death.* Annual Review of Immunology, 1998. **16**(1): p. 395-419.

162. Henson, S.M. and A.N. Akbar, *KLRG1—more than a marker for T cell senescence.* AGE, 2009. **31**(4): p. 285-291.
163. Reinhardt, R.L., H.E. Liang, and R.M. Locksley, *Cytokine-secreting follicular T cells shape the antibody repertoire.* Nat Immunol, 2009. **10**(4): p. 385-93.
164. Liu, X., et al., *Genome-wide Analysis Identifies Bcl6-Controlled Regulatory Networks during T Follicular Helper Cell Differentiation.* Cell Rep, 2016. **14**(7): p. 1735-1747.
165. Yu, X., et al., *The surface protein TIGIT suppresses T cell activation by promoting the generation of mature immunoregulatory dendritic cells.* Nat Immunol, 2009. **10**(1): p. 48-57.
166. Wing, J.B., et al., *Regulatory T cells control antigen-specific expansion of Tfh cell number and humoral immune responses via the coreceptor CTLA-4.* Immunity, 2014. **41**(6): p. 1013-25.
167. Griffith, J.W., C.L. Sokol, and A.D. Luster, *Chemokines and chemokine receptors: positioning cells for host defense and immunity.* Annu Rev Immunol, 2014. **32**: p. 659-702.
168. Böttcher, J.P., et al., *Functional classification of memory CD8+ T cells by CX3CR1 expression.* Nature Communications, 2015. **6**(1): p. 8306.
169. Yamazaki, T., et al., *CCR6 Regulates the Migration of Inflammatory and Regulatory T Cells.* The Journal of Immunology, 2008. **181**(12): p. 8391-8401.
170. Crabtree, G., *Contingent genetic regulatory events in T lymphocyte activation.* Science, 1989. **243**(4889): p. 355-361.
171. Benoist, C. and D. Mathis, *Regulation of major histocompatibility complex class-II genes: X, Y and other letters of the alphabet.* Annu Rev Immunol, 1990. **8**: p. 681-715.
172. Shaffer, A.L., et al., *Blimp-1 orchestrates plasma cell differentiation by extinguishing the mature B cell gene expression program.* Immunity, 2002. **17**(1): p. 51-62.
173. Wollenberg, I., et al., *Regulation of the germinal center reaction by Foxp3+ follicular regulatory T cells.* J Immunol, 2011. **187**(9): p. 4553-60.
174. Kawamoto, S., et al., *Foxp3(+) T cells regulate immunoglobulin a selection and facilitate diversification of bacterial species responsible for immune homeostasis.* Immunity, 2014. **41**(1): p. 152-65.
175. Sage, P.T., et al., *Defective TFH Cell Function and Increased TFR Cells Contribute to Defective Antibody Production in Aging.* Cell Rep, 2015. **12**(2): p. 163-71.
176. Levy, Y. and J.C. Brouet, *Interleukin-10 prevents spontaneous death of germinal center B cells by induction of the bcl-2 protein.* The Journal of Clinical Investigation, 1994. **93**(1): p. 424-428.
177. Xin, G., et al., *Single-cell RNA sequencing unveils an IL-10-producing helper subset that sustains humoral immunity during persistent infection.* Nature Communications, 2018. **9**(1): p. 5037.
178. Choe, J. and Y.S. Choi, *IL-10 interrupts memory B cell expansion in the germinal center by inducing differentiation into plasma cells.* 1998. **28**(2): p. 508-515.
179. Middendorp, S., et al., *Mice deficient for CD137 ligand are predisposed to develop germinal center-derived B-cell lymphoma.* Blood, 2009. **114**(11): p. 2280-9.
180. Miles, B., et al., *Follicular regulatory T cells impair follicular T helper cells in HIV and SIV infection.* Nat Commun, 2015. **6**: p. 8608.

181. Li, L., et al., *Block of both TGF-β and IL-2 signaling impedes Neurophilin-1+ regulatory T cell and follicular regulatory T cell development.* Cell Death & Disease, 2016. **7**(10): p. e2439-e2439.
182. Adachi, O., et al., *Targeted disruption of the MyD88 gene results in loss of IL-1- and IL-18-mediated function.* Immunity, 1998. **9**(1): p. 143-50.
183. Burns, K., et al., *MyD88, an adapter protein involved in interleukin-1 signaling.* J Biol Chem, 1998. **273**(20): p. 12203-9.
184. Pan, F., et al., *Eos mediates Foxp3-dependent gene silencing in CD4+ regulatory T cells.* Science, 2009. **325**(5944): p. 1142-6.
185. Hem, S.L., C.T. Johnston, and H. HogenEsch, *Imject Alum is not aluminum hydroxide adjuvant or aluminum phosphate adjuvant.* Vaccine, 2007. **25**(27): p. 4985-6.
186. HogenEsch, H., D.T. O'Hagan, and C.B. Fox, *Optimizing the utilization of aluminum adjuvants in vaccines: you might just get what you want.* npj Vaccines, 2018. **3**(1): p. 51.
187. Haynes, N.M., et al., *Role of CXCR5 and CCR7 in Follicular Th Cell Positioning and Appearance of a Programmed Cell Death Gene-1^{High} Germinal Center-Associated Subpopulation.* The Journal of Immunology, 2007. **179**(8): p. 5099-5108.
188. Cyster, J.G., et al., *Follicular stromal cells and lymphocyte homing to follicles.* Immunol Rev, 2000. **176**: p. 181-93.
189. Cimmino, L., et al., *Blimp-1 attenuates Th1 differentiation by repression of ifng, tbx21, and bcl6 gene expression.* J Immunol, 2008. **181**(4): p. 2338-47.
190. Ogawa, C., et al., *Blimp-1 Functions as a Molecular Switch to Prevent Inflammatory Activity in Foxp3(+)RORgammat(+) Regulatory T Cells.* Cell Rep, 2018. **25**(1): p. 19-28.e5.
191. Nakamura, N., et al., *An epidermal growth factor receptor/Jak2 tyrosine kinase domain chimera induces tyrosine phosphorylation of Stat5 and transduces a growth signal in hematopoietic cells.* J Biol Chem, 1996. **271**(32): p. 19483-8.
192. Ohtani, T., et al., *Dissection of signaling cascades through gp130 in vivo: reciprocal roles for STAT3- and SHP2-mediated signals in immune responses.* Immunity, 2000. **12**(1): p. 95-105.
193. Bhattacharyya, S., et al., *NFATc1 affects mouse splenic B cell function by controlling the calcineurin–NFAT signaling network.* The Journal of Experimental Medicine, 2011. **208**(4): p. 823-839.
194. Ahyi, A.N., et al., *IFN regulatory factor 4 regulates the expression of a subset of Th2 cytokines.* J Immunol, 2009. **183**(3): p. 1598-606.
195. Man, K., et al., *Transcription Factor IRF4 Promotes CD8(+) T Cell Exhaustion and Limits the Development of Memory-like T Cells during Chronic Infection.* Immunity, 2017. **47**(6): p. 1129-1141.e5.
196. Hedrich, C.M., et al., *Stat3 promotes IL-10 expression in lupus T cells through trans-activation and chromatin remodeling.* Proc Natl Acad Sci U S A, 2014. **111**(37): p. 13457-62.
197. Hutchins, A.P., D. Diez, and D. Miranda-Saavedra, *The IL-10/STAT3-mediated anti-inflammatory response: recent developments and future challenges.* Brief Funct Genomics, 2013. **12**(6): p. 489-98.

198. Boles, K.S., et al., *A novel molecular interaction for the adhesion of follicular CD4 T cells to follicular DC.* Eur J Immunol, 2009. **39**(3): p. 695-703.
199. Chacón-Salinas, R., et al., *Mast Cell-Derived IL-10 Suppresses Germinal Center Formation by Affecting T Follicular Helper Cell Function.* The Journal of Immunology, 2011. **186**(1): p. 25-31.
200. Kurtulus, S., et al., *TIGIT predominantly regulates the immune response via regulatory T cells.* The Journal of Clinical Investigation, 2015. **125**(11): p. 4053-4062.
201. Gibson, H.M., et al., *Induction of the CTLA-4 gene in human lymphocytes is dependent on NFAT binding the proximal promoter.* J Immunol, 2007. **179**(6): p. 3831-40.
202. Rudd, C.E., A. Taylor, and H. Schneider, *CD28 and CTLA-4 coreceptor expression and signal transduction.* Immunol Rev, 2009. **229**(1): p. 12-26.
203. Pan, M., et al., *Enhanced NFATc1 nuclear occupancy causes T cell activation independent of CD28 costimulation.* J Immunol, 2007. **178**(7): p. 4315-21.
204. Xu, K., et al., *GATA3, HDAC6, and BCL6 Regulate FOXP3+ Treg Plasticity and Determine Treg Conversion into Either Novel Antigen-Presenting Cell-Like Treg or Th1-Treg.* Front Immunol, 2018. **9**: p. 45.